Roles and regulation of the iron-sulphur proteins, HCP, NapG and NapH, induced during anaerobic growth of *E. coli*

by

Nina Filenko

A thesis submitted to
the University of Birmingham
for the degree of
DOCTOR OF PHILOSOPHY

School of Biosciences
The University of Birmingham
March 2005

AT THE BEHEST OF THE UNIVERSITY, THE FOLLOWING PAGES OF THIS THESIS HAVE NOT BEEN SCANNED:

APPENDIX A

APPENDIX B

Synopsis

The periplasmic nitrate reductase (Nap) has been shown to support anaerobic growth of *Escherichia coli* K-12 under nitrate-limiting conditions. Two of the Nap proteins, NapG and NapH, are predicted to contain four and two [4Fe-4S] clusters, respectively. In this thesis it is reported that, during fermentative growth, Nap plays a role in redox balancing. This role is most pronounced in a strain that lacks menaquinol and therefore cannot use the menaquinol-dependent fumarate reductase to fulfil a redox balancing role during glucose fermentation. Nitrate stimulated the growth of both a Δ*menBC* Δ*napGH* and an isogenic Δ*menBC nap*$^+$ strain to the same extent, even although the Nap activity was extremely low. This showed that the residual 1% electron flow in the strain deleted for NapG and NapH was sufficient to fulfil this redox balancing function. Using artificial quinones, NapG and NapH were shown to be linked to oxidation of quinones with high midpoint redox potentials. NapF$^+$ and NapF$^-$ strains were grown anaerobically after either aerobic or anaerobic growth and NapF was shown to be involved in adaptation from aerobic to anaerobic growth.

The hybrid cluster protein (HCP) contains two Fe-S clusters, one of which is a hybrid [4Fe-2S-2O] cluster. Despite intensive study, its physiological function is unclear. *E. coli* HCP is detected after anaerobic growth with nitrate or nitrite, so a possible role for it in some stage of the nitrogen cycle has been proposed. To study the regulation of HCP, an *hcp::lacZ* fusion was constructed and transformed into *fnr, arcA* and *norR* mutant strains of *E. coli.* Transcription from the *hcp* promoter was induced during anaerobic growth. Only the *fnr* mutant was defective in *hcp* expression, suggesting that transcription from the promoter in response to anaerobiosis is dependent on FNR. Nitrate and nitrite further induced transcription from the *hcp* promoter. The parental strain and the *narL*, *narP* and *narLnarP* mutants were grown anaerobically in medium supplemented with nitrite or nitrate. The nitrite and nitrate response of the *hcp* promoter was mediated by both of the response regulator proteins, NarL and NarP. It is argued that NarL plays a dual role at the *hcp* promoter acting as an activator during growth in the presence of a low concentration of nitrite or nitrate and as both repressor and activator in the presence of high nitrite or nitrate

concentrations. Gel retardation assays were used to show that FNR and NarL form a complex with the *hcp* promoter, thus confirming that their effect on transcription is direct. A technique involving the rapid amplification of cDNA ends (RACE) was used to demonstrate that transcription of the *hcp-hcr* operon initiates at a thymine nucleotide located 31 bp upstream of the translation-initiation codon.

A Δ*hcp* strain was constructed by homologous recombination. When grown in medium supplemented with nitrate, the growth rate and yield of the parental strain and the Δ*hcp* mutant were the same, suggesting that HCP is not involved in nitrate-dependent growth. Both HCP^+ and HCP^- strains were equally sensitive to nitric oxide and hydroxylamine. It was concluded therefore that HCP is unable to protect bacteria against nitric oxide or hydroxylamine toxicity *in vivo*. HCP was overexpressed from a recombinant plasmid and subsequently purified on a nickel column for biochemical studies. A qualitative method using reduced methyl viologen as an electron donor was developed for use in attempts to identify a possible substrate of HCP *in vitro*. Nitrite, nitrate and hydroxylamine were tested, but no evidence was presented that any of them can be used as an electron acceptor.

Dedicated with love and thanks

to my family

Acknowledgements

First I would like to thank my supervisor Professor Jeff Cole for the wealth of his guidance and assistance throughout the project and preparation of this thesis. I am grateful to everyone with whom I worked for the last three years. Especially I would like to thank Harma Brondijk for getting me started when I first came to the laboratory and to Sudesh Mohan for help with Western analysis and other protein techniques. I would also like to thank Eve for general help in the laboratory in the beginning of my project. Special thanks go to all the residents of ground floor, particularly to Lesley for her help with subcloning of the *hcp* gene (which resisted getting subcloned) and for her cheerful personality, and also thanks to Tim for his corrections of this thesis. Thank you to both Jeff and Tim for being patient to my ability to put "a" and "the" articles in the wrong place in a sentence (did I get it right this time?). I am grateful to Fred Hagen from Wageningen University for sharing with us the results on enzyme activity of HCP. I would like to thank Professor Steve Busby for his genuine interest in the project and input on the discussion on the *hcp* gene regulation. Special thanks to the members of Steve Busby lab, especially to Doug Browning for his help on DNA retardation assays and to Dave Lee for his assistance on nickel-NTA purification.

Enormous thanks to my family who supported and believed in me - without them I would not have come that far. I am grateful to my dad who always wanted me to study and to my mum and grandma for moral support and taking care of my son when I was not with him. Thanks to my husband Dmitry and son Anton for joining me in the UK for the part of my stay here. Thanks go to all my friends in the UK who I really enjoyed spending time with: Susanne, Nora, Christina, Dongling, Martin, Angeliki and Gavin, for some good talks, laughs and sightseeing together. Thanks are also due to my Ukrainian friends, in particular to Pasha, Nicolas, Julia, and Ira for wishing always to keep in touch.

Finally, I am indebted to the Darwin Trust of Edinburgh for awarding a studentship throughout the three years in the UK.

Contents

List of figures

List of tables

Abbreviations

Å	angstrom
AAP	abridged anchor primer
ABC	ATP binding cassette
α CTD	α subunit carboxy-terminal domain
ADP	adenosine diphosphate
ARNT	aryl hydrocarbon receptor nuclear translocator
APS	ammonium persulphate
ATP	adenosine triphosphate
BSA	bovine serum albumin
bp	base pair
CFU	colony forming unit
CIAP	calf intestinal alkaline phosphatase
CRP	cAMP receptor protein
Cys, C	cysteine
DEPC	diethylpyrocarbonate
DMK	demethylmenaquinone
DMSO	dimethyl sulfoxide
DNA	deoxyribonucleic acid
dNTP	2'-deoxynucleoside 5'-triphosphate (N = A, C, G, or T)
E. coli	*Escherichia coli*
EMSA	electromobility shift assays
FAD .	flavin adenine dinucleotide
Fis	factor for inversion stimulation
FNR	fumarate and nitrate reduction
GFP	green fluorescent protein
HA	hydroxylamine
HCP	hybrid cluster protein
His, H	histidine
H-NS	histone-like nucleoid-structuring protein
HPK	histidine protein kinase
IHF	integration host factor

IPTG	Isopropyl-β-D-thiogalactopyranoside
Kb	kilo base
kDa	kilo Dalton
LB	Lennox broth
MAD	multiple-wavelength anomalous dispersion
MCD	magnetic circular dichroic spectroscopy
MK	menaquinone
MKH_2	menaquinol
Mo-bis-MGD	molybdenum-bis-molybdopterin guanine dinucleotide cofactor
MS	minimal salts (medium)
Nap	nitrate reductase in the periplasm
NOSW	nitric oxide saturated water
NTA	nitrilo-acetic acid
OD	optical density
ONPG	o-nitrophenyl-β-galactopyranoside
ORF	open reading frame
PAGE	polyacrylamide gel electrophoresis
PAS	acronym from PER, ARNT and SIM
PER	period clock protein
PCR	polymerase chain reaction
PEP	phosphoenolpyruvate
PNK	polynucleotide kinase
PTS	PEP-dependent carbohydrate phosphotransferase system
PVDF	polyvinylidene difluoride
RACE	rapid amplification of cDNA ends
RNA	ribonucleic acid
RNase	ribonuclease
RNAP	RNA polymerase
RNI	reactive nitrogen intermediates
RNS	reactive nitrogen species
RR	response regulator
RT	reverse transcriptase
SD	standard deviation

SDS	sodium dodecyl sulphate
SIM	single-minded protein
Tat	twin-arginine translocation pathway
TdT	terminal deoxynucleotidyl transferase
T_m	melting temperature
TMAO	trimethylamine N-oxide
UQ	ubiquinone
UQH_2	ubiquinol
UV	ultra violet
v/v	volume per volume
w/v	weight per volume

CHAPTER 1
INTRODUCTION

Iron and sulphur are versatile elements. Inorganic iron and sulphur are part of many proteins with different functions: regulatory proteins and enzymes mediating electron transport and involved with carbon, oxygen, hydrogen, and nitrogen metabolism. Clusters involving iron and sulphur (Fe-S clusters) are one of the most ancient and ubiquitous classes of electron transfer groups (reviewed in Beinert et al., 1997, and Johnson, 1998). Unlike more complex cytochromes and flavines, Fe-S clusters are among the simplest electron transfer systems. They have been suggested as the first to be produced during chemical evolution. Common types of cluster include [2Fe-2S], [3Fe-4S], and [4Fe-4S] cores, and one or more of these units are found in more than 120 distinct classes of protein. The most surprising result to appear in recent years was the resolution of the unprecedented structure of a hybrid [4Fe-4S-2O] cluster. The primary function of FeS clusters lies in mediating one-electron redox processes. That is why they are integral components of respiratory and photosynthetic electron transfer chains, and a host of redox proteins involved in different types of cell metabolism. They also constitute the substrate-binding sites of a wide range of enzymes (Johnson, 1998). The term "iron-sulphur proteins" refers to those proteins in which a non-haem iron is ligated to inorganic sulphur or cysteine sulphur.

This thesis is concerned with some specialised non-haem Fe-S proteins of *Escherichia coli*, NapG, NapH and hybrid cluster protein (HCP), which are expressed under anaerobic conditions in the presence of nitrate. Based on their primary structures, NapG and NapH are predicted to contain four [4Fe-4S] clusters. HCP has two types of cluster, [2Fe-2S] and [4Fe-4S-2O] (a hybrid cluster) (Krockel et al., 1998; van den Berg et al., 2000). NapG and NapH are the subunits encoded by the periplasmic nitrate reductase operon, *nap*, which in *E. coli* is expressed in the presence of nitrite and low concentrations of nitrate. The expression of HCP is

also elevated in the presence of nitrate and nitrite. NapG and NapH are involved in nitrate reduction (Brondijk et al., 2002). HCP has been proposed to reduce hydroxylamine (Wolfe et al., 2002; Cabello et al., 2004). Although a physiological role for HCP has not yet been established, this protein is presumably involved in some aspect of nitrogen metabolism.

In this chapter, the role of nitrate reduction in the nitrogen cycle will first be described. Secondly, the structure of *E. coli* nitrate reductases will be introduced with particular emphasis on the periplasmic nitrate reductase. The regulation of genes involved in anaerobic respiration will be described and finally, an overview of the hybrid cluster protein will be presented.

1.1. The biological nitrogen cycle

Nitrogen is a component of the two essential biological macromolecules: proteins and nucleic acids. Nitrogen is present in the environment in oxidation states between +5 and –3. Interconversions of these nitrogen species constitute the global biogeochemical nitrogen cycle, which is sustained by biological processes with bacteria playing a predominant role (reviewed by Richardson, 2001). The nitrogen cycle is shown in **figure 1.1**. Inorganic nitrogen is assimilated into organic matter by nitrate assimilation and dinitrogen fixation. Dinitrogen fixation is performed by bacteria such as Klebsiella pneumoniae and Azotobacter vinelandii and it depends on the nitrogenase reaction, which proceeds without free intermediates. Denitrification constitutes a respiratory reduction of nitrate (NO_3^-) to nitrite (NO_2^-), nitric oxide (NO), nitrous oxide (N_2O) and dinitrogen (N_2) by denitrifying bacteria. There is also a short way in the nitrogen cycle of reducing nitrite to ammonia avoiding the production of nitric and nitrous oxides (Cole and Brown, 1980). Nitrification is the process whereby ammonia (NH_4^+)

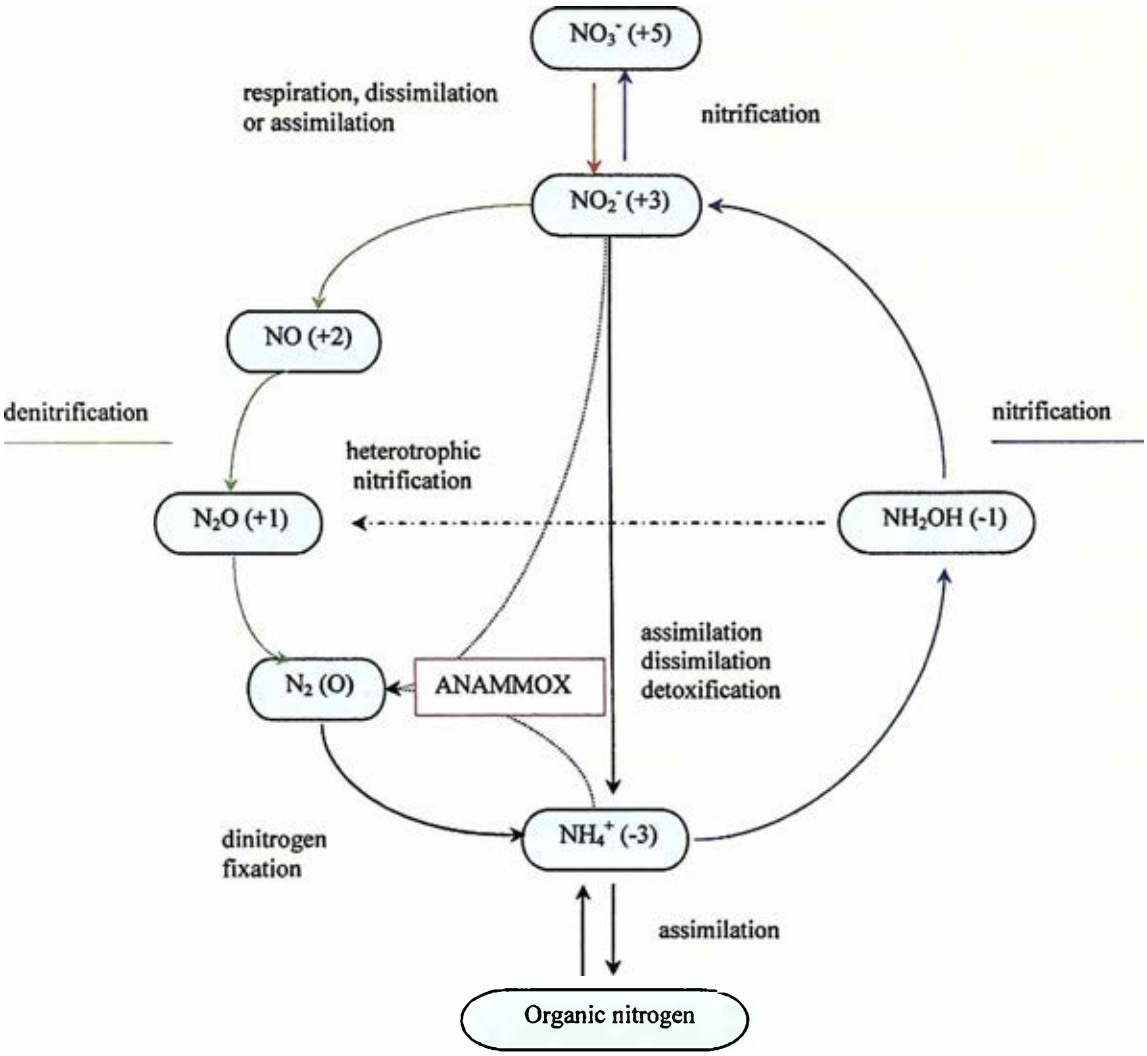

Figure 1.1. The biological nitrogen cycle. The oxidation state of nitrogen is given in brackets for each intermediate. Denitrification constitutes a respiratory reduction of nitrate (NO_3^-) to nitrite (NO_2^-), nitric oxide (NO), nitrous oxide (N_2O) and dinitrogen (N_2). The oxidation of ammonia (NH_4^+) to nitrite, via hydroxylamine (NH_2OH) constitutes the first part of nitrification. Dinitrogen fixation depends on the nitrogenase reaction, which proceeds without free intermediates. ANAMMOX, ANaerobic AMMonia OXidation, is a process in which nitrite and ammonia combine to produce dinitrogen and water.

is oxidized to nitrate via hydroxylamine (NH_2OH) and nitrite by the combined action of two species such as *Nitrozomonas europaea*, ammonia oxidizer, and *Nitrobacter vulgaris*, nitrite oxidizer. ANAMMOX, ANaerobic AMMonia OXidation, is a process in which nitrite and ammonia combine by planctomycetes to produce dinitrogen and water (van de Graaf et al., 1995; Jetten et al., 2001; Jetten et al., 2005).

Nitrate reduction by bacteria plays a key role in the nitrogen cycle, which has important effects in many ways, such as in agricultural activities. Denitrification is an important route for the loss of nitrogen from the biosphere. There is worldwide concern over the excessive use of fertilizers because nitrogen oxides generated by denitrification are a significant cause of the green-house effect. They are also a source of ozone- damaging gases that have a major impact both in the environment, and as a cause of public health problems (Richardson et al., 1998, Moreno-Vivian et al., 1999). Therefore, nitrate reduction by bacteria has been a major research topic for many years.

Nitrate reduction can be performed with three different purposes. It can be used in a respiratory process to generate energy (Haddock and Kendall-Tobias, 1975; Berks et al., 1995a; Richardson, 2000). Nitrate reduction is also used by bacteria when grown on very reduced substrates to dissipate the excess of reducing power (Ellington et al., 2002; Ellington et al., 2003a). Assimilatory nitrate reductases use nitrate reduction to assimilate nitrate into organic compounds (Gangeswaran and Eady, 1996; Gangeswaran et al., 1993; Rubio et al., 1996).

1.2. Respiratory process in bacteria

Respiration involves the transfer of electrons from a low redox-potential electron donor such as NADH through a range of redox cofactors to a high redox-potential electron acceptor such as

oxygen or nitrate. The free energy released during this electron transfer process is used to generate a trans-membrane proton electrochemical gradient (or proton motive force, Δp) that in turn can drive the synthesis of ATP. The prokaryotic respiratory system has a very flexible design, which enables the cell to survive changes of growth conditions and environmental challenges (**figure 1.2**). Most bacterial respiratory systems comprise several dehydrogenases that transfer electrons to a pool of quinones, which in turn is reoxidised by terminal oxidases that pass electrons to the final electron acceptor. Before focusing on nitrate respiration, a brief overview of different components of *E. coli* anaerobic respiratory system will be given.

1.2.1. Dehydrogenases involved in anaerobic respiration in *E. coli*

E coli encodes several dehydrogenases: formate-, glycerol-3-phosphate-, and NADH-dehydrogenases, and uptake hydrogenases (Ingledew and Poole, 1984). During anaerobiosis, formate is generated from the cleavage of pyruvate. *E. coli* expresses three enzymes capable of oxidising formate to CO_2. Formate dehydrogenase H (FDH_H) is used during fermentative growth. Formate dehydrogenases FDH_N, encoded by the *fdnGHI* locus and FDH_O, encoded by the *fdoGHI* genes, couple the oxidation of formate to the reduction of an electron acceptor and the generation of Δp (Jormakka et al., 2002b). FDH_N contains 11 redox centres aligned in a single chain, which extends almost 90 Å (Jormakka et al., 2002a).

The anaerobic glycerol-3-phosphate dehydrogenase is encoded by the *glpABC* operon. It is maximally expressed during anaerobic growth in the presence of fumarate, but it also couples the oxidation of glycerol-3-phosphate to the reduction of nitrate, TMAO and DMSO (Miki and Lin, 1975). GlpB mediates electron transfer from the soluble GlpAC dimer to the terminal electron acceptor fumarate via the membrane-bound menaquinone pool (Varga

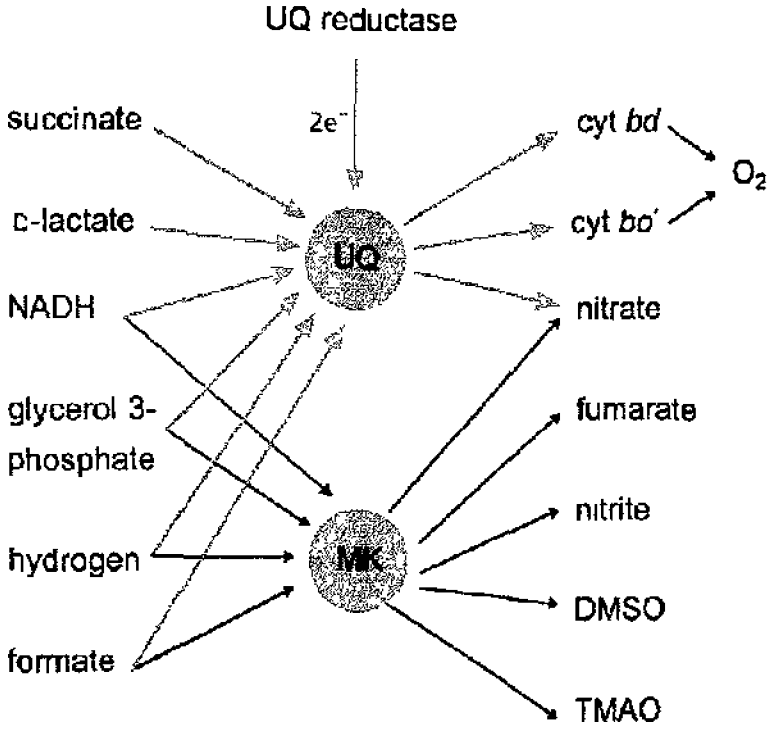

Figure 1.2. Respiratory system of *E. coli.* *E coli* respiratory systems comprises several dehydrogenases that transfer electrons from electron donors to a pool of quinones ubiquinone (UQ) and menaquinone (MK). UQ and MK are in turn reoxidised by terminal oxidases that pass electrons to the final electron acceptor. From Soballe and Poole, 1999.

and Weiner, 1995).

NADH is the most important electron donor for the respiratory chains of *E. coli* during growth with many substrates. *E. coli* contains two membrane-bound enzymes that couple NADH oxidation to reduction of the quinone pool. NADH dehydrogenase I is encoded by the *nuo* operon and consists of 14 subunits (Weidner et al., 1993). Its expression is stimulated in the presence of electron acceptors oxygen and nitrate compared with fermentative growth. NADH dehydrogenase II is encoded by the *ndh* gene. Its expression is maximal during aerobic growth and is repressed in the absence of oxygen by FNR (regulator of fumarate and nitrate reduction) (Green and Guest, 1994).

E. coli encodes four distinct uptake [NiFe] hydrogenases (denoting that H_2 is oxidised, not generated). Hydrogenases 1 and 2 are encoded by the *hyaABCDF* and *hybOhybABCDEFG* operons, whose transcription is regulated in response to oxygen and nitrate (Menon et al., 1991; Richard et al., 1999). Synthesis of hydrogenase 2 is induced when cells are grown anaerobically on non-fermentable carbon sources such as hydrogen and fumarate or glycerol and fumarate (Ballantine and Boxer, 1985). The physiological function of hydrogenase 1 is not clear. Hydrogenase 3 forms part of the formate hydrogen-lyase complex (FHL), which, during fermentation, converts formate produced by pyruvate formate-lyase to carbon dioxide and molecular hydrogen (Böhm et al., 1990). Hydrogenase 4, encoded by the *hyf* operon, is a part of another form of formate hydrogen lyase (Bagramyan et al., 2001). Optimum expression of *hyf* requires the presence of cyclic AMP receptor protein-cyclic AMP complex (Self et al., 2004).

1.2.2. Quinones

Quinones are best known as lipid-soluble components of membrane-bound electron transport chains. An important property of quinones is their hydrophobicity, which allows free movement between partner reductants and oxidants in the membrane. The quinone structure has isoprenoid side chains of various length depending on the species (reviewed in Soballe and Poole, 1999).

Bacterial respiratory quinones can be divided into two groups. The first comprises benzoquinone termed ubiquinone or coenzyme Q. The abbreviation for ubiquinone is UQ or UQ-n, where n refers to the number of isoprenoid units in the side chain. The second group contains the naphthoquinones, menaquinone (vitamin K_2; MK or MK-n) and demethylmenaquinone (DMK or DMK-n). The reduced forms of the quinones are referred to as quinols and are named ubiquinol (UQH_2), menaquinol (MKH_2) and demethylmenaquinol ($DMKH_2$), respectively. Animal cells synthesize only UQ, but MK is obtained from the diet.

Escherichia coli uses 3 different types of quinone as redox mediators – ubiquinone, menaquinone and demethylmenaquinone. They are produced in variable amounts depending on the growth conditions (Bentley and Meganathan, 1982). The cellular concentration of ubiquinone is the same during aerobiosis and anaerobiosis; menaquinone and demethylmenaquinone are produced in higher amounts during anaerobiosis. With *E. coli* mutants deficient in either UQ or MK and DMK it was demonstrated that UQ serves as a redox mediator in aerobic and nitrate respiration while the naphthoquinones fulfil the same function in anaerobic respiration with nitrite, nitrate, fumarate, dimethyl sulphoxide (DMSO) and trimethylamine N-oxide (TMAO) as the acceptors (Wissenbach et al., 1990). Thus, nitrate respiration in *E. coli* has a unique position because electrons from both UQ and MK, but not DMK, can be used for nitrate reduction (Soballe and Poole, 1999).

The selectivity of quinones for particular electron donors and acceptors could be due to differences in the midpoint redox potential between UQ/UQH_2 (E_m = 113 mV) and MK/MKH_2 couples (E_m = -74 mV) (Gennis and Stewart, 1996). Thus, MK is more suitable for a respiratory chain with lower-potential electron acceptors such as fumarate, whereas UQ is well suited for oxygen and nitrate respiration.

1.2.3. Terminal reductases involved in anaerobic respiration in *E. coli*

In addition to nitrate, *E. coli* can use nitrite, TMAO, DMSO and fumarate as terminal electron acceptors in the absence of oxygen. Before focusing on nitrate reductases a brief overview of other terminal reductases will be given. *E. coli* expresses two nitrite reductases; both catalyse the six-electron reduction of nitrite to ammonia. The nitrite reductase Nir uses NADH as an electron donor and is encoded by the *nirBDC* operon (Harborne et al., 1992). The alternative nitrite reductase, Nrf, uses formate as an electron donor and is encoded by the *nrfABCDEFG* operon (Hussain et al., 1994). The role of Nir is to detoxify nitrite formed in the cytoplasm as a product of nitrate reduction. In contrast, reduction of nitrite by the Nrf pathway provides energy for anaerobic growth (Page et al., 1990).

Fumarate is the weakest oxidising agent used by *E. coli* as a terminal electron acceptor during anaerobic respiration. Reduction of fumarate to succinate is catalysed by fumarate reductase (Cole et al., 1985), which contains covalently attached FAD at the active site of the enzyme. The *frdABCD* operon is induced by FNR during anaerobiosis and repressed by NarL in response to nitrate (Jones and Gunsalus, 1987).

DMSO reductase is encoded by the *dmsABC* operon. It reduces dimethyl sulphoxide (DMSO) to dimethyl sulphide, but also has broad range of specificity, being capable of reducing

a wide variety of S-oxides and N-oxides (Weiner et al., 1988). To reduce trimethylamine oxide (TMAO), *E. coli* synthesises two homologous systems. One, the TorCAD, is strongly induced by TMAO, whereas the other, TorYD, is expressed at a low level (Silvestro et al., 1989; Gon et al., 2000).

1.3. Nitrate reductases

Three types of nitrate reductase, each fulfilling a different physiological role, can be found in some, but not all, Gram-negative bacteria (reviewed in Philippot and Hojberg, 1999; Stolz and Basu, 2002). The active site of all three enzymes is molybdenum-bis-molybdopterin guanine dinucleotide cofactor (Mo-bis-MGD). The three types are the soluble, assimilatory nitrate reductase (NAS) located in the cytoplasm, the membrane-associated nitrate reductase (NAR) and a soluble periplasmic nitrate reductase (Nap). *E. coli* expresses two isoenzymes of membrane bound nitrate reductase, NRA and NRZ, and a periplasmic nitrate reductase, Nap (**figure 1.3**).

1.3.1. Assimilatory nitrate reductases

Assimilatory nitrate reductases are widely distributed. Nitrate is assimilated into the pool of organic nitrogen compounds by plants, eukaryotic and prokaryotic micro-organisms. Assimilatory nitrate reductases in several phototrophic and heterotrophic bacteria have been studied at the biochemical or genetic level. Nitrate assimilation by bacteria is reviewed by Lin and Stewart (1998). The first reduction step in nitrate assimilation is the two-electron reduction of nitrate to nitrite; this is followed by the six-electron reduction of nitrite to ammonia. The ammonia so formed is then predominantly incorporated into either glutamine or glutamate (Ogawa et al., 1995). Expression of *nas* genes is subjected to dual control: ammonia repression

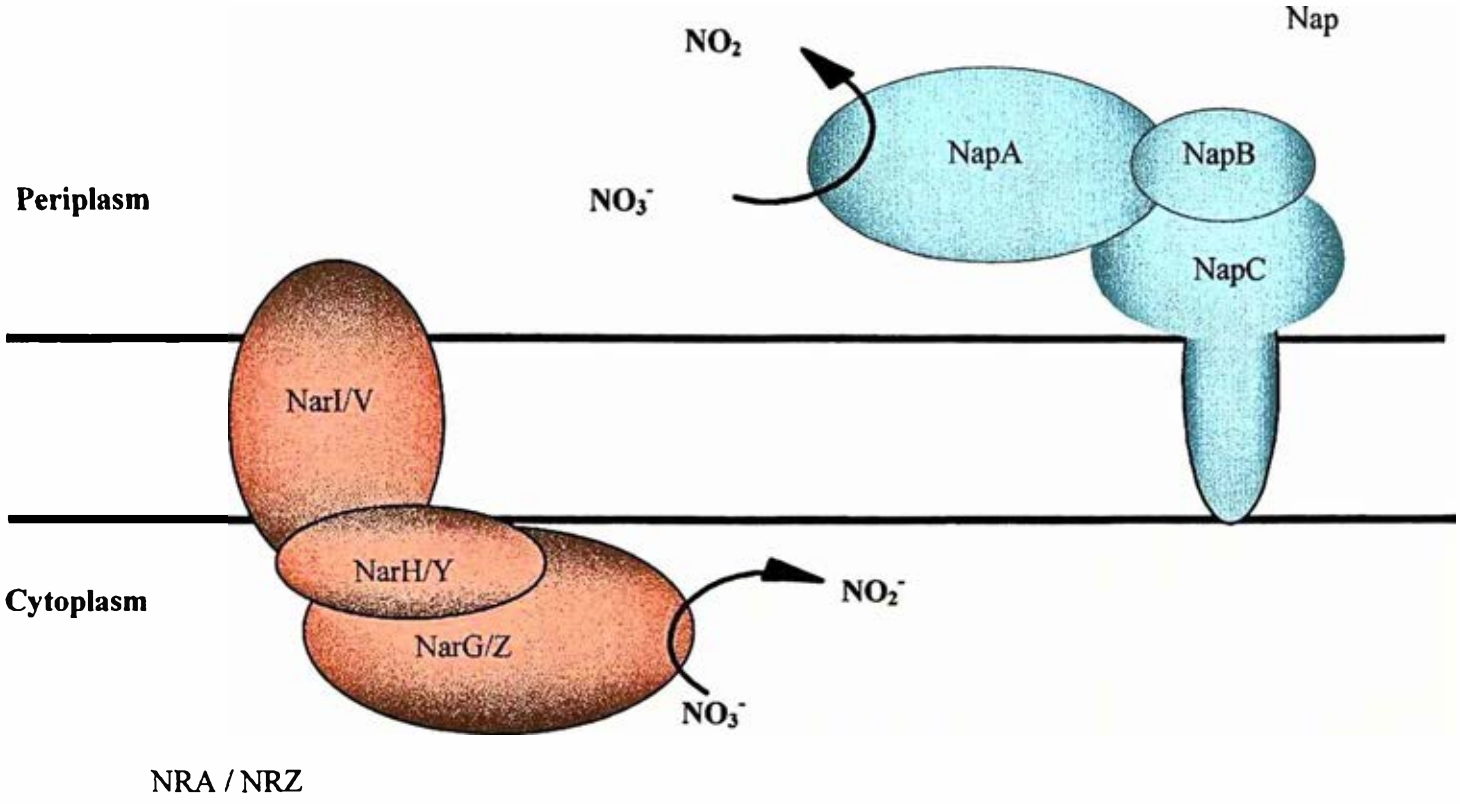

Figure 1.3. Nitrate reductase A, nitrate reductase Z and the periplasmic nitrate reductase of *E. coli*. *E. coli* expresses two isoenzymes of membrane bound nitrate reductase, NRA and NRZ, and a soluble periplasmic nitrate reductase, Nap. Each active enzyme contains 3 subunits.

by the general nitrogen regulatory system (Ntr) and specific nitrate or nitrite induction (Goldman et al., 1994; Lin and Stewart, 1998).

1.3.2. The respiratory nitrate reductase A (NRA)

The respiratory nitrate reductase A (NRA) has become one of the best-characterised anaerobic respiratory enzymes (Magalon et al., 1997; Blasco et al., 2001; Rothery et al., 2001). NRA is the most active nitrate reductase expressed during anaerobic growth in *E. coli* in the presence of excess nitrate; for many years it was believed to be the only one present. The *narG, narH* and *narI* genes encode the α-, β-, and γ-subunits, respectively. The third gene in the operon, *narJ*, encodes a soluble protein that is not part of the mature enzyme complex (Eaves et al., 1998). The α-subunit contains Mo-bis-MGD cofactor at the active site of the enzyme and the β-subunit is an FeS protein. The γ-subunit is a b-type cytochrome that anchors the αβ complex to the membrane (Blasco et al., 1992b). Formate is the preferred electron donor for NRA, although the oxidation of NADH, lactate and glycerol-3-phosphate can be coupled via the quinone pool to nitrate reduction (Wimpenny and Cole, 1967; Cole and Wimpenny, 1968; Wallace and Young, 1977). Approximately 500 bp upstream of the *narGHJI* operon, and in the same orientation, is the *narK* gene encoding an integral membrane protein acting as a nitrite extrusion and nitrate uptake protein (Rowe et al., 1994; Clegg et al., 2002). The *narL* and *narX* genes, encoding the nitrate sensor NarX and the DNA-binding regulator NarL, form another operon in the *chlC* locus and are transcribed in the opposite direction to *narGHJI*.

1.3.3. The respiratory nitrate reductase Z (NRZ)

The second membrane-bound nitrate reductase, nitrate reductase Z, has been identified in few organisms including *E. coli* and *Salmonella typhi*. This enzyme is very similar to nitrate reductase A. First, the two enzymes have the same $\alpha\beta\gamma$ subunit composition. The α and β subunits of NRZ, encoded by *narZ* and *narY* genes, correspond to the α and β subunits of NRA coded by *narG* and *narH*, with 76% and 75% identity, respectively (Bonnefoy et al., 1997). There is also 87% identity between NarI and NarV (the γ subunit of the protein). Formation of relatively active heterologous nitrate reductases between NRA and NRZ of *E. coli* was achieved (αA βZ γZ), which implicates the possibility that heterologous nitrate reductases could be formed *in vivo* (Blasco et al., 1992a).

The structural genes encoding NRZ are clustered in the *chlZ* locus, which is located at 32 min on the *E. coli* chromosome and encoded by a five-gene *narUZYWV* operon (Bonnefoy et al., 1997; Clegg, 2002). The *narW* and *narU* genes encode a chaperone-like protein and a NarK-like protein 74% identical in sequence to NarK, respectively (Bonnefoy et al., 1997). The function of NarU is to provide both nitrate and nitrite transport (Clegg et al., 2002; Jia and Cole, 2005). The *chlZ* region does not contain a regulatory gene (*narXL* homologue) upstream of *narU*.

Another difference between NRA and NRZ lies in the regulation of expression of the two proteins. NRA is strongly induced by nitrate during anaerobic growth, but NRZ is expressed at a very low, constitutive level. It was shown that *E. coli* NRZ is only slightly regulated by FNR and that its expression is highly growth phase dependent and is controlled by RpoS, the alternative sigma factor (Blasco et al., 1990; Chang et al., 1999). Expression studies, using operon fusions and nitrate reductase assays, revealed that the *narUZYWV* operon is controlled mainly at the level of transcription and is induced 10-fold at the onset of stationary phase in rich

media (Chang et al., 1999). The physiological role of the NarU-NarZ system appears to be to provide a selective advantage in the survival of stationery phase bacteria, or during stress imposed by very slow, nutrient-limited growth (Clegg, 2002).

1.4. Periplasmic nitrate reductase Nap

The assimilatory and membrane-associated respiratory nitrate reductases have been studied for many years, but it is only recently that periplasmic nitrate reductases (Nap) have attracted growing interest (reviewed in Potter et al., 2001). So far, proteins of the Nap complex have been purified from various bacteria including enterobacteria, denitrifiers and non-sulphur photosynthetic bacteria, such as *Rhodobacter capsulatus* (Richardson et al., 1990), *Paracoccus denitrificans* (Sears et al., 1995), *P. pantotrophus* (Bell et al., 1990; Berks et al., 1995b), *Ralstonia eutropha* (formerly *Alcaligenes eutrophus;* Siddiqui et al., 1993), *Desulfovibrio desulfuricans* (Dias et al., 1999) and *Azospirillum brasilense* (Steenhoudt et al., 2001).

Nap fulfils different roles in different groups of bacteria. In *Haemophilus influenzae* and *Pseudomonas* sp. strain G179 Nap is the only nitrate reductase present and its role is clearly to support nitrate respiration (Bedzyk et al., 1999, Liu et al., 1999). In *E. coli,* which expresses not only Nap, but also NRA and NRZ, the Nap enzyme is used during nitrate respiration in nitrate-limited environments (Potter et al., 1999). Brondijk et al. (2002) have shown that Nap in *E. coli* couples more effectively to menaquinol oxidation than to ubiquinol oxidation and that conversely, nitrate reductase A couples more effectively with ubiquinol than with menaquinol.

Paracoccus pantotrophus and *Ralstonia eutropha* express membrane bound, periplasmic and assimilatory nitrate reductases. In *Paracoccus pantotrophus* Nap is used for redox balancing during aerobic respiration on highly reduced carbon sources, for example, during growth on

butyrate as the main source of carbon and energy (Richardson et al., 2001; Sears et al., 2000; Ellington et al., 2002 and 2003b). Redox balancing is the process by which bacteria utilise an electron acceptor to dissipate excess reductant generated during metabolism of a carbon source that is more reduced than the average oxidation state of the biomass (Sears et al., 2000). In *Rhodobacter sphaeroides*, where Nap is the sole nitrate reductase, it can also function as an electron sink during photosynthesis (Reyes et al., 1996; Reyes et al., 1998).

1.4.1. NapA, B, C and D – four common components of all Nap enzymes

The *nap* operon was originally named the "aeg 46.5" operon as it was detected as "anaerobically expressed genes" located at minute 46.5 on the *E. coli* linkage map (Grove et al., 1996). The seven *napFDAGHBC* genes of *E. coli* are followed by eight *ccmABCDEFGH* genes, which encode proteins essential for cytochrome c maturation (Tanapongpipat et al., 1998). The *ccm* genes are transcribed from the *napF* and *ccmA* promoters, and also from a weak promoter, which is suggested to permit transcription of the downstream *ccmEFGH* genes.

The *nap* gene clusters of different bacteria reveal considerable heterogeneity in their composition (**figure 1.4**), but most of the *nap* clusters have four genes in common: *napDABC* (with exceptions in *Campylobacter jejuni*, *Wollinella succinogenes*, *Symbiobacterium thermophilum* and *Desulfovibrio desulfuricans*; Parkhill et al., 2000; Simon et al., 2003; Marietou and Mohan, personal communication). The conservation of *napA*, *napB* and *napC* is expected as they encode the periplasmic molybdoprotein, NapA, a di-haem cytochrome, NapB, and a putative tetra-haem quinol dehydrogenase, NapC. The *napD* gene encodes a possible pathway-specific chaperone, NapD. Potter and Cole (1999) showed that products of the *napABCD* genes are all essential for the Nap activity in *E. coli*.

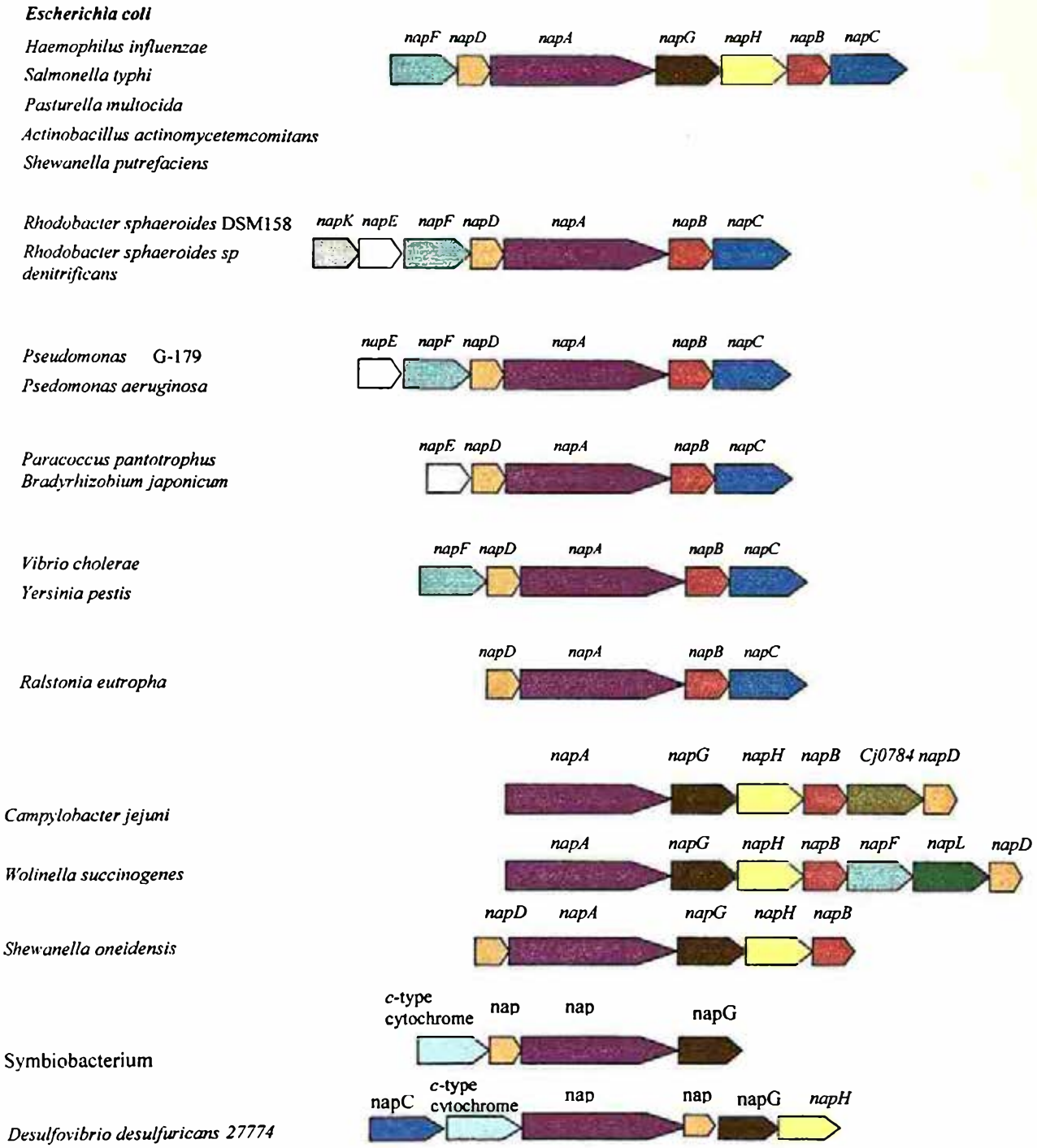

Figure 1.4. Organization of genes encoding periplasmic nitrate reductase. The *nap* operons from various bacteria are shown. The genes are drawn approximately to scale, and the arrows indicate the direction of transcription.

The NapA protein contains Mo-bis-MGD and [4Fe-4S] as cofactors. Although some hyperthermophilic archaea synthesise a number of enzymes with tungsten at the active site, none of the utilised approaches revealed evidence that tungsten could replace molybdenum at the active site of *E. coli* NapA (Gates et al., 2003). NapA is a 90 kDa protein with a 36-residue leader peptide, which includes the double-arginine (RR) motif (Thomas et al., 1999). This motif is typical of proteins to which complex redox cofactors are attached in the cytoplasm and which are transported to the periplasm via the twin-arginine translocation, Tat, pathway (reviewed in Berks et al., 2000a and 2000b). The pre-NapA leader sequence is both unexpectedly long and is cleaved at the unprecedented sequence G-Q-Q (Thomas et al., 1999).

The crystal structure of the NapA from *Desulfovibrio desulfuricans* was determined at 1.9 Å resolution by multiple-wavelength anomalous dispersion (MAD) (Dias et al., 1999). The protein is folded into four domains comprising both alpha-helices and beta-sheets and all four domains are involved in cofactor binding. The [4Fe-4S] centre is located near the periphery of the molecule, whereas the MGD cofactor extends across the interior of the molecule. The molybdenum atom is positioned 12 Å from the [4Fe-4S] cluster (Dias et al., 1999). A facile electron-transfer pathway connects the di-haem NapB, molybdenum and the [4Fe-4S] cluster.

The NapB protein from *Haemophilus influenzae* was overproduced (Brigé et al., 2001) and its crystal structure was resolved at 1.25 Å by MAD spectrometry (Brigé et al., 2002). Finally, the structure of the NapAB complex from *R. sphaeroides* was determined at a resolution of 3.2 Å (Arnoux et al., 2003 and **figure 1.5**). The NapB subunit binds to the large NapA subunit with haem II in close proximity to the [4Fe-4S] cluster of NapA. The N- and C-terminal extremities of NapB adopt an extended conformation, embracing the NapA subunit (Arnoux et

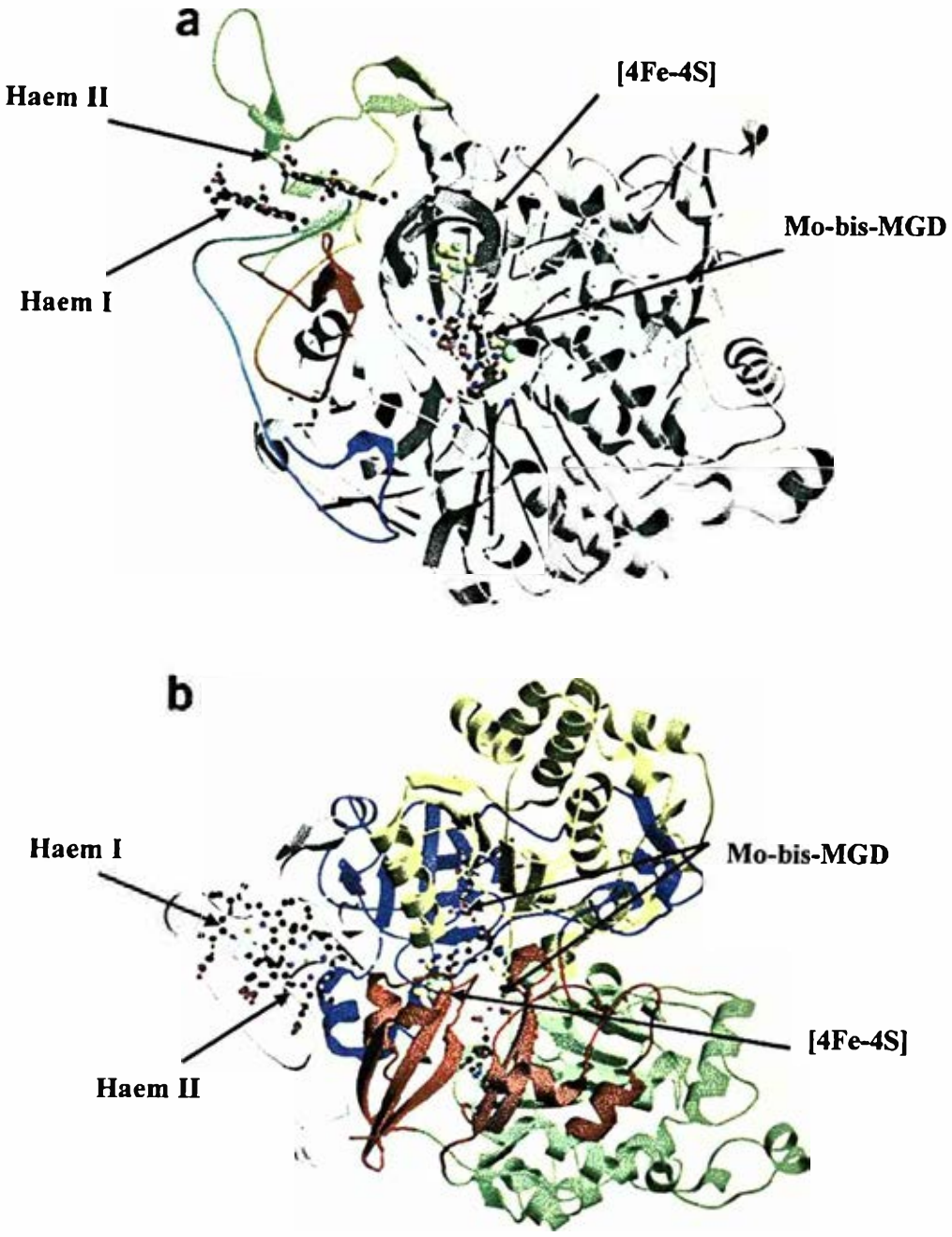

Figure 1.5. Views of the overall fold of the NapAB complex from *R. sphaeroides*.
a: NapA is represented as a white ribbon, and NapB is colored from blue to red from the N to the C terminus, respectively. Mo-bis-MGD cofactor and [4Fe-4S] cluster of NapA and the two haems of NapB are indicated. **b:** The same view as in **a**, rotated by 90 °C. NapB is white, and the four structural domains of NapA are coloured as follows: domain I, red; domain II, green; domain III, yellow; domain IV, blue. Adapted from Arnoux et al., 2003.

al., 2003). Based on the protein from *Haemophilus influenzae* a model of the NapAB complex was proposed, in which the four redox centres are positioned in a virtually linear configuration, which spans a distance of nearly 40 Å (Brigé et al., 2002). This suggests an efficient pathway for the transfer of electrons from NapB to a nitrate molecule at the catalytic site of NapA.

The *nap* gene cluster of *D. desulfuricans* does not encode a NapB (Marietou and Mohan, personal communication; see also **figure 1.4**). It is proposed that at some point in evolution NapA must have recruited the di-naem NapB as a redox partner (Richardson, personal communication). The molecular interaction with the primordial NapB would not have initially been strong, which perhaps is still reflected by the weak NapA-NapB interaction of γ-proteobacterium *E. coli*. As the NapA and NapB co-evolved, the interaction would have become stronger, which is exemplified by the tight heterodimeric NapA-NapB complex of α-proteobacterium *R. sphaeroides* (Dias et al., 1999; Richardson, personal communication).

Each haem-iron centre of NapC has a bis-histidinyl coordination. Four proximal ligands arise from each of four Cys-X_2-Cys-His haem-binding motifs; candidates for the four distal ligands are four other histidine residues. A model of organisation of NapC into two domains, each containing a di-haem pair, was proposed (Cartron et al., 2002). In this model, each haem pair obtains one distal haem ligand from its own domain and a second one from the other domain. One of the Nap systems, known to be independent of NapC, is that one of *Wolinella succinogenes*. The *nap* cluster of this bacterium lacks the *napC* gene, and neither of two other members of the NapC/NirT family encoded by the genome are required for nitrate respiration (Simon et al., 2003).

1.4.2. Nap E, F, G, H and K - additional proteins of Nap systems

Apart from *napA, napB, napC and napD*, additional genes are not the same among different organisms (**figure 1.4**). The *napE* gene has been found in *T. pantotropha*, *R. sphaeroides*, *P. aeruginosa* and *B. japonicum nap* operons (Reyes et al., 1998; Liu et al., 1999; Delgado et al., 2003). NapK and NapE are integral membrane proteins of currently unknown function.

The genome of *E. coli* contains 3 additional genes for putative iron-sulphur proteins NapF, NapG and NapH. It has been shown recently that electron transfer from ubiquinol to NapAB is almost totally dependent upon NapGH and it was originally proposed that NapGH form an energy-conserving ubiquinol dehydrogenase (Brondijk et al., 2002). The topology model of the *E. coli* periplasmic nitrate reductase complex is shown in **figure 1.6**. Sequence analysis of NapF, NapG and NapH predicts them to bind four [4Fe-4S] clusters. NapF, G and H are 16, 20 and 32 kDa proteins, respectively. Based on the primary structure, NapF is a hydrophilic protein with a hydrophobic region in its C-terminus. Although it has an N-terminal double-arginine motif that might be required for translocation across the cytoplasmic membrane of *E. coli* by the twin-arginine translocation system, its mutation did not affect nitrate dependent growth. NapF from *E. coli* was shown to be loosely associated with the membrane facing the cytoplasm (Nilavongse, 2003). This partially agrees with the finding of Olmo-Mira et al. (2004) who showed NapF of *R. sphaeroides* to be located in the cytoplasm. The 6xHis-tagged NapF protein of this bacterium displayed spectral properties indicative of Fe-S clusters, but these features were rapidly lost, suggesting cluster lability. NapA could not be detected in an isogenic *ΔnapF* strain of *R. sphaeroides*, and also the recovery of NapA, which had previously been treated with 2,2'-dipyridyl to remove the [4Fe-4S] cluster, was achieved in the presence of NapF. Based on these observations, a role for NapF was proposed in assembling the [4Fe-4S]

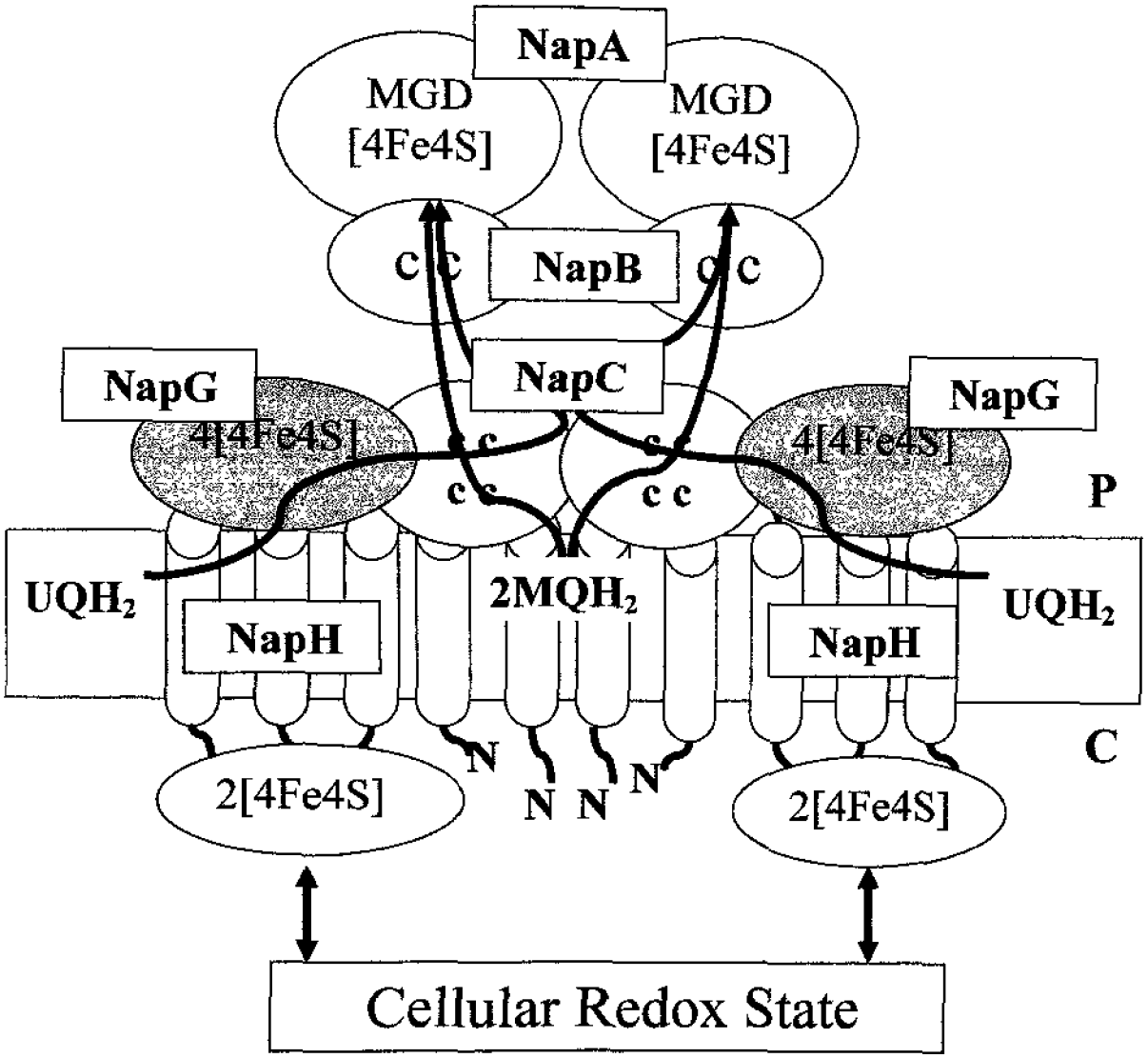

Figure 1.6. Working model for electron transfer from the cytoplasm via ubiquinone, NapH and NapG to the NapCBA complex in the periplasm. Nap*A*, *B* and *C* proteins are common components of all Nap enzymes. NapA is a periplasmic molybdoprotein, NapB is a di-haem cytochrome and NapC a putative quinol dehydrogenase. The putative iron-sulphur proteins NapG and NapH participate in oxidation of *ubiquinol, but oxidation of menaquinol is independent from* NapG and NapH (Brondijk et al., 2002; Brondijk et al., 2004). P: periplasm; C: cytoplasm.

centre of the catalytic subunit NapA (Olmo-Mira et al., 2004).

NapG is encoded by the fourth gene in the *nap* operon. Like NapF, the N-terminal sequence of NapG includes a twin arginine motif. Alignment of NapG coding sequences from several bacteria reveals a consensus sequence of Leu-Arg-Pro-Pro-(Gly/Phe)-Ala. The first proline in this consensus sequence is located 35 or 36 amino acid residues after the twin arginine motif and 13 residues before the first cysteine motif. Mutagenesis of the twin-arginines showed that RR is essential for NarG function, presenting strong evidence that NapG is exported into the periplasm (Brondijk et al., 2004).

The fifth gene of the *nap* operon encodes NapH, an integral membrane protein with four transmembrane helices (Brondijk et al., 2004). The proposed cytoplasmic C-terminal domain contains one of the four cysteine clusters. This region of the polypeptide is thus likely to bind one non-haem [4Fe-4S] cluster. One of the other three cysteine clusters is found in the cytoplasmic loop between helices 2 and 3 (**figure 1.6**).

1.4.3. Energy conservation by NRA and NRZ and energy dissipation by Nap

As active centres of the NRA/Z and Nap enzymes are located at the opposite sides of the membrane, the enzymes differ in terms of energy conservation (**figure 1.3**). NRA generates energy by a redox loop mechanism (Jones et al., 1980; reviewed in Jormakka et al., 2003). The quinol is oxidised by the NarI/V subunit at the periplasmic face of the cytoplasmic membrane. Protons are ejected into the periplasm while the electrons flow back to the cytoplasm across the membrane through the two NarI/V haems. The electrons then pass, via the NarH/Y iron-sulphur centres, to the cytoplasmically located NarG/Z MGD cofactor, where nitrate is reduced to nitrite.

The reduction also involves consumption of two protons. This electron-transfer process ensures that the free energy is conserved as a proton motive force.

In the case of the *E. coli* periplasmic nitrate reductase, the quinol is thought to be oxidised by NapC at the periplasmic face of the cytoplasmic membrane. The electrons flow into the periplasm, where during the reduction of nitrate to nitrite, the protons released by quinol oxidation become consumed. Thus, in contrast to the membrane-bound nitrate reductases A and Z, the free energy in the QH_2/NO_3^- redox pair is not conserved as a proton motive force, but is dissipated. Interestingly, in *Paracoccus pantotrophus* the Nap complex is expressed under aerobic conditions. This expression of an energy-dissipating system raised the possibility of a role for Nap in redox balancing (Richardson et al., 1998; Ellington et al., 2002). However, despite not creating an electrochemical gradient, periplasmic nitrate reductase can participate indirectly in respiration, by functioning as a part of electron transport chain with a proton-translocating enzyme, such as NADH-dehydrogenase I (NuoA-N enzyme).

1.5. Regulation of genes involved in anaerobic respiration

The expression of most bacterial genes is regulated at the initiation of transcription. Bacterial promoters contain different elements that are recognised by RNA polymerase holoenzyme (RNAP). The –10 and –35 hexamer elements are contacted by specific surfaces in the RNAP σ^{70} subunit. Upstream (UP)-elements, which are located upstream of the –35 region at many promoters, are contacted by the RNA polymerase α subunit carboxy-terminal domain (α CTD) (reviewed in Rhodius and Busby, 1998). Different promoters contain different combinations of

these elements: in some cases recognition of these elements by RNAP is sufficient for transcription initiation, but in other cases an activator, or activators, are required.

To adapt to a new environment, *E. coli* must be able to repress synthesis of enzymes that are no longer needed and induce those that are required for the metabolism of available substrates. Oxygen is the preferred electron acceptor, but in the absence of oxygen nitrate becomes the most favourable electron acceptor. Gene expression in response to oxygen availability is mediated either by FNR or by the ArcB/ArcA system. Both systems can either repress or activate expression from relevant operons. Further regulation in the presence of nitrate or nitrite is ensured by the NarX/NarL and NarQ/NarP systems (Stewart, 1993).

1.5.1. FNR

Anaerobic induction of respiratory enzyme synthesis is in many cases regulated by the transcription regulator protein FNR. At most target promoters two FNR monomers bind to a 22 bp sequence, resulting in the activation of transcription initiation by RNA polymerase (Jayaraman et al., 1988; Bell et al., 1989; Bell and Busby, 1994). FNR can also function as a repressor of genes involved in aerobic metabolism as well as an autorepressor of the *fnr* gene itself (reviewed in Spiro and Guest, 1990). Recently it was shown that FNR can respond not only to oxygen, but also to nitric oxide, with major implications for gene regulation in bacteria (Cruz-Ramos et al., 2002). Global gene expression profiling of *E. coli* showed that more than 40% of genes are either directly or indirectly modulated by FNR, although this extent of regulation by FNR should be taken with caution as microarray techniques may raise biased data (Salmon et al., 2005). In another study, it was shown that 184 operons comprised of 465 genes are regulated by FNR and/or O_2 (Kang et al., 2005). The expression of many genes known to be

involved in anaerobic respiration and fermentation was increased under anaerobic growth conditions, while that of genes involved in aerobic respiration and the tricarboxylic acid cycle (TCA) were repressed. Ninety-one genes with no presently defined function were also altered in expression, six of which were found to be directly regulated by FNR (Kang et al., 2005).

The *fnr* gene is located at 29 min on the *E. coli* chromosome. The FNR protein is homologous to the well-characterised transcription regulator, CRP (cyclic AMP receptor protein) (Shaw et al, 1983; Kolb et al., 1993). In contrast to CRP, FNR contains a cysteine-rich N-terminal extension, which is essential for FNR function (Shaw and Guest, 1982). Four essential cysteines coordinate an iron-sulphur centre of FNR (Green et al., 1993). Mossbauer spectroscopy was used to identify two forms of Fe-S centre in native FNR namely $[4Fe\text{-}4S]^{2+}$ and $[2Fe\text{-}2S]^{2+}$. These and other observations have led to a model for iron-sulphur centre transition in FNR (**figure 1.7**; see also Unden and Schirawski, 1997; Kiley and Beinert, 1998). According to this model an equilibrium exists between the active dimeric FNR-$[4Fe\text{-}4S]^{2+}$ and inactive monomeric FNR-$[2Fe\text{-}2S]^{2+}$ depending on the concentration of oxygen.

The site of FNR binding at most promoters is centred between base pairs 41 and 42 upstream from the transcript start point (i.e. –41.5) (Jayaraman et al., 1989). Promoters in which the FNR-binding site is located at this position are referred to as class II FNR-dependent promoters (Wing et al., 1995). Studies of the FNR-activated *napF* control region indicated that the FNR binding site is at position –64.5 (Choe and Reznikoff, 1993; Darwin and Stewart, 1995b; Darwin et al., 1998). *napF* exemplifies another class of FNR activated promoters called class I FNR-dependent promoters.

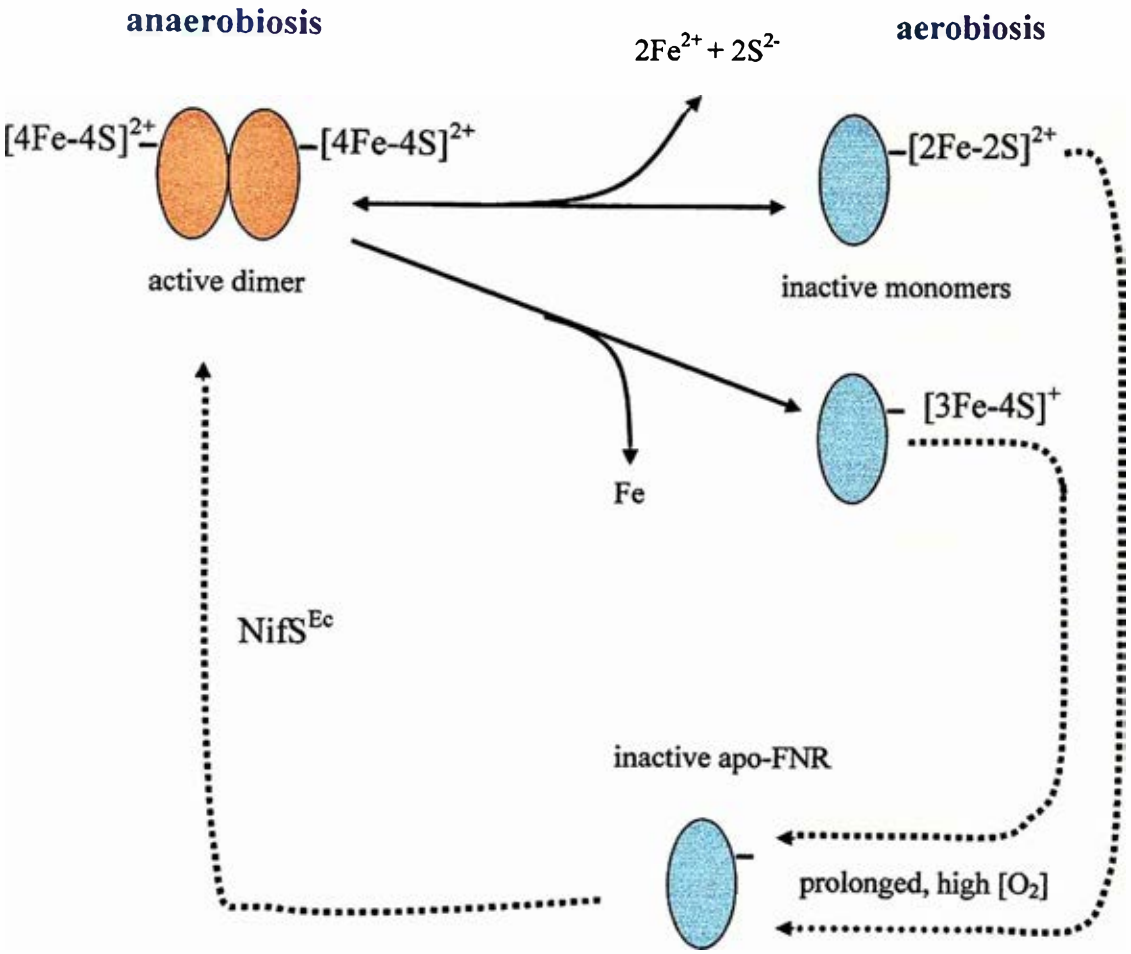

Figure 1.7. A model of the oxygen-sensing mechanism of *E. coli* FNR. An equilibrium exists between the active dimeric FNR-$[4Fe\text{-}4S]^{2+}$ in the absence of oxygen and inactive monomeric FNR-$[2Fe\text{-}2S]^{2+}$ in the presence of oxygen. The active $[4Fe\text{-}4S]^{2+}$ centre may also degrade aerobically to a $[3Fe\text{-}4S]^{+}$ centre. When continuously exposed to oxygen, the FNR monomer loses its iron-sulfur centre to form apo-FNR. Active FNR-$[4Fe\text{-}4S]^{2+}$ can be regenerated by $NifS^{Ec}$. Dotted lines show unproven pathways. Adapted from, Kiley and Beinert, 1998.

1.5.2. The ArcB/ArcA and the Nar two-component signal transduction systems

Proteins involved in anaerobic respiration are also regulated by two-component systems ArcB/ArcA, NarX/NarL and NarQ/NarP. The number of two-component systems is highly variable in the eubacteria (reviewed in Stock et al., 2000). In the enteric bacteria *E. coli* and *S. typhimurium*, about 30 different two-component systems are known to occur.

Each two-component system consists of a histidine protein kinase and a response regulator element. In all cases the former protein contains the histidine protein kinase domain (HPK) and the latter one the response regulator domain (RR). The regulation exploits the phosphorelay scheme (Kwon et al., 2000). The HPK domain catalyses the reversible phosphorylation of a conserved histidine residue within the HPK domain at the expense of ATP, producing ADP. The phosphorylated HPK domain is dephosphorylated by the RR domain by means of a reversible reaction in which the phosphoryl group is transferred to a conserved aspartate within the response regulator domain. The phosphorylated RR domain may be dephosphorylated by a number of mechanisms including a self-catalysed autophosphatase activity, a regulated phosphatase activity of the HPK, and dephosphorylation by distinct phosphatases (Stewart, 1998).

The ArcB/ArcA regulatory system

The ArcB/ArcA signal transduction system comprises the membrane-associated ArcB sensor kinase and its cognate response regulator, ArcA (Iuchi and Lin, 1988). Under microaerobic conditions, ArcB undergoes autophosphorylation and then catalyses the transphosphorylation of ArcA. The sequence of most conserved bases, recognized by ArcA-P, is 5'-GTTAATTTAAATGTTA-3' (Georgellis et al., 2001). Phospho-ArcA (ArcA-P) subsequently

represses a wide variety of aerobic enzymes such as enzymes of the tricarboxylic acid cycle, and activates some others (cytochrome *d* operon and pyruvate formate lyase operons). Microaerobic control of *cydAB* (cytochrome *d* oxidase) gene expression involves ArcA/B in conjunction with FNR. Analysis of the ArcA/B modulon of *E. coli* revealed that 9% of all reading frames are affected either directly or indirectly by ArcA-P (Liu and Wulf, 2004). The data also suggest that the Arc regulon overlaps partly with the FNR regulatory network. This is not surprising as ArcA is regulated by FNR (Compan and Touati, 1994). The *arcA* and *arcB* genes are located at minute 0 and 69.5, respectively, on the *E. coli* chromosome. Expression of *arcA* is positively regulated by both ArcA and FNR during anaerobic growth and as a consequence FNR indirectly regulates the synthesis of many aerobic respiratory enzymes (Compan and Touati, 1994). No equivalent regulation has been observed for *arcB* (Lynch and Lin, 1996).

ArcB contains a PAS domain (**figure 1.8**), the common domain of many sensor proteins that monitor changes in light, redox potential, oxygen and overall level of energy of a cell (reviewed in Taylor and Zhulin, 1999). PAS is an acronym formed from the names of the proteins in which the imperfect repeat sequences were first recognised: the *Drosophila* period clock protein (PER), vertebrate aryl hydrocarbon receptor nuclear translocator (ARNT), and the *Drosophila* single-minded protein (SIM). Recent studies suggest that the PAS domain comprises a region of approximately 100 to 120 amino acids. In PYP (photoactive yellow protein), which is the structural prototype for the three-dimensional PAS domain, four segments have been delineated: the N-terminal cap, the PAS core, the helical connector and the ß-scaffold (**figure 1.8**). The PAS core has the highest density of conserved residues in PAS domains. The mechanism of oxygen sensing by ArcB is not entirely elucidated, although redox-sensing rather than sensing of oxygen per se was proposed (Iuchi et al., 1990). And indeed, recently quinones

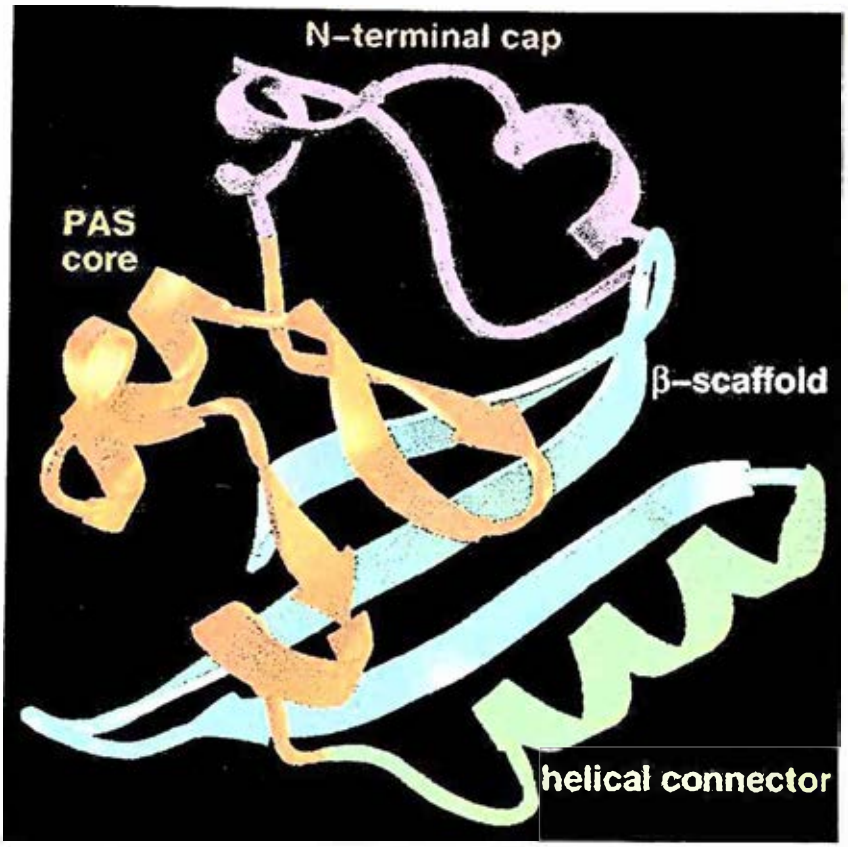

Figure 1.8. Structure of PAS domain. The proposed PAS three-dimensional fold is illustrated on the structure of PYP (photoactive yellow protein) from *Ectothiorhodospira halophida*. The PYP is a bacterial blue-light receptor. The PAS domain contains the N-terminal cap (purple), the PAS core (gold), the helical connector (green) and the ß-scaffold (blue). The PAS core has the highest density of conserved residues in PAS domains. From Taylor and Zhulin, 1999.

were shown to be a redox signal for the Arc system: it was demonstrated that the oxidised forms of quinones are the ArcB-specific signals that silence ArcB kinase activity, whereas reduced forms permit the ArcB autophosphorylation (Georgellis et al., 2001).

The Nar (NarX/NarL and NarQ/NarP) regulatory system

Expression of operons involved in anaerobic respiration is also modulated in response to the availability of nitrate and nitrite. This establishes priorities for operons involved in nitrate/nitrite reduction amongst other anaerobically expressed operons. This expression is mediated by another two-component, dual, regulatory system, - the Nar system. Homologous membrane-bound sensor proteins, NarX and NarQ, monitor the availability of nitrate and nitrite in the medium. They control the phosphorylation state of homologous DNA-binding response regulators NarL and NarP by phosphorylating or dephosphorylating them (Rabin and Stewart, 1993; Wang et al., 1999; Wang and Gunsalus, 2000). The phosphorylated response regulators then bind to the control regions of target operons and regulate their expression. The regulation of gene expression by the Nar two-component system is shown in **figure 1.9**. Two-component signalling represents only one of several possible regulatory mechanisms for response to nitrate and nitrite. For example, *Paracoccus pantotrophus* employs an FNR-like nitrate-responsive regulator (Wood et al., 2001).

Generally it is thought that both sensor proteins NarX and NarQ interact with both response regulator proteins NarL and NarP (Rabin and Stewart, 1993), although it was shown that cytoplasmic domains of the two sensor proteins differ in their ability to interact with NarL (Schröder et al., 1994). Different roles for NarX and NarQ were proposed in nitrate and nitrite control in which NarQ is the major phospho-kinase to generate active NarL (NarL-phosphate)

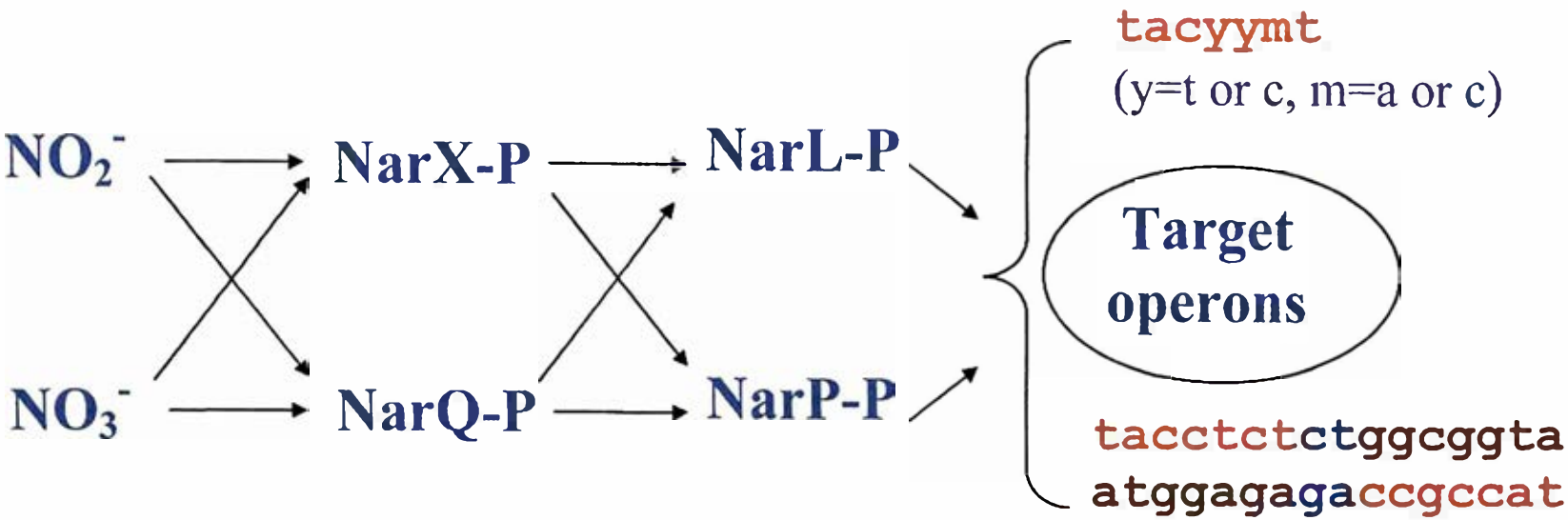

Figure 1.9. The NarXLQP regulatory system. In the presence of nitrate or nitrite in the medium, homologous membrane-bound sensor proteins, NarX and NarQ, autophosphorylate and then control the phosphorylation state of homologous DNA-binding response regulators, NarL and NarP, by phosphorylating or dephosphorylating them (Rabin and Stewart, 1993; Wang et al., 1999; Wang and Gunsalus, 2000). The phosphorylated response regulators then bind to the control regions of target operons and regulate their expression.

when nitrate is present, whereas NarX serves as a major phosphatase when nitrate is absent. There is some disagreement as to whether nitrite or nitrate is a superior ligand (Rabin and Stewart, 1993; Lee et al., 1999). A chemostat was used to show that nitrate is a stronger regulatory signal than nitrite by at least 2 to 3 orders of magnitude (Wang et al., 1999; Lee et al., 1999; Wang and Gunsalus, 2000).

The presence of dual Nar two-component regulatory systems is a peculiarity confined to one branch of the enterobacteria represented by *Escherichia coli* and *Salmonella enterica.* Sequenced genomes of the other bacteria each contain only two genes: *narX* and *narL* in *Pseudomonas aeruginosa* and *Ralstonia solanaceum* and *narQ* and *narP* in *Vibrio cholerae*, *Haemophilus influenzae*, *Pasteurella multocida* and *Yersinia pestis* (reviewed in Stewart, 2003). One noteworthy observation is that *narXL* genes are specifically associated with the structural genes for membrane-bound nitrate reductase, *narGHJI*, whereas organization and linkage of the *narQ* and *narP* genes is quite variable.

In *E. coli*, the *narX* and *narL* genes form an operon in the *chlC* locus and are transcribed in the opposite direction to the *narK* gene, coding for a nitrate/nitrite antiporter, and the *narGHJI* operon. The *narQ* and *narP* genes are located at 53 and 46 min, respectively, on the *E. coli* genetic map (Nohno et al., 1989; Stewart, 1994; Darwin and Stewart, 1995a). The primary sequence of NarP shares 44% identity with NarL and the putative NarP helix-turn-helix DNA-binding element is identical to that of NarL at 12 out of 20 positions (Rabin and Stewart, 1993). Alignment of the primary amino acid sequences of NarX and NarQ revealed that they are homologous with 28% identity (Rabin and Stewart, 1992). The 8 amino acid motif of NarX and NarQ (residues 53-60 and 49-56 respectively) known as the P-box is essential for signal sensing

and discrimination between nitrate and nitrite. Mutations in the P-box lead to ligand insensitivity or loss of discrimination between the ligands (Williams and Stewart, 1997; Chiang et al., 1997).

A consensus heptameric DNA binding sequence for both NarL and NarP is TACYYMT, where Y=C or T and M=A or C (Dong et al., 1992, Tyson et al., 1993; Tyson et al., 1994). DNAse I footprinting experiments (Darwin et al., 1997) showed that NarP only binds to these heptamer sequences organised as an inverted repeat with a 2 bp spacing (referred to as 7-2-7 sites). NarL protein recognises not only 7-2-7 sites, but also heptamers in other arrangements.

The interplay between two metabolites, two sensors, two response regulators and different affinities of consensus sequences for NarL and NarP at different regulatory regions inevitably means that complex and diverse regulatory interactions are involved in different contexts. Ultimately it is the amount of active (phosphorylated) NarL and NarP that determines the level of expression of target genes. There is yet another layer of complexity to the system: the *narXL*, *narQ* and *narP* genes are all regulated (Darwin and Stewart, 1995a). Expression of the *narP* and *narQ* genes is weakly repressed by nitrate which is mediated by NarL. The *narP* and *narQ* genes are induced under anaerobic conditions independently of FNR or ArcA whereas the *narXL* operon is unaffected by anaerobiosis. The NarL and NarP proteins are required for full nitrate induction of the *narXL* operon expression.

The Nar regulon (operons regulated by the Nar system) includes about 15 operons (Darwin and Stewart, 1996; **table 1.1**). These operons can be classified into two types. The first group includes operons for nitrate reductase A (*narGHJI*), fumarate reductase (*frdABCD*) and nitrite export/nitrate import (*narK*) and is regulated only by NarL. The second group of operons, for which the regulatory regions contain not only single heptamers, but also 7-2-7 sites, is controlled by both NarL and NarP. This group includes operons for formate-dependent nitrite

Table 1.1 NarL and NarP regulated promoters in *E. coli*

Key: +, positive regulation; -, negative regulation; n/d, not determined. Adapted from Darwin and Stewart, (1996).

Enzyme	Locus	Effect of NarL	Effect of NarP
Nitrate reductase A	*narGHJI*	+	none
Periplasmic nitrate reductase	*napFDAGHBC*	-	+
NADH-dependent nitrite reductase	*nirBDC*	+	+
Formate-dependent nitrite reductase	*nrfABCDEFG*	+/-	+
Nitrate/nitrite regulation	*narXL*	+	+
	narQ	-	none
	narP	-	none
Nitrite transport protein NarK	*narK*	+	none
Molybdate uptake	*modE*	+	n/d
Formate dehydrogenase N	*fdnGHI*	+	+
NADH dehydrogenase I	*nuoA-N*	+	+
Alcohol dehydrogenase	*adhE*	-	n/d
Pyruvate formate lyase	*pfl*	-	-
DMSO reductase	*dmsABC*	-	n/d
Fumarate reductase	*frdABCD*	-	none
Hybrid cluster protein	*hcp*	(?)	(?)

reductase (*nrfABCDEFG*), NADH-dependent nitrite reductase (*nirBDC*) and the periplasmic nitrate reductase (*napABCD*) (Darwin et al., 1997). This work (chapter 3) describes regulation of the hybrid cluster protein by the Nar system.

There are several distinct patterns of operon expression known, including induction by nitrate for *narG* and *fdnG* operons, and repression by nitrate for the *frdA* operon. The organisation of five *E. coli* promoters that are regulated by FNR and NarLP is shown in **figure 1.10.** In the case of NADH-dependent nitrite reductase, encoded by the *nir* operon, anaerobic expression can be increased by both nitrite and nitrate (Tyson et al., 1993). Anaerobic transcription activation of the *nirB* operon is co-dependent on both FNR and either NarL or NarP transcription factors as mutations in the NarL/NarP-binding site at the *nirB* promoter decrease FNR-dependent anaerobic induction (Tyson et al., 1993). In the absence of NarL or NarP the FNR-dependent expression from the *nir* promoter is suppressed by three DNA binding proteins, Fis (factor for inversion stimulation), IHF (integration host factor) and H-NS (histone-like nucleoid structuring protein), which bind to the upstream elements (Wu et al., 1998; Browning et al., 2000). An important role of NarL and NarP is to counteract these repressing proteins.

The activity of the *nrf* operon, encoding the alternative formate-dependent nitrite reductase, is activated by nitrite and nitrate at low concentration, but repressed by nitrate at high concentration. The *nrfA* promoter has an inverted 7-2-7 repeat centred around –74.5 and also three other single heptamers (**figure 1.10**). The expression of this promoter is activated by NarL-P and NarP-P binding to the inverted repeat, but during high nitrate conditions is repressed by NarL-P occupation of heptamers situated at –50 and –22, which excludes binding of FNR and RNAP, respectively (Tyson et al., 1994; Wang and Gunsalus, 2000).

Figure 1.10. Architecture of five *E. coli* promoters that are regulated by FNR and NarLP. The rightward-facing arrows on the right are the transcription start sites. The orange inverted arrows show the FNR (regulator of fumarate and nitrate reduction) binding sites, the green arrows are NarL recognition sites, the ocean-grey inverted arrows denote 7-2-7 recognition sites for both NarL and NarP. ModE is involved in regulation of genes in response to molybdenum. Fis is factor for inversion stimulation, IHF is integration host factor and H-NS is histone-like nucleoid structuring protein. Lines with arrowheads denote activation; lines with straight ends denote repression. Adapted from Tyson et al., 1994; Li et al., 1994; Darwin and Stewart, 1996; Darwin et al., 1998; Browning et al., 2000 and McNicholas and Gunsalus, 2002.

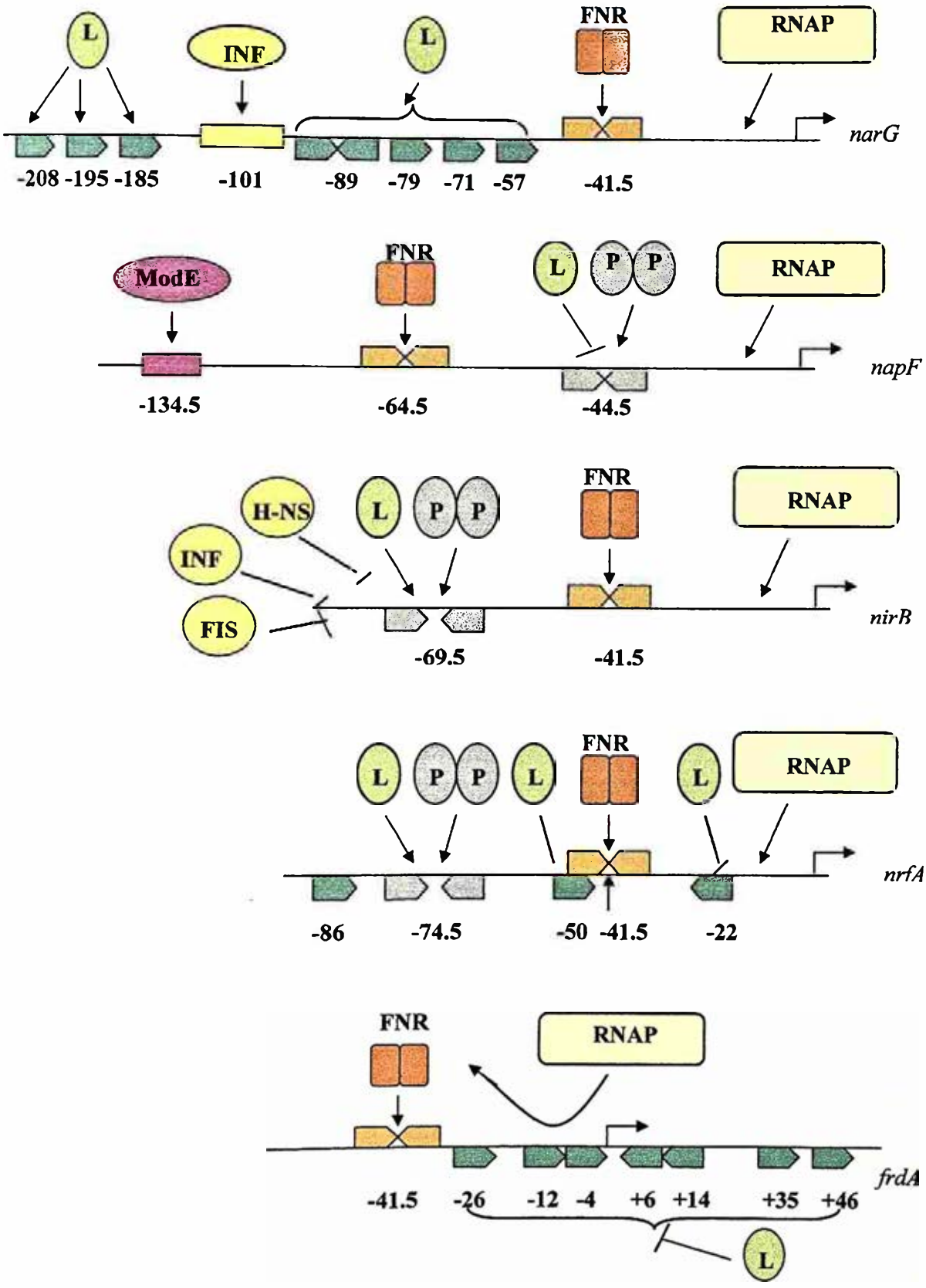
L
INF
L
FNR
RNAP
narG
-208 -195 -185
-101
-89 -79 -71 -57
-41.5
ModE
FNR
L P P
RNAP
napF
-134.5
-64.5
-44.5
H-NS
INF
FIS
L P P
FNR
RNAP
nirB
-69.5
-41.5
L P P L
FNR
L
RNAP
nrfA
-86
-74.5
-50 -41.5
-22
FNR
RNAP
frdA
-41.5
-26
-12 -4
+6 +14
+35 +46
L

The *napF* operon reveals even more complicated regulation: it is activated by nitrate at low concentration and by nitrite, but repressed by nitrate at high concentration (Darwin and Stewart, 1995b; Darwin et al., 1998). Amongst all operons mentioned above the *napF* operon has unique features with respect to its FNR-, NarL- and NarP-dependent regulation. The *napF* control region directs synthesis of two transcripts whose 5' ends differ by about 3 nucleotides (Choe and Reznikoff, 1993). Results indicate that the downstream promoter (P1) is responsible for FNR and NarP-regulated *napF* operon expression, whereas transcription from the upstream (P2) promoter is activated only weakly by the FNR protein and is inhibited by phospho-NarL and phospho-NarP proteins (Stewart et al., 2003). The physiological function of the promoter P2 is unknown. The FNR-binding site is centred at position –64.5 with respect to P1 (**figure 1.10**), which by analogy with CRP-dependent promoters indicates that it is a naturally occurring example of a class I FNR-dependent promoter. Besides other peculiarities, nitrate and nitrite activation of the *napF* operon is solely dependent on NarP but antagonised by the NarL protein. Both NarL and NarP proteins are able to bind to the common binding region of the *napF* promoter centred at –44.5 bp, but NarL fails to activate transcription in the presence of FNR. One of the possible explanations is that the binding of NarL may not have the required effect on the DNA structure to enable FNR to be an efficient activator. It may not bend DNA in the same way as NarP (Darwin et al., 1998).

The NarX sensor protein exhibits a differential response to nitrate and nitrite in interactions with NarL (Rabin and Stewart, 1993). In response to nitrate at high concentration, the NarX protein primarily phosphorylates NarL, whereas in response to nitrite and nitrate in low concentration, it primarily dephosphorylates phospho-NarL. This results in high levels of phospho–NarL (NarL-P) in the presence of a high concentration of nitrate and much lower levels

in response to nitrite and low nitrate. In contrast, it appears that the phospho-NarP (NarP-P) concentration is similar in the presence of nitrate or nitrite (Rabin and Stewart, 1993; Wang and Gunsalus, 2000). It was demonstrated that two nitrate reductase operons, *narG* and *napF*, are differentially expressed in a complementary pattern (Wang et al., 1999). In *E. coli* at high nitrate concentration the ratio NarL-P/NarP-P is high. This results in *narG* operon expression, activated by NarL-P. Under these conditions the *napF* operon is not transcribed because NarL-P binds to the *napF* promoter, but is unable to activate its transcription. The membrane-bound nitrate reductase is thus a "high-substrate-induced" operon (Wang et al., 1999; see also Potter et al., 1999). When the concentration of nitrate decreases to about 1 mM, NarL-P becomes primarily dephosphorylated, which results in a high NarP-P/NarL-P ratio. NarP-P is not able to activate the *narG* promoter, lacking the 7-2-7 site (**figure 1.10**), so this operon is switched off. Conversely, this provides a higher occupation by NarP-P of the *napF* 7-2-7 target site and increased transcription activation from the *napF* promoter.

Other genes regulated by the Nar system include those encoding pathways for the reduction of alternative electron acceptors. The expression of genes encoding DMSO reductase (*dmsABC*) and fumarate reductase (*frdABCD*) are repressed by phospho-NarL to ensure preferential use of nitrate and nitrite as electron acceptors. The NarL heptamers are scattered around the transcription start site of the *frdA* promoter (**figure 1.10**); so that binding of NarL displaces RNA polymerase (Stewart and Berg, 1988; Li et al., 1994). Synthesis of dehydrogenases is also tuned according to the metabolism type so that alcohol dehydrogenase (*adhE*) and pyruvate-formate lyase (*pfl*), which non-oxidatively cleaves pyruvate to yield formate and acetyl CoA, are repressed by phospho-NarL whereas formate dehydrogenase (*fdnG*) and NADH dehydrogenase (*nuoA-N*) are activated by both NarL and NarP (**table 1.1**).

1.5.3. Carbon catabolite repression

Some operons of the Nar regulon are also subject to catabolite repression. The *E. coli nir* promoter is repressed by Cra (catabolite repressor-activator) when cells are grown in minimal medium with glycerol and fumarate (Tyson et al., 1997a). The term carbon catabolite repression (CCR) is currently in use to describe the general phenomenon in microorganisms whereby the presence of some carbon sources in the medium can repress expression of certain genes and operons, whose gene products are often concerned with the utilization of alternative carbon sources. While the final outcome of CCR is uniform (reduced expression of certain genes and operons) the mechanisms leading to repression may be quite diverse (reviewed in Bruckner and Titgemeyer, 2002). This includes mechanisms preventing carbohydrate-specific induction (inducer exclusion) and transcriptional control by global regulators.

Carbohydrate transport and concomitant phosphorylation is achieved by components of the phosphoenolpyruvate (PEP)-dependent carbohydrate phosphotransferase system (PTS) (Postma et al., 1993). The system consists of sugar-specific PTS permeases, also referred to as enzymes II (EII), and two general PTS proteins, enzyme I (EI) and histidine-containing protein (HPr), that participate in the phosphorylation of all PTS-transported carbohydrates. Inducer exclusion is a regulatory phenomenon whereby a carbohydrate inhibits uptake of another carbon source. In *E. coli*, inducer exclusion is mediated by the glucose-specific enzyme IIA ($EIIA^{glc}$) of the PTS (Postma et al., 1993). When a PTS substrate, for example glucose, is present, the phosphate group of PTS proteins is drained to the incoming sugar. Consequently, $EIIA^{glc}$ exists predominantly in its unphosphorylated form. This form of $EIIA^{glc}$ binds to non-PTS sugar permeases, that are specific for other sugars such as lactose, maltose, melibiose, and raffinose.

As a result, transport of these sugars is inhibited and due to this the respective operons remain poorly expressed.

One of the best studied consequences of the availability of carbohydrates is the activation of global transcriptional control systems. In enteric bacteria an activation mechanism that uses the CRP protein is realized (Busby et al., 1994) and CCR is the result of diminished activation of promoters for catabolic genes or operons. In *E. coli*, CRP (cAMP receptor protein, also known as CAP) activates transcription at more than 100 promoters and is in some cases also involved in repression. CRP needs the allosteric effector cAMP in order to bind efficiently to DNA. Global regulation by CRP is dependent on the intracellular amount of cAMP and on autoregulation of CRP levels (Ishizuka et al., 1994). The intracellular cAMP level, in turn, is adjusted by adenylate cyclase, whose activity depends on the phosphorylated form of $EIIA^{glc}$ ($P\text{-}EIIA^{glc}$) (Postma et al., 1993). Besides controlling carbohydrate catabolic genes, CRP is directly involved in the modulation of a large number of other cellular processes. It also exerts indirect control by influencing expression of global regulators such as FIS (Nasser et al., 2001); therefore, the role of CRP goes far beyond regulation of sugar utilization.

1.5.4. Other regulation of Nap expression

Transcription of the *Paracoccus pantotrophus nap* operon is negatively regulated under anaerobiosis so that expression is restricted to aerobic growth, but only when the carbon source is highly reduced (Sears et al., 2000). In *Rhodobacter sphaeroides*, nitrate reduction is mainly regulated at the level of enzyme activity by both nitrate and the level of reduction of electron donors (Gavira et al., 2002).

The *nap* operon is also regulated by the availability of molybdenum in the medium. The *modABC* genes code for a high-affinity ABC-type molybdate uptake system in which ModA binds molybdate in the periplasm, ModB is the transmembrane component of the permease, and ModC provides the energiser function on the cytoplasmic side of the membrane. In the presence of molybdenum, ModE represses transcription of the *modABC* genes (Self et al., 2001). A ModE protein binding site centred at –134.5 relative to the transcription start confers molybdate-responsive *napF* operon expression, but deletion of this site renders expression independent of ModE (McNicholas and Gunsalus, 2002). A *Bradyrhizobium japonicum modA* mutant was constructed that was not able to grow anaerobically with nitrate and lacked nitrate reductase activity (Bonnard et al., 2005).

1.6. Hybrid cluster protein

Another focus of this work was a study of *E. coli* hybrid cluster protein (HCP), which is presumably involved in the nitrogen cycle. HCP contains two Fe-S clusters: either a cubane [4Fe-4S] cluster with spin-admixed S = 3/2 ground-state paramagnetism (*D. vulgaris* and *D. desulfuricans*) or [2Fe-2S] cluster (*E. coli*) and a hybrid [4Fe-4S-2O] cluster. This soluble, cytoplasmic protein has been extensively studied because of the unusual properties of its redox-active iron clusters. Initial characterisation by electron paramagnetic resonance (EPR) and Mössbauer spectroscopy suggested the presence of an Fe/S cluster with magnetic properties similar to those of synthetic [6Fe–6S] model compounds (Moura et al., 1992; Pierik et al., 1992a; Pierik et al., 1992b). These compounds were previously named 'prismane' clusters, hence the name 'prismane protein' was initially proposed for the HCP.

Hybrid cluster protein occurs in three domains of life, bacteria, archaea and eucaryota, but only in unicellular organisms and only in facultative or strict anaerobes. Nevertheless, the *hcp* genes have not been encountered in all strains for which the genomes have now been completely sequenced. The *hcp* genes are not found, for example, in the genomes of *Bacillus subtilis, Pyrococcus horikoshii, Archeoglobus fulgidus*, nor in several other bacterial species with small genomes (e.g. *Mycobacterium* sp., *Haemophilus influenzae*). **Table 1.2** shows the species distribution for HCP. The gene for the HCP protein has been sequenced in more than 40 organisms, but structural, physiological and enzymic studies have been carried out in only some of them. These include *Desulfovibrio vulgaris* (Pierik et al., 1992a; Pierik et al., 1992b; Stokkermans et al., 1992a; Cooper et al., 2000), *Desulfovibrio desulfuricans* (van den Berg et al., 1994; Aragao et al. 2003), *E. coli* (van den Berg et al., 2000; Wolfe et al., 2002), *Shewanella oneidensis* (Beliaev et al., 2002), *Clostridium perfringens* (Briolat and Reysset, 2002), *Salmonella enterica* (Kim et al., 2003) and *Rhodobacter capsulatus* (Cabello et al., 2004).

Differences in primary structures allow the distinction of three classes of putative HCPs (Cooper et al., 2000). Genes for class 1 HCPs have been found only in strictly anaerobic bacteria and in the methanogenic archaeon *Methanococcus jannaschii*. A distinctive feature of class 1 HCPs is the spacing of the N-terminal cysteine ligands for the cubane cluster: Cys-X_2-Cys-X_{7-8}-Cys-X_5-Cys. This is different from typical cubane binding motifs where the final ligand is donated from the C-terminal end of the molecule (Hinks et al., 2002). Genes for class 2 HCPs are found in facultatively anaerobic Gram-negative bacteria and the spacing of the N-terminal cysteines is Cys-X_2-Cys-X_{11}-Cys-X_6-Cys. Class 3 HCPs are found in hyper-thermophilic bacteria and archaea. Class 3 proteins have the same spacing of the N-terminal cysteines as class

Table 1.2. Species distribution for hybrid cluster protein

Kingdom	Family	Species
Eukaryota	Entamoebidae	*Entamoeba histolytica*
	Parabasalidea	*Trichomonas vaginalis*
	Diplomonadida	*Giardia lamblia* *Giardia intestinalis* *Spironucleus barkhanus*
Bacteria	Thermotogae	*Thermotoga maritima*
	Proteobacteria Alphaproteobacteria	*Rhodospirillum rubrum*
	Gamma proteobacteria	*Acidithiobacillus ferrooxidans* *Shewanella oneidensis* *Vibrio vulnificus* *Photobacterium phosphoreum* *Enterobacteriaceae:* *Escherichia coli* *Salmonella typhimurium* *Salmonella typhi* *Yersinia pestis*
	Delta proteobacteria	*Desulfuvibrio desulfuricans* *Desulfuvibrio vulgaris*
	Fusobacteria	*Fusobacterium nucleatum*
	Chlorobi	*Chlorobium tepidum*
	Firmicutes	*Thermoanaerobacter tengcongensis* *Clostridium acetobutylicum* *Clostridium perfringens* *Bacillus cereus*
Archaea	Euryarchaeota	*Methanothermobacter thermoautotrophicum* *Methanopyrus kandleri* *Methanocaldococcus jannaschii* *Methanosarcina mazei* *Pyrococcus abyssi* *Pyrococcus furiosus*

1 proteins but have a deletion of 116 amino acids downstream of the N-terminal cysteine cluster. This deletion corresponds to one of the two three-helix bundles in domain 1 of *D. vulgaris* HCP.

Hybrid cluster protein belongs to the carbon monoxide (CO) dehydrogenase (CODH) family of proteins. The CODH catalyses the reversible oxidation of CO to CO_2. Overall sequence similarity of HCP and CODH is weak, but sequence similarity of the active site binding domain is strong. CODH dimer has five metal clusters of 3 types *B*, C and D (Dobbek et al., 2001; Drennan et al., 2001): a 4Fe4S cluster that bridges the two subunits and that is termed the D cluster, a pair of 4Fe4S clusters referred to as B clusters, and a pair of clusters referred to as C clusters. The C cluster constitutes the active site of the enzyme. This cluster from *Rhodospirillum rubrum* CODH is reported to contain Ni4Fe4S while that from *Carboxydothermus hydrogenoformans* CODH is reported to contain Ni4Fe5S (Dobbek et al., 2001; Drennan et al., 2001). In both cases the nickel atom is associated with a 3Fe4S unit and is bridged to a fourth iron atom.

1.6.1. Characterisation of HCP in sulphate reducing bacteria

The hybrid-cluster proteins were initially purified from species of the strictly anaerobic sulphate-reducing bacterial genus *Desulfovibrio*: *D. vulgaris* (Hildenborough) (Pierik et al., 1992b) and *D. desulfuricans* (Moura et al., 1992). The gene encoding the HCP protein of *Desulfovibrio vulgaris* (Hildenborough) has been cloned and sequenced (Stokkermans et al., 1992a). The gene encodes a polypeptide composed of 553 amino acids (60 kDa). The polypeptide contains nine Cys residues. Four of these residues are gathered in a Cys-X_2-Cys-X_7-Cys-X_5-Cys motif located towards the N-terminus of the protein, which serve as ligands to a conventional cubane cluster. In the transconjugant *D. vulgaris* cells the prismane protein was 25-fold overproduced and

characterized by molecular mass, isoelectric point, iron content and spectroscopic properties (Stokkermans et al., 1992a).

The amino acid sequence of *Desulfovibrio desulfuricans* HCP is highly similar to that of the corresponding protein from *D. vulgaris* (Hildenborough) and also contains a cysteine motif that is involved in coordination of the Fe-S cluster (Stokkermans et al., 1992b). The hybrid cluster protein of *D. desulfuricans* is composed of 544 amino acids. *Desulfovibrio vulgaris* HCP was shown to be a stable monomeric protein, which has a molecular mass of 52 kDa, as determined by sedimentation-equilibrium centrifugation (Pierik et al., 1992b). The prismane protein has a slightly acidic amino acid composition and isoelectric point (pI = 4.9). The shape of the protein is approximately globular. Its cytoplasmic localisation was inferred from subcellular fractionation studies (Pierik et al., 1992b).

HCP was previously thought to contain 6Fe-6S clusters with 4 valency states, 3+, 4+, 5+ and 6+, which were identified in the titration experiments (Pierik et al., 1992a). The fully oxidized 6+ state appeared to be diamagnetic at low temperature. The aerobically isolated prismane protein is predominantly in the one-electron-reduced 5+ state. The nature of the HCP redox states was later supported on the HCP of *D. desulfuricans* overproduced in *D. vulgaris* cells (van den Berg et al., 1994). The redox titration demonstrated that the [Fe-S] cluster in this protein might attain four different redox states with midpoint potentials for the transitions of approximately -220, +50/-25 and +370 mV, respectively. In the +5-state, virtually all of the iron was in an S = 9/2 spin state, which indicated a cluster that is more complex than common [4Fe-4S] or [2Fe-2S] clusters (van den Berg et al., 1994).

Later, contrary to the previous result low-temperature magnetic circular dichroic spectroscopy (MCD) showed three paramagnetic redox states of the HCP, 3+, 4+ and 5+

(Marritt et al., 1995). Each of the redox states showed a distinctive low-temperature MCD spectrum unlike that observed for any other iron-sulphur clusters. Finally, with Mossbauer spectroscopy HCP was shown to contain the hybrid cluster (Krockel et al., 1998). The Mossbauer parameters of HCP in its isolated, its one-electron-reduced, and its oxidized states indicated that it represents a 4Fe cluster with an unusual mixture of bridging and terminal ligands and metal coordinations, a hybrid cluster. It was also shown to contain an additional 4Fe unit, which according to its Mossbauer parameters was a [4Fe-4S] cubane structure. These findings were contrary to the former hypothesis of one or two [6Fe-6S] cluster(s) as the prosthetic group of this protein (Pierik et al., 1992a; Moura et al., 1992).

The three-dimensional structure of the hybrid cluster protein from *Desulfovibrio vulgaris* (Hildenborough) has been determined at 1.6 Å resolution using synchrotron X-ray radiation (Cooper et al., 2000). The protein can be divided into three domains: an N-terminal mainly alpha-helical domain and two similar domains comprising a central beta-sheet flanked by alpha-helices (**figure 1.11**). The protein contains two 4Fe clusters with an edge-to-edge distance of 10.9 Å. Four cysteine residues at the N-terminus of the protein are ligands to the iron atoms of a conventional [4Fe-4S] cubane cluster. The second hybrid cluster with a variety of protein ligands, namely two μ2-sulphido and two μ2-oxo bridges, is ligated to the protein via three cysteine residues, a cysteine persulphide, two glutamate residues, and a histidine residue (**figure 1.12**) (Cooper et al., 2000). The hybrid cluster is buried in the centre of the protein, but is accessible through a large hydrophobic cavity that runs the length of domain 3. The hybrid cluster is also accessible by a hydrophilic channel. At the present time the significance of these channels is not known.

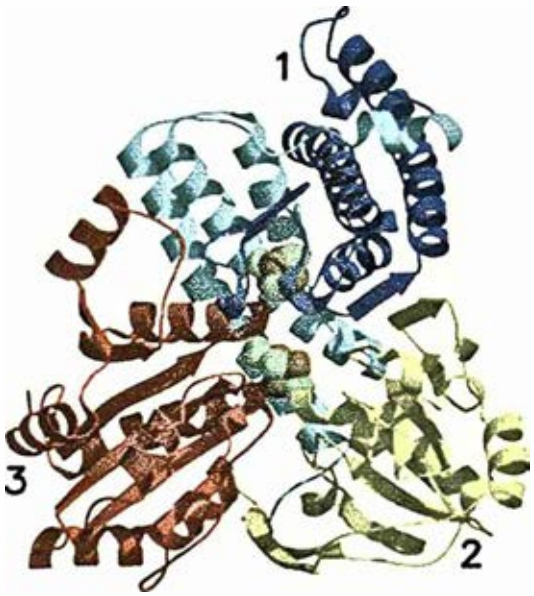

Figure 1.11. A schematic representation of the 3-D structure of hybrid cluster protein from *D. vulgaris* (from Cooper et al., 2000). Domain 1 is depicted in blue (light and dark), domain 2 in light green and domain 3 in red. The iron, sulphur and oxygen atoms of the clusters are shown as brown, green, and red spheres, respectively. The cubane cluster is the upper of the two clusters.

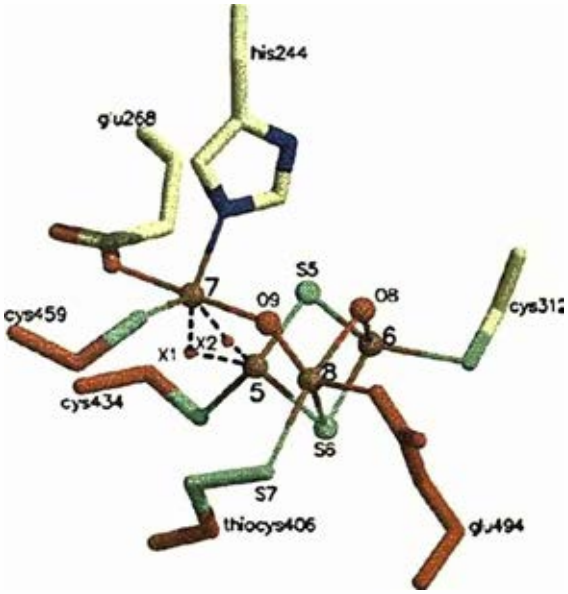

Figure 1.12. View of the hybrid cluster from *D. vulgaris* HCP (from Cooper et al., 2000). Iron, sulphur and oxygen atoms are represented as brown, green and red spheres, respectively. Ambiguous atoms X_1/X_2 are shown as smaller spheres and their bonds with dotted lines. The carbon atoms of protein ligands from domain 2 are in light green and those from domain 3 in red.

Both naturally oxidized and dithionite-reduced structures from *D. vulgaris* and *D. desulfuricans* were elucidated at higher, 1.25 Å resolution (Macedo et al., 2002; Aragao et al., 2003). The structural changes in the HCP in moving between the reduced and the oxidized state and *vice versa* have been compared. They show the large movements of Fe8 and S7 atoms and involve gain or loss of the two bridging O atoms O8 and O9 (Macedo et al., 2003).

1.6.2. *Thiobacillus ferrooxidans* HCP as a part of an electron transport chain

HCP was also found to be encoded by plasmid pTF5 in *Thiobacillus ferrooxidans* (Dominy et al., 1997). The plasmid contains a region of approximately 5 to 6 kb that is also found on the chromosome. This region was sequenced and found to encode four complete ORFs, which when translated had a high percentage of amino acid similarity to [3Fe-4S,4Fe-4S] ferredoxins, proteins of the FNR regulator family, prismane-like proteins and the NADH oxidoreductase subunit of a methane monooxygenase (Dominy et al., 1997). Ferredoxins, prismane-like proteins and NADH oxidoreductases are redox-active proteins, so it is likely that the proteins on pTF5 represent an electron transport system of as yet unknown function.

1.6.3. Characterisation of HCP in *Escherichia coli*

HCP of *E coli* was overproduced and isolated (van den Berg et al., 2000). EPR spectroscopy showed the presence of a hybrid cluster in the *E. coli* protein with characteristics similar to those in the proteins of anaerobic sulphate reducing bacteria. EPR spectra of the reduced *E. coli* hybrid-cluster protein, however, gave evidence for the presence of a [2Fe-2S] cluster instead of a [4Fe-4S] cluster.

The *hcp* gene encoding the hybrid-cluster protein in *E. coli* and other facultative anaerobes occurs, in contrast with *hcp* genes in obligate anaerobic bacteria and archaea, is found in a small operon with a gene encoding a putative NADH oxidoreductase. This NADH oxidoreductase was also isolated and shown to contain FAD and a [2Fe-2S] cluster as cofactors (van den Berg et al., 2000). It catalysed the reduction of the hybrid-cluster protein with NADH as an electron donor. Midpoint potentials (25 °C, pH 7.5) for the Fe/S clusters in both proteins indicate that electrons derived from the oxidation of NADH (E_m NAD^+ /NADH couple = -320 mV) are transferred along the [2Fe-2S] cluster of the NADH oxidoreductase (E_m = -220 mV) and the [2Fe-2S] cluster of the hybrid-cluster protein (E_m = -35 mV) to the hybrid cluster (E_m = 0, +85 and +365 mV for the three redox transitions). Western hybridisation demonstrated that in the facultative anaerobes *Escherichia coli* and *Morganella morganii* the protein is only detected after cultivation under anaerobic conditions in the presence of nitrate or nitrite, which suggested a role for HCP in nitrate or nitrite respiration (van den Berg et al., 2000).

E. coli HCP has also been implicated in reduction of hydroxylamine *in vitro*. One interesting feature of the amino acid ligands to the hybrid cluster is their similarity to the ligands to the FeNiS active-site cluster of *Rhodospirillum rubrum* carbon monoxide dehyrogenase (CODH; the C cluster) (Garavelli et al., 2000). It was shown previously that upon substitution of some key residues that bind the CODH C cluster the specificity of the CODH was altered, effectively converting it from an enzyme that catalyzes CO oxidation to one that has some hydroxylamine (NH_2OH) reductase activity (Heo et al., 2002). The activity was 28.8 ± 4.6 μmol of NH_2OH reduced min^{-1} mg of $protein^{-1}$. It has also been found that, by inserting iron into the vacant position of Ni-deficient CODH, in a sense creating an Fe-CODH, a similar hydroxylamine reductase activity can be produced. These findings led to the investigation and

discovery of a similar hydroxylamine reductase activity for the HCP from *Escherichia coli* (Wolfe et al., 2002). It was shown that NH_3 was produced in a 1:1 ratio with NH_2OH loss when HCP was incubated with NH_2OH. Therefore, it was proposed that HCP catalyzes the reduction of NH_2OH to NH_3 and H_2O. Upon addition of NH_2OH to the fully reduced HCP, an increase in the absorbance at 420 nm was observed, indicating that the FeS clusters in HCP are oxidized. The coupling of hydroxylamine reduction with the oxidation of the Fe clusters present in HCP shows strong evidence that in fact HCP is responsible for hydroxylamine reduction *in vitro*. In addition, HCP reduced NH_2OH analogs CH_3NHOH and hydroxyquinone. The product (NH_3) and product analog (NH_2NH_2) showed only minor effects on the hydroxylamine reductase activity of HCP. Changing the pH of the assay solution had a dramatic effect on the V_{max} of the enzyme. The highest recorded activity occurred at pH 9.0, with the V_{max} at this pH reaching 458 ± 19 μmol of NH_2OH reduced min^{-1} mg of $protein^{-1}$ (Wolfe et al., 2002). These data suggest that pH affects the reaction mechanism of the enzyme due to ionization of key residues.

Though the above study provides some evidence that HCP may function as a hydroxylamine reductase *in vitro*, other functions of HCP cannot be completely ruled out (Wolfe et al., 2002). It is possible to imagine the role of this enzyme as a scavenger of potentially toxic by-products of nitrate metabolism. If at some point in the metabolism of nitrate and nitrite small amounts of NH_2OH are produced, it would be necessary to have present an enzyme that could quickly metabolize this compound before it could act on the cell. Therefore it is feasible that HCP could provide this detoxification, which would be necessary for organisms to carry out nitrate metabolism safely (Wolfe et al., 2002).

1.6.4. *Clostridium perfringens* HCP and oxidative stress

The *hcp* gene of *Clostridium perfringens* has been shown to be involved in the oxidative response (Briolat and Reysset, 2002). *Clostridium perfringens* is a ubiquitous Gram-positive pathogen that is present in the air, soil, animals, and humans. It is suggested that *C. perfringens* possesses a complex oxidative stress response that provides protection against the adverse effects of the reactive oxygen species encountered both *in vivo* and *in vitro*. *C. perfringens* encodes a classical Mn superoxide dismutase, but no catalases have been found in this bacterium (Poyart et al., 1995). In contrast, components of the alternative oxidative stress protection system recently described in the sulphate-reducing bacterium *Desulfovibrio vulgaris* (Lumppio et al., 2001) have been identified in one strain of *C. perfringens* (Lehmann et al., 1996). This system consists of two non-haem proteins, rubrerythrin (Rbr) and rubredoxine oxidoreductase (Rbo). Rbo has superoxide reductase activity that catalyzes the reduction of O_2 to H_2O_2 without dismutation. Rbr is the terminal component of NADH peroxidase that catalyzes the reduction of hydrogen peroxide to water. Nonetheless, the ability of *C. perfringens* to survive when it is faced with a wide variety of natural and accidental oxidative stresses suggests that many genes are involved in this adaptive response.

Tn*916* mutagenesis was used to isolate *C. perfringens* mutants including the *hcp* mutant with altered oxidative stress response (Briolat and Reysset, 2002). The clones were screened, and Tet^r mutants with higher or lower sensitivities to air, a superoxide-generating compound plumbagin, or to hydrogen peroxide and to peroxyl radical-generating compounds (H_2O_2, ethanol) were identified. To confirm that the prismane protein was implicated in the oxidative stress response, the prismane-encoding gene was disrupted by an erythromycin resistance cassette (Prismane::*ermc'*). The sensitivities to H_2O_2 and plumbagin of the mutant strain were

compared to those of the same strain harboring the wild-type prismane gene cloned on an expression vector. In anaerobic conditions, the knockout mutant was more resistant to H_2O_2 than the complemented strain. In contrast, both strains were very sensitive to plumbagin, suggesting that the overproduction of the protein was toxic to the cells in the presence of oxygen. The result with H_2O_2 implies that the hybrid cluster protein is somehow negatively related to oxidative stress.

1.6.5. Induction of HCP expression by NO and its role in *Salmonella* virulence

Promoter-GFP (green fluorescent protein) libraries of *Salmonella enterica* were screened with acidified nitrite as an inducer (Kim et al., 2003). Acidified nitrite is used as an *in vitro* model to mimic reactive nitrogen intermediates (RNI) (Feelish and Stamler, 1996). Two acidified-nitrite-inducible promoters were identified (Kim et al., 2003). One of these was located upstream of a locus, which corresponds to *E. coli hcp-hcr* (*nipAB*, nitrite-activated promoter, according to authors' nomenclature).

Nitric oxide (NO) exhibits multiple modes of antimicrobial activity. NO possesses a free electron that is reactive with many other intracellular molecules, which can result in the generation of even more destructive RNI such as peroxynitrite (MacMicking et al., 1997). In addition, RNI can cause damage to DNA by a variety of chemical mechanisms and are thereby mutagenic (Christen et al., 1996). Moreover, NO also possesses signalling roles for host processes such as the inflammatory response and cytokine regulation (Nathan and Shiloh, 2000).

The *nipAB::GFP* expression was 9 times higher when the promoters were induced with 1 mM acidified nitrite. It was also shown that nitrite-induced activation of the *nipAB.:lacZ* promoter exhibits pH dependence. The *nipAB* fusion displayed the maximal induction near pH

6.5. When using acidified nitrite for the generation of RNI, NO production would be expected under more acidic conditions. The observation that maximal induction occurred at pH 6.5 implies that the substrate may be different to nitrogen oxide (Kim et al., 2003). The authors suggest that hydroxylamine could be one of the candidates taking into account the recent report that HCP displays hydroxylamine reductase activity (Wolfe et al., 2002).

The *nipAB* promoter was also upregulated in activated RAW264.7 macrophage-like cells, which produce NO via the inducible nitric oxide synthase (iNOS). The induction was inhibited by aminoguanidine, an inhibitor of iNOS. It was concluded that these genes are regulated by physiological nitrogen oxides (Kim et al., 2003).

Small inoculating doses (10^3 to 10^6 CFU) of the *hcp-hcr* mutant showed unexpectedly increased ability to cause lethal infection 2 to 3 weeks after challenge, compared to a similar challenge dose of the wild-type bacteria. Perhaps the mutant cells fail to metabolise NO to the same degree as the wild type, leading to an excessive concentration of NO and subsequent host damage and/or immunosuppression. The absence of these bacterial genes in some way diminishes the ability of mice to clear a low dose infection (Kim et al., 2003).

1.6.6. *Shewanella oneidensis* HCP expression under nitrate reducing conditions

Recently changes in mRNA and protein expression profiles of *Shewanella oneidensis* MR-1 during a switch from aerobic to nitrate-reducing conditions were examined using DNA microarrays and two-dimensional polyacrylamide gel electrophoresis (2-D PAGE) (Beliaev et al., 2002). It was shown that transcription of genes encoding a periplasmic nitrate reductase (*napBHGA*), cytochrome c_{552}, and HCP was elevated 8- to 56-fold in response to the presence of

nitrate. Protein identification by mass spectrometry indicated that the expression of prismane protein correlated with the microarray data.

Beliaev et al. (2002) also used the DNA microarrays to examine the transcriptional effects under fumarate and nitrate reducing conditions of an insertional disruption in the chromosomal *etrA* locus. The predicted *S. oneidensis* EtrA (electron transport regulator) protein (Saffarini and Nealson, 1993) shares a high degree of amino acid sequence identity with *E. coli* FNR protein. The gene encoding HCP was induced approximately three-fold in an $EtrA^+$ background under fumarate-reducing conditions. The ratio (R) of mRNA of the parental strain to that of the *etrA* mutant was 2.89±1.62. The expression of HCP under nitrate-reducing conditions exhibited a marginal decrease (R=0.59±0.06).

1.6.7. HCP and hydroxylamine assimilation by *Rhodobacter capsulatus*

DNA sequencing revealed that the nitrate assimilation gene region, *nas*, in *R. capsulatus* includes the *hcp* gene (Cabello et al., 2004). It was suggested that expression of the *hcp* gene is probably regulated by a nitrite-sensitive repressor encoded by the adjacent *nsrR* gene. The 6-histidine-HCP from *R. capsulatus* was overproduced in *E. coli* and purified. It showed hydroxylamine reductase activity (K_m = 1 mM) as previously reported for *E. coli* HCP. This activity was oxygen-sensitive and was inhibited by sulphide and iron reagents (Cabello et al., 2004). It was shown that *R. capsulatus* grew well with 1 mM hydroxylamine as the sole nitrogen source under anaerobic phototrophic conditions, although a long lag-phase was observed. Hydroxylamine uptake was measured, ammonium was transiently accumulated in the medium, and ammonium assimilation was prevented by L-methionine-D, L-sulfoximine, a glutamine synthetase inhibitor (Cabello et al., 2004). However, an *R. capsulatus* strain lacking the whole

hcp-nas region did not grow with 1 mM hydroxylamine. In addition, the hydroxylamine reductase activity detected in the extracts of cells grown on hydroxylamine as a sole nitrogen source was also inhibited by oxygen and by iron and sulphur reagents and it showed the same temperature optima (40 °C) as the purified HCP protein. It was also shown that *E. coli* cells overproducing HCP from *R. capsulatus* tolerate hydroxylamine better during anaerobic growth (Cabello et al., 2004). These findings indicated that the *hcp* gene product could be involved in assimilation of hydroxylamine by *R. capsulatus*.

1.7. Aims of this investigation

Prior to start of this investigation the crystal structure of HCP had been determined, which together with spectroscopic studies showed that it has two FeS clusters as redox active sites (Cooper et al., 2000; Macedo et al., 2002, Aragao et al., 2003). HCP is accumulated under nitrite or nitrate respiring conditions in *E. coli* and the *hcp* promoter of *S. enterica* is induced by acidic nitrite as a source of reactive nitrogen species (van den Berg et al., 2000; Kim et al., 2003). This indicated that HCP is involved in the nitrogen cycle. The finding that the *hcp* mutant in *C. perfringens* has lower sensitivity to peroxide suggested that HCP is linked to oxidative stress (Briolat and Reysset, 2002).

It had been established before that the multi-subunit periplasmic nitrate reductase, Nap, supports nitrate dependent growth of *E. coli* under nitrate-limiting conditions (Potter et al., 1999). It was shown that electron transport from ubiquinol, whose oxidized/reduced couple has higher midpoint redox potential than that of menaquinol, is dependent on NapG and NapH (Brondijk et al., 2002).

The aims of the work presented in this thesis were to study the transcription regulation of the *hcp* gene and to investigate whether HCP is involved in several steps of the nitrogen cycle. Secondly, the aims were to establish whether Nap is involved in redox balancing and to investigate the roles of NapF, NapG and NapH. The objectives were to:

1. construct an *hcp::lacZ* fusion to determine whether transcription from the *hcp* promoter is affected by different electron acceptors, hydroxylamine and nitric oxide, and whether it is regulated by FNR, ArcA, NorR, NarL and NarP;
2. identify whether HCP is involved in nitrate-dependent growth and whether it protects against hydroxylamine and nitric oxide toxicity;
3. develop a qualitative assay to study whether HCP reduces nitrite, nitrate and hydroxylamine *in vitro*;
4. determine whether NapG and NapH are involved in the oxidation of quinols with higher midpoint redox potentials;
5. determine whether the deletion of *napF*, *napG* and *napH* affects activity of the *napF* promoter and nitrate-reductase activity of NapA;
6. identify the impact of Nap on redox balancing in strains able to synthesize only ubiquinone or menaquinone during growth in the presence of glucose and nitrate.

CHAPTER 2

MATERIALS AND METHODS

2.1. Materials

2.1.1. Suppliers

Chemicals, reagents and media were purchased from Difco, Oxoid and Sigma. Restriction endonucleases were obtained from New England Biolabs. Calf intestinal alkaline phosphatase (CIAP) and T4 DNA ligase were supplied by Gibco BRL. Bio-X-Act DNA polymerase and *Taq* polymerase were obtained from Bioline. Enzymes and appropriate buffers were stored at -20 °C. Radioactive isotopes were supplied by Amersham International. QIAquick PCR purification kit, QIAquick gel extraction kit, QIAprep miniprep kit and RNeasy Mini kit for isolation of RNA were obtained from Qiagen. The RACE kit was purchased from Invitrogen. pGEM-T Easy ligation kit was obtained from Promega.

2.1.2. Media

Liquid and solid media were prepared by dissolving the quantities specified below in distilled water, followed by autoclaving at 120 °C and 1 atmosphere for 15 minutes.

LB (Lennox broth) contained 10 g/l tryptone, 5 g/l yeast extract and 5 g/l NaCl. MS (minimal salts) medium was composed of 33 mM KH_2PO_4, 60 mM K_2HPO_4, 7.6 mM $(NH_4)_2SO_4$, 0.5 mM $MgCl_2$, 1 μM ammonium molybdate, 1 μM sodium selenate and 1ml/l of *E. coli* sulphur-free salts. The *E. coli* sulphur-free salts contained 82 g of $MgCl_2 \cdot 7H_2O$, 10 g of $MnCl \cdot 4H_2O$, 4 g of $FeCl_2 \cdot 6H_2O$, 1 g of $CaCl_2 \cdot 6H_2O$ and 20 ml of concentrated HCl per litre of distilled water. SOC medium contained 20 g bacto-tryptone, 5 g yeast extract, 0.58 g NaCl, 0.189 g KCl, 2.03 g $MgCl_2 \cdot 6H_2O$, 2.46 g $MgSO_4 \cdot 7H_2O$ per 980 ml of distilled water. Glucose (20 ml of 20% w/v solution) was added after autoclaving.

Nutrient agar medium (NA) contained 28 g of nutrient agar per l of distilled water. For agar plates, approximately 25 ml of molten agar was poured into Petri dishes and allowed to set. Plates were dried at 60 °C and stored at 4 °C prior to use.

2.1.3. Antibiotics

Stock solution of the sodium salt of ampicillin (100 mg/ml) was prepared in water. The solution was sterilised by filtration and stored at -20 °C. The stock solution was added to the liquid medium to give the final concentration of 100 μg/ml ampicillin (Amp). To prepare the agar plates, the autoclaved medium was cooled to 48 °C before adding the stock solution of ampicillin to the final concentration of 100 μg/ml. Plates containing ampicillin were stored at 4 °C for not longer than 2 weeks before use.

Solid chloramphenicol was dissolved in 100 % ethanol at a concentration of 34 mg/ml. Chloramphenicol is stable for at least a year when prepared in this way. The stock solution was stored at -20 °C. The stock solution was added to the liquid medium to give the final concentration of 10 μg/ml chloramphenicol (Cm). To prepare the agar plates, the autoclaved medium was cooled as described for Amp and the stock solution of Cm was added to the final concentration of 10 μg/ml. The plates were stored at 4 °C and used within 1 to 5 days.

2.1.4. Buffers and solutions

All buffers and solutions used are described in **table 2.1.**

2.1.5. Preparation of nitric oxide saturated water (NOSW)

Sterile water (5 ml) was placed in a tube, which was then closed with a rubber stopper. Two needles were inserted into the rubber stopper, one of which was connected to the nitrogen

Table 2.1. Buffers and solutions used in this work

Name	Composition
(a) General buffers	
Tris-EDTA (TE) buffer (pH 8.0)	10 mM Tris-HCl and 1 mM EDTA (diaminoethanetetra-acetic acid).
Phosphate buffer (50 mM, pH 7.5)	7.26 g of K_2HPO_4 and 1.13 g of KH_2PO_4 per litre.
(b) Buffers for agarose gel electrophoresis	
Stock 5xTBE buffer	0.445 M Tris-HCl (pH 8.0), 0.445 M boric acid and 0.01 M EDTA (pH 8.0).
0.8% agarose solution	0.8 g of agarose in 100 ml 1xTBE buffer.
Sample buffer	0.025% (w/v) bromophenol blue, 10% (v/v) glycerol in 10 mM Tris-HCl (pH 7.5) and 1 mM EDTA.
(c) Buffers for sequencing	
BigDye reaction mix	Included in a ready format the dye terminators, deoxynucleoside triphosphates, AmpliTaq DNA polymerase, $MgCl_2$ and Tris-HCl buffer, pH 9.0.
Dye terminators	A-BigDye terminator v3.0, C-BigDye terminator v3.0, G-BigDye terminator v3.0 and T-BigDye terminator v3.0.
Deoxynucleoside triphosphates	dATP, dCTP, dITP and dUTP. This mix included dITP in place of dGTP and dUTP in place of dTTP.
Big Dye (terminator) ready reaction mix	2 µl of BigDye reaction mix (as above) and 6 µl of dilution buffer.
250 mM EDTA	Was used to dilute DNA in sequencing purification step.

(d) Solutions for RNA isolation	
0.1% DEPC (diethyl pyrocarbonate)	Water and solutions were treated with 0.1% DEPC, 1 ml of which was added to 1 l of water or solution to be treated and shaken vigorously to dissolve the DEPC. The solution was incubated for 12 to 16 hours at 37 °C and autoclaved for 15 minutes at 121 °C to remove any trace of DEPC.
TE (resuspension buffer) with lysozyme	Lysozyme was diluted in TE to a final concentration of 400 µg/ml.
RLT (denaturing buffer) with β-mercaptoethanol	Immediately before use 10 µl of β-mercaptoethanol were added to 1ml of RLT.
RPE (washing buffer)	RPE buffer was supplied as a concentrate. Before using it for the first time, 4 volumes of ethanol were added to obtain a working solution.
(e) Buffers for transcription start mapping by 5' RACE system (provided with a kit)	
Wash buffer	Was prepared by adding 49 ml 70 % ethanol to 1 ml of wash concentrate.
10x reverse transcription buffer	25 mM $MgCl_2$ and 0.1 M DTT.
5x tailing buffer	50 mM Tris-HCl (pH 8.4), 125 mM KCl and 7.5 mM $MgCl_2$.
(f) Buffers for French press and purification of proteins on Ni-NTA column	
Formate buffer	5 mM formate and 50 mM phosphate, pH 7.5
Tris-HCl buffer	50 mM Tris-HCl, pH 8.0, 250 mM NaCl and 5% glycerol.
(g) Buffers for Folin protein assay	

Folin A solution	2% Na_2CO_3 in 0.1 M NaOH.
Folin B solution	1 ml 1% $CuSO_4$ and 1 ml 2% Na Tartrate in 100 ml of A solution.
Folin Reagent	Contained Folin/Ciocalteu's Phenol Reagent and H_2O in ratio 10:7.
(h) Buffers and solutions for SDS polyacrylamide gel electrophoresis (SDS-PAGE) of proteins	
Ultrapure Protogel ™	30% (w/v) acrylamide and 0.8% NN' methylenbisacrylamide) used for both the stacking and the resolving gel.
Stock resolving gel buffer	Contained 0.75 M Tris-HCl pH 8.3. Tris (18.17 g) was dissolved in 100 ml of deionised water and the pH adjusted to 8.3 using HCl. The solution was stored at 4 °C.
Stock stacking gel buffer	1.25 M Tris-HCl pH 6.8. Tris (30.29 g) was dissolved in 100 ml of deionised water, and the pH adjusted to 6.8 using HCl. The volume of 200 ml was prepared and stored as described above for the stock resolving gel buffer.
10x electrode buffer (stock solution)	150 g glycine was dissolved in 800 ml distilled water. Tris (15g) was added, the volume was made to 1 l using deionised water and the solution was stored at room temperature.
Electrode buffer (working solution)	5 ml of 20% SDS (w/v) were added to 100 ml 10x electrode buffer and diluted with 895 ml of distilled water.
Ammonium persulphate solution (APS)	Was prepared at 8% (w/v), aliquoted and stored at -20 °C until required.
Sample buffer	Was prepared by dissolving 5 g of bromophenol blue, 2 g of SDS and 20 ml of glycerol in 0.1x stock stacking gel buffer to a final volume of 92 ml. This

	was then dispensed into 1 ml aliquots and stored at room temperature. Immediately prior to use, 87 µl of β-mercaptoethanol were added to each aliquot.
(i) Buffers for Coomassie brilliant blue staining of SDS-PAGE gels	
Stain solution	0.2% (w/v) Coomassie brilliant blue, 50% (v/v) methanol and 10% (v/v) glacial acetic acid. The solution was filtered to remove undissolved solid and stored at room temperature.
Destain solution	40% (v/v) methanol and 10% (v/v) acetic acid.
Shrink solution	48% (v/v) methanol and 20% (v/v) glycerol.
(j) Buffers for Western blotting	
Blotting buffer	14.4 g of glycine, 3.0 g of Tris, 200 ml of MeOH in total volume of 1l.
PBS buffer (pH 7.4)	8.0 g NaCl, 0.2 g KH_2PO_4, 1.32 g Na_2HPO_4, 0.2 g KCl and 0.2 g NaN_3 in 1 l of solution.
10 mM Tris-HCl buffer, pH 7.5	Was used for washing step.
(k) Acrylamide gel buffers for separation of DNA fragments	
Acrylamide gel buffer for separation of DNA fragments after digest	7.5% acrylamide, 15% glycerol and 1x TBE. This buffer was prepared by adding 125 ml of 30% acrylamide, 75 ml of glycerol and 100 ml of 5x TBE to the total volume of 500 ml.
Acrylamide gel buffer for band-shift assays	6% acrylamide, 2% glycerol and 0.25x TBE. This buffer was prepared by adding 60 ml of 30% acrylamide, 6 ml of glycerol and 15 ml of 5x TBE to the total volume of 300 ml.
(l) Buffers for band shifts	

Buffer for dilution of purified FNR protein	20 mM Hepes, pH 8.0, 5 mM $MgCl_2$, 50 mM potassium glutamate, 2 mM DTT and 1mg/ml BSA.
Buffer for dilution of purified NarL protein	20mM potassium Epps (N [2-hydroxyethyl] piperazine-N'-3-propanesulfonic acid) pH 8.0, 125 mM potassium glutamate, 1.5 mM DTT and 5% glycerol.
10x buffer for band-shifts	200 mM Hepes pH 8.0, 50 mM $MgCl_2$, 500 mM potassium glutamate and 10 mM DTT.
Running buffer for the DNA gel	0.25x TBE.
Herring sperm DNA	Was diluted to a concentration of 500 μg ml^{-1} and was stored at -20 °C.
(m) Buffers for methyl viologen assay	
Sodium dithionite buffer	9.6 g/l sodium dithionite in 0.1 M sodium bicarbonate and 0.5 M $NaNO_3$.
Buffer D	Equal volumes of sodium dithionite buffer and 0.2 mM methyl viologen.
(n) Buffers from QIAprep miniprep spin kit	Use
P1	Resuspension buffer.
P2	Lysis buffer.
N3	Precipitation buffer.
PB and PE	Wash buffers.
EB	Elution buffer (10 mM Tris-HCl, pH 8.5).
(o) Buffers from Qiaquick PCR purification kit and Qiaquick gel extraction kit	
PB	Binding buffer.
QG	Solubilization and binding buffer.
PE	Washing buffer.
EB	Elution buffer (10 mM Tris-HCl, pH 8.5).

cylinder. The water was bubbled with gaseous nitrogen for 5 minutes. The same needle was connected to the nitric oxide cylinder and the water was saturated with nitric oxide for 10 minutes. The second needle was taken out, the tubing connecting to the nitric oxide cylinder was closed and the tube with water was inverted so that NOSW was kept under the atmosphere of nitric oxide. If prepared in this way, the concentration of NO in NOSW is 20 mM. When needed, the required amount of NOSW was taken and added to the cell culture.

2.2. Bacterial and chemical methods

2.2.1. Strains

Strains used during this study were derivatives of *E. coli* K-12 and are listed in **table 2.2**. They were purified by streaking to single colonies onto agar plates containing appropriate antibiotics (ampicillin or chloramphenicol). Plates were incubated at 37 °C unless stated otherwise and stored at 4 °C. Liquid cultures were prepared by inoculating sterile medium with a single colony from an agar plate and grown at 37 °C unless stated otherwise. Agar plates were kept for several weeks at 4 °C for short term storage of bacteria. For longer term storage, 0.625 ml of an overnight liquid culture was mixed with 0.375 ml of a sterile solution of 40% (v/v) glycerol and stored at -80 °C.

2.2.2. Growth of strains

For growth curve experiments *E. coli* strains were grown anaerobically in MS medium supplemented with 2.5 g/l nutrient broth, 20 mM $NaNO_3$ and 0.4% (w/v) glucose. Glycerol (0.4% v/v) was used instead of glucose for growth of HCP mutant strains. Cultures were grown at 37 °C and the optical density at 650 nm was monitored throughout the growth cycle.

Table 2.2. Bacterial strains used in this work

Bacterial strains	Relevant genotype	Reference
RK4353	*ΔlacU169 araD139 rpsL gyrA*	Stewart and McGregor, 1982
RV	*F'Lac*$^-$ prototroph	Page et al., 1990
JCB4041	RK4353 *ΔnarZ::Ω ΔnarG-I ΔnarL::Tn10*	Brondijk et al., 2002
JCB4081a	JCB4041 *ΔnrfAB ΔnirBDC::km*	Brondijk et al., 2004
JCB4083a	JCB4041 *ΔnapGH ΔnrfAB ΔnirBDC::km*	Brondijk et al., 2004
JCB4042	JCB4041 *ΔnapF*	Brondijk et al., 2002
JCB4043	JCB4041 *ΔnapGH*	Brondijk et al., 2002
JCB4044	JCB4041 *ΔnapFGH*	Brondijk et al., 2002
JCB4045	JCB4041 *ΔnapC*	Brondijk et al., 2002
JCB4141	RK4353 *ΔnarZ::Ω ΔnarG-I narL::Tn10 ΔmenBC*	Brondijk et al., 2002
JCB4142	JCB4141 *ΔnapF*	Brondijk et al., 2002
JCB4143	JCB4141 *ΔnapGH*	Brondijk et al., 2002
JCB4144	JCB4141 *ΔnapFGH*	Brondijk et al., 2002
JCB4145	JCB4141 *ΔnapC*	Brondijk et al., 2002
JCB4241	RK4353 *ΔnarZ::Ω ΔnarG-I narL::Tn10 ΔubiAB*	Brondijk et al., 2002
JCB4242	JCB4241 *ΔnapF*	Brondijk et al., 2002
JCB4243	JCB4241 *ΔnapGH*	Brondijk et al., 2002
JCB4244	JCB4241 *ΔnapFGH*	Brondijk et al., 2002
JCB4245	JCB4241 *ΔnapC*	Brondijk et al., 2002
JCB4999	RK4353 *hcp::cat*	This work
JCB5000	RK4353 *Δhcp*	This work

JCB4340	JCB4041 *hcp::cat*	This work
JCB4341	JCB4041 *Δhcp*	This work
JCB4011	RK4353 *ΔnarZ::Ω,ΔnapA-B*	Potter et al., 1999
JCB4310	JCB4011 *hcp::cat*	This work
JCB4311	JCB4011 *Δhcp*	This work
JCB4141	JCB4041 *ΔMenBC*	Brondijk et al., 2002
JCB4441	JCB4141 *Δhcp*	This work
JCB387	*Δnir Δlac*	Page et al., 1990
JCB38705	JCB387 *arcA::cat*	This work
JCB3871	JCB387 *Δfnr*	Page et al., 1990
JCB38715	JCB3871 *arcA::cat*	This work
JCB302	*Δ(nirB-cysG) chl*$^{+}$ *RV*	Page et al., 1990
JCB3875	JCB387 *narP253::Tn10*	Page et al., 1990
JCB3893	JCB302 *narXnarL*	Constructed by L. Griffiths for this project
JCB3894	JCB302 *narXnarLnarQnarP*	Constructed by L. Griffiths for this project
JCB4401	RK4353 *norR::cat*	Constructed by M. Campos for this project
JM109	*recA ΔlacZ*	Promega
JW0857	*recA1 endA1 gyrA96*	Kitagawa et al., in preparation.

For large-scale growth strains were grown anaerobically in 1 l or 2 l cultures in MS medium supplemented with 2.5 g/l nutrient broth and 0.4% (w/v) glucose. $NaNO_3$ (20 mM) was added if required.

Unless otherwise specified, for measurements of β-galactosidase activity an overnight culture was grown in 2 ml of LB at 37 °C and was used to inoculate the required selective medium. Strains were grown aerobically in LB medium. For 5 ml aerobic cultures, 50 µl of overnight culture were taken. The cultures were grown until the OD_{650} was 0.15 to 0.3. Strains were grown anaerobically in MS medium supplemented with 0.4% glycerol, 20 mM fumaric acid, 20% LB (2 g/l tryptone, 1 g/l yeast extract, 1 g/l NaCl), 100 µg/ml ampicillin, with or without 2.5 mM $NaNO_2$ or 20 mM $NaNO_3$. For10 ml anaerobic cultures 0.4 ml of overnight culture were used. The cultures were grown until the OD_{650} was 0.5 to 0.8. For measurements of β-galactosidase activity during the growth cycle, strains were grown anaerobically in MS medium supplemented with 0.4% glucose, 10% LB (1 g/l tryptone, 0.5 g/l yeast extract, 0.5 g/l NaCl), 100 µg/ml ampicillin, with or without 2.5 mM $NaNO_2$ or 20 mM $NaNO_3$.

2.2.3. Preparation of cell-free extracts

Preparation of cytoplasmic proteins by French pressure cell

Cultures were grown anaerobically on a large scale as described previously. Bacteria were harvested by centrifugation at 5 000 g for 15 minutes. The pellet was resuspended in 40 ml of formate buffer and pelleted by centrifugation at 5 000 g for 20 minutes. The supernatant was discarded and the pellet resuspended in 5 ml of formate buffer using a glass homogeniser and passed through a French pressure cell at 10 000 psi. Each bacterial sample was passed through the French press 2 to 3 times, and during the procedure the bacteria were kept on ice. The resultant suspension, consisting of unbroken cells, periplasm, membrane,

cytoplasm and inclusion bodies was centrifuged at 40 000 g for 30 minutes to separate soluble cytoplasmic proteins and inclusion bodies. The supernatant contained cytoplasmic proteins and was used for further analysis.

Sonication procedure

For sonication, the cell culture was grown on a large scale. The optical density of the cells was taken, the cells were centrifuged at 5 000 g for 15 minutes and the pellet was resuspended in 10 mM phosphate buffer, 150 mM NaCl, pH 6.5 to an OD_{650} of 125. Before sonication, the probe was cooled down on ice and rinsed with ethanol. The probe was inserted into the tube with cells and the pulse of 1 minute 20 seconds was applied to the cell culture. The procedure was repeated twice. The OD_{650} of the cell culture was checked after sonication. If the cell walls had been broken, the optical density at 650 nm decreased.

2.2.4. β-galactosidase assay

For β-galactosidase assays the method described by Jayaraman et al. (1987) was used. The culture (2 ml) was lysed with 30 µl each of 1% Na^+-deoxycholate and toluene. After aeration at 37 °C for 20 minutes the cultures were placed on ice. The lysate (0.1 ml of undiluted or of 10-fold diluted depending on the expected activity) was added to 2 ml of assay buffer, and pre-warmed at 30 °C. The reaction was started by the addition of 0.5 ml of pre-warmed 13 mM ONPG. $NaCO_3$ (1 M, 1 ml) was added to stop the reaction when a sufficiently yellow colour had developed. The OD_{420} was measured and the β-galactosidase activity was calculated from the formula:

$A = OD_{420} \cdot 1000 \cdot D \cdot C \cdot V / (OD_{650} \cdot t \cdot \varepsilon \cdot L)$

Key:

OD_{420}: optical density of cell lysate at 420 nm;

D: dilution factor;

C: coefficient used to convert OD_{650} to mg dry weight (C=2.5);

V: volume of the assay mixture in ml (V=3.5);

OD_{650}: optical density at 650 nm of cell culture before lysis;

t: the incubation time in minutes;

ε: the molar extinction of o-nitrophenol (ε=4.5) (L $mmol^{-1}$ cm^{-1})

L: the volume of lysate that was used in ml.

Cultures were assayed in duplicate and reported values are averages from at least two independent experiments.

2.2.5. Determination of nitrate reductase activities using the artificial electron donor, methyl viologen

Methyl viologen is an electron donor that in the presence of nitrate donates electrons directly to the catalytic subunit of nitrate reductases. Reduced methyl viologen is blue and becomes colourless upon oxidation (Jones and Garland, 1977). A simple assay has been developed in which methyl viologen is used as an artificial electron donor for the reduction of nitrate to nitrite (Showe and DeMoss, 1968). The presence of nitrite in the assay mixture is then determined colorimetrically and from this, the rate of nitrate reduction can be estimated.

Bacteria were grown as described previously until the desired OD_{650} had been reached. At this point, the cultures were placed on ice until required. At the start of the experiment, the bacteria were centrifuged for 2 minutes at 8 000 g at room temperature and the pellet resuspended in 50 mM potassium phosphate buffer (pH 7.4) to an OD_{650} of about 1.0. A sample of the bacterial suspension was diluted if required to 200 µl with 50 mM phosphate buffer in a small test tube. Each culture was assayed in duplicate. Following addition of 50 µl of 2 mM methyl viologen, the tubes were incubated at 30 °C in a water

bath. A freshly made solution of sodium dithionite buffer was prepared, which consisted of 0.5 M sodium nitrate and 0.1 M sodium bicarbonate, de-aerated with nitrogen gas whilst 9.6 $g \cdot l^{-1}$ of sodium dithionite dissolved. After 5 minutes the assay was started by the addition of 50 µl sodium dithionite buffer. During this time methyl viologen passed electrons through NapA to nitrate. The test tubes were gently inverted to mix the contents, without aerating them, to give a uniform blue colour. After a 5-minute incubation, the reaction was stopped by vigorous aeration. Cell debris was sedimented by centrifugation at 8 000 g for 3 minutes, and the concentration of nitrite in 50 µl samples of the supernatant was determined.

2.2.6. Determination of hybrid cluster protein activity using the modified methyl viologen assay

Sodium bicarbonate (0.2 M, 10 ml) was added to10 ml of 1 M $NaNO_3$, 1 M $NaNO_2$ or 1 M NH_2OH individually, or in mixtures containing two or all three elements and de-aerated by bubbling with nitrogen gas. To prepare sodium dithionite buffer, sodium dithionite was added to the above solution to the final concentration 9.6 $g \cdot l^{-1}$. Equal volumes (5 ml each) of sodium dithionite buffer and 0.2 mM methyl viologen were mixed, and aliquots of this solution (buffer D) were added to different volumes of either a cytoplasmic protein fraction containing overexpressed HCP, or to purified HCP. Two negative controls were buffer D left at room temperature and buffer D with added formate buffer instead of HCP fraction. The time required for the methyl viologen to be oxidised was determined.

2.2.7. Determination of quinol-nitrate oxido-reductase activities *in vitro*

A pre-culture of the appropriate *E. coli* strain was diluted 20-fold into LB supplemented with 20 mM Na^+ nitrate and 0.4% glucose and grown anaerobically at 37 °C for 3 to 3.5 hours. Cells were harvested and washed with 50 mM K^+ phosphate, pH 7.0. Bacteria were

resuspended in K^+ phosphate buffer to an OD_{650} of ≈ 40 and stored on ice. When required, the bacterial suspension was diluted to an OD_{650} of 2.0 in N_2-saturated K^+ phosphate buffer and incubated at room temperature. Quinones were dissolved to 50 mM in methanol and reduced by diluting 2-fold with 0.5% $NaBH_4$ in 50% (v/v) methanol. After 5 minutes incubation the residual $NaBH_4$ was degraded by the addition of 0.1 volume of 0.1 M HCl. The reaction was started by the addition of 2.5 mM $NaNO_3$ and 1 mM reduced quinol to the cell suspension. Samples were removed at intervals, and the quantity of nitrite produced was determined (Pope and Cole, 1984).

2.3. Recombinant DNA techniques

2.3.1. Separation of DNA samples by agarose gel electrophoresis

Stock 5xTBE buffer was diluted 5-fold to give a working solution that was used for agarose gel electrophoresis. The agarose was dissolved in 1xTBE by boiling in a microwave oven and poured into a gel plate. When set, the gel was transferred to the gel apparatus and covered with 1xTBE buffer. DNA samples were mixed in a 1:4 ratio with sample buffer and separated by electrophoresis through an agarose gel at 3 V/cm of gel. After electrophoresis the gels were stained in a solution of 0.1 μg/ml ethidium bromide (EtBr) for 15 minutes. Ethidium bromide intercalates between stacked bases of DNA molecules and this allows DNA to be visualised by irradiation with ultraviolet light using a transilluminator.

2.3.2. Small-scale isolation of plasmid DNA ('mini-prep')

Plasmids used in this work are described in **table 2.3** and **figures 2.1** to **2.4**. The QIAprep Mini-prep Spin Kit was used to purify small amounts of plasmid DNA. The procedure is based on alkaline lysis of bacteria followed by absorption of DNA onto a silica membrane in the presence of high salt. This protocol s designed for the purification of up to 20 μg of

Table 2.3. Plasmids used in this work

Plasmid	Description	Reference/Source
pAA182	11.2 kb Amp^R promoter probe vector with ColE1 origin of replication. Carries the *lac* operon without the *lac* promoter (figure 2.1).	Jayaraman et al., 1987
pNF383	The *hcp* regulatory region (383 bp) cloned into pAA182 to create the *hcp:lacZ* fusion (figure 2.2).	This work
pKD3	Amp^R and Cm^R marker used as a PCR template to create a replacement of a gene of interest with a *cat* cassette	Datsenko and Wanner, 2000
pKD46	Amp^R marker with ts-origin of replication (active at 30°C). Expresses λ *red* β, γ and *exo* genes (the products of which enable homologous recombination) under control of the *paraB* promoter.	Datsenko and Wanner, 2000
PCP20	Amp^R and Cm^R marker, which has a ts-origin of replication. Expresses the FLP recombinase gene under the control of heat-sensitive promoter.	Datsenko and Wanner, 2000
pGEM T-Easy	Has β-galactosidase coding sequence interrupted by a polylinker with an oligo-dT tail at the each end. The vector can be used for cloning of PCR products and blue/white screening of recombinants (figure 2.3).	Promega
pCA24n1	5.2 kb vector, encodes Cm resistance and the HCP protein under the control of *t5-lac* promoter. GFP (green fluorescent protein) is cloned in frame with HCP from C-terminal end. *t5-lac* promoter can be activated by IPTG (figure 2.4).	Kitagawa et al., in preparation.
pCA24n2	Derivative of pCA24n1. Lacks GFP coding sequence.	Kitagawa et al., in preparation.

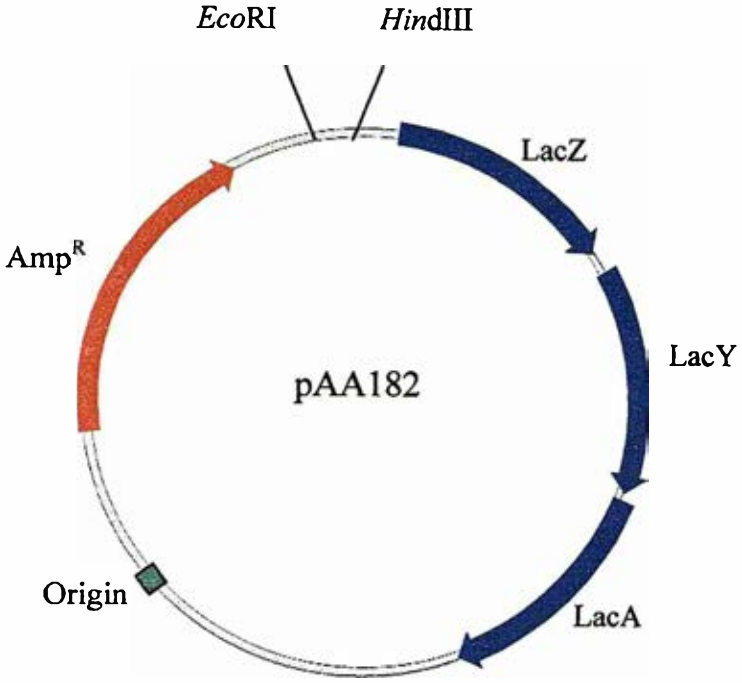

Figure 2.1. Restriction map of the plasmid pAA182. The plasmid pAA182 is a 11.2 kb Amp^r promoter probe vector with ColE1 origin of replication. It carries the *lac* operon (*lacZ*, *lacY* and *lacA* genes) without the *lac* promoter. If an active promoter is placed before the *lac* operon, β-galactosidase encoded by the *lacZ* is expressed. The β-galactosidase is a reporter protein and its activity is indicative of the activity of the tested promoter.

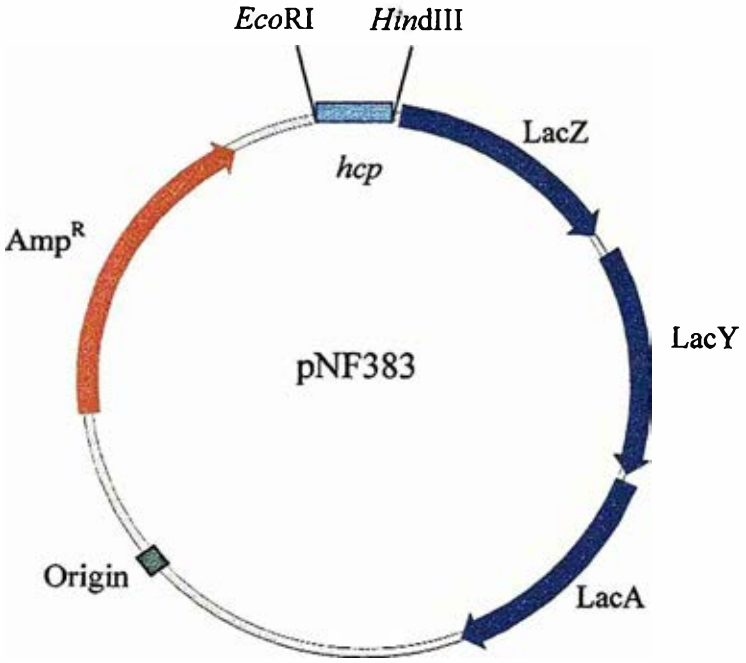

Figure 2.2. Restriction map of the plasmid pNF383. The plasmid pNF383 contains 383 bp of regulatory region of the *hcp* gene, which encodes the hybrid cluster protein. The plasmid pNF383 is a derivative of pAA182 and carries the *lacZ* gene under the control of the *hcp* regulatory region. Plasmid pNF383 was used under different growth conditions and in different gene backgrounds to check for β-galactosidase activity, which is indicative of the activity of the *hcp* promoter.

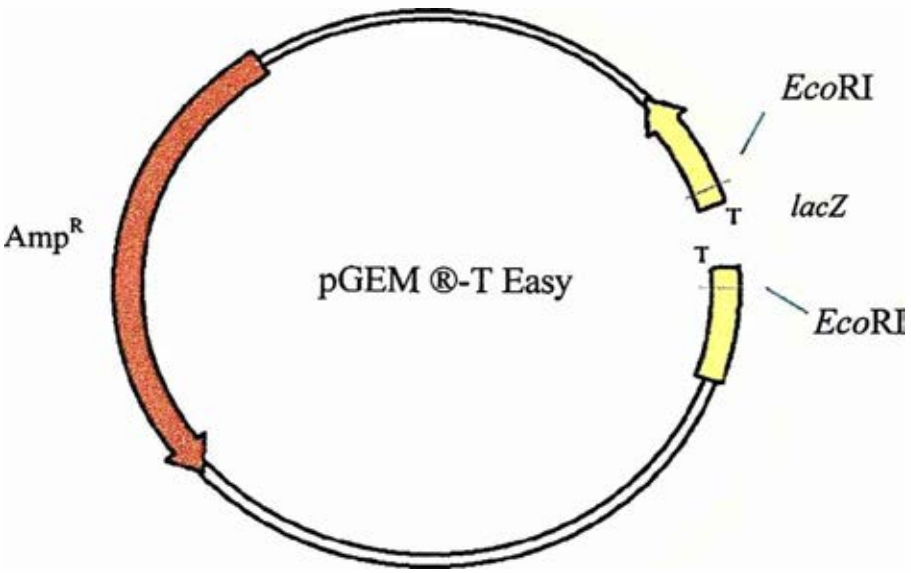

Figure 2.3. Restriction map of the plasmid pGEM ®-T Easy. The plasmid pGEM ®-T Easy was used for cloning of PCR products and blue/white screening of recombinants. It is a 3 015 bp Amp^r vector and is supplied in a linearized form. It carries β-galactosidase coding sequence interrupted by a polylinker with an oligo-dT tail at the each end. The insert must have an oligo-dA tail at the 3´ end of each single strand to complement oligo-dT. If the fragment is ligated to the plasmid, the coding sequence of the β-galactosidase becomes interrupted and the colour formation is stopped as a result. Most of the colonies, which contain the insert, appear white on IPTG/X-Gal plates.

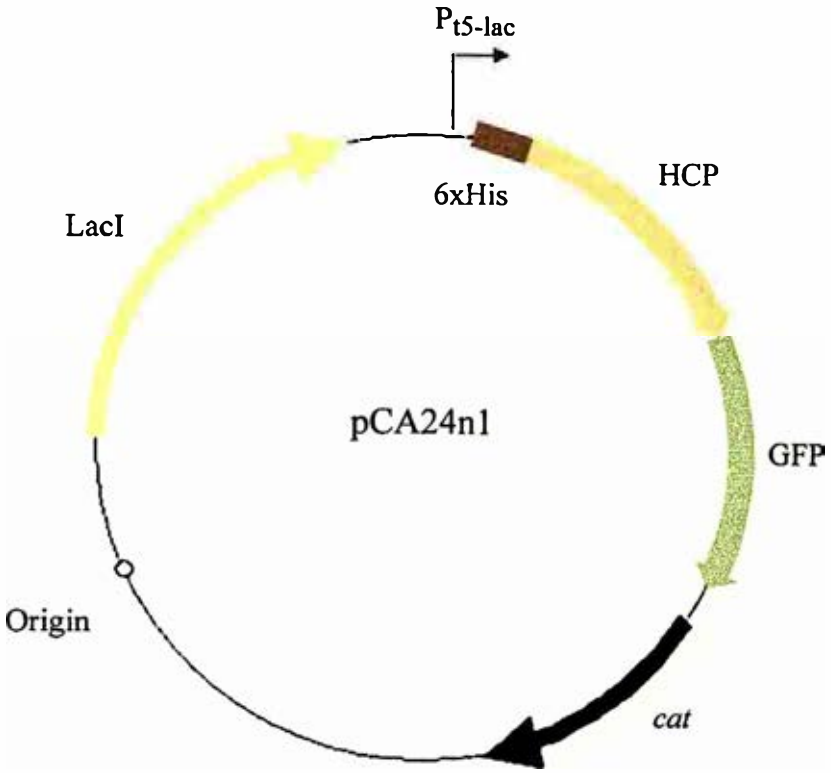

Figure 2.4. Restriction map of the plasmid pCA24n1. PCA24n1 is a 5.2 kb vector that encodes Cm resistance and the HCP protein under the control of *t5-lac* promoter. GFP (green fluorescent protein) is cloned in frame with HCP from C-terminal end. *t5-lac* promoter can be activated by IPTG, but normally is repressed by LacI placed in *cis*. The HCP protein has a tag of 6 consecutive histidine residues (6xHis tag) at its N-terminal end. 6xHis is separated from HCP by seven spacer amino acids. IPTG (isopropyl-beta-D-thiogalactoside) was used at 0.1 mM to induce expression of the cloned *hcp* gene.

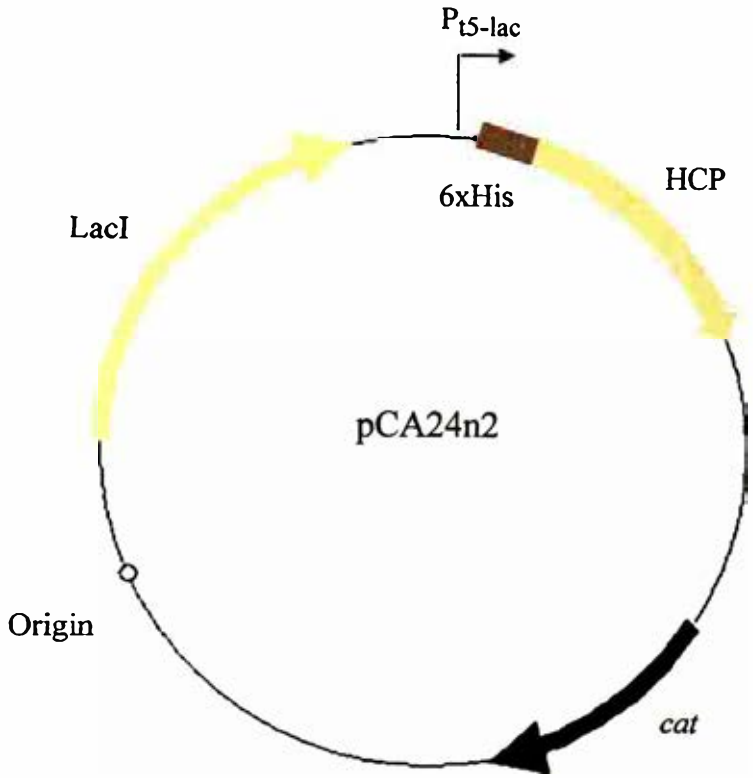

Figure 2.5. Restriction map of the plasmid pCA24n2. Plasmid pCA24n2 is a 4.8 kb derivative of pCA24n1 that lacks GFP coding sequence. Encodes Cm resistance and the HCP protein with 6xHis tag under the control of the *t5-lac* promoter.

high-copy plasmid DNA from 1 to 5 ml overnight cultures of *E. coli* in LB.

A single bacterial colony picked from a freshly retransformed culture was used to inoculate 5 ml of LB containing appropriate antibiotics. The culture was incubated aerobically overnight at 37 °C with shaking. The culture (1.5 ml) was transferred to a microcentrifuge tube and harvested by centrifugation at 15 000 g for 1 minute. The cell pellet was resuspended thoroughly in 250 µl of buffer P1 containing 1 mg/ml RNase A. To lyse the cells, the cell suspension was gently mixed with 250 µl of buffer P2 and incubated at room temperature for 5 minutes. Cell walls, proteins and chromosomal DNA were precipitated by addition of 350 µl buffer N3 containing a high concentration of salt and detergent. After centrifugation at full speed for 10 minutes, a white pellet formed and the supernatant was applied onto a QIAprep column. To absorb DNA onto the silica membrane, the column was centrifuged at 8 000 g for 1 minute. The flow-through was discarded and the column was washed with0.5 ml of buffer PB and centrifuged for 1 minute. The flow-through was discarded and the column was washed with 0.75 ml of buffer PE followed by centrifugation for 1 minute. The column was centrifuged for another minute to dry the membrane and then transferred to a fresh microcentrifuge tube. Buffer EB (50 µl) was then added to the centre of the membrane, the column was left to stand at room temperature for 1 minute, and the plasmid DNA was eluted by centrifugation for 1 minute.

2.3.3. Restriction of DNA fragments

The following components were added to restriction digests: 2 µl of 10x restriction buffer, 1 to 5 units of the restriction endonuclease (see below), 2 to 5 µl of plasmid DNA and water to the final volume of 20 µl. A unit of a restriction endonuclease is defined as an amount of the

enzyme, which cuts 1 μg of λ phage DNA in 1 hour. The required weight X (in μg) of the plasmid DNA was calculated in the following way:

$X = 1 \cdot B_1 \cdot A_2 / (A_1 \cdot B_2)$

Where A_1 is the molecular weight of λ phage in kb (= 50);

A_2 is the molecular weight of the plasmid of interest;

B_1 is the number of restriction sites of the specific restriction endonuclease per one molecule of λ phage and

B_2 is the number of restriction sites of the specific restriction endonuclease per one molecule of the plasmid of interest.

The restriction reaction was left at the temperature optimal for the specific restriction endonuclease and then purified using a Qiaquick PCR purification kit. Alternatively, the fragments were separated by gel electrophoresis and purified using a QIAquick gel extraction kit.

2.3.4. Dephosphorylation of a vector DNA

To prevent self-ligation of vector in subsequent ligation reactions the 5′ phosphates were removed with calf intestinal alkaline phosphatase (CIAP). This enzyme cleaves terminal 5′ phosphate groups of linear DNA molecules thus preventing the recircularisation of the vector plasmid during the ligation reactions. Although the optimal reaction conditions of CIAP are 1 mM $MgCl_2$, 50 mM Tris-HCl (pH 8.0) and 50 mM NaCl, it is also active in most restriction endonuclease buffers. After the DNA had been digested with appropriate restriction endonucleases, 5 units of CIAP were added and the reaction mixture was incubated at 37 °C for 30 minutes. A further 5 units of CIAP were then added and the mixture was incubated for a further 30 minutes at 37 °C.

2.3.5. Ligation reaction

The vector was prepared from a parent plasmid by appropriate restriction digestion. T4 DNA ligase catalyses the formation of phosphodiester bonds between 5′ phosphate groups and 3′ hydroxyl groups of DNA fragments. The vector DNA fragment was purified from restriction endonuclease and calf intestinal phosphatase with the Qiaquick PCR purification kit. The insert was generated by a PCR reaction. A typical ligation reaction involved 1 to 2 µl (50 to 100 ng) of dephosphorylated vector DNA, 1 µl (10 to 50 ng) of insert DNA, 2 µl of 10x ligase buffer and 1 unit of T4 DNA ligase. The volume was made up to 10 µl with sterile distilled water. A formula used to calculate the amount of insert to take into the ligation reaction is shown below (section 2.3.10). The reaction was incubated overnight at 4 °C and 5 to 10 µl were used for the transformation procedure.

2.3.6. Purification of DNA by phenol/chloroform extraction

In order to purify DNA after electroelution or to concentrate DNA samples, phenol/chloroform extraction and ethanol precipitation were used to enable the removal of proteins or ethidium bromide from the DNA sample and the resuspension in fresh buffer. Alternatively, to purify 100 bp to 10 kb DNA from enzymic reactions and PCR, a more convenient protocol, using a Qiaquick PCR purification kit, was applied.

Phenol/chloroform extraction

If necessary, the volume of the DNA sample was made up to at least 200 µl with sterile distilled water. An equal volume of phenol/chloroform/isoamyl alcohol (25:24:1 v/v) was added to the sample in a microcentrifuge tube, and the sample was vortexed vigorously for 15 seconds until a white emulsion formed. The sample was centrifuged in a microcentrifuge at 21 000 g for 2 minutes to enable the separation of aqueous and organic phases. The upper

aqueous layer was transferred to a fresh microcentrifuge tube. The organic phase and interface were then 'back-extracted' by adding an equal volume of TE buffer, vortexing and centrifuging as described above to separate the two phases. Again the upper aqueous layer was removed and combined with the previous aqueous layer.

Alcohol precipitation

DNA samples were precipitated in order to concentrate the DNA and to remove traces of chloroform present after phenol/chloroform extraction. A one-tenth volume of 3M Na acetate (pH 5.2), one-hundredth volume of 1M $MgCl_2$ and 2 volumes of cold (-20 °C) 100% ethanol or 0.6 volume of 100% isopropanol were added to the DNA sample. The mixture was placed at –20 °C for at least 30 minutes or, for small DNA fragments (<500 bp), overnight. The sample was centrifuged at 21 000 g for 15 minutes at 4 °C and the supernatant was discarded. Cold ethanol (1 ml at 80% (v/v)) was added, the DNA was vortexed and centrifuged for 15 minutes. The supernatant was removed, the DNA pellet was vacuum-dried for 10 minutes and the dry pellet was resuspended in TE buffer or sterile distilled water.

2.3.7. DNA purification by Qiaquick PCR purification kit

QIAquick PCR purification kits were used to remove DNA polymerase and free nucleotides from PCR reactions or enzymes from digestion and dephosphorylation reactions. The system for both PCR purification and gel extraction combines the convenience of spin-column technology with selective binding properties of a uniquely designed silica-gel membrane. DNA absorbs to the silica membrane under high salt and appropriate pH while contaminants pass through the column, and the pure DNA is then eluted using a low-salt solution.

One volume of reaction solution was mixed with five volumes of PB buffer and applied to a QIAquick spin column. To allow DNA to bind to the membrane, the sample was

centrifuged for 30 to 60 seconds. The flow-through was discarded, a membrane cartridge was placed back in the same column, washed with 0.75 ml of buffer PE and centrifuged for 30 to 60 seconds. An additional 1-minute centrifugation was required to dry the membrane. To elute the DNA, 50 µl of buffer EB (elution buffer) was added to the centre of the silica membrane and the column was centrifuged for 1 minute. Alternatively, for increased DNA concentrations, 30 µl of buffer EB was added to the center of the QIAquick membrane and the column was incubated at room temperature for at least 1 minute, and then centrifuged.

2.3.8. Recovery of DNA fragments from gels with QIAquick gel extraction kit

PCR products or restriction digestion fragments were routinely extracted using a QIAquick gel extraction kit. The DNA fragments were first separated by gel electrophoresis on an appropriate agarose gel, stained with ethidium bromide and viewed under UV light (360 nm). Special attention was paid not to illuminate the DNA for a long time with UV light. The corresponding band was excised from the gel and transferred to a 1.5 ml microcentrifuge tube. The gel slice was then dissolved in 3 volumes of buffer QG at 50 °C for 10 minutes or until the gel had dissolved completely. If after incubation at 50 °C the colour of the mixture was not yellow, 10 µl of 3M sodium acetate were added. The absorption of DNA to the Qiaquick membrane is efficient only at pH < 7.5 and addition of sodium acetate provides the required acidic conditions. The suspension was mixed with 1 volume of isopropanol and applied immediately onto the QIAquick spin column. The DNA was absorbed onto the silica membrane by centrifugation for 1 minute and the flow-through was discarded. The column was washed with 0.5 ml of buffer QG and the flow-through was discarded. Buffer PE (0.75 ml) was added and the column was centrifuged for 1 minute. An additional 1-minute centrifugation was used to dry the membrane. To elute the DNA, 50 µl of buffer EB was

added onto the silica membrane and incubated at room temperature for at least 1 minute. The pure DNA was then obtained by centrifugation.

2.3.9. Recovery of DNA fragments from gels with electroelution

DNA fragments were eluted from the polyacrylamide gels (Maniatis et al., 1982). A gel slice containing the DNA fragment of interest was excised from the polyacrylamide gel using a razor blade. The slice was then placed into a piece of dialysis tubing (1 cm width) that had been washed with distilled water and sealed at one end with a clip. TBE (200 µl at 0.1x concentration) was added into the tubing and the second clip was attached after the removal of the air bubbles. The tubing was then placed in a horizontal electrophoresis gel apparatus filled with 100 ml of 0.1×TBE. A microscope slide was placed on top of the dialysis tubing to prevent it moving or touching the buffer meniscus. A constant current of 20 to 30 mA was passed through the dialysis tubing, perpendicular to the gel slice, for 20 minutes. After electroelution, the dialysis tubing was placed on the transilluminator (366 nm wavelength) to check that the DNA had moved out of the gel slice into the buffer. The buffer in the tubing was transferred to a microfuge tube. Any residual sample was washed out of the tubing with approximately 200 µl of TE buffer and combined with the first sample. The buffer containing the DNA fragment was cleaned from any proteins by extracting them with phenol/chloroform.

2.3.10. Ligation into pGEM®-T Easy

The following components were mixed in a total volume of 10 µl: 5 µl of 2x rapid ligation buffer, 1 µl of pGEM®-T Easy Vector, X µl of PCR product to achieve 1:1 or 3:1 molar ratio of insert:vector (see the formula below), 1 µl of T4 DNA ligase and deionised water. The 2x

rapid ligation buffer was vortexed vigorously before each use. The reaction was mixed by pipetting and incubated overnight at 4 °C. Separately a control ligation was prepared with 2 µl of control insert DNA.

The formula to calculate the amount of PCR product X, which is to be taken into the ligation reaction, was as follows:

$X = (50\ ng \cdot a)/3.0 \cdot b$

Where 50 ng is an amount of vector taken into the ligation reaction;

a is a size of the insert in kb;

3.0 is the size of the vector in kb;

b is a required molar ratio of insert:vector (for example 1/1 or 3/1).

2.3.11. Transformation of ligation mix into JM109 competent cells

For each ligation reaction and also for determining the transformation efficiency two LB plates were prepared, containing 100 µg/ml Amp, 0.5 mM IPTG and 80 µg/ml X-Gal. The plates were equilibrated to room temperature before use. The tubes containing the ligation reactions were centrifuged to collect the contents at the bottom of the tube. Half of the volume of each ligation reaction (5 µl) was added to a sterile 1.5 ml microcentrifuge tube on ice. Another tube with 0.1 ng of uncut plasmid was set up on ice for determination of the transformation efficiency of the competent cells. Frozen JM109 high efficiency competent cells were removed from –80 °C and placed on ice until thawed. The cells were mixed by gently flicking the tube and 50 µl of the cells were gently transferred into each prepared tube with the ligation mix and the control insert DNA. To determine the transformation efficiency 100 µl of competent cells was added to the tube with 0.1 ng of uncut plasmid. All tubes were flicked gently and placed on ice. After 20 minutes the cells were heat-shocked for 50 seconds in a water bath at exactly 42 °C. During this time the cell membrane becomes permeabilised

and the DNA molecules easily enter the cell. The tubes were returned immediately to ice for 2 minutes and 950 or 900 µl room temperature LB was added to the cells transformed with ligation reaction and with uncut plasmid, respectively. After 1 hour at 37 °C, 90 or 900 µl of each transformation reaction were plated onto LB/ampicillin/IPTG/X-Gal plates. For the transformation control, the cell culture diluted 10-fold with LB was used and 100 µl were plated. The plates were incubated overnight at 37 °C. The white colonies contained the recombinant plasmid with an insert.

2.3.12. Preparation of competent cells

Competent bacteria were prepared as described by Maniatis et al. (1982). A test tube containing 2 ml of sterile LB was inoculated with a single colony of bacteria from an agar plate. The tube was aerated overnight at 37 °C, unless otherwise stated. A 20 ml tube containing 2 ml of sterile LB was inoculated with 50 µl of the overnight culture and incubated at 37 °C for 2 to 3 hours. The bacteria were transferred into sterile microfuge tubes and pelleted by centrifugation at 8 000 g for 2 minutes. The supernatant was discarded and the pellet was resuspended in 0.75 ml of ice-cold, sterile 0.1 M $CaCl_2$ After incubation on ice for at least one hour, the bacteria were again pelleted and resuspended in 50 µl of ice-cold 0.1 M $CaCl_2$. The bacteria were used for the successive transformation. For long term storage, the bacteria could also be kept at -80 °C.

2.3.13. Transformation of *E. coli* with plasmid DNA

Plasmid DNA (1 to 3 µl) was added to 50 µl of competent cells and mixed gently. After incubation on ice for 30 minutes, the microfuge tubes were transferred to 42 °C for 1 minute to heat shock the bacteria and 0.2 ml of LB was added immediately. The tubes were incubated at 37 °C for one hour. This allows recovery of the bacteria and expression of the

antibiotic resistance encoded by the plasmid. Bacteria (20 µl and 200 µl samples) were plated onto the agar plates containing appropriate antibiotic and incubated overnight at 37 °C.

2.3.14. Subcloning of the *hcp* promoter into pAA182

The *hcp* promoter region of gene *ybjW* (*hcp*) was isolated by PCR amplification of genomic DNA from an *E. coli* K-12 strain. Based on the sequence of the same strain in this region (entry NC_000913 in the GenBank *nucleotide* database, Blattner et al., 1997), two primers were designed for amplification of the *hcp* promoter and its cloning into the promoter probe vector, pAA182 (Jayaraman et al., 1987). The primers hcp-prom1 and hcp-prom2 (**table 2.4**) were used to amplify a 0.4-kb fragment between nucleotides 912 971 and 913 339 in genomic *E. coli* DNA. These primers created unique *Eco*RI and *Hin*dIII restriction sites at the 5' and 3' ends, respectively, of the amplified fragment. Plasmid pNF383 was constructed by ligating the *Eco*RI/*Hin*dIII-digested PCR fragment into pAA182 that had been digested with the same enzymes (**figure 2.2**).

2.3.15. Polymerase chain reaction (PCR)

PCR reaction is a technique used to replicate DNA between two short oligonucleotides (known as primers) using thermostable DNA polymerases.

Primers were synthesised by Alta Bioscience (University of Birmingham, UK). Each primer was supplied as a dry solid and subsequently resuspended in sterile distilled water to a final concentration of 100 µM. The primers used in this work are listed in **table 2.4.**

For synthesis of the *hcp* promoter Bio-X-Act DNA (Bioline) polymerase was used. This enzyme has 3'-5' exonuclease activity, and consequently proof-reading capacity. When

Table 2.4. Primers used in this work

Name of primer	Sequence (5'-3')	Description
hcp-prom1	AAA**GAATTC**TGATTCGCCGCAGCC	Both primers were used to amplify a 383 nt fragment between nucleotides 912 971 and 913 353 in genomic *E. coli* DNA. Contain *EcoRI and HindIII restriction sites (in bold), respectively.*
hcp-prom2	AAAAAA**AAGCTT**CCTGCGCGTATGAGC	
$KD3_{C1}$	TTATACGCAAGGCGACAAGG	Forward test primer for the *cat* cassette from pKD3.
$KD3_{C2}$	GATCTTCCGTCACAGGTAGG	Reverse test primer for the *cat* cassette from pKD3.
hcp-del1	TTAACCTTAAACATGTATATTAAATATAACTT *TAAAAGGTGTGTAGGCTGGAGCTGCTTC*	Was used to delete the *hcp* gene. Homologous to 40 bp upstream of the *hcp*; contains P1 priming site from pKD3.
hcp-del2	*CACGGGCATTGATTCGTTGGCATCGTCATCGA* CAAACTCCCATATGAATATCCTCCTTAG	Was used to delete the *hcp* gene. Homologous to 40 bp downstream of the *hcp*; contains P2 priming site from pKD3
hcp-upstream	ATCGGGAGCGCGGCG	Locus-specific primer for the *hcp* gene; anneals upstream of the *hcp* gene.
hcp-downstream	TCGGCGTGACGCGCG	Locus-specific primer for the *hcp* gene; anneals downstream of the *hcp* gene.
arcA-del1	ACTTCCTGTTTCGATTTAGTTGGCAATTTAGG TAGCAAACGTGTAGGCTGGAGCTGCTTC	Was used to delete the *arcA* gene. Homologous to 40 bp upstream of the *arcA*; contains P1 priming site from pKD3.
arcA-del2	CGCTAAAAAGCGCCGTTTTTTTTGACGGTGGT AAAGCCGACATATGAATATCCTCCTTAG	Was used to delete the *arcA* gene. Homologous to 40 bp downstream of the *arcA*; contains P2 priming site from pKD3.

arcA-upstream	CGCCGGTTGTTGTAT
arcA-downstream	TCTTGCTGGCGCTTT
hcp-RACE1	GCAATCGCTTCACGACGCTA
hcp-RACE2	CGACCGACAATACGCGGAGAATCG
Abridged anchor primer (AAP)	GGCCACGCGTCGACTAGTAGGGGIIGGGIIGGGIIG
Abridged universal amplification primer (AUAP)	GGCCACGCGTCGACTAGTA

Locus-specific primer for the *arcA* gene; anneals upstream of the *arcA* gene.
Locus-specific primer for the *arcA* gene; anneals downstream of the *arcA* gene.
Anneals to the *hcp* RNA about 400 nt from the 5'-end. Corresponds to GSP1 in figure 2.6. Was used to prime the *hcp* cDNA synthesis.
Anneals to the *hcp* cDNA about 350 *nt* from its 3'-end (corresponds to GSP2 in figure 2.6). Was used to generate the *hcp* DNA in the first and second rounds of RACE PCR reaction and also to sequence the PCR fragment.
Is complementary to the poly-C tail of cDNA (underlined) and contains *Mlu*I, *Sal*I and *Spe*I restriction sites for subsequent cloning. Deoxyinosine residues (I) were selectively placed to decrease the melting temperature of the primer. The primer was used with hcp-RACE2 during the first round of RACE PCR (see also step 4 of figure 2.6).
Contains the 5'-end part of AAP (not underlined) and contains *Mlu*I, *Sal*I and *Spe*I restriction sites. Was used with hcp-RACE2 during the second round of RACE PCR.

proof-reading was not required, for example checking that a bacterial strain contains a certain mutation, BioTaq polymerase (Bioline) was used.

Plasmid DNA or chromosomal DNA was used as a PCR template. When chromosomal DNA was a template, a single bacterial colony was resuspended in 50 µl of water and incubated at 100 °C for 10 minutes. This was briefly centrifuged and 5 µl of the supernatant were used in the PCR reaction. Each 50 µl of reaction mixture contained 36.75 µl of H_2O, 5 µl of the appropriate 10x buffer, 1.5 µl of 50 mM $MgCl_2$, 5 µl of template DNA, 0.5 µl of each primer, 0.5 µl of 25 mM dNTP mixture (G, A, T and C) and 0.25 µl (1.25 units) of polymerase.

The polymerase chain reaction consists of three stages. First, high temperature is used to separate the two strands of DNA (denaturation). Secondly, the reaction is cooled to the temperature at which the primers anneal to the DNA. Finally, the temperature is increased to the optimum temperature of the DNA polymerase for DNA replication to occur between the two primers (extension or elongation). This cycle of three stages is repeated between 25 and 30 times.

For each PCR reaction, a general program was adapted to account for melting temperatures of the primers involved, the expected size of the desired fragment, and the DNA polymerase used. The parameters were:

Annealing T °C was taken as the lower annealing temperature (T_m) of the two primers. If either primer had a 5' overhang only the T_m of the annealing part was considered. Annealing temperature of the primers was calculated with the formula:

$$T_m = 64.9 + (G\% + C\%) \cdot 0.41 - 600/n$$

where G% and C% are the percentages of guanidine and cytosine bases in the primer and n is the total length of the primer in nucleotides.

Elongation T °C was 68 °C for Bio-X-Act polymerase and 72 °C for BioTaq polymerase. Elongation time was estimated by assuming that 1 kb of DNA is polymerised per minute. Number of cycles was 25 for Bio-X-Act and 30 for BioTaq. **Table 2.5, a** shows one example of such reaction designed to amplify 1 kb DNA using two primers with melting temperatures of 60 °C with BioTaq DNA polymerase.

2.3.16. DNA Sequencing

DNA was sequenced using a modified Sanger method, which is based on a template dependent polymerization of DNA with incorporation of modified nucleotides (terminator nucleotides). Sample processing (electrophoresis and output of data) were provided by the Genomics laboratory, the University of Birmingham, using the Applied Biosystems 3700 DNA Analyser and Roboseq 4204. The results were available through the Genomics data collection site of the School of Biosciences central server.

For each reaction the following reagents were added to a separate tube: 8 µl of terminator ready reaction mix, template (see below), 3.2 pmols of a primer and sterile water to a total volume of 20 µl. The solution was mixed well and spun briefly. Sequencing in this work was done with two types of a template: PCR product and a double stranded plasmid. Depending on whether the PCR product or plasmid DNA was used, 3 to 10 ng or 50 to 100 ng of DNA, respectively, was taken into the reaction. The sequencing program used is shown in **table 2.5, b.**

The entire content of the sequencing reaction mix was pipetted into a 1.5 ml microfuge tube. EDTA (250 mM, 2 µl) and non-denatured 95% ethanol (64 µl) were added, the tube was vortexed briefly and left at room temperature for 15 minutes. The tube was placed in a microcentrifuge with its orientation marked and centrifuged for 20 minutes at the maximum speed. The supernatant was carefully aspirated and discarded. The pellet was

Denaturing	Annealing	Extension	No. of cycles
94 °C, 5 minutes			x1
94 °C, 30 seconds	60 °C, 30 seconds	72 °C, 1 minute	x30
		72 °C, 7 minutes	x1

a

Denaturing	Annealing	Extension	No. of cycles
96 °C, 2 minutes			x1
96 °C, 10 seconds	50 °C, 5 seconds	60 °C, 4 minutes	x25
		Store at 5 °C	x1

b

Denaturing	Annealing	Extension	No. of cycles
94°C,2 minutes			x1
94°C, 30 seconds	55 °C, 30 seconds	72 °C, 1 minute	x35
		72 °C, 7 minutes	x1

c

Table 2.5. PCR programs used in this work. **a**: an example of a reaction designed to amplify 1 kb of DNA with BioTaq DNA polymerase using two primers with melting temperatures of 60 °C; **b**: the program used for sequencing; **c**: the program used in the RACE technique (section 2.4.2) to amplify DNA with poly-C tailed cDNA as a template.

usually invisible. Ethanol (70%, 250 µl) was added and the tube was vortexed briefly. The tube was placed in the microcentrifuge in the same orientation as in the previous centrifugation step and spun for 10 minutes at the maximum speed. The supernatant was carefully aspirated. The washing with 70% ethanol was repeated and the supernatant was carefully aspirated . The sample was dried in a vacuum centrifuge for 10 to 15 minutes or to dryness. Hi Di Formamide (10 µl) was added to the sample and DNA was resuspended for 30 minutes before taking the sample to the 3700 DNA Analyser.

2.3.17. Generation of the *hcp* and *arcA* deletion mutants

The method of Datsenko and Wanner (2000) was used in this work. This involves the initial replacement of the gene of interest with a chloramphenicol resistance cassette (*Cm*^{r}) with subsequent deletion of this cassette (**figure 2.5**).

The standard PCR mixture included plasmid pKD3 as a template, primers, and BioXact DNA polymerase. Primers hcp-del1 with hcp-del2 were used for deletion of the *hcp* gene. All primers used in this work are listed in **table 2.4**. The PCR product carried the Cm resistance cassette flanked by DNA homologous to the upstream and downstream regions of the *hcp* gene (**figure 2.5**, step 1). The PCR product was purified with QIAquick PCR purification kit and resuspended in elution buffer (10 mM Tris-HCl, pH 8.0).

E. coli strain RK4353 was transformed with plasmid pKD46 encoding AraC, ParaB, Exoγ, and Exoβ enzymes under control of the *paraB* promoter. The enzymes are required for deletion of a gene. This plasmid has a temperature-sensitive origin of replication (*ts-ori*) that is active at 30 °C.

For subsequent electroporation with Cm^r cassette the transformants were grown in 5 ml SOC cultures with 100 µg/ml ampicillin and 10 mM L-arabinose at 30 °C to an OD_{600} of 0.6. Arabinose was used to activate transcription from the *paraB* promoter. The cells were

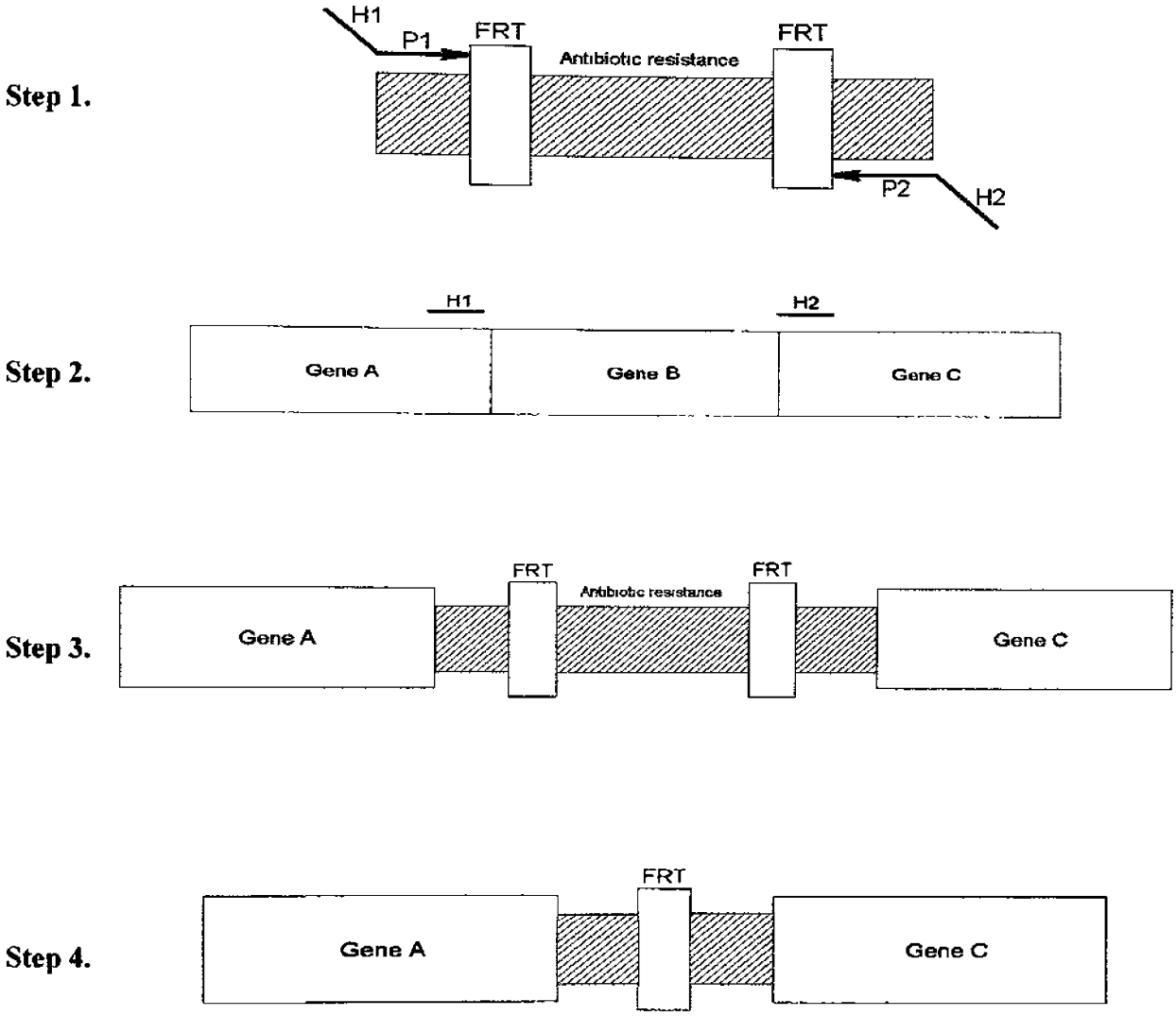

Figure 2.6. Inactivation of chromosomal genes using PCR products. The method of Datsenko and Wanner (2000) involves the initial replacement of the gene of interest with an antibiotic resistance cassette with subsequent deletion of this cassette. **Step 1:** Antibiotic resistance gene, flanked by FRT (FLP-recognition target) sites, is PCR amplified using primers with H1 and H2 extensions homologous to the upstream and downstream regions of the gene to be deleted. **Step 2:** Strain is transformed with a plasmid encoding λ Red recombinase. **Step 3:** Recombination between the H1 and H2 sites on the chromosome and corresponding sites on the PCR product occurs, which leads to the replacement of gene of interest with an antibiotic resistance cassette. **Step 4:** The replacement mutant is transformed with an FLP expression plasmid to eliminate the antibiotic resistance cassette by recombination between FRT sites.

made electrocompetent by concentrating them 100-fold and washing them three times with ice-cold 10% glycerol. For electroporation, 50 µl of cells and 100 ng of PCR product were placed in a 0.1 cm gap cuvette and a 1.8 kV/cm pulse was applied. The shocked cells were carefully added to 1 ml SOC medium, incubated for 1 hour at 37 °C. During this time, recombination between the H1 and H2 sites on the chromosome and corresponding sites on the PCR product occurs, which leads to the replacement of gene of interest with an antibiotic resistance cassette (**figure 2.5**, step 3). One-half was spread onto an agar plate to select Cm^r transformants and grown at 37 °C. If no transformants had grown within 24 hours, the remainder of the electroporated sample was spread after overnight incubation at room temperature. To ensure the loss of the helper plasmid, pKD46, the colonies were grown at 37 °C for 3 hours followed by growth at 43 °C for 2 hours and plated first on medium without antibiotic. After primary selection of each colony on both media without antibiotic and with ampicillin, the mutants were maintained on a medium without antibiotic.

Three PCR reactions were set up to show that the candidate mutants have the *cat* cassette instead of the gene to be deleted. The test primers for the Cm^r cassette were $KD3_{C1}$ and $KD3_{C2}$ (**table 2.3**). The locus-specific primers for the *hcp* gene were hcp-upstream and hcp-downstream (**table 2.3**). Two reactions were set up by using locus-specific primers in combination with the respective common test primer (hcp-upstream with $KD3_{C1}$ and hcp-downstream with $KD3_{C2}$). A third reaction was set up with the locus-specific primers. The latter reaction was repeated after elimination of the antibiotic resistance gene.

To eliminate the antibiotic resistance gene, Cm^r mutants were transformed with the Amp^r plasmid, pCP20, which has a temperature-sensitive origin of replication and encodes the FLP recombinase under the control of a heat-activated promoter. Ampicillin-resistant transformants were selected at 30 °C. To induce FLP recombinase synthesis, the colonies were grown at 37 °C for 3 hours followed by 43 °C for 2 hours. During this incubation

pCP20 is not able to replicate, whereas FLP recombinase becomes expressed, which leads to elimination of antibiotic resistance cassette by FRT sites (**figure 2.5**, step 4). The cultures were then tested for loss of Cm and Amp resistances.

To generate the *arcA* mutant, strain JCB387 and primers arcA-del1 and arcA-del2 were used as described above. The locus-specific primers for the *arcA* gene were arcA-upstream and arcA-downstream.

2.3.18. Bacteriophage P1 transduction

E. coli phage P1 is able to infect bacteria and produce viral particles (approximately 1 in 1000) that accidentally contain only bacterial DNA instead of viral DNA. Due to the generalised transduction, this bacterial DNA represents any part of the host bacterial genome including the region where a gene of interest is replaced with the chloramphenicol resistance cassette (*geneX::cat*). Consequently by growing the phage on an appropriate host strain, it is possible to use the phage transducing particles to introduce a gene of interest into another host strain. About 10% of phage transductions of chromosomal DNA undergo a homologous recombination and have exchanged DNA (that is recipient strain will acquire *geneX.:cat*). The rest of the donor bacterial DNA within the phage particle is introduced into the recipient but does not get exchanged with host chromosome and since it does not replicate, it is effectively diluted out by further growth.

Bacteriophage P1 transduction was used to create deletions of the *hcp* and *arcA* genes in different genetic backgrounds. P1 transduction of *hcp::cat* from strain JCB4999 was used for deletion of the *hcp* gene in JCB4011, JCB4041 and JCB4141. Deletion of the *arcA* gene in JCB3871 was achieved by transduction of *arcA::cat* from strain JCB38705. Donor strains were grown overnight at 37 °C, diluted with 0.5 ml of $LBCa^{2+}$ (LB supplemented with 2 mM $CaCl_2$) and aerated until the OD_{650} had reached 0.7 to 0.8. To 2 ml of $LBCa^{2+}$, kept at 45

°C, 0.1 ml of each P1 dilution (10^{-4}, 10^{-5} and 10^{-6}) and 0.1 ml of cell culture were added, mixed and poured onto an LA-agar plate (LB supplemented with 1.25% agar, 0.2% glucose and 2 mM $CaCl_2$). Plates were incubated overnight at 37 °C. A plate that gave nearly visible individual plaques was used for isolation of the P1 preparation. To each plate, 2 ml of $LBCa^{2+}$ were added and the soft agar was broken up using a glass spreader. This was then homogenised with 10 ml of chloroform using a homogeniser and centrifuged at 8 000 g for 15 min. The clear supernatant containing the phage particles was transferred into a sterile tube with 1 ml of chloroform, vortexed and stored at 4 °C.

Recipient strains were grown overnight in 1 ml of $LBCa^{2+}$, transferred into 20 ml of $LBCa^{2+}$ and grown until OD_{650} had reached 0.7 to 0.8. The culture was centrifuged at 3 600 g for 5 minutes, resuspended in 0.5 ml of $LBCa^{2+}$ and 0.1 ml of a 10^{-1} diluted P1 preparation was added. After 20 minutes of incubation at 37 °C, 1 ml of MS was added to the culture and it was centrifuged at 3 600 g for 5 minutes. To eliminate P1, the supernatant was discarded, the cell pellet was resuspended in 4 ml of MS by vortexing and centrifuged at 3 600 g for 5 minutes. The last step was repeated twice. The final cell pellet was resuspended in 2 ml of LB, aerated at 37 °C for 1 hour and centrifuged. Finally, the pellet was resuspended in 0.2 ml of MS and plated onto a Cm selective medium.

2.4. Isolation of RNA and transcription start mapping

2.4.1. Isolation of total RNA with on-column DNA digestion

Before the isolation of RNA, water and solutions were treated with 0.1% DEPC (diethyl pyrocarbonate). DEPC is a strong, but not absolute, inhibitor of RNases, which inactivates RNases by covalent modification. It is commonly used at a concentration of 0.1% to inactivate RNases on glass or plasticware or to create RNase free solutions and water.

Total RNA was isolated using a Qiagen RNeasy Mini Kit according to the manufacturer's instructions. A specialised high-salt buffer system allows up to 100 μg of RNA longer that 200 bp to bind to the RNeasy silica-gel membrane. Biological samples were first lysed and homogenised in the presence of a highly denaturing guanidine isothiocyanate (GITC)-containing RLT buffer, which immediately inactivates RNases to ensure isolation of intact RNA. Ethanol was added to provide appropriate binding conditions, and the sample was then applied to an RNeasy mini column where the total RNA bound to the silica-gel membrane. The contaminants were effectively washed away and RNA was then eluted with 30 μl of RNase free water.

For each miniprep not more than $1x10^9$ bacteria were used. Bacteria were harvested by centrifuging at 5 000 g for 5 minutes at 4 °C. The supernatant was decanted and all remaining medium was removed by aspiration. The bacterial pellet was loosened by flicking the bottom of the tube. The bacteria were resuspended thoroughly in 100 μl of 400 μg/μl lysozyme in TE buffer by vortexing and incubated at room temperature for 3 to 5 minutes. Buffer RLT (350 μl, containing 1% (v/v) β-mercaptoethanol) was added to the sample and this was mixed by vigorous vortexing. Ethanol (96-100%, 250 μl) was added to the lysate and mixed thoroughly by pipetting. The sample was applied to a RNeasy mini column placed in a 2 ml collection tube, centrifuged for 15 seconds at ≥8 000 g and the flow-through was discarded.

This was followed by on-column DNase digestion. RW1 (washing buffer, 350 μl) was pipetted into the RNeasy mini column and the column was centrifuged for 15 seconds at ≥8 000 g. DNase I stock solution (10 μl) was added to 70 μl of buffer RDD and mixed gently by inverting the tube. The DNase I incubation mix (80 μl) was pipetted directly onto the RNeasy silica-gel membrane, which was placed on the benchtop (20 °C). After 15 minutes, 350 μl of buffer RW1 was added and the column was centrifuged for 15 seconds at ≥8 000 g.

Buffer RW1 (700 µl) was added to the RNeasy column and this was centrifuged for 15 seconds at ≥8 000 g to wash the column. The flow-through and collection tube were discarded. The RNeasy column was transferred into a new 2 ml collection tube. Buffer RPE (500 µl) was pipetted onto the column, this was centrifuged for 15 s at ≥8 000 g and the flow-through was discarded. Another 500 µl of buffer RPE was added to the tube. The tube was centrifuged for 2 minutes at ≥8 000 g to dry the RNeasy silica-gel membrane. To eliminate any chance of possible buffer RPE carryover the RNeasy column was placed in a new collection tube and centrifuged at full speed for 1 min. To elute, the RNeasy column was transferred to a new 1.5 ml tube, 30 µl of RNase-free water were added directly onto the RNeasy silica-gel membrane and the tube was centrifuged for 1 minutes at 8 000 g.

2.4.2. Transcription start mapping by 5' RACE system

The transcription start site of the *hcp* gene was determined using the RACE system (Rapid Amplification of cDNA Ends). The principle of RACE is shown in **figure 2.6.** A preparation of mRNA is first hybridised with a gene-specific oligodeoxynucleotide primer (GSP1), complementary to the target RNA, and this primer is extended with reverse transcriptase. Following reverse transcription, the first strand product is purified from unincorporated dNTPs and GSP1. TdT (Terminal deoxynucleotidyl transferase) is used to add homopolymeric poly-C tails to the 3'-ends of the cDNA. Tailed cDNA is then amplified by PCR using a complementary homopolymer-containing anchor primer and a second gene-specific primer (GSP2), which anneals 3' in respect to GSP1. This allows amplification of unknown sequences between the GSP2 and the 5' end of the mRNA. The amplified DNA is then sequenced and the transcription start site is determined as the first nucleotide downstream of polyG tail (complementary to polyC tail of cDNA).

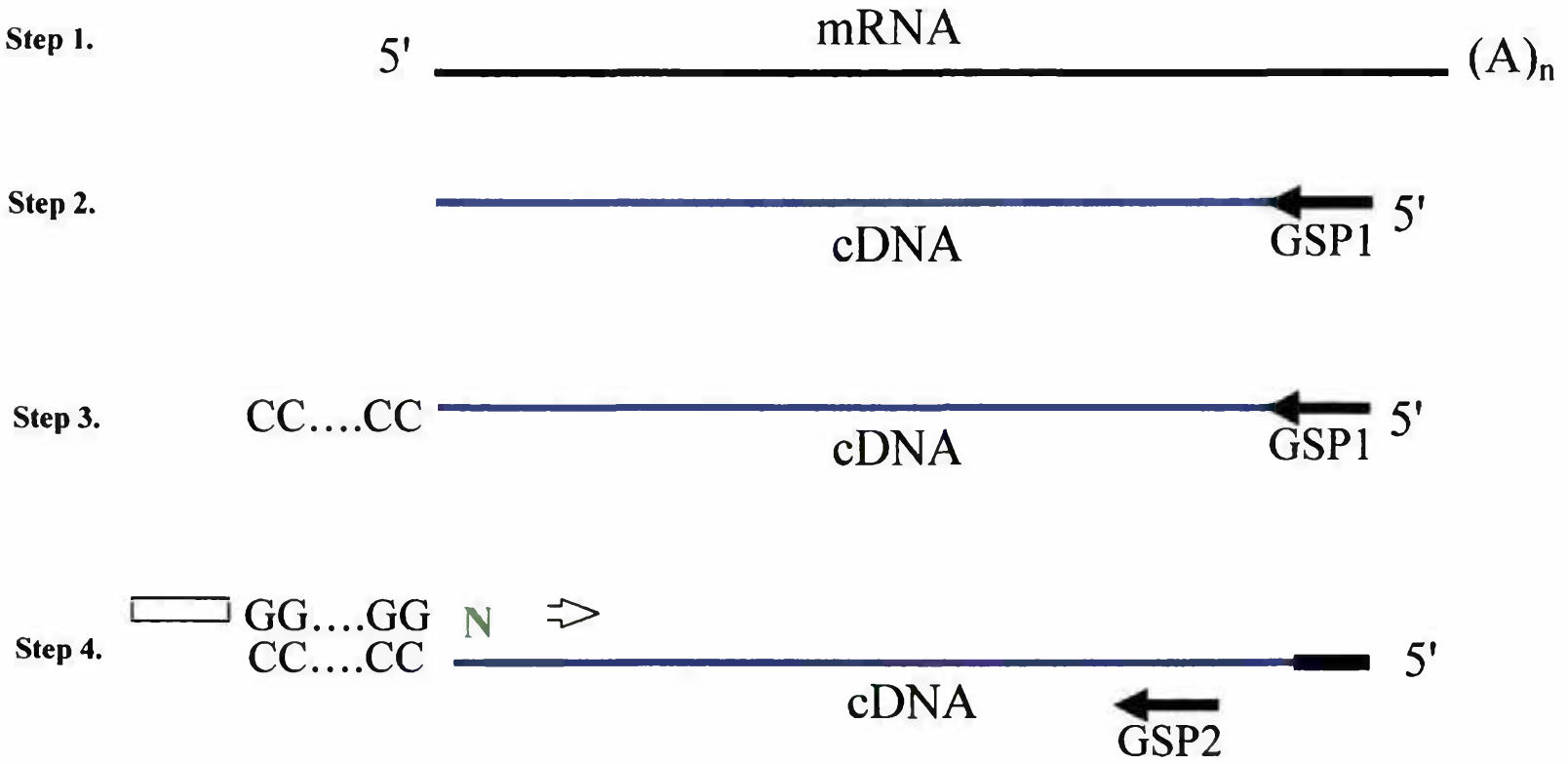

Figure 2.7. RACE method to identify the transcription start point. The transcription start site of the *hcp* gene was determined using the RACE system (Rapid Amplification of cDNA Ends). A preparation of mRNA (step 1) is first hybridised with a gene-specific oligodeoxynucleotide primer (GSP1), complementary to the target RNA, and this primer is extended with reverse transcriptase (step 2). TdT (Terminal deoxynucleotidyl transferase) is used to add homopolymeric poly-C tails to the 3'-ends of the cDNA (step 3). Tailed cDNA is then amplified by PCR using a complementary homopolymer-containing anchor primer and a second gene-specific primer (GSP2), which anneals 3' in respect to GSP1 (step 4). This allows amplification of unknown sequences between the GSP2 and the 5' end of the mRNA. The amplified DNA is then sequenced using GSP2 and the transcription start site is determined as the first nucleotide (green N) downstream of polyG tail (complementary to polyC tail of cDNA).

Design of gene specific 5' RACE primers

For transcription start mapping, two or three primers specific to RNA of the gene of interest are required. The requirements for the primers were the following. The first primer (GSP1) should anneal about 400 bp downstream of a putative transcription start site. The second primer (GSP2) anneals about 350 bp downstream from the putative transcription site. If required, the third primer (GSP3) is used, which anneals 3' in respect to GSP2. All primers read towards the transcription site and all have the sequence of the complementary strand. The primers should be approximately 20 bp long and have high G:C content in the 5'- and central regions. To have higher specificity, the primers must also contain a fairly unstable 3' end, for that no more than two G or C residues should be included in the last five 3'- bases.

First strand cDNA synthesis

The first step in the synthesis of the cDNA is annealing of the primer. The primer is extended using reverse transcriptase, and the RNA is digested leaving the labelled cDNA. RNA-primer mixtures were prepared in sterile microfuge tubes. RNA (1 to 5 µg), 2.5 pmoles of primer and DEPC-treated water were added to a final volume of 15.5 µl. Each sample was incubated at 65 °C for 5 minutes, then placed on ice for at least 1 minute. The following reaction mixture was prepared with each component being added in the indicated order: 2.5 µl of 10x RT buffer; 2.5 µl of 25 mM $MgCl_2$; 1 µl of 10 mM dNTP mix and 2.5 µl of 0.1 M DTT. The reaction was mixed gently, collected by brief centrifugation and incubated at 42 °C for 1 minute. After the SuperScriptTM II reverse transcriptase had been added the reaction was mixed gently and incubated at 42 °C for 50 minutes. To inactivate the reverse transcriptase, the reaction was incubated at 70 °C for 15 minutes. The reaction was then centrifuged for 20 seconds and placed at 37 °C. To degrade RNA, 1 µl of RNase mix was

added, the reaction was mixed gently and thoroughly and incubated at 37 °C. After 30 minutes the reaction was collected by brief centrifugation and placed on ice.

S.N.A.P Column Purification of cDNA

The binding solution was equilibrated to room temperature. For each sample to be purified about 100 µl of sterilised distilled water was equilibrated at 65 °C. A volume of 120 µl of binding solution (6M NaI) was added to the first strand reaction. The cDNA/NaI solution was transferred to a S.N.A.P column and centrifuged at 8 000g for 20 seconds. The cartridge insert was removed from the tube and the flowthrough transferred to a microcentrifuge tube. This solution was saved until the recovery of the cDNA was confirmed. The cartridge insert was placed back into the tube. Cold (4 °C) 1x wash buffer was added to the cartridge and the column was centrifuged at 8 000 g for 20 seconds. The flowthrough was discarded and the wash step was repeated three additional times. The cartridge was washed twice with 400 µl of cold (4 °C) 70% ethanol as described in washing step with the wash buffer. After removing the final ethanol, the tube was centrifuged at 8 000g for 20 seconds to elute the cDNA.

TdT Tailing of cDNA

The column purified cDNA was concentrated into a volume of 10 µl in a concentrator at 40 °C for 15 minutes. The following components were added into the tube and mixed gently: DEPC treated water, 5x tailing buffer, 2 mM dCTP and SNAP purified cDNA sample to a total final volume of 24 µl. The final composition of the tailing reaction was 10 mM Tris-HCl (pH 8.4), 25 mM KCl, 1.5 mM $MgCl_2$, 200 µM dCTP and cDNA. Enzyme TdT (1 µl) was added, the reaction was mixed gently and incubated for 10 minutes at 37 °C. The TdT

was heat inactivated for 10 minutes at 65 °C. The contents of the reaction were collected by brief centrifugation and placed on ice.

PCR with poly-C tailed cDNA as a template

The poly-C tailed cDNA was taken into the first round of PCR reaction with gene specific primer GSP2 and AAP, which anneals to the poly-C tail. The program used is shown in **table 2.5, c.** The PCR product from the first PCR reaction was diluted 100-fold and 5 µl of it were taken into the second PCR reaction using primers GSP2 and AUAP (**table 2.3**). Alternatively, if the first round of PCR generated some DNA products as a result of non-specific annealing, an aliquot of the PCR reaction was run on an agarose gel, the DNA band of expected size was excised, purified with QIAquick gel extraction kit and used as a template for the second round of PCR. The program for the second round of PCR was as above except that the number of cycles was 30.

2.5. Analysis of proteins and chemical methods

2.5.1. Folin protein assay

The soluble protein content of cytoplasmic fraction and Ni-NTA purified protein extract were assayed as described by Lowry et al. (1951). Under alkaline conditions the divalent copper ion forms a complex with peptide bonds in which it is reduced to a monovalent ion. Monovalent copper ions and the radical groups of tyrosine, tryptophan, and cysteine react with Folin reagent to produce an unstable product that becomes reduced to molybdenum/tungsten blue. Standards were 20, 40, 60, 80 and 100 µg of bovine serum albumin (BSA) solution. As samples 50 or 100 µl of ten- and one hundred-fold diluted supernatant and pellet fraction or undiluted purified protein extract, respectively, were assayed. Samples were diluted to 0.6 ml with distilled water and assayed in duplicate. A 3 ml

sample of Folin B solution was added to each tube. The samples were then mixed twice. After 10 minutes of incubation at room temperature, 0.3 ml of Folin reagent was added to all tubes and the samples were mixed twice. After a further 30 minutes of incubation at room temperature the absorbance at 750 nm was measured. Protein concentrations were calculated using the standards as a reference as following. For the standards, the best-fit line of regression of amount of the protein on the absorbance at 750 nm was plotted and an equation $y = ax + b$ was calculated; where y is the amount of the protein, x is the absorbance at 750 nm, and a and b are the regression coefficients.

2.5.2. Purification of His-tagged proteins on Ni-NTA column

HCP protein was overexpressed with a tag of 6 histidine residues fused to the N-terminus. To purify it from all other cellular proteins Ni-NTA-agarose was used. Nitrilo-acetic acid (NTA) has four chelation sites for nickel ions, which have high affinity to the His-tagged proteins. The bound His-tagged protein is then washed with a buffer and eluted with imidazole as a competitor for binding to the nickel ions.

A 10 ml column (Biorad) was put on a stand and loaded with Ni-NTA resin. The binding capacity of the resin is 5 to 10 mg of protein per 1 ml of resin, consequently the volume used corresponded to the amount of protein to be purified. The column was equilibrated with 10 ml of Tris-HCl buffer and the protein suspension was loaded onto the resin and mixed gently. The mixture was shaken for 1 hour at 4 °C in a vertical shaker for the His-tagged protein to bind to the Ni^{+}-charged resin. The column was washed 5 times with 10 ml of Tris-HCl buffer and 0.5 ml of 250 mM imidazole in Tris-HCl buffer was added to elute the bound protein. This last elution step was repeated and two 0.5 ml portions of 1 M imidazole were added to elute any remaining proteins bound to the nickel ions.

2.5.3. SDS polyacrylamide gel electrophoresis (SDS-PAGE) of proteins

SDS-PAGE was used to separate proteins according to their molecular weight. The apparatus consisted of two glass plates (Bio-rad, 18 cm^2), which were held parallel and separated from one another by 0.75 mm spacers placed along three lengths. The running acrylamide gel contained 15% acrylamide, 0.375 M Tris, 0.1% SDS, 0.08% APS and 0.05% TEMED. The 8% APS and TEMED were added and the solution swirled gently immediately before applying. The running polyacrylamide gel was pipetted between the vertical glass plates to 75% to 80% of their total height. A layer of 0.1% SDS was applied to the top of the running gel to prevent drying out and the solution was left for 40 minutes to polymerize. The 0.1% SDS overlay on the resolving gel was poured off and the acrylamide stacking gel was layered on top of the polyacrylamide resolving gel. The stacking gel is used to improve resolution of the protein bands. It contained 6% acrylamide, 0.125 M Tris, 0.1% SDS, 0.08% APS and 0.05% TEMED. The 8% APS and TEMED were added immediately before applying as described above. A comb was inserted and the gel was polymerised for another 40 minutes. The protein samples were mixed with the sample buffer and heated at 100 °C for 10 minutes before loading. After removal of the comb, the wells were washed with 1x electrode buffer to eliminate unpolymerised acrylamide and the gel attached to a vertical electrophoresis tank. The lower spacer was removed and space between plates washed with electrophoresis buffer to eliminate any air. The samples were loaded into pre-washed wells and a constant voltage of 60-80 V was applied for 15 to 17 hours.

2.5.4. Coomassie Brilliant Blue staining of SDS-PAGE gels

To visualize protein bands, the gel was dismantled and stained with Coomassie brilliant blue, which binds to free amino groups in the side chains of amino acids, especially lysine.

Standard marker proteins were separated on each SDS-PAGE gel so that the size of the other proteins could be estimated. The markers were: myosin (205 kDa), β-galactosidase (116 kDa), phosphorylase b (97 kDa), fructose-6-phosphate kinase (84 kDa), bovine serum albumine (BSA) (66 kDa), glutamic dehydrogenase (55 kDa), ovalbumin (45 kDa), glyceraldehyde-3-phosphate dehydrogenase (36 kDa), carbonic anhydrase (29 kDa), trypsinogen (24 kDa), trypsin inhibitor (20 kDa), α-lactalbumine (14 kDa), and aprotinin (6.5 kDa). The gel was stained by shaking gently in 200 ml of Coomassie brilliant stain solution for 30 minutes at room temperature. The gel was then rinsed in destain solution and was placed in 300 ml destain solution and left shaking. The destain solution was changed every 30 min, until the background of the gel was clear. Finally, the gel was left for 1 hour in 300 ml of shrink solution and dried overnight between two framed sheets of gel drying film.

2.5.5. Western blotting

Western blotting detected proteins separated by SDS-PAGE using specific antibodies. Proteins separated by SDS-PAGE gel were denatured and transferred to the PVDF membrane. The immobilized proteins were then hybridized with primary antibodies. After hybridization the antibodies were detected by enzyme linked immunoassay, using a secondary antibody conjugated to alkaline phosphatase. Alkaline phosphatase catalyses a colour reaction with 5-bromo-4-chloro-3-indolyl phosphate and nitro blue tetrazolium salt to produce an insoluble blue/purple precipitate enabling visualisation of the protein-antibody complex.

Following electrophoresis, the gel was soaked in blotting buffer. The PVDF membrane was soaked in methanol and then in blotting buffer and the blot was mounted onto the blot transfer system, avoiding air bubbles. A voltage of 200 mV was applied across the

blot and the proteins were left to transfer for 1 hour. After blotting, the membrane was incubated in PBS with 0.5% Tween buffer for 1 hour, which was changed and the membrane shaken for another hour. This blocking step decreased non-specific binding of proteins to the membrane. The membrane was shaken for 3 hours at room temperature with the primary antibodies diluted in PBS + 0.1% Tween + 0.1% BSA. The membrane was washed 3 times for 5 minutes each in PBS + 0.1% Tween to remove non-specifically bound antibodies and was incubated with secondary antibody conjugate in PBS + 0.1% Tween + 0.1% BSA for 1 hour. The membrane was washed 3 times for 5 minutes each in PBS + 0.5% Tween and subsequently washed with 10 mM Tris-HCl, pH 7.5 for 5 minutes to remove NaN_3, which interferes with colour reaction. To detect the secondary antibodies, a 5-bromo-4-chloro-3-indolyl phosphate/nitro blue tetrazolium tablet was dissolved in 10 ml of water and the solution was added to the membrane. When the bands started developing, the reaction was stopped with water that was changed several times. The membrane was dried between two sheets of Whatman paper.

2.5.6. Determination of nitrite concentration

The concentration of nitrite in the supernatant was determined by removing 50 µl of the solution from assay on determination of nitrate reductase activity. Distilled water (450 µl) and 1 ml of each of two nitrite detection reagents: 1% (w/v) of sulphanilamide in 1 M HCl; and 0.02% (w/v) of naphthylethylene diamine dihydrochloride were added to this. The assay was calibrated in triplicate by diluting 30 µl of 1 mM sodium nitrite with 470 µl of distilled water and adding the two nitrite detection reagents. A blank consisted of 500 µl of distilled water and the two nitrite detection reagents. After vortexing twice the tubes were left for 30 minutes before the optical density at 540 nm was determined. The specific nitrate reductase activity at room temperature was calculated from the formula:

$$Specific\ activity = \frac{OD_{540} \cdot M \cdot N \cdot V_1}{t \cdot V_2 \cdot OD_{650} \cdot S \cdot V_3}$$

Units are: nmol nitrate reduced.(mg dry weight)$^{-1}$.min^{-1}

Key:			*Constant values*
OD_{540}	:	optical density of the sample at 540 nm	
M	:	coefficient used to convert OD_{650} to mg dry weight	2.5
N	:	amount of nitrite present in the standard (nmol)	30
V_1	:	total assay volume (ml)	1.09
t	:	incubation time for assay (min)	5
V_2	:	volume of cells assayed for activity (ml)	0.075
OD_{650}	:	optical density at 650 nm of cell suspension	
S	:	average optical density of nitrite standards at 540 nm	
V_3	:	volume of supernatant assayed for nitrite (ml)	50

The presence of nitrite ions in the culture was determined with qualitative nitrite assay. To 400 µl of bacterial culture, 200 µl of 1% sulphanilamide and 200 µl of N-naphthylethylene diamine dihydrochloride were added. If nitrite was present in the culture, a red colour developed.

2.6. Analysis of protein-DNA interactions by electromobility shift assays (EMSA)

2.6.1. Radioisotope labelling of DNA fragments

DNA, after being digested with restriction endonucleases, treated with phosphatase and purified, was labelled in a 20 µl total volume. The following components were added into the reaction: 8 to16 µl of DNA, 1 µl of T4 polynucleotide kinase (PNK), 2 µl of 10x PNK buffer,

1 µl of $^{\gamma 32}$P ATP and H_2O to a final volume of 20 µl. The DNA was labelled at 37 °C for 30 minutes. The unincorporated nucleotides were removed using a G50 spin column.

2.6.2. Preparation of Sephadex G-50

Sephadex G-50 (5 g) was autoclaved in 100 ml of TE buffer and allowed to settle. The excess TE was decanted and discarded. Fresh TE (150) was added, the suspension was mixed and settled and the excess TE was discarded. The step of adding a new portion of TE, mixing and discarding excess TE was repeated twice. These washes removed under-sized particles to leave a homogenous G-50 suspension. Finally, the excess TE was decanted and discarded and approximately 50 ml TE was added to G-50, mixed and settled before use. G-50 was stored at 4 °C.

2.6.3. Preparation of spin columns and purification of the labelled fragment from unincorporated nucleotides

A micro bio-spin chromatography column (BioRad) was placed in an empty, clean 1.5 ml centrifuge tube. The column was filled with approximately 400 µl of the settled G-50 suspension prepared as above and TE buffer was drained out of the column. The column was centrifuged at 1 500 g for 1 minute. The column volume when packed should be approximately 200 µl. The column was placed in a fresh microfuge tube, the sample was applied to the top of the column in a volume of 20 µl (i.e. one tenth column volume) and centrifuged at 1 500 g for 1 minute. The speed and duration of centrifugation should be the same as those used to pack the column. The DNA fragments used for following band-shifts were cleaned by passing them through two successive G-50 spin columns. The labelled DNA fragment was present in approximately 20 µl of eluate from the column whereas unincorporated nucleotides were retained in the column.

The concentration of DNA in the eluate was calculated by assuming that up to 50% of the labelled fragment had been lost. The number of counts of the labelled fragment was estimated. For each band-shift reaction 0.1 to 0.5 ng of the labelled fragment was used i.e. in the order of 0.2 µl of the 20 µl total labelled fragment. The fragment was stored at -20 °C.

2.6.4. Electromobility shift assays (EMSA) with FNR and NarL

FNR and NarL were diluted to appropriate concentrations in buffer for dilution of FNR and buffer for dilution of NarL, respectively. Each concentration of FNR or NarL to be used (1 µl) was aliquoted into fresh microfuge tubes. The aliquots were stored in the cold room while preparing the band-shift cocktail. The following components for one reaction were added: 1 µl of 10x binding buffer, 1 µl of 50% glycerol, 0.5 µl of 10 mg ml^{-1} BSA, 0.5 µl of 500 µg ml^{-1} herring sperm DNA, acetyl phosphate to the final concentration 50 mM, 0.2 µl of $^{\gamma 32}P$ labelled DNA fragment and H_2O to 9 µl. The cocktail was distributed in 9 µl aliquots into microfuge tubes. The appropriate FNR and NarL dilutions (1 µl) were added to the microfuge tubes, mixed by gently pipetting a few times and briefly spun in a microfuge. The tubes were transferred to the 37 °C block and incubated for 30 minutes. The gel apparatus was set up, and pre-run at 12 V/cm of gel. The 10 µl band-shift samples were loaded into the appropriate wells and bromophenol blue/xylene cyanol FF DNA loading buffer (10 µl) was loaded into an adjacent well, with which to monitor the progress of the gel. The gel was run at the voltage as above for approximately 2.5 to 3 hours until the bromophenol blue had reached the bottom of the gel.

The gel was fixed in a solution of 10 % (v/v) methanol + 10 % (v/v) acetic acid for 5 to 10 minutes. When properly fixed, the bromophenol blue dye turned a green colour. After fixing, the solution was retained and re-used several times. The gel was dried with filter paper. The top of the gel was covered with cling film so that no radioactivity could be

transferred to the drier and the gel was dried for approximately 1 hour. In the meantime the phosphorimager screen was exposed to daylight in order to blank it. The dried gel was covered with fresh cling film and exposed to the phosphorimager screen for 3 to 24 hours depending on the intensity of the labelled fragment. The amount of DNA in the band shift reaction was adjusted if necessary in order to see the fragment on the autoradiograph.

2.7. Computer programs used during this study

GCG package of programs developed by the Genetics Computer Group, the University of Wisconsin, Madison (*http://gcg.com*) was used for bioinformatic analysis of nucleotide sequences. This program suite works under the Unix operating system. Programs *Reverse* and *Map* were used for converting a DNA sequence into a reverse and complementary sequence and for producing a double strand sequence from a single strand, respectively. The latter program was also used to search for restriction sites. *Pileup* was used to create a pairwise alignment of two sequences.

Mfold (*http://bioweb pasteur.fr/seqanal/interfaces/mfold-simple.html*) was used to analyze secondary structure of mRNA and cDNA molecules.

Chromas was employed to visualize sequencing data generated by the ABI 3700 Sequence analyzer.

Quantity One was used to analyze ethidium-bromide stained DNA visualized under UV light and developed phosphoimager screen.

Statistics package *Minitab* was used for statistical analysis of data as to calculate regression coefficients, the slope of the regression line and the growth rate of the cultures.

Precision Scan Pro was used to scan Coomassie stained gels and Western blots. The gels and blots were scanned at 600 or 300 dpi resolution in the 256-color mode. The initial files were saved in the bitmap format (*.bmp).

Adobe PhotoDeluxe Business Edition was used to process the files saved in HP Precision Scan Pro. Brightness/contrast and size were adjusted with options quality and size, respectively.

CHAPTER 3

Regulation of transcription of the *E. coli* *hcp* gene encoding the hybrid cluster protein

3.1. Introduction

The hybrid cluster protein (HCP) contains two non-haem iron-sulphur clusters, a conventional [2Fe-2S] cluster and the hybrid [4Fe-2S-2O] cluster. HCP has been proposed to be involved in some step of the nitrogen cycle (van den Berg et al., 2000; Kim et al., 2003). Prior to the start of this project, how the *hcp* promoter is regulated had not been studied.

To define the *hcp* regulatory region, the transcription start site was identified. The *hcp* regulatory region was cloned into a promoter probe vector to construct an *hcp::lacZ* fusion suitable for studying the effects of alternative electron acceptors such as fumarate, DMSO and TMAO on *hcp* promoter activity. How the *hcp* promoter is regulated by FNR, ArcA, NorR, NarL and NarP was also determined.

3.2. Analysis of the structure of the *hcp* promoter

The transcription start of the *hcp* gene had not been determined by the start of this project. A 383 nt fragment of DNA that included the sequence upstream from the *hcp* open reading frame and a part of the open reading frame was searched for the presence of possible binding sites of some regulatory proteins and for possible promoter consensus sequences. The sequence of the *hcp* promoter was obtained as entry NC_000913 from the GenBank NCBI nucleotide database (Blattner et al., 1997). The program Findpatterns in the GCG package (Genetics Computer Group, the University of Wisconsin) was used to search for the consensus DNA binding sequences for different regulator proteins. The results of the search are shown in **figure 3.1.** A potential transcription start and –10 box were located 64 and 74.5 bp upstream from the translation start. The potential –10 box matched the consensus at four out of six nucleotides. A putative FNR binding site was centred between 39 and 40 bp upstream from the suggested transcription start (position –39.5 bp). A putative

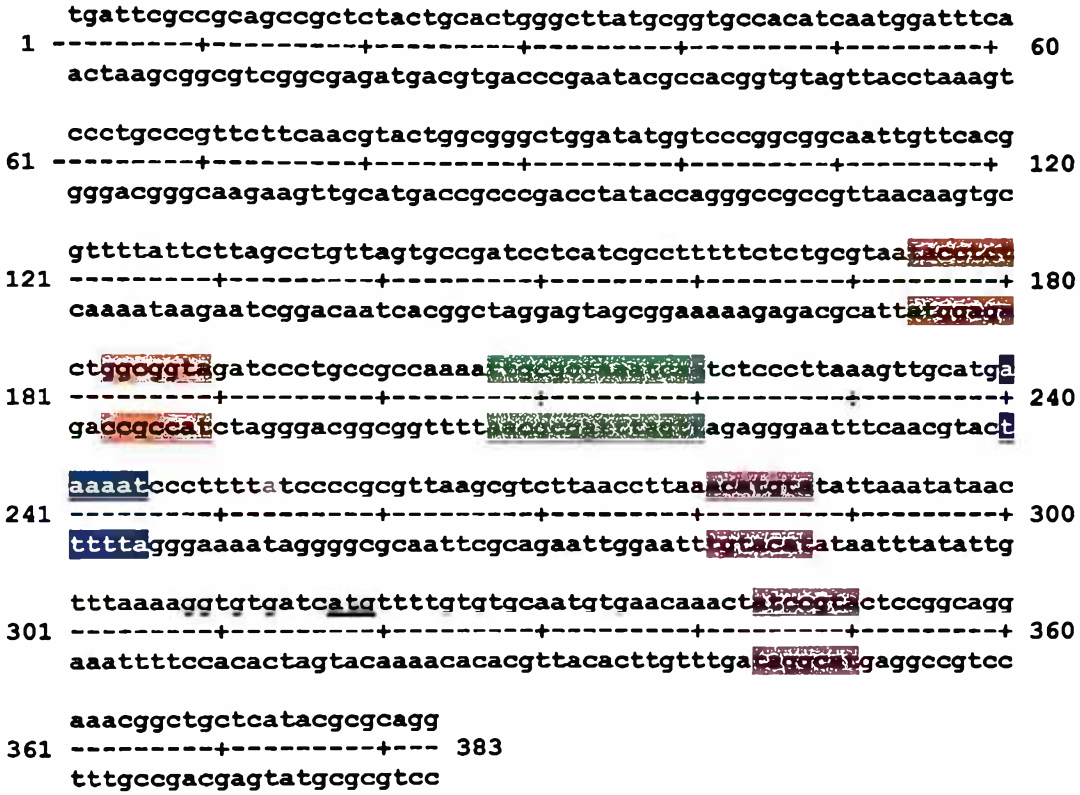

Figure 3.1. Structure of the *hcp* promoter. A 383 nt fragment of the *hcp* regulatory region was searched for the presence of possible binding sites of some regulatory proteins and for possible promoter consensus sequences. A potential transcription start (shown in red) and –10 box (blue) are located 64 and 74.5 bp upstream from the translation start, respectively. The translation start site is underlined. A putative FNR binding site is centred between 39 and 40 bp from the potential transcription start (position –39.5 bp) (in green). A possible 7-2-7 binding site for both NarL and NarP located 71.5 bp upstream from the potential transcription start is shown in red. Two putative NarL heptamers located 31 and 94 bp downstream from the proposed transcription start site are shown in pink.

binding site for both NarL and NarP transcription factors organised as a 7-2-7 inverted repeat was also identified located 71.5 bp upstream from the possible transcription start (135.5 bp upstream from the translation start). The *hcp* promoter also contained two NarL binding heptamers in a reverse direction located 31 and 94 bp downstream from the putative transcription start. No consensus DNA binding sequence for the ArcA protein was found in the *hcp* regulatory region, and there was no recognisable –35 consensus sequence. Thus, based on this sequence analysis, it was suggested that the *hcp* promoter might be regulated by FNR, NarL and NarP proteins.

3.3. Transcription start site of the *hcp/hcr* operon

To facilitate the *in vitro* work, the transcription initiation site of the *hcp/hcr* operon was determined. Strain RK4353 and its *hcp* derivative, JCB5000, were grown anaerobically in MS medium supplemented with glucose and nitrate. Total RNA from both strains was isolated with an RNeasy kit from Qiagen. As the columns are designed for a maximal number of 10^9 bacteria, either $0.5 \cdot 10^9$ or $1 \cdot 10^9$ cells were extracted (**figure 3.2**). Both quantities of bacteria yielded RNA of good quality, so the RNA preparation from the $1 \cdot 10^9$ cell sample was used to ensure the maximal presence of the *hcp* RNA transcript. Total RNA of RK4353 expressing HCP was used as a template in a reverse transcription reaction to synthesise cDNA. The cDNA was poly-C tailed and used as a template for two successive PCR reactions: first with a gene-specific primer and a primer complementary to the poly-C tail; and the second with another gene-specific primer and abridged universal amplification primer. The PCR product was sequenced, which showed a poly-G tail (complementary to poly-C tail) upstream from the 5'-TATATTAAA-3' sequence (**figure 3.3**), indicating that the transcription start site is located at a thymine nucleotide 31 bp upstream from the translation initiation codon (**figure 3.4**).

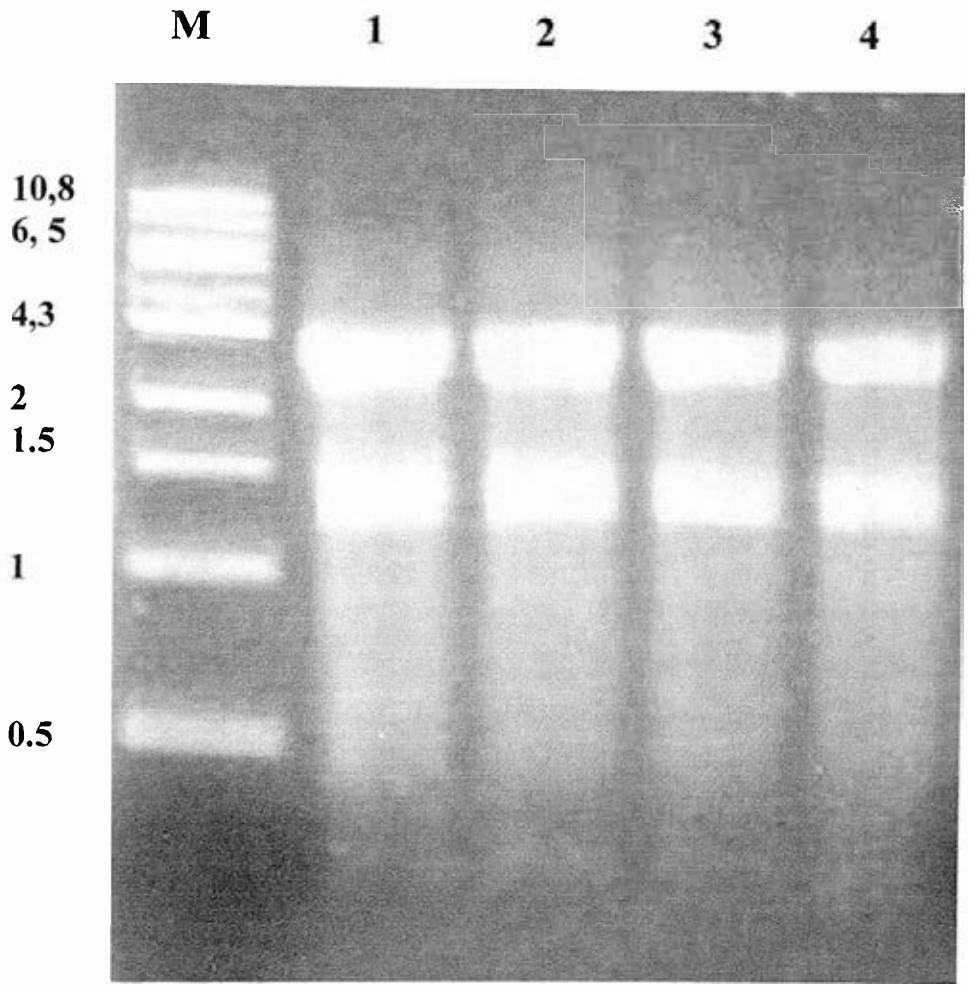

Figure 3.2. Isolation of total RNA from strains RK4353 and JCB5000. Strains RK4353 and JCB5000 (RK4353 *Δ hcp*) were grown anaerobically in MS medium supplemented with glucose and nitrate. Total RNA from both strains was isolated with an Invitrogen RNeasy kit. **Lane M**: marker DNA ladder, 1 kb DNA ladder (NEB); the sizes of the fragments are given to the left; **lane 1**: RNA isolated from strain RK4353 using $1 \cdot 10^9$ cells; **lane 2**: RNA isolated from strain RK4353 using $0.5 \cdot 10^9$ cells; **lane 3**: RNA isolated from $1 \cdot 10^9$ cells of strain JCB5000; **lane 4**: RNA isolated from $0.5 \cdot 10^9$ cells of strain JCB5000.

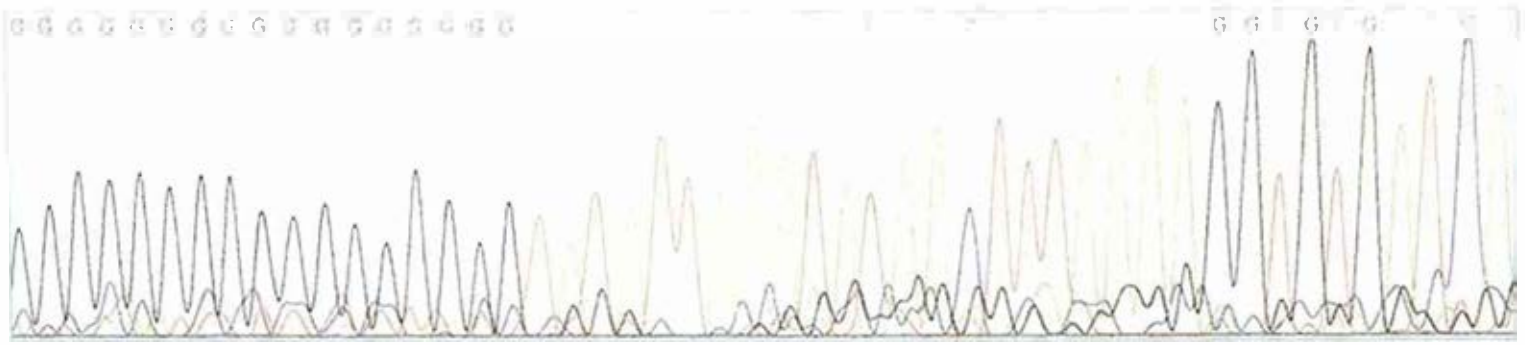

Figure 3.3. Transcription start mapping of the *hcp/hcr* operon. Total RNA of strain RK4353 expressing HCP was isolated and used as a template in a reverse transcription reaction to synthesise cDNA. The cDNA was poly-C tailed and used as a template for a PCR reaction, and the PCR product was sequenced. The poly-G tail (complementary to poly-C) was located upstream from the sequence 5'-TATATTAAA-3', indicating that the transcription start site is located at the first thymine nucleotide of this sequence.

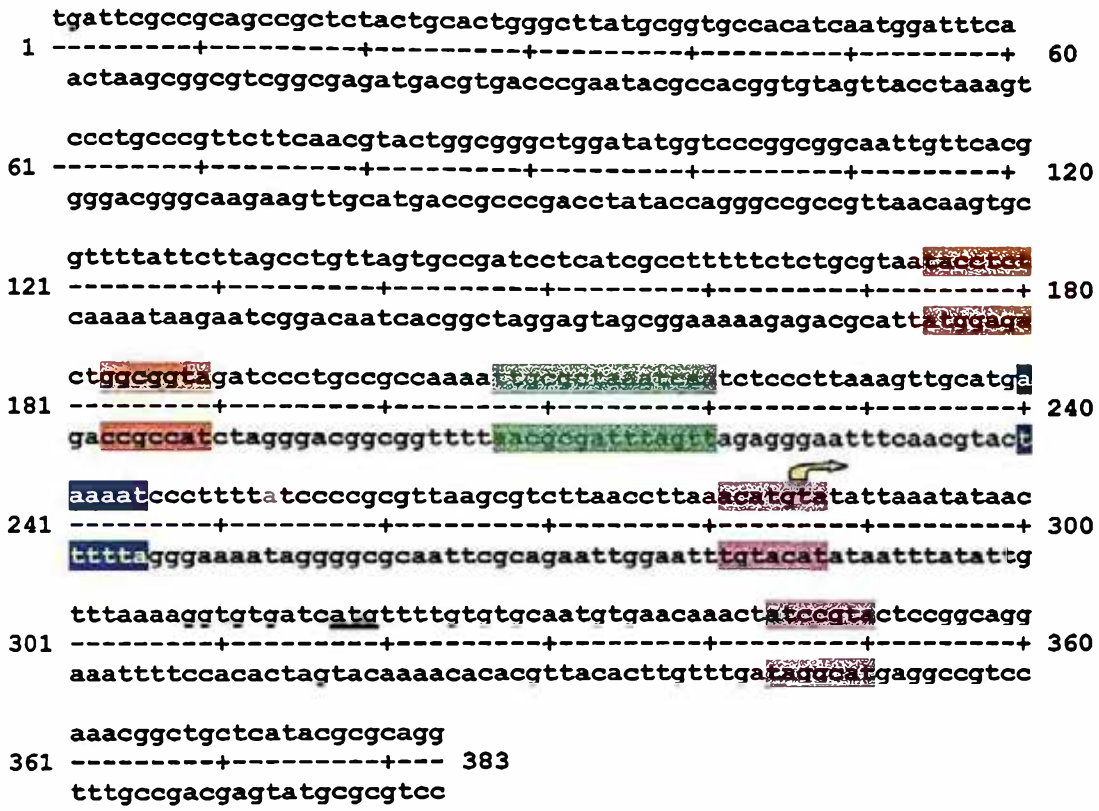

Figure 3.4. Transcription start site of the *hcp/hcr* operon. One transcription start site of the *hcp/hcr* operon was identified and was shown to be located at a thymine nucleotide 31 bp upstream of the translation-initiation codon. The transcription start site is indicated with an arrow. This locates the FNR binding consensus sequence and the NarL/NarP 7-2-7 consensus sequence at nucleotides 72.5 and 104.5 upstream from the transcription start site, respectively. The demonstrated transcription initiation site places the two NarL single heptamers 2 nucleotides upstream and 61 nt downstream from the transcription start site.

The PCR product was also subcloned into the pGEM-Teasy vector, and several clones containing the recombinant plasmid were sequenced. This confirmed the transcription start site to be located at the thymine nucleotide previously identified by sequencing of the PCR product (**figure 3.3**). This transcription initiation site located the FNR binding sequence at nucleotide 72.5 upstream from the transcription start (**figure 3.4**). This promoter arrangement is similar to that of the *napF* (for nitrate reductase in the periplasm) gene, indicating that the *hcp* promoter is a class I FNR-dependent promoter (Wing et al., 1995). The initiation site placed the NarL/NarP 7-2-7 consensus sequence at 104.5 nucleotides upstream, and two NarL single heptamers 2 nucleotides upstream and 61 nt downstream from the transcription start site.

3.4. Construction of the pNF383 plasmid to test the activity of the *hcp* promoter under different conditions

To monitor the *hcp* promoter activity, the promoter was cloned into a *lacZ* expression vector, pAA182, to create an *hcp*::*lacZ* fusion. Two primers, hcp-prom1 with an *Eco*RI site and hcp-prom2 with a *Hin*dIII site, were used to amplify the *hcp* regulatory region. The DNA fragment was subcloned into the *Eco*RI-*Hin*dIII vector fragment of pAA182, which created the recombinant plasmid, pNF383. The recombinant plasmid was sequenced to confirm the presence of the *hcp* regulatory region.

Strain RK4353 was transformed with either the promoterless vector pAA182 or with pNF383. The transformants were grown to exponential phase either aerobically in LB or anaerobically in MS medium supplemented with glycerol and fumarate, and the ß-galactosidase activity of each culture was measured. As expected no enzyme activity was observed in the strain transformed with the promoterless plasmid pAA182 after growth under aerobic or anaerobic conditions (**figure 3.5**). Enzyme activity in RK4353/pNF383

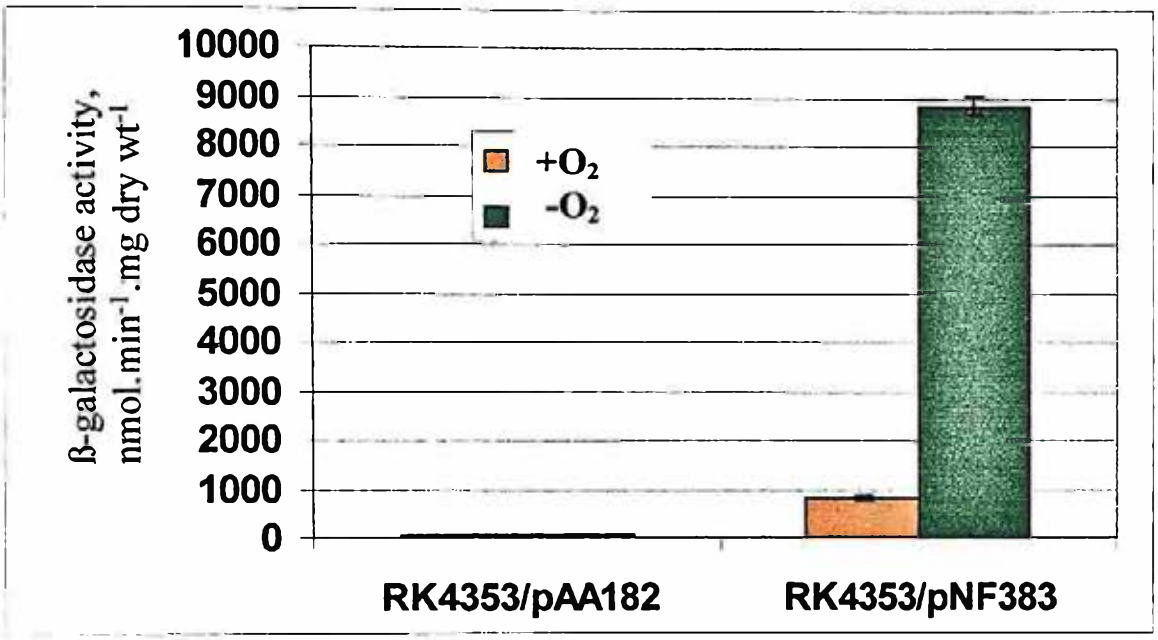

Figure 3.5. Transcription from the *hcp* promoter in plasmid pNF383 during aerobic and anaerobic growth. Strain RK4353 was transformed with either the promoterless pAA182 plasmid or with an *hcp::lacZ* fusion plasmid, pNF383. The transformants were grown to exponential phase either aerobically in LB or anaerobically in MS medium supplemented with glycerol and fumarate, and the ß-galactosidase activity of each culture was measured. Units of β-galactosidase activity are nmol.min^{-1}.mg dry weight^{-1}. Values are the averages of data from two independent cultures each assayed in duplicate. The error bars indicate the standard deviation of the mean.

was about 800 and 9 000 units after aerobic and anaerobic growth, respectively, confirming that the *hcp.:lacZ* fusion had been successfully constructed in pNF383. This also showed that the *hcp* promoter was almost inactive under aerobic conditions and became activated during anaerobic growth. This finding is consistent with a previous report that HCP was present in cultures that had been grown anaerobically (van den Berg et al., 2000).

3.5. Construction of the *arcA* deletion strains

There are two systems that regulate transcription of different genes in response to anaerobiosis, the FNR protein and ArcB-ArcA two-component system. To check whether the *hcp* promoter is dependent on the ArcB-ArcA two-component signal transduction system, an ArcA deletion mutant was created using the one-step method of Datsenko and Wanner (2000).

The *arcA* gene in strain JCB387 was replaced with a chloramphenicol resistance cassette (*cat*). The *cat* cassette with the *arcA* flanking regions was generated by PCR using the primers arcA-del1 and arcA-del2 and pKD3 plasmid DNA as a template. Strain JCB387 was transformed first with plasmid pKD46, encoding the proteins required for homologous recombination, and then with the above PCR product. Chloramphenicol resistant transformants were selected.

The JCB387 parental strain and its *arcA::cat* derivative strain, JCB38705, were tested for the presence of the *cat* cassette with the following primers: $KD3_{c1}$ and $KD3_{c2}$ that are the forward and the reverse primers to the *cat* cassette and arcA-upstream and arcA-downstream primers that are the locus-specific primers to the *arcA* gene. The following pairs of primers were used: $KD3_{c1}$ with arcA-upstream; $KD3_{c2}$ with arcA-downstream; and arcA-upstream with arcA-downstream. As expected, no PCR product was generated in the parental strain, JCB387, with $KD3_{c1}$ and $KD3_{c2}$ primers that anneal to the *cat* cassette (**figure 3.6**). All

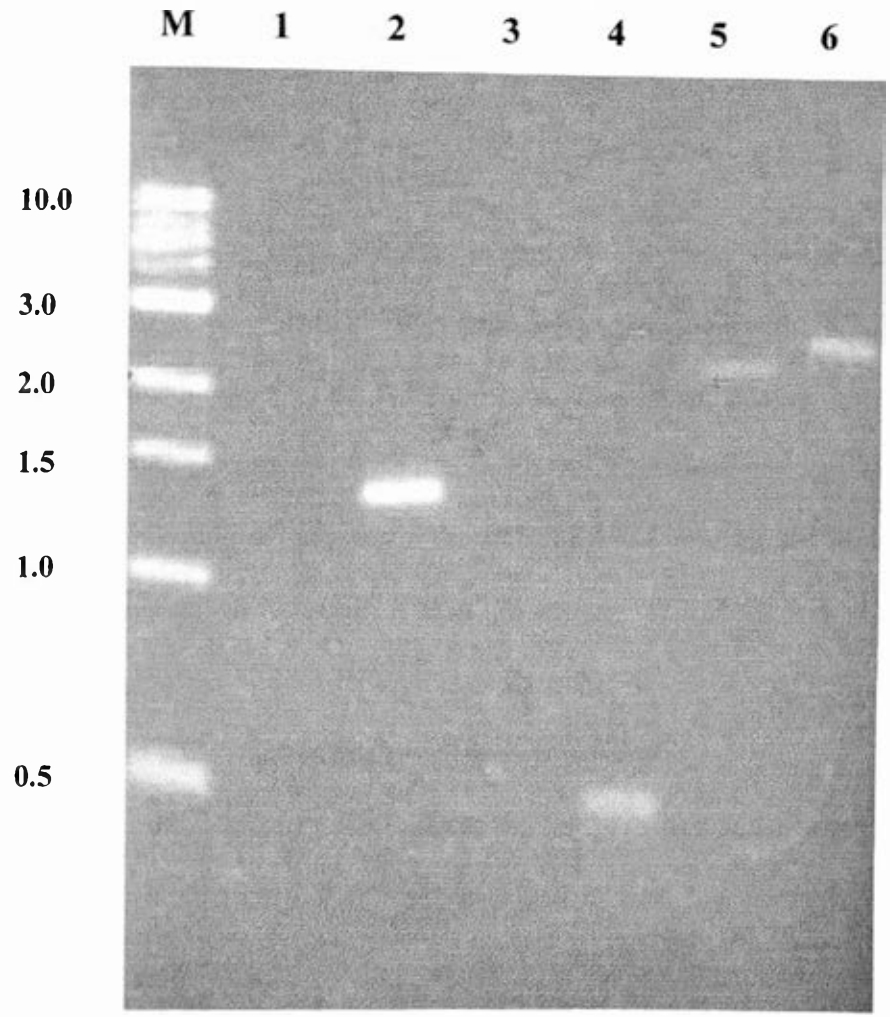

Figure 3.6. PCR products amplified from DNA of strains JCB387 and JCB38705 (*arcA::cat*) to check the presence of the *cat* cassette. The *arcA* gene was replaced with a chloramphenicol resistance cassette (*cat*) and the JCB387 parental strain and the mutant were tested with 3 pairs of primers for the presence of the *cat* cassette. The following pairs of primers were used: $KD3_{c1}$ with arcA-upstream, $KD3_{c2}$ with arcA-downstream and arcA-upstream with arcA-downstream. **Lane M:** 1 kb DNA marker; **lane 1:** JCB387 with $KD3_{c1}$ and arcA-upstream pair of primers; **lane 2:** JCB387*arcA::cat* with $KD3_{c1}$ and arcA-upstream; **lane 3:** JCB387 with $KD3_{c2}$ and arcA-downstream; **lane 4:** JCB387*arcA::cat* with $KD3_{c2}$ and arcA-downstream; **lane 5:** JCB387 with arcA-upstream and arcA-downstream; **lane 6:** JCB387*arcA::cat* with arcA-upstream and arcA-downstream.

combinations of primers in JCB387 *arcA::cat* generated DNA products of a correct size, namely approximately 1.4 kb, 0.4 kb and 2.5 kb DNA bands when $KD3_{c1}$ with arcA-upstream, $KD3_{c2}$ with arcA-downstream and arcA-upstream with arcA-downstream pairs of primers, respectively, had been used. It was concluded that the *arcA* gene in strain JCB387 had been replaced by the *cat* cassette.

To create an *arcA fnr* double mutant, the *arcA::cat* cassette was transferred from JCB38705 to strain JCB3871 by phage P1 transduction with selection for chloramphenicol resistant transductants. The Cm resistant transductants were purified and tested for the presence of the *cat* cassette with $KD3_{c1}$, $KD3_{c2}$, arcA-upstream and arcA-downstream primers. The presence of the *cat* cassete in the JCB3871 was confirmed with three combinations of the primers as described for strain JCB38705 above.

3.6. Fnr and ArcA dependence of the *hcp* promoter

To monitor the *hcp* promoter activity in the presence and absence of FNR and ArcA, the pNF383 plasmid with the *hcp::lacZ* fusion was transformed into the strains JCB387 (*fnr*$^+$ *arcA*$^+$ *Δlac*), JCB38705 (*fnr*$^+$ *arcA::cat Δlac*), JCB3871 (*fnr arcA*$^+$ *Δlac*) and JCB38715 (*fnr arcA::cat Δlac*). Bacteria were grown either aerobically in LB or anaerobically in MS supplemented with glycerol and fumarate, and β-galactosidase activities were determined. As expected, in the *fnr*$^+$ *Δlac* strain, JCB387, expression was very low during aerobic growth but induced during anaerobic growth (**figure 3.7**, panel 1). Absolutely no anaerobic induction was observed in the FNR-deficient strain, JCB3871 (**figure 3.7, panel 3**), which suggested that under anaerobiosis FNR is an activator of the *hcp* promoter.

Under anaerobic conditions β-galactosidase expression was not significantly different in the *arcA*$^+$ and *arcA* strains. In the *fnr*$^+$ *arcA Δlac* mutant during aerobic growth β- galactosidase

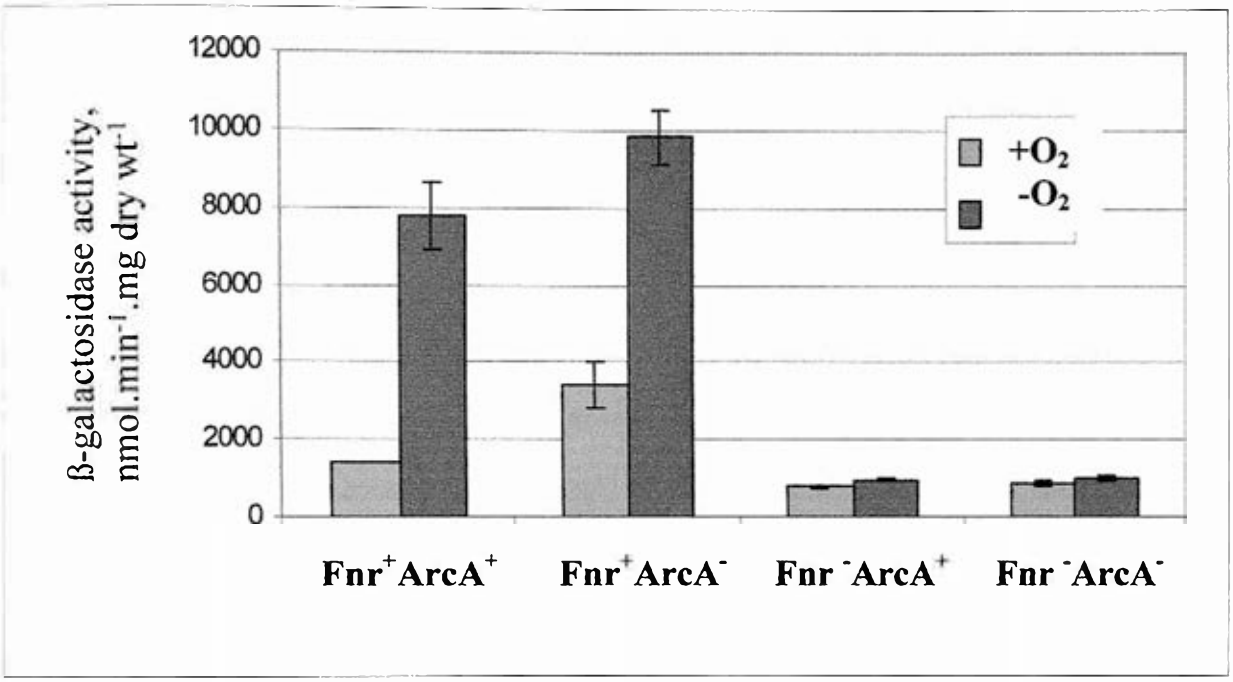

Figure 3.7. Effect of Fnr and ArcA on transcription at the *hcp* promoter. The parental strain (JCB387) and strains lacking either ArcA (JCB38705) or FNR (JCB3871), or both FNR and ArcA (JCB38715) were transformed with the *hcp::lacZ* fusion plasmid pNF383. The purified transformants were grown both aerobically in LB and anaerobically in MS medium supplemented with glycerol and fumarate. The β-galactosidase activity of each culture was measured. Units of β-galactosidase activity are nmol.min^{-1}.mg dry weight^{-1}. Values are the averages of data from two independent cultures each assayed in duplicate. The error bars indicate the standard deviation of the mean.

expression from the *hcp* promoter was 2.4 times higher than in the *fnr*$^{+}$*arcA*$^{+}$*Δlac* strain, which might be explained by some indirect influence of ArcA on the promoter as there is no binding site of ArcA in the *hcp* regulatory region. It was concluded that anaerobic induction of the *hcp* promoter is due to the transcription regulator, FNR, and that the ArcB/ArcA system apparently plays no direct role in the regulation of the *hcp* promoter.

3.7. NorR dependence of the *hcp* promoter

Transcription of the *hcp* gene was observed to increase in infected with *S. enterica* macrophages upon induction of nitric oxide synthase (NOS) (Kim et al., 2003), which implicates HCP in the detoxification of nitric oxide. There are three enzymes capable of reducing NO in *E. coli*: two nitric oxide reductases, HMP and NorV; and nitrite reductase, NrfA (Poock et al., 2002). NorV is regulated by the transcription regulator NorR. To test whether NorR regulates transcription from the *hcp* promoter, a strain defective in the synthesis of NorR, JCB4401, was prepared by P1 transduction of a *norR::cat* cassette into *E. coli* strain RK4353. Strains RK4353 and JCB4401 were transformed with plasmid pNF383, carrying the *hcp::lacZ* fusion. The strains were grown anaerobically in MS medium supplemented with LB, glucose and nitrate as an electron acceptor. The transformants were assayed for β-galactosidase activity at different stages of growth (**figure 3.8**).

Despite some minor differences in the β-galactosidase activity in *norR*$^{+}$ and *norR* strains observed at 0.5 and 0.95 OD_{650} units, generally *norR*$^{+}$ and *norR* strains did not show any statistically significant differences in transcription from the *hcp* promoter. Thus, it was concluded that NorR is not a regulator of HCP under the conditions tested.

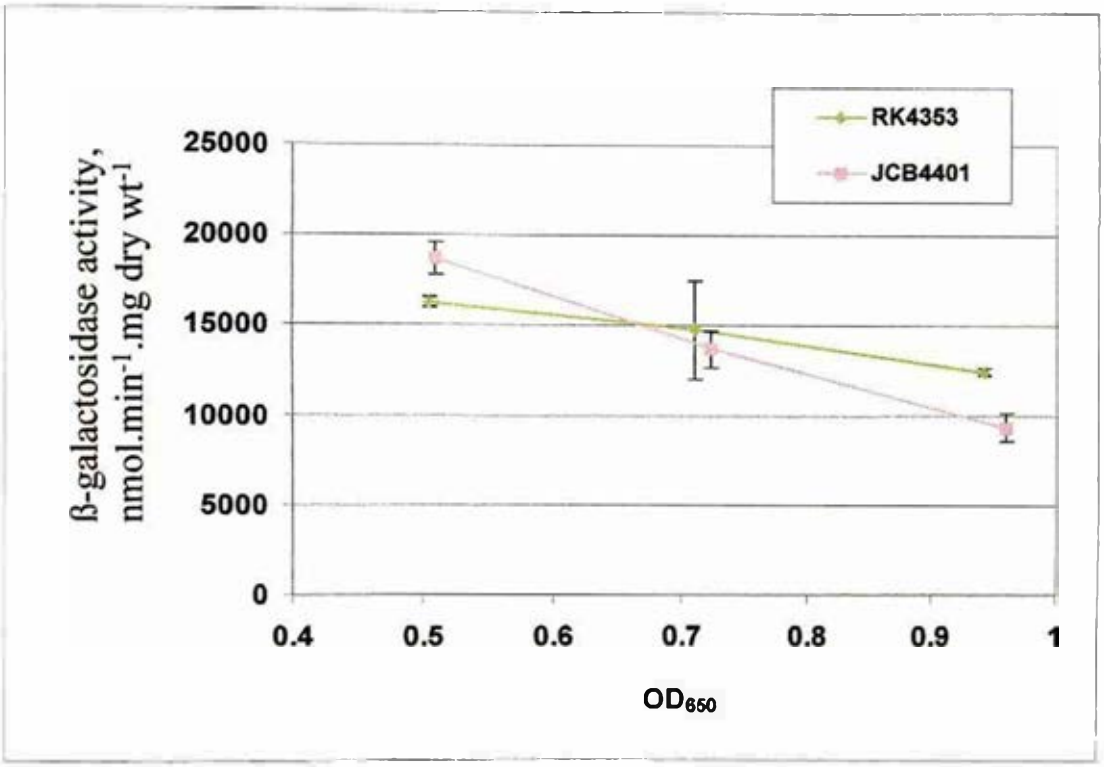

Figure 3.8. NorR dependence of the *hcp* promoter. Strains RK4353 and JCB4401 (RK4353 *norR*) were transformed with the *hcp::lacZ* fusion plasmid pNF383 and grown anaerobically in MS medium supplemented with nitrate. The β-galactosidase activity was assayed at different stages of growth. Units of β-galactosidase activity are nmol ONP formed.min^{-1}.mg dry weight^{-1}. Values are the averages of data from two independent cultures. The error bars indicate the standard deviation of the mean.

3.8. The effect of fumarate, DMSO and TMAO on transcription activation at the *hcp* promoter

When oxygen is absent from the medium, other electron acceptors can be used by bacteria. Preference is given to nitrate and nitrite, but when they are not present, fumarate, DMSO or TMAO can be reduced, which is then linked to the formation of the electrochemical proton gradient. As HCP is expressed in the absence of oxygen, fumarate, DMSO or TMAO were tested for their ability to activate transcription from the *hcp* promoter. Strain RK4353 transformed with pNF383 was grown anaerobically in MS medium supplemented with 20% LB, 0.4% glycerol (v/v) and also anaerobically in the same medium supplemented with 20 mM fumarate, 70 mM DMSO or 90 mM TMAO as electron acceptors. The cultures were assayed for β- galactosidase activity when the OD_{650} was between 0.5 and 0.8 (**figure 3.9**). The activity of the *hcp* promoter after anaerobic growth with glycerol was 4 000 units and the activities of the promoter after growth in the presence of fumarate, DMSO or TMAO were approximately the same, 4300, 3700, and 4100 units, respectively (**figure 3.9**). It was concluded that fumarate, DMSO and TMAO had no effect on the rate of transcription from the *hcp* promoter.

3.9. The effect of glucose on the *hcp* promoter

Many promoters are subject to carbon catabolite repression. To find out whether the *hcp* promoter is also subject to carbon catabolite repression and to test the ability of glucose to repress the *hcp* promoter, strain RK4353 was transformed with the *hcp::lacZ* fusion plasmid pNF383 and grown in MS, LB medium supplemented either with 0.4% (v/v) glycerol and 20 mM fumarate or with 0.4% (w/v) glucose. The cultures were grown aerobically, anaerobically, anaerobically with nitrite and anaerobically with nitrate and the β-galactosidase activity was measured when the OD_{650} was between 0.5 and 0.8 units

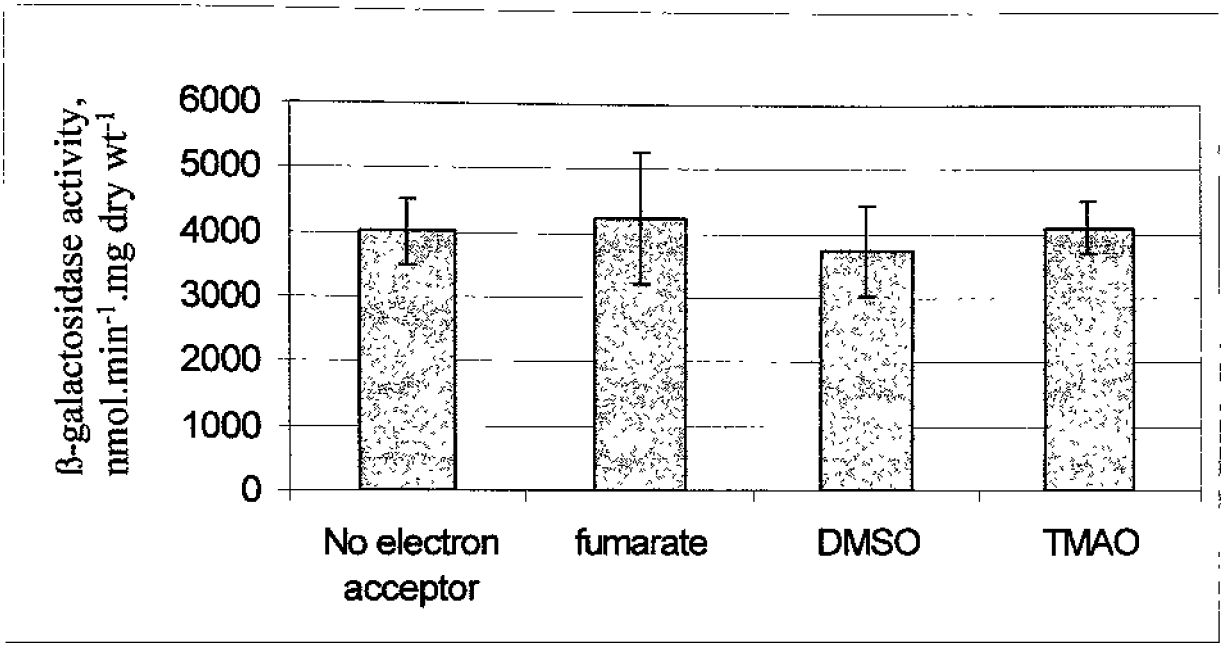

Figure 3.9. Effect of fumarate, DMSO and TMAO on transcription from the *hcp* promoter. Strain RK4353 was transformed with plasmid pNF383 and grown anaerobically with or without 20 mM fumarate, 70 mM DMSO and 90 mM TMAO as electron acceptors. The cultures were assayed for β-galactosidase activity when OD_{650} was between 0.5 and 0.8. Values are the averages of data from two independent cultures each assayed in duplicate. The error bars indicate the standard deviation of the mean.

(**figure 3.10**). The β-galactosidase activities in cultures grown aerobically, anaerobically and anaerobically with nitrite in medium supplemented with glucose were only slightly lower than those in medium supplemented with glycerol, but were not significantly different. This suggested that the *hcp* promoter is not catabolite repressed by glucose.

3.10. The effect of nitrite and nitrate on transcription from the *hcp* promoter measured during the growth cycle

Previously in this work it was shown that the *hcp* promoter became activated during anaerobiosis and that this activation was mediated by FNR. It has also been reported that HCP was found in cultures grown anaerobically in the presence of nitrite or nitrate (van den Berg et al., 2000). The effect of nitrite and nitrate on transcription from the *hcp* promoter in plasmid pNF383 was therefore determined. As bacteria grow faster with glucose than with glycerol as the main carbon and energy source, and because glucose does not decrease transcription from the *hcp* promoter, glucose was used as a carbon source instead of glycerol. Strain JCB302 was transformed with the *hcp::lacZ* fusion plasmid pNF383 and grown anaerobically in MS medium supplemented with 10% (v/v) LB and 0.4% (w/v) glucose, and also anaerobically in the same medium supplemented with nitrite or nitrate. The cultures were assayed for β-galactosidase activity at different optical densities during growth (**figure 3.11a**). After anaerobic growth promoter activity was around 19 000 units. The activity was increased upon addition of nitrate and still further increased upon addition of nitrite. Thus, it was shown that transcription from the *hcp* promoter is activated by both nitrite and nitrate.

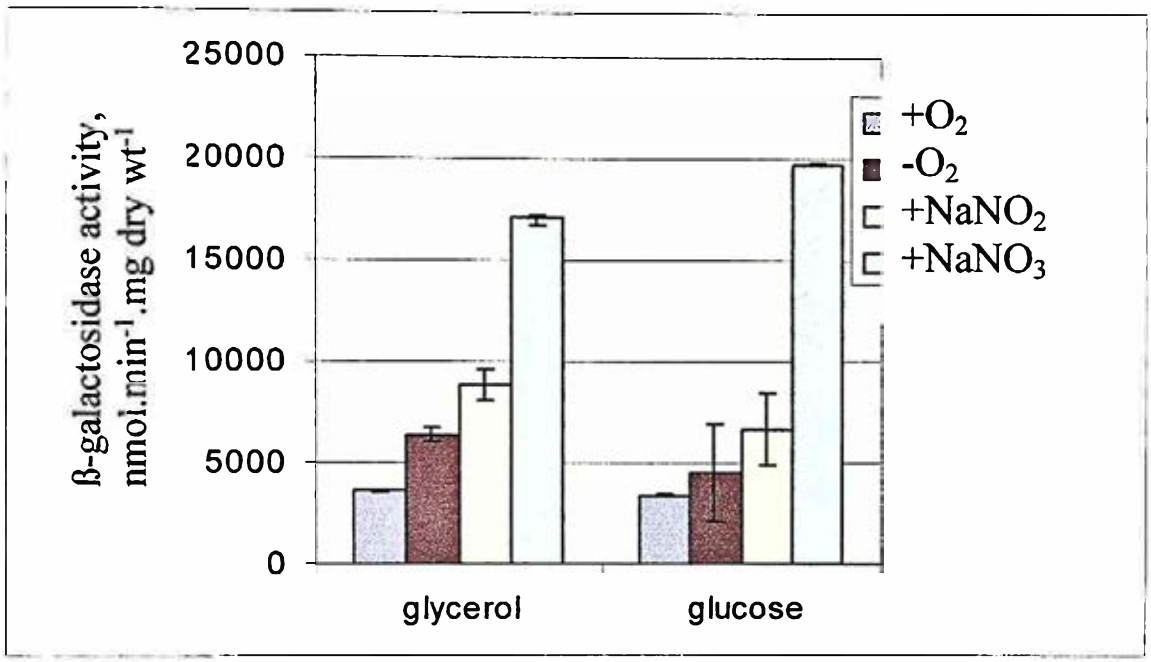

Figure 3.10. Effect of glucose on transcription from the *hcp* promoter. Strain RK4353 was transformed with pNF383 carrying an *hcp::lacZ* fusion and was grown in MS medium supplemented with either 0.4% glycerol and 20 mM fumarate or with 0.4% glucose. The β-galactosidase activity was measured when the culture OD_{650} was between 0.5 and 0.8. Values are the averages of data from two independent cultures each assayed in duplicate. The error bars show the standard deviation of the mean. The β-galactosidase activities in cultures grown with glucose were not significantly different from those grown in medium supplemented with glycerol, as calculated with the t-test.

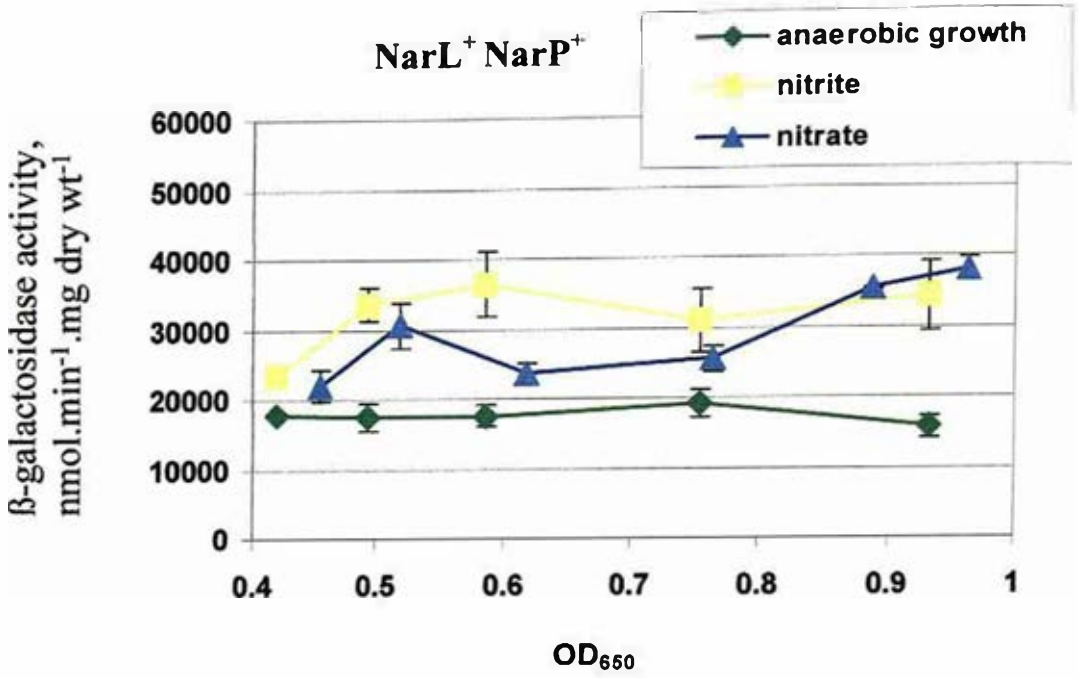
NarL+ NarP+
anaerobic growth
nitrite
nitrate
ß-galactosidase activity, nmol.min-1.mg dry wt-1
60000
50000
40000
30000
20000
10000
0
0.4
0.5
0.6
0.7
0.8
0.9
1
OD650

a)

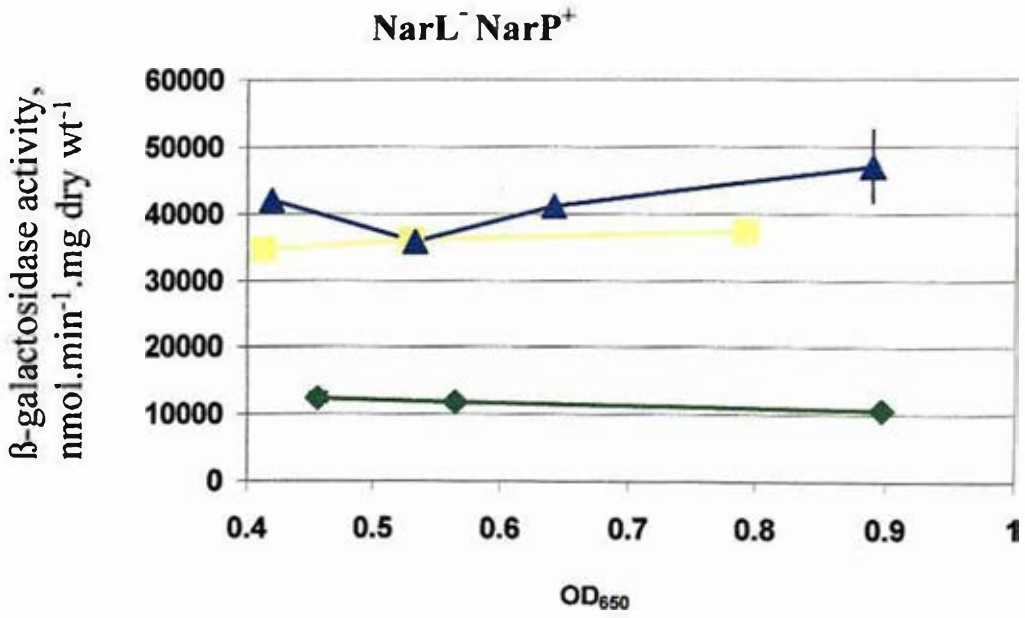
NarL- NarP+
ß-galactosidase activity, nmol.min-1.mg dry wt-1
60000
50000
40000
30000
20000
10000
0
0.4
0.5
0.6
0.7
0.8
0.9
1
OD650

b)

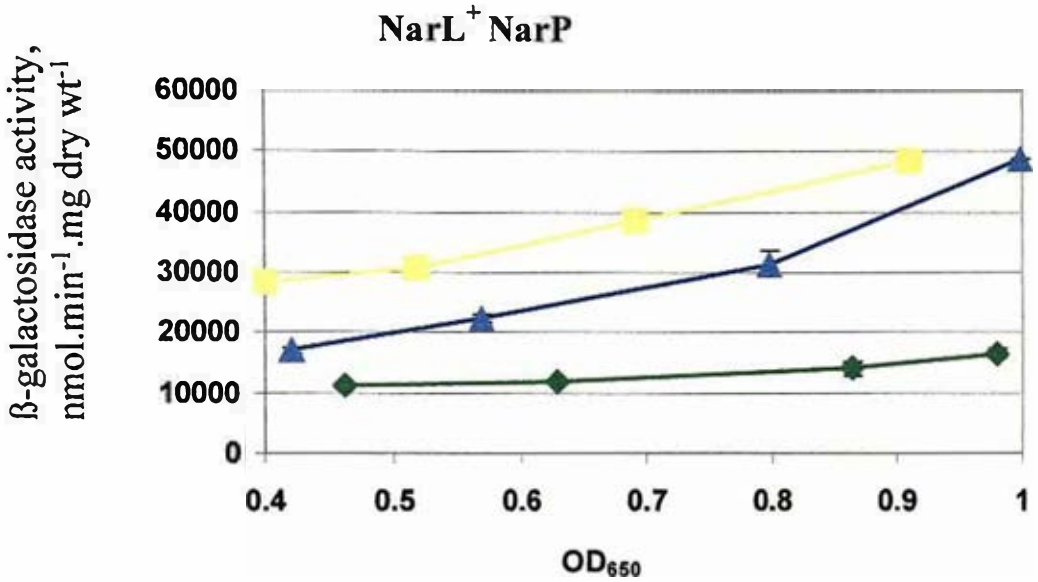
NarL+ NarP
ß-galactosidase activity, nmol.min-1.mg dry wt-1
60000
50000
40000
30000
20000
10000
0
0.4
0.5
0.6
0.7
0.8
0.9
1
OD650

c)

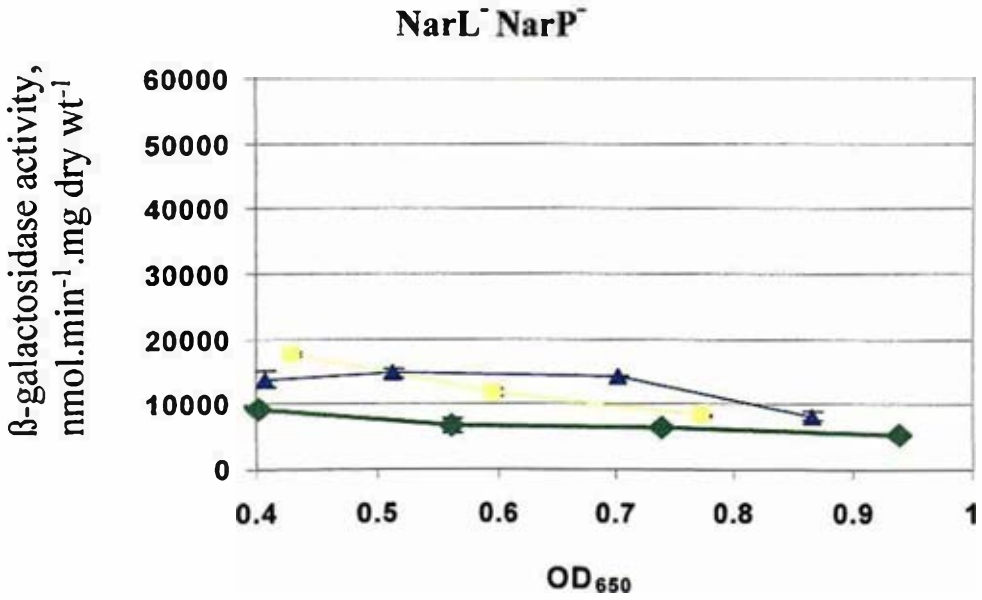
NarL- NarP-
ß-galactosidase activity, nmol.min-1.mg dry wt-1
60000
50000
40000
30000
20000
10000
0
0.4
0.5
0.6
0.7
0.8
0.9
1
OD650

d)

Figure 3.11. The effect of nitrite and nitrate and response regulators NarL and NarP on transcription from the *hcp* promoter measured during the growth cycle. The parental strain, JCB302, and the *narL* mutant, JCB3893, the *narP* mutant, JCB3875 and the *narLnarP* mutant, JCB3894, were transformed with pNF383 and grown anaerobically (green), anaerobically with nitrite (yellow) and anaerobically with nitrate (blue). The β-galactosidase activities of the cultures were measured at different optical densities during growth. **a:** the parental strain, JCB302; **b:** the *narL* mutant, JCB3893; **c:** the *narP* mutant, JCB3892; **d:** the *narL narP* mutant, JCB3894. Values are the averages of data from two independent cultures each assayed in duplicate. The error bars show the standard deviation of the mean; some of the error bars are hidden by the bullet points.

3.11. The effect of response regulators NarL and NarP on nitrite and nitrate dependent expression from the *hcp* promoter measured during the growth cycle

In many bacteria nitrite- and nitrate-activated transcription is mediated by the Nar system, which comprises two sensor kinase proteins, NarX and NarQ, and two response regulators, NarL and NarP. To find out whether the response of the *hcp* promoter to nitrate and nitrite is also regulated by the Nar system, *narL* and *narP* derivatives of strain JCB302 were used. The *narL* mutant (JCB3893), *narP* mutant (JCB3875) and *narL narP* double mutant (JCB3894) were transformed with pNF383 and grown under the same conditions as described above. The β-galactosidase activities of the cultures were measured at different stages of growth.

In the *narL* mutant, *hcp* promoter activity during anaerobic growth was only about half that of the parental strain JCB302 (**figure 3.11b**). As it was shown that anaerobic activation of the *hcp* promoter is dependent on FNR, this is consistent with a previously reported result demonstrating that NarL can act as a coactivator of FNR during transcription (Wu et al., 1993). Nitrite-mediated expression of the *hcp* promoter was similar in the parental strain and in the *narL* mutant, and varied between 30 000 and 40 000 units. However, nitrate-mediated activation of the *hcp* promoter in the *narL* mutant was approximately 1.5 times higher than in the parental strain, suggesting that, in the presence of nitrate, NarL might act as a weak repressor of the *hcp* promoter. Retention of activity of the *hcp* promoter in response to both nitrate and nitrite and in the absence of NarL suggested also that NarP was acting as an activator at this promoter.

In the *narP* mutant, *hcp* promoter activity during anaerobic growth was also only about half that of the parental strain (**figure 3.11c**). The promoter activity during anaerobic growth with nitrite gradually increased from 30 000 to 50 000 units. The promoter activity

also increased from 15 000 to 50 000 units during growth in the medium supplemented with nitrate.

In the *narL narP* double mutant the nitrite- and nitrate-mediated activity of the *hcp* promoter was almost completely abolished, although some residual activity was detected (**figure 3.11d**). So, based on this series of experiments, it was concluded that NarP is an activator of the *hcp* promoter, whereas NarL might act both as an activator and a repressor depending on concentration of nitrate and nitrite.

3.12. FNR and NarL form a complex with the *hcp* promoter as shown by gel retardation assays

The sequence analysis of the *hcp* regulatory region suggested that it contains FNR and NarL binding sites. Also, the previous experiments established that both FNR and NarL regulate transcription from the *hcp* promoter. The binding of FNR and NarL to the *hcp* regulatory region prepared by digesting plasmid pNF383 with *Eco*RI and *Hind*III was investigated by gel retardation (band-shift) assays. The gel-purified promoter fragment was labelled with radioactive γ^{32}ATP and mixed with FNR or NarL at a range of concentrations. The final concentrations used were from 0.25 to 1 μM FNR or from 0.4 to 3.2 μM NarL. The reactions were incubated at 37 °C for 30 minutes and run on non-denaturing acrylamide gels for 3 to 4 hours. The gels were fixed, dried, and the fragments were detected using autoradiography.

It was shown that a shift of the free DNA band appeared starting from the concentration of 0.5 μM of FNR, indicating that FNR molecules form a complex with the *hcp* promoter (**figure 3.12a**). A single shift was observed at 0.25 and 0.5 μM concentration, which was in agreement with the presence of one FNR consensus binding site at the *hcp* region. Additional shift was observed at the highest, 1 μM, concentration of FNR, which was apparently due to the non-specific binding of FNR to the *hcp* regulatory region.

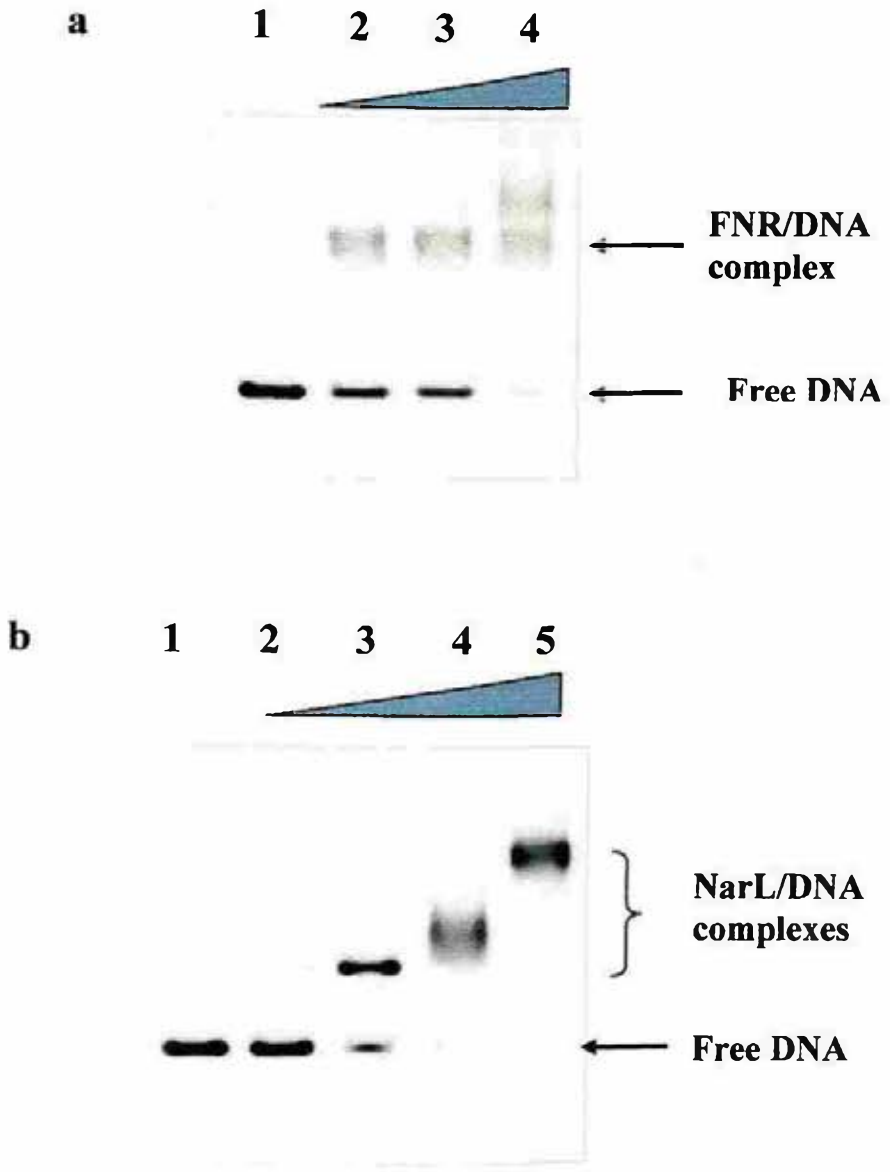

Figure 3.12. Formation of a complex of the *hcp* promoter with FNR and NarL. The *hcp* regulatory region was prepared by digesting plasmid pNF383 with *Eco*RI and *Hin*dIII. The *hcp* regulatory region was labelled with radioactive γ^{32}ATP and mixed with FNR or NarL at a range of concentrations. The reactions were incubated at 37 °C for 30 minutes and run on PAGE for 3 to 4 hours. The gels were fixed and dried, and the phosphoscreen was developed. Free DNA and complexes of DNA with FNR and NarL are denoted. **a:** gel retardation assay with FNR. Lane1. No FNR; Lane 2. 0.25 μM FNR; Lane 3. 0.5 μM FNR; Lane 4. 1.0 μM FNR. **b:** gel retardation assays with NarL. Lane 1. No NarL; Lane 2. 0.4 μM NarL; Lane 3. 0.8 μM NarL; Lane 4. 1.6 μM NarL; Lane 5. 3.2 μM NarL.

The results for NarL indicate that the *Eco*RI/*Hin*dIII fragment of the *hcp* regulatory region contains three NarL binding sites, which is in agreement with data of the *hcp* promoter sequence analysis. The first shift was observed at 0.4 μM NarL concentration, and two more shifts occurred at 1.6 μM and 3.2 μM concentration of NarL (**figure 3.12b**), suggesting that one site is a high affinity binding site, and two others are low affinity binding sites. Apparently, the first, second and the third shifts occur as a result of binding of NarL to one, two or three consensus sites at the same time, respectively. In conclusion, both FNR and NarL bind to the *hcp* promoter, suggesting that the effect of NarL and FNR on the *hcp* promoter observed *in vivo* is a result of direct binding of these regulators at the *hcp* regulatory region.

CHAPTER 4

Overproduction, purification and functional studies of the hybrid cluster protein of *E. coli*

4.1. Introduction

Despite intensive study, the physiological function of HCP is unknown. HCP accumulates in *E. coli* under nitrite or nitrate respiring conditions and the *hcp* promoter of *S. enterica* is induced by acidic nitrite as a source of reactive nitrogen species (van den Berg et al., 2000; Kim et al., 2003). This indicates that HCP might play some role in nitrogen metabolism. The finding that an *hcp* mutant of *C. perfringens* is less sensitive to peroxides suggests that HCP is linked to oxidative stress (Briolat and Reysset, 2002).

The objective of the work presented in this chapter was to construct Δ*hcp* strains to find out whether HCP confers any advantage to *E. coli* during growth in the presence of nitrate. Also investigated was whether HCP protects *E. coli* against hydroxylamine and nitric oxide toxicity *in vivo*. Another objective was to overexpress HCP and to develop a qualitative *in vitro* assay to study whether HCP reduces nitrite, nitrate or hydroxylamine.

4.2. Construction of *hcp* mutants

When bacteria are grown anaerobically on a non-fermentable carbon source and NO_3^- as an electron acceptor, growth occurs due to reduction of NO_3^- by either NAP or NRA. If HCP were involved in nitrate reduction, deletion of the *hcp* gene would affect nitrate-dependent growth. To test this hypothesis, the *hcp* gene was deleted from strains expressing both NAP and NRA, only NAP, or only NRA.

The method of Datsenko and Wanner (2000) was used to create strain JCB5000 (RK4353 *Δhcp*). First, the *hcp* gene in strain RK4353 was replaced with a chloramphenicol resistance cassette (*cat*) to give the strain JCB4999 (RK4353 *cat::hcp*). The *cat* cassette flanked by DNA upstream and downstream of the *hcp* gene was generated by PCR using hcp-del1 and hcp-del2 primers and the plasmid pKD3 as a template. Strain RK4353 was transformed with plasmid pKD46, the transformant was electroporated with the above linear

PCR product and the chloramphenicol resistant colonies were purified. To eliminate the *cat* cassette, strain JCB4999 was transformed with plasmid pCP20 and grown at 30 °C. Enzymes encoded by pCP20 are required for the excision of the *cat* cassette by recombination between two FLP sites. The RK4353 parental strain, JCB4999 and JCB5000 were tested for the presence or absence of the *hcp* gene and the *hcp::cat* cassette by PCR using the primers hcp-prom EcoRI and hcp-hcr rev BamHI that are the forward and the reverse locus-specific primers to the *hcp* gene. In all three strains, DNA products of the correct size were generated, namely of 2.0 kb, 1.8 kb and 1.0 kb in strains RK4353, JCB4999 and JCB5000, respectively (**figure 4.1, a**). So, it was demonstrated that in JCB4999 the *hcp* gene had been successfully replaced with a *cat* cassette and that in JCB5000 the *cat* cassette had been deleted. To create the *hcp* deletion in other genetic backgrounds the *hcp::cat* casette was transferred from JCB4999 to JCB4011 (RK4353 *ΔnapA-B*) and to JCB4041 (RK4353 *ΔnarG-I*) by phage P1 transduction.

Bacteriophage P1, propagated on the donor strain, JCB4999, was used to transduce the acceptor strains, and chloramphenicol resistant transductants were selected. Purified transductants were designated strains JCB4310 (JCB4011 *hcp::cat*) and JCB4340 (JCB4041 *hcp::cat*), respectively. The Cm resistant transductants were purified and tested for the presence of the *cat* cassette with primers hcp-upstream/$KD3_{c1}$ and hcp-downstream/$KD3_{c2}$. The presence of the *cat* cassette in JCB4310 and JCB4340 was confirmed with both combinations of primers (**figure 4.1, b**).

To remove the *cat* cassette, strains JCB4310 and JCB4340 were transformed with plasmid pCP20 and grown first at 37 °C and subsequently at 42 °C. The candidates were tested with two pairs of primers: hcp-upstream with $KD3_{c1}$ and with hcp-downstream and $KD3_{c2}$. No PCR product was generated in either candidate with both pairs of primers, which demonstrated that the *cat* cassette, to which $KD3_{c1}$ and $KD3_{c2}$ anneal, had been lost. The *hcp*

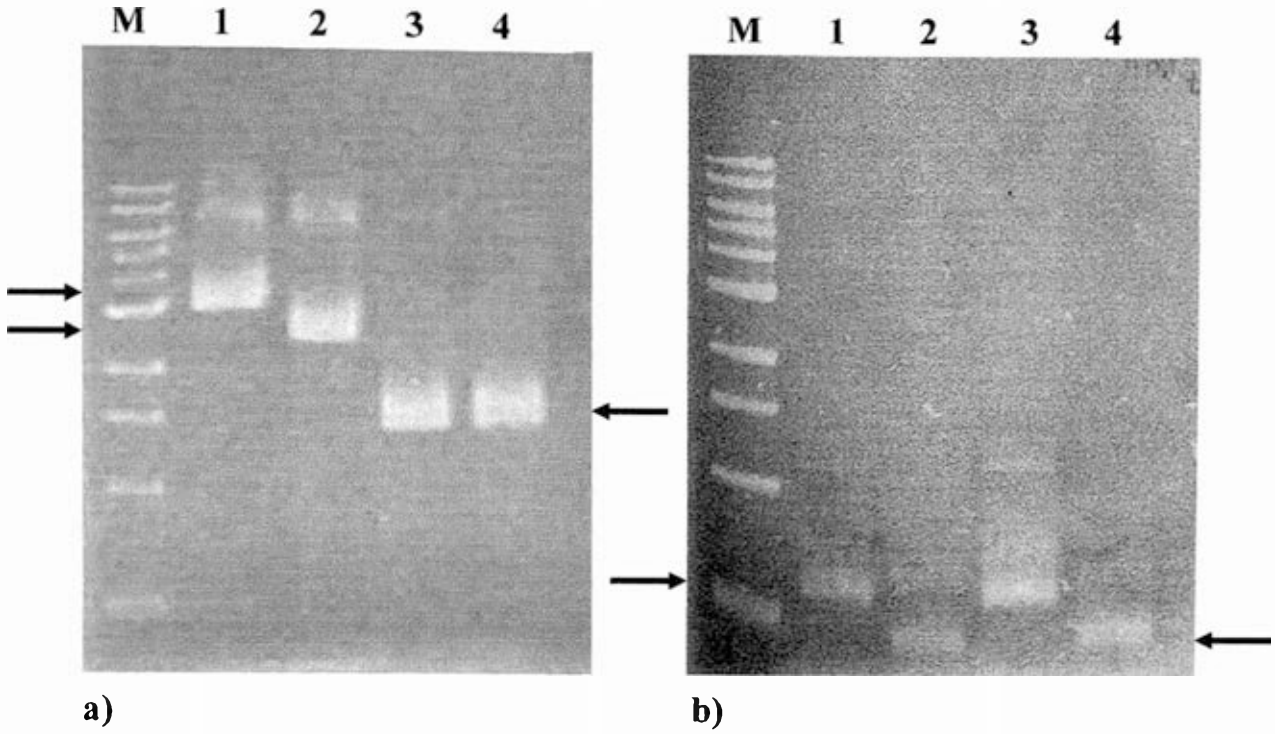

Figure 4.1. PCR analysis for the presence of the *cat* cassette and the *hcp* gene in strains RK4353, JCB4011 and JCB4041 and their *Δhcp* derivatives.

a. The *hcp* gene was replaced with a chloramphenicol resistance cassette (*cat*) and the *cat* cassette was subsequently deleted. Strains RK4353, JCB4999 (RK4353 *hcp::cat*) and JCB5000 (RK4353 *Δhcp*) were grown on agar plates and tested by colony PCR with primers hcp-prom EcoRI and hcp-hcr rev BamHI. **Lane M**: 1 kb DNA marker. The sizes of bands in kb are given to the left; **lane 1:** RK4353 as a template; **lane 2**: JCB4999 as a template; **lanes 3 and 4**: two different clones of JCB5000 as a template.

b. To create the *hcp* deletion in other genetic backgrounds the *hcp::cat* was transferred from JCB4999 to JCB4011 (RK4353 *ΔnapA-B*) and JCB4041 (RK4353 *ΔnarG-I*) by phage P1 transduction, which created strains JCB4310 (JCB4011 *hcp::cat*) and JCB4340 (JCB4041 *hcp::cat*). The Cm resistant derivatives of the recipient strains were purified and tested for the presence of the *cat* cassette with two pairs of primers. **Lane M**: 1 kb DNA marker; **lane 1:** JCB4310 with primers hcp-upstream and $KD3_{c1}$; **lane 2**: JCB4310 with hcp-downstream and $KD3_{c2}$; **lanes 3** JCB4340 with hcp-upstream and $KD3_{c1}$; **lane 4**: JCB4310 with hcp-downstream and $KD3_{c2}$.

null derivatives of JCB4310 and JCB4340 were designated JCB4311 (RK4353 *ΔnapA-B Δhcp*) and JCB4341 (RK4353 *ΔnarG-I Δhcp*), respectively.

4.3. HCP and nitrate-dependent growth

To test whether HCP is involved in nitrate-dependent growth, parental strains RK4353, JCB4011, JCB4041 and also JCB5000, JCB4311 and JCB4341 as their *hcp* null derivatives were grown anaerobically in MS medium supplemented with 2.5 g/l nutrient broth, 0.4% (v/v) glycerol and 20 mM $NaNO_3$. The OD_{650} of the cultures was measured every hour during growth (**figure 4.2**). Slight differences in optical density were noticed between RK4353 or JCB4011 and their *hcp* derivatives at the lag phase of growth, being lower for the *hcp* strains. However, no difference in optical density was observed during the exponential phase of growth within each of three pairs of the wild type and the *hcp* deletion mutant. There was also no significant difference in the cell yield between a parental strain and its *hcp* derivative for each pair of strains. Therefore, it was concluded that HCP is not essential for nitrate dependent growth of strains expressing only NRA, only NAP, or both NRA and NAP.

4.4. Effect of hydroxylamine on anaerobic growth in the presence of a non-fermentable carbon source

Previous reports that HCP from both *E. coli* and other bacteria is a hydroxylamine reductase raised the possibility that it might protect *E. coli* from hydroxylamine toxicity. It was also possible that HCP might enable *E. coli* to grow anaerobically in the presence of a non-fermentable carbon source with hydroxylamine as a terminal electron acceptor. To test these possibilities, strain RK4353 was grown in MS supplemented with 2.5% LB, glycerol and a range of hydroxylamine concentrations, but no other terminal electron

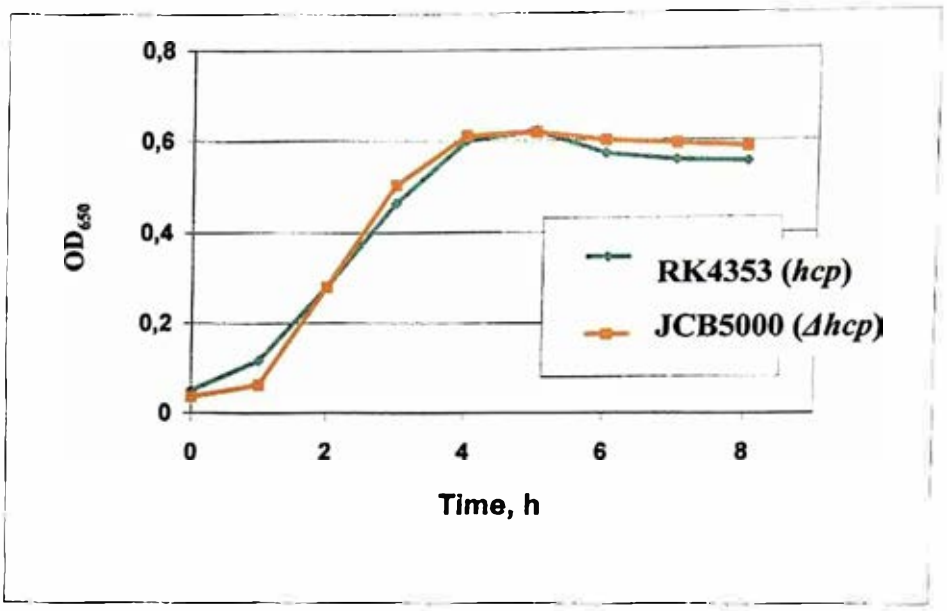
0,8
0,6
0,4
0,2
0
OD650
0
2
4
6
8
Time, h
RK4353 (hcp)
JCB5000 (Δhcp)

a)

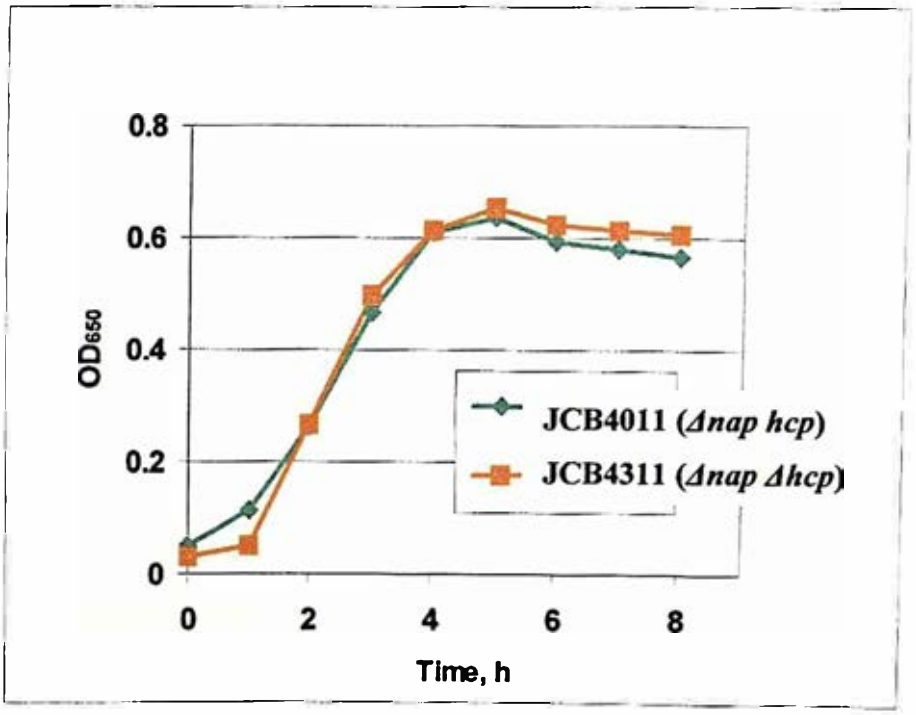
0.8
0.6
0.4
0.2
0
OD650
0
2
4
6
8
Time, h
JCB4011 (Δnap hcp)
JCB4311 (Δnap Δhcp)

b)

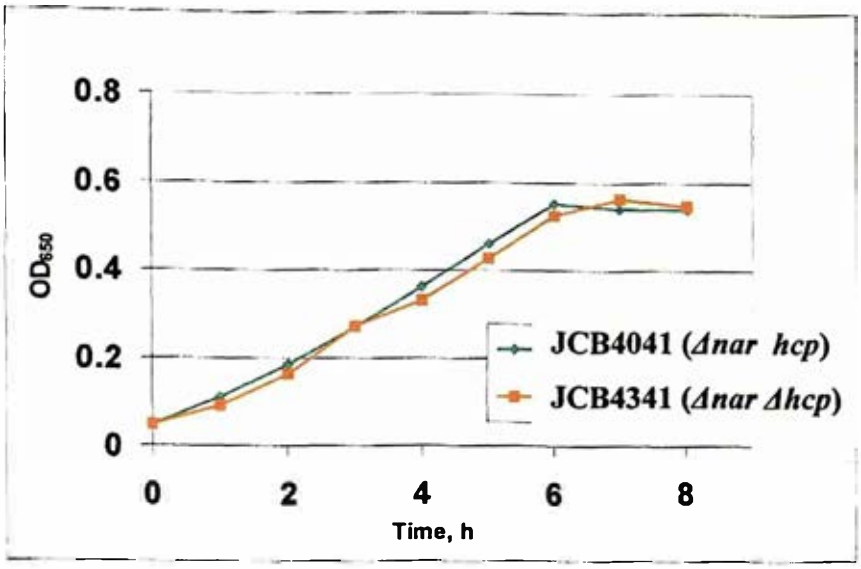

c)

Figure 4.2. Effect of an *hcp* mutation on nitrate-dependent growth. Strains RK4353 and JCB5000 (RK4353 *Δhcp*) (**a**), JCB4011 (*ΔnapA-B*) and JCB4311 (JCB4011 *Δhcp*) (**b**), JCB4041 (*ΔnarG-I*) and JCB4341 (JCB4041 *Δhcp*) (**c**) were grown in MS medium supplemented with 2.5 g/l nutrient broth, 0.4% (v/v) glycerol and 20 mM $NaNO_3$. The OD_{650} was measured every hour during the growth cycle.

acceptor. Virtually no growth was detected even after 66 h in cultures supplemented with 1mM or higher concentrations of hydroxylamine, and even 0.5 mM hydroxylamine strongly inhibited growth (**figure 4.3, a**). Lower concentrations of hydroxylamine inhibited the rate of growth, but did not significantly affect the final growth yield. Consequently, no evidence was obtained that hydroxylamine can be used as a terminal electron acceptor. Furthermore, in the absence of the LB supplement, even 0.2mM hydroxylamine was sufficient to strongly inhibit growth (**figure 4.3, b**).

To determine whether HCP protects *E. coli* against hydroxylamine toxicity, strain RK4353 and its *hcp* derivative were grown in the same medium with a range of hydroxylamine concentrations, but nitrate was also added as a terminal electron acceptor. Growth of both strains was again totally inhibited by 1mM hydroxylamine, and at lower concentrations there were no significant differences in hydroxylamine toxicity between the two strains (**figure 4.4**). It was concluded that HCP does not significantly protect *E. coli* against hydroxylamine toxicity.

4.5. Effect of hydroxylamine on transcription activation at the *hcp* promoter

Hydroxylamine was tested for its ability to activate transcription from the *hcp* promoter. Strain RK4353 transformed with pNF383 was grown anaerobically in MS medium supplemented with fumarate and glycerol in the presence or absence of 0.1 mM hydroxylamine. The cultures were assayed for β-galactosidase activity when the OD_{650} of the cultures was between 0.5 and 0.8. Similar β-galactosidase activities were detected in both cultures, 8 000 and 9 500 units for cultures grown without and with 0.1 mM HA, respectively (**figure 4.5**). Thus, the presence of hydroxylamine during growth did not significantly activate transcription from the *hcp* promoter. A substrate of an enzyme does not always activate transcription of a gene encoding this enzyme (da Costa et al., 2003),

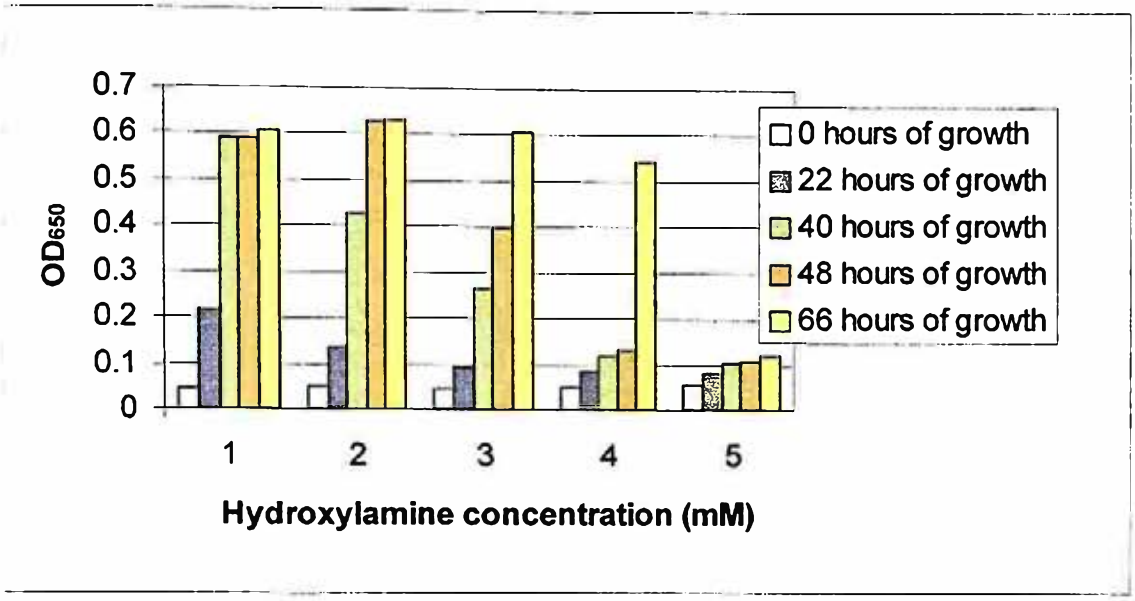

a)

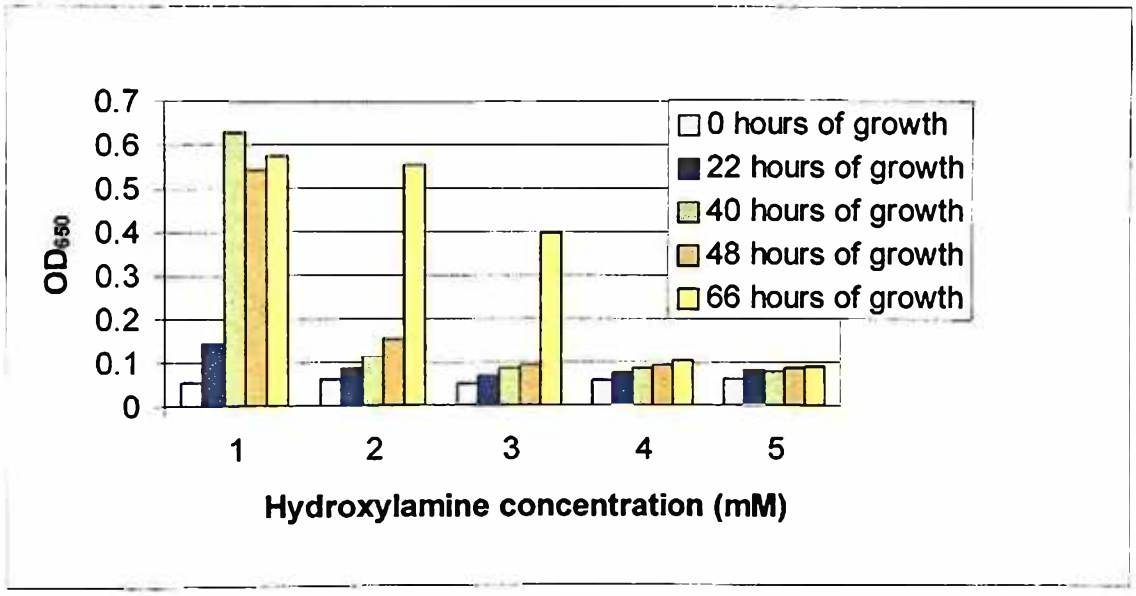

b)

Figure 4.3. Hydroxylamine as an electron acceptor. Strain RK4353 was grown in MS supplemented with LB, glycerol, a range of HA from 0 to 1 mM and no other electron acceptor. The optical density was measured after 22, 40, 48 and 66 hours of growth. **a:** Medium supplemented with 2.5% LB; **b:** These experiments were repeated twice; the data for a single experiment are shown.

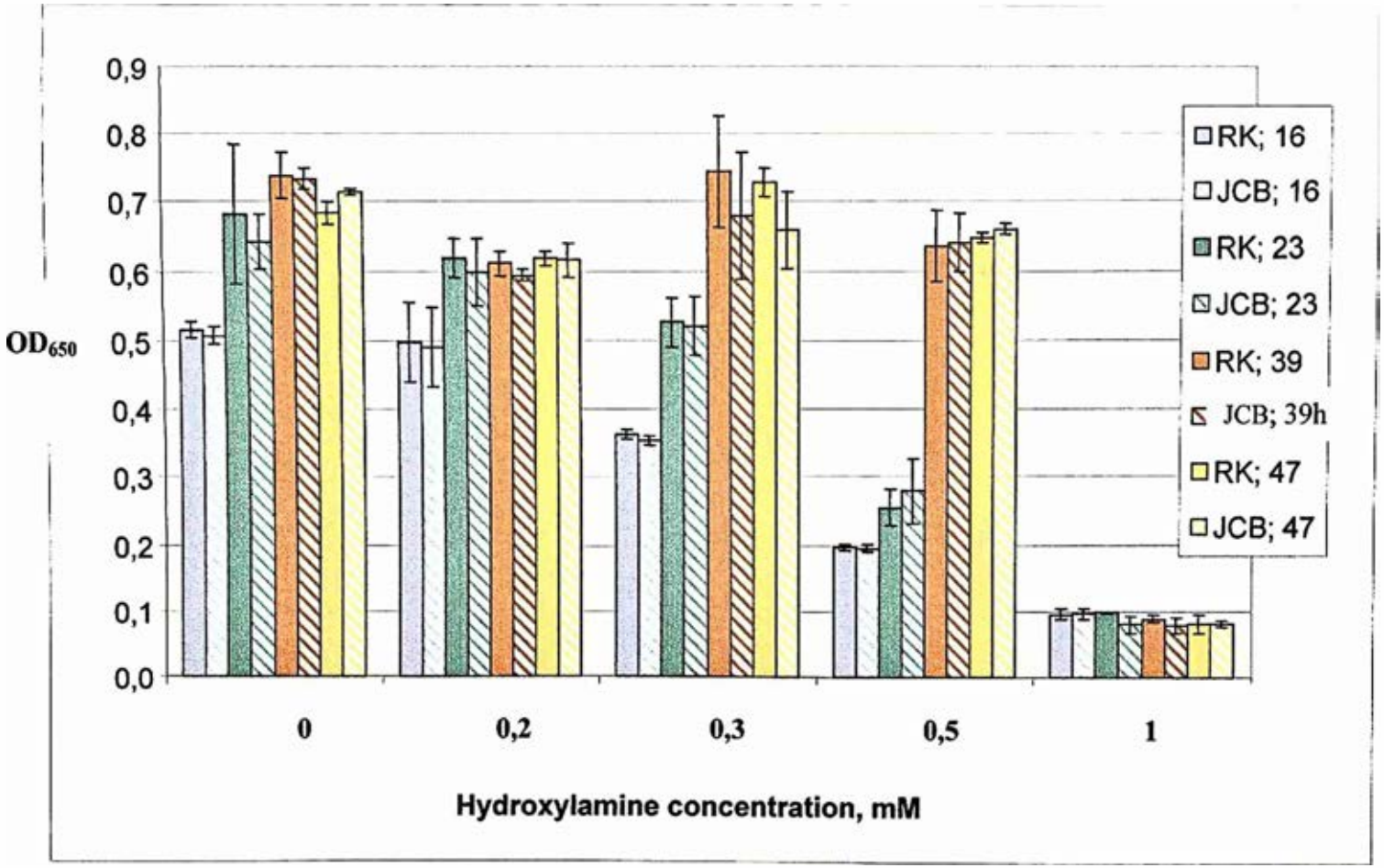

Figure 4.4. Possible detoxification of hydroxylamine by HCP. Strains RK4353 and JCB5000 (RK4353 *Δhcp*) were grown anaerobically in MS medium supplemented with 2.5% LB, 0.4% glycerol, 20 mM $NaNO_3$ and also with 0.2; 0.3; 0.5 or 1 mM of hydroxylamine. The optical densities were measured after 16, 23, 39 and 47 h of growth.

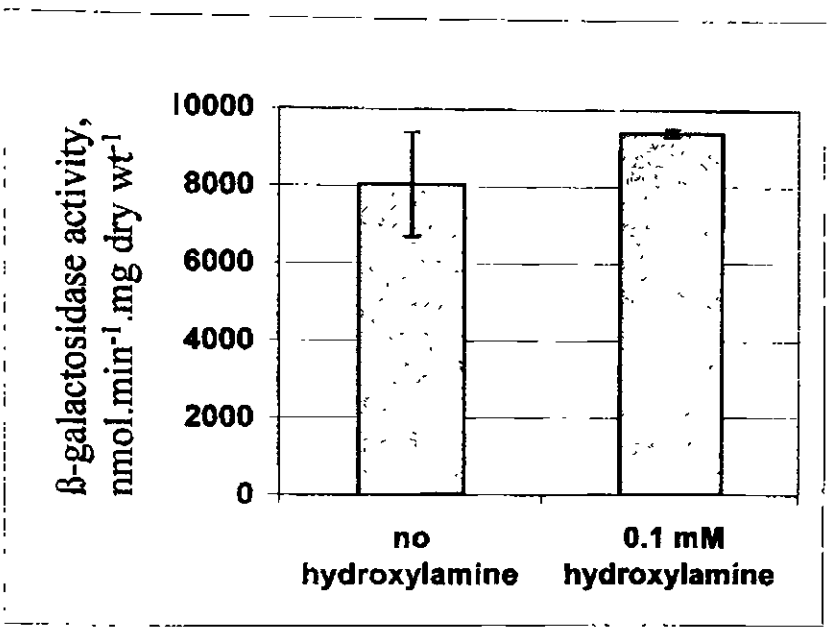

Figure 4.5. Effect of hydroxylamine on transcription activation at the *hcp* promoter. Strain RK4353 transformed with pNF383 was grown anaerobically in MS medium supplemented with glycerol and fumarate with or without 0.1 mM hydroxylamine. The β-galactosidase activity was measured when the OD_{650} of the cultures was between 0.5 and 0.8. The β-galactosidase activities are stated as the mean value of two independent cultures each assayed in duplicate with the standard deviation shown by error bars.

thus, the ability of HCP to reduce and therefore detoxify hydroxylamine *in vitro* was determined.

4.6. HCP and nitric oxide detoxification

It was previously shown that the *hcp/hcr* promoter in *S. enterica* is upregulated in the presence of acidified nitrite, which is a source of reactive nitrogen species including nitric oxide (NO) (Kim et al., 2003). It was also demonstrated that in infected with *S. enterica* macrophages, upon induction of NO synthase, the *hcp/hcr* promoter is also activated (Kim et al., 2000), suggesting a role for HCP as an NO reductase. Thus, the possibility of HCP being an NO reductase *in vivo* was tested. If HCP is an NO reductase, an HCP mutant would be expected to be more sensitive to growth inhibition by NO that the parental strain.

Strains RK4353 and JCB5000 were grown anaerobically in MS supplemented with glucose and nitrate with or without nitric oxide saturated water (NOSW). Overnight cultures were diluted 40-fold and grown anaerobically for two hours. The cultures were saturated with nitrogen gas to ensure fully anaerobic conditions. When the OD_{650} had increased to between 0.4 and 0.5 units, NOSW was added to a final concentration of 0.1 mM NO. Every hour, the optical density was measured, the cultures were saturated with nitrogen gas and further NOSW was added. NO was observed to be toxic to the *E. coli* culture, resulting in lower yields of the cultures supplemented with NO. After 4 hours, RK4353 grown either with or without NO had reached the stationary phase of growth, but the OD_{650} was 0.8-0.9 and 1.2-1.3, respectively (**figure 4.6**).

During the exponential phase strain JCB5000 grew in the absence of NO at the same rate as the parental strain, RK4353, and the optical density of the culture at stationary phase was slightly, but not significantly, as calculated with the t-test, lower than that of the parental strain. JCB5000 grown in medium supplemented with NO had at all stages of

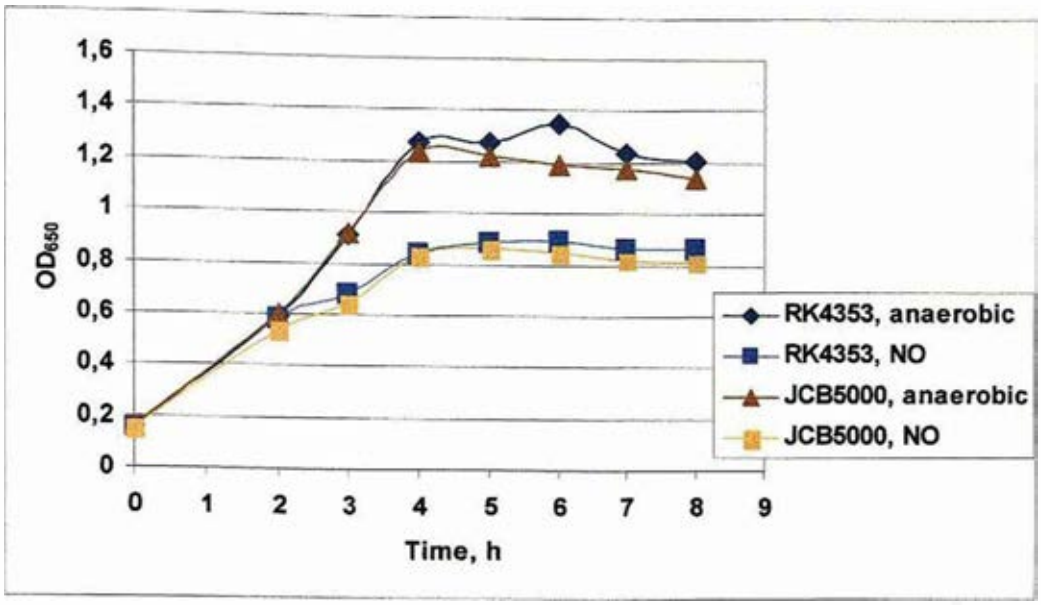

Figure 4.6. HCP and nitric oxide detoxification. Strains RK4353 and its *hcp* derivative, JCB5000, were grown anaerobically in MS supplemented with glucose and nitrate with or without nitric oxide saturated water (NOSW). The cultures were saturated with nitrogen gas to ensure fully anaerobic conditions. When the OD_{650} had reached 0.4-0.5 units, NOSW was added to the final concentration of 0.1 mM NO. The optical density of the cultures was measured every hour, and after the optical density had been measured, the cultures were again saturated with nitrogen gas and more NOSW was added.

growth similar optical density to that of the parental strain under the same conditions. As no decrease in growth of the *hcp* mutant in the presence of NO was noticed, which would be expected if HCP detoxified nitric oxide, it was concluded that HCP is not involved in NO detoxification under the conditions tested.

4.7. Identification of HCP in the culture with Western blotting

In the above experiments, no difference in optical density *in vivo* was observed between *hcp*$^+$ and *hcp* strains that had been grown in medium supplemented with hydroxylamine or nitric oxide. Neither was there a difference noticed within three pairs of *hcp*$^+$ and *hcp* strains when they were grown under nitrate respiring conditions. In order to validate these results it was important to exclude the possibility that this lack of difference might be due to low expression or absence of expression of HCP in the *hcp*$^-$ strain. To check the amount of HCP in both HCP$^+$ and HCP$^-$ strains, strains JCB302 (*hcp*$^+$ *chl*), JCB4041 (*hcp*$^+$ *ΔnarG-I*), RK4353 (*hcp*$^+$ *ΔnarG-I*) and JCB5000 (*Δhcp ΔnarG-I*) were grown to the middle of the exponential phase under anaerobic conditions in MS medium supplemented with 5% LB, 0.4% glycerol and 20 mM $NaNO_3$. The bacteria were collected by centrifugation, sonicated and centrifuged. The supernatant proteins were separated by SDS-PAGE, denatured and transferred to the PVDF membrane. The membrane with immobilized proteins was blocked with PBS buffer containing 0.5% Tween. The membrane was hybridized with primary goat antibodies against HCP from *Desulfovibrio vulgaris*. After the washing step, the membrane was incubated with secondary anti-goat antibodies that had been raised in rabbit and conjugated for alkaline phosphatase. The secondary antibodies were detected with 5-bromo-4-chloro-3-indolyl phosphate/nitro blue tetrazolium as a substrate of alkaline phosphatase. It was shown that during anaerobic growth in the above medium, HCP had accumulated in the

three *hcp*$^+$ strains but was not detectable in the *hcp* strain (**figure 4.7,** lanes 1-3 and 4, respectively).

As the antibodies used in this study had been raised against *D. vulgaris* HCP and not *E. coli* HCP, they consequently reacted non-specifically with other *E. coli* proteins as well as with HCP itself. To partially reduce the non-specific binding of antibodies to other *E. coli* proteins, two changes to the standard method were applied. First, the proteins separated by SDS-PAGE were transferred onto two successive membranes. This allowed transfer of smaller proteins to onto the first membrane, which was later discarded. The medium-sized and large proteins including HCP were then transferred from the gel onto the second membrane. Secondly, prior to incubation of the proteins immobilized to the membrane with primary antibodies, 20 µl of antibodies were mixed with 100 µl of supernatant proteins and incubated for 1 hour 30 minutes at 37 °C with subsequent incubation at 4 °C for the same time. This allowed unspecific binding of antibodies to the rest of the supernatant proteins. This mix was then used in place of primary antibodies. Despite still quite pronounced bands of the proteins, which non-specifically reacted with primary antibodies, the intensity of the band corresponding to HCP was quite high in the *hcp*$^+$ strains while this band was absent from the *hcp* strain. In this way it was shown that the absence of a phenotypic difference between the mutant and the parental strain was not due to the failure of the *hcp*$^+$ strain to accumulate HCP protein.

4.8. Overproduction of the hybrid cluster protein

Purified HCP was required to test its function *in vitro*. Initial attempts to subclone the *hcp/hcr* coding region into the overexpression vector pET11c were unsuccessful. Two HCP overexpression plasmids, pCA24n1 and pCA24n2, kindly provided by Dr. Mori, Nara Institute, were therefore used. In both of the plasmids the *hcp* coding region is preceded by

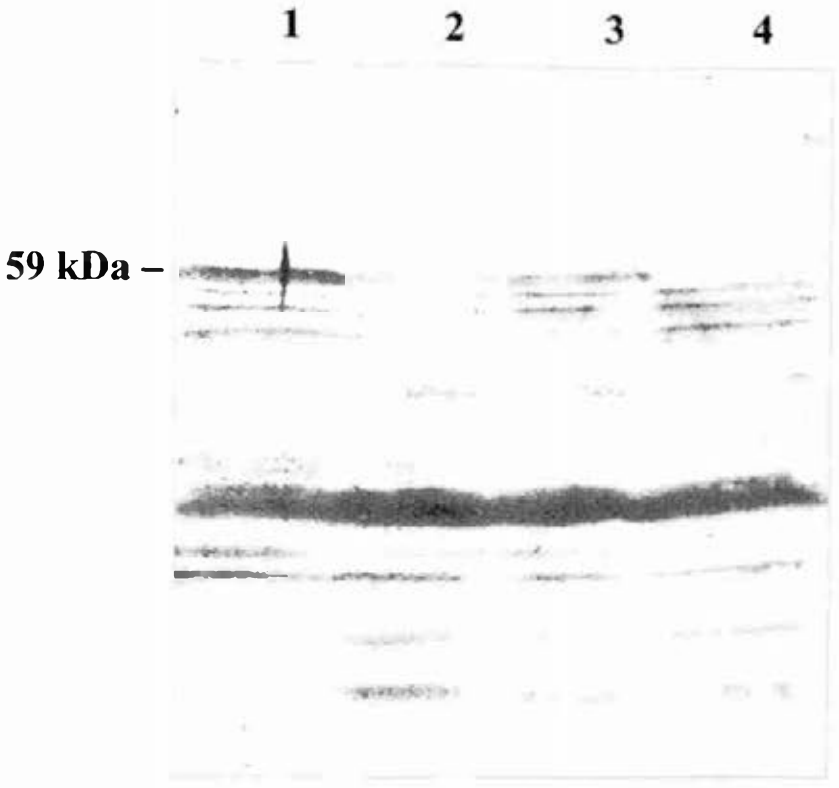

Figure 4.7. Identification of HCP in *hcp*$^+$ strains with Western blotting. JCB302 (*hcp*$^-$ *chl*), JCB4041 (*hcp*$^+$ *ΔnarG-I*), RK4353 (*hcp*$^+$ *ΔnarG-I*) and JCB5000 (*Δhcp ΔnarG-I*) were grown under anaerobic conditions in MS medium supplemented with LB, glycerol and $NaNO_3$ until the middle of the exponential phase. The bacteria were collected, sonicated and centrifuged. The supernatant proteins were separated by SDS-PAGE, denatured and transferred to the PVDF membrane. The membrane with immobilized proteins was blocked with PBS buffer containing 0.5% Tween and hybridized with primary antibodies raised in goat against HCP from *Desulfovibrio vulgaris*. After a washing step, the membrane was incubated with secondary rabbit anti-goat antibodies, conjugated to alkaline phosphatase. The secondary antibodies were detected with 5-bromo-4-chloro-3-indolyl phosphate/nitro blue tetrazolium as a substrate of alkaline phosphatase. **Lane 1**: proteins of strain JCB302; **lane 2**: proteins of strain JCB4041; **lane 3**: proteins of strain RK4353; **lane 4**: proteins of strain JCB5000. The band of 59 kDa, corresponding to HCP, is indicated.

a sequence encoding six consecutive histidine residues (6xHis tag) under the control of the IPTG-inducible *t5-lac* promoter, and they produce HCP fused to green fluorescent protein (GFP) and native HCP, respectively. To find out which condition is the best for maximal production of hybrid cluster protein, the strain JW0857 was transformed with pCA24n1 or pCA24n2. The transformants were grown at 37 °C under two different conditions: either aerobically in Lennox Broth (LB) medium with 10 μg/ml Cm; or anaerobically in LB supplemented with 20 mM $NaNO_3$, 0.4% glucose and 10 μg/ml Cm. The *t5-lac* promoter was induced with 0.1 mM IPTG. Bacteria in the exponential phase of growth were lysed in sample buffer, the proteins were separated by SDS-PAGE and stained with Coomassie blue. Induction of both free HCP and HCP-GFP fusion protein was observed after both aerobic and anaerobic growth (**figure 4.8**, lanes 1-4). Recognizing the possibility that HCP might be an enzyme, and that the GFP tertiary structure might obscure its activity, the plasmid encoding native HCP was used for all subsequent experiments. Furthermore, as HCP contains two Fe-S clusters, which might be inactivated in the presence of oxygen, during further experiments HCP was overproduced under anaerobic conditions to minimize inactivation of the Fe-S clusters.

Strains JW0857 (*hcp*$^+$), RK4353 (*hcp*$^+$) and JCB5000 (*Δhcp*) were transformed with plasmid pCA24n2 encoding native HCP. The transformants and untransformed JCB5000 were grown anaerobically in LB, 20 mM $NaNO_3$, 0.4% glucose and 10 μg/ml Cm as appropriate at 37 °C, and expression of HCP was induced by addition of 0.1 mM IPTG. The colour of bacteria transformed with pCA24n2 was dark red due to the FeS clusters of accumulated HCP (**figure 4.9, a**). Bacteria were broken in the French press, and the soluble cytoplasmic fraction and the insoluble fraction containing unbroken cells, membranes and inclusion bodies were separated by ultracentrifugation. After growth under the above conditions, all of the HCP was present in the insoluble (pellet) fraction indicative of HCP

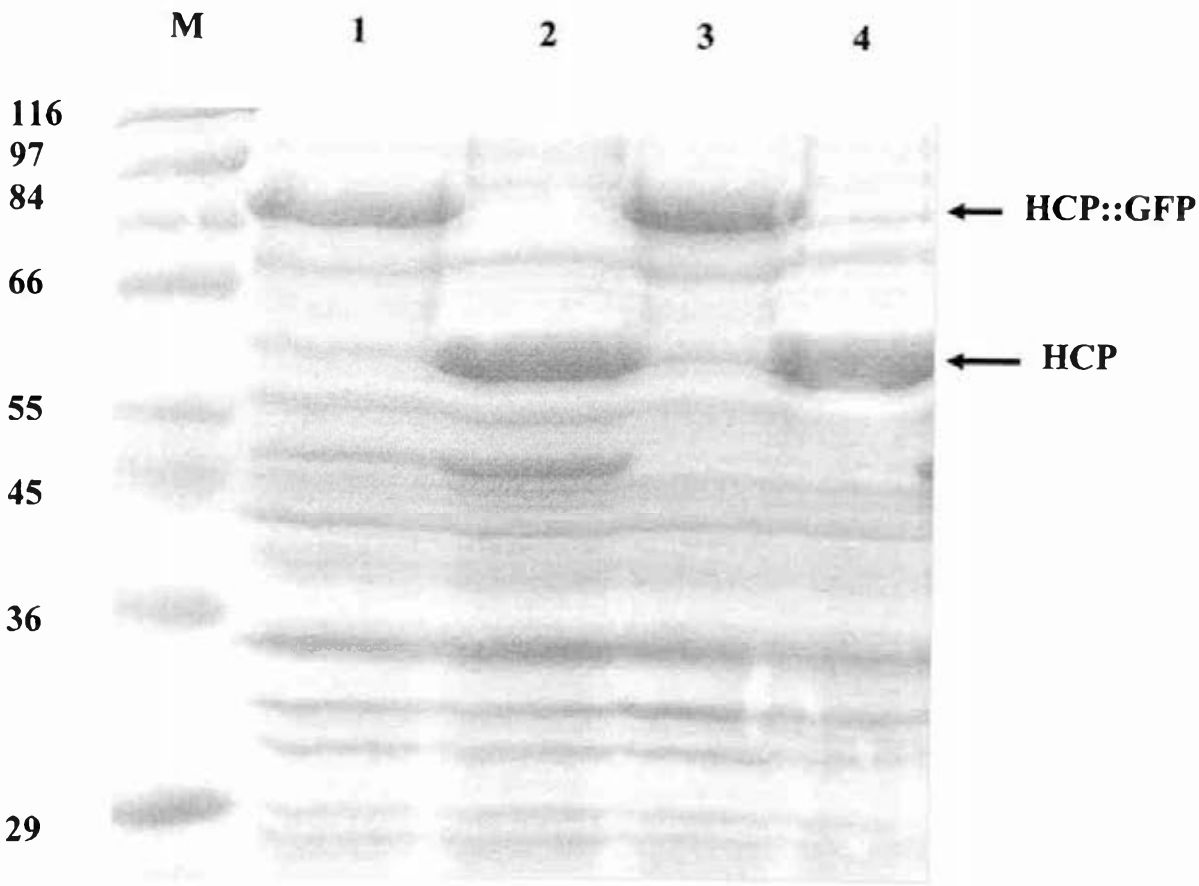

Figure 4.8. Overexpression of HCP from strain JW0857. Strain JW0857 was transformed with plasmids pCA24n1 or pCA24n2, producing HCP fused to GFP or free HCP, respectively. The transformants were grown either aerobically in LB and 10 μg/ml Cm or anaerobically in LB, 20 mM $NaNO_3$, 0.4% glucose and 10 μg/ml Cm. The *t5-lac* promoter was induced with 0.1 mM IPTG. Whole cell extract was separated by SDS-PAGE and stained for proteins. **Lane M**: wide range protein Sigma marker (precise sizes in kDa are given to the left); **lane 1**: JW0857/*pCA24n1* expressing HCP::GFP, grown aerobically; **lane 2**: JW0857/*pCA24n2* expressing HCP, grown aerobically; **lane 3**: JW0857/*pCA24n1* expressing HCP::GFP, grown anaerobically; **lane 4**: JW0857/*pCA24n2* expressing HCP, grown anaerobically.

a **b**

Figure 4.9. Culture with overexpressed HCP. Strain JCB5000 (*Δhcp*) was transformed with plasmid pCA24n2 encoding HCP. The transformant and untransformed JCB5000 were grown anaerobically in LB, 20 mM $NaNO_3$, 0.4% glucose and 10 µg/ml Cm as appropriate at 37 °C. Expression of HCP was induced by addition of 0.1 mM IPTG and the strains were grown until the late exponential phase. **a**: JCB5000/ pCA24n2. The colour of bacteria is dark red due to the FeS clusters of accumulated HCP; **b**: JCB5000 as negative control.

being accumulated in inclusion bodies (**figure 4.10,** lanes 4 and 5).

In subsequent experiments, several more growth and induction conditions were tested to optimize HCP accumulation in the soluble fraction suitable for purification. RK4353/pCA24n2 was grown anaerobically on a small scale in 100 ml of LB, 20 mM $NaNO_3$, 0.4% glucose and 10 μg/ml Cm at room temperature (20 °C) and at 37 °C. At each temperature the *t5-lac* promoter, controlling expression of the *hcp*, was either induced with 0.1 mM IPTG or not induced. Bacteria were broken in the French press, and the cytoplasmic and insoluble fractions were separated by ultracentrifugation. It was demonstrated that induction of the *t5-lac* promoter by IPTG is essential for expression of HCP at both temperatures (**figure 4.11**, lanes 3, 4 and 8). However, HCP accumulated in the soluble fraction only after growth at room temperature. These conditions were therefore used to grow strain RK4353/pCA24n2 anaerobically in 2 l of LB, 20 mM $NaNO_3$, 0.4% glucose and 10 μg/ml Cm. The *t5-lac* promoter was induced with 0.1 mM IPTG. Bacteria were broken in the French press, and the cytoplasmic and insoluble fractions were separated by ultracentrifugation. Soluble cytoplasmic proteins were separated by SDS-PAGE and stained with Coomassie blue. A band of 59 kDa, corresponding to HCP, was visible and HCP amounted to about 5% of the total cellular protein.

4.9. Purification of HCP

Nickel-charged resin was used to purify HCP-6His from other cytoplasmic proteins. The proteins bound to the nickel-charged resin were washed with buffer C and eluted twice with 0.5 ml of 0.25 M imidazole in buffer C, and twice with 0.5 ml of 1 M imidazole in buffer C. Equal amounts of protein were separated by SDS-PAGE and stained with Coomassie Blue. As shown in **figure 4.12** (lanes 5-8), HCP was eluted with other cytoplasmic proteins in all four eluates, although its relative amount increased in the final eluate. This suggested that

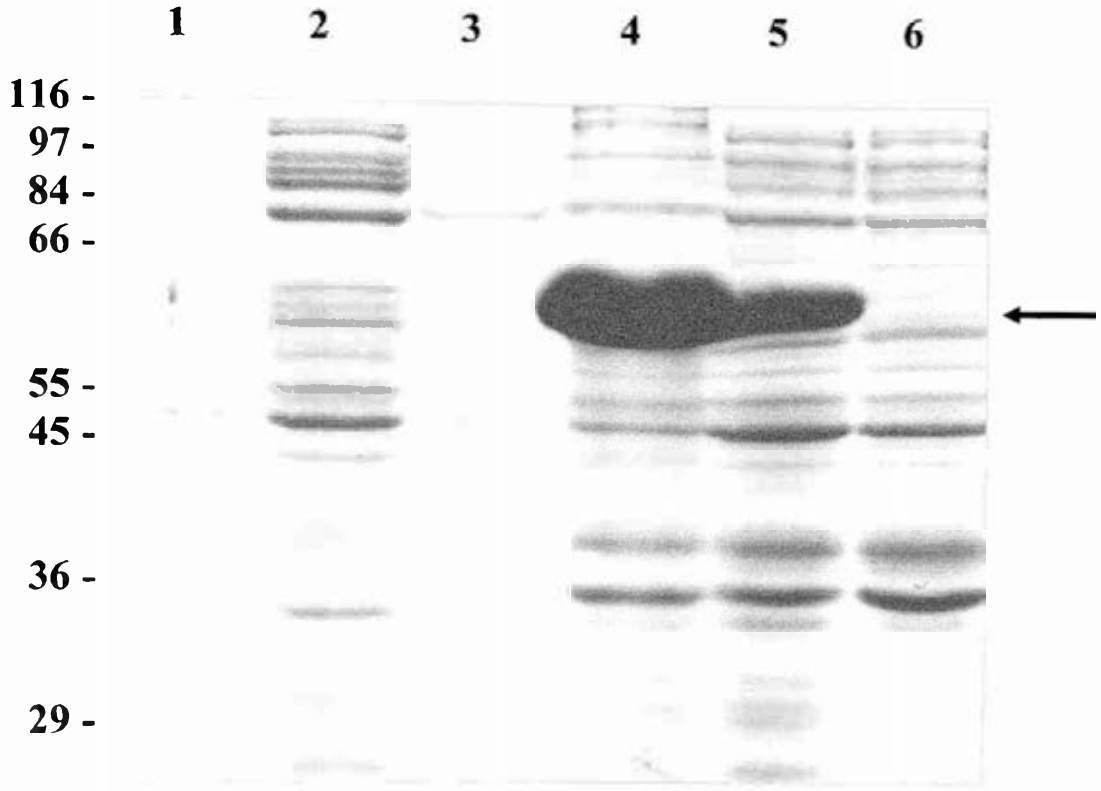

Figure 4.10. Location of HCP, overexpressed at 37 °C, in supernatant and pellet fractions of JW0857/ pCA24n2 and RK4353/ pCA24n2. Strains RK4353 (*hcp*$^+$), JCB5000 (*Δhcp*) and JW0857 (*hcp*$^+$) were transformed with pCA24n2 encoding native HCP. The transformants were grown anaerobically in LB, 20 mM $NaNO_3$, 0.4% glucose and 10 μg/ml Cm at 37 °C, and HCP expression was induced by addition of 0.1 mM IPTG. Bacteria were broken in the French press and soluble supernatant and insoluble pellet fractions were separated by ultracentrifugation. Proteins in each sample were separated by SDS-PAGE and stained with Coomassie blue.
Lane 1: JW0857/pCA24n2, supernatant fraction; **lane 2**: RK4353/pCA24n2, supernatant; **lane 3**: JCB5000/pCA24n2, supernatant; **lane 4**: JW0857/pCA24n2, pellet fraction; **lane 5**: RK4353/pCA24n2, pellet; **lane 6**: JCB5000/pCA24n2, pellet.

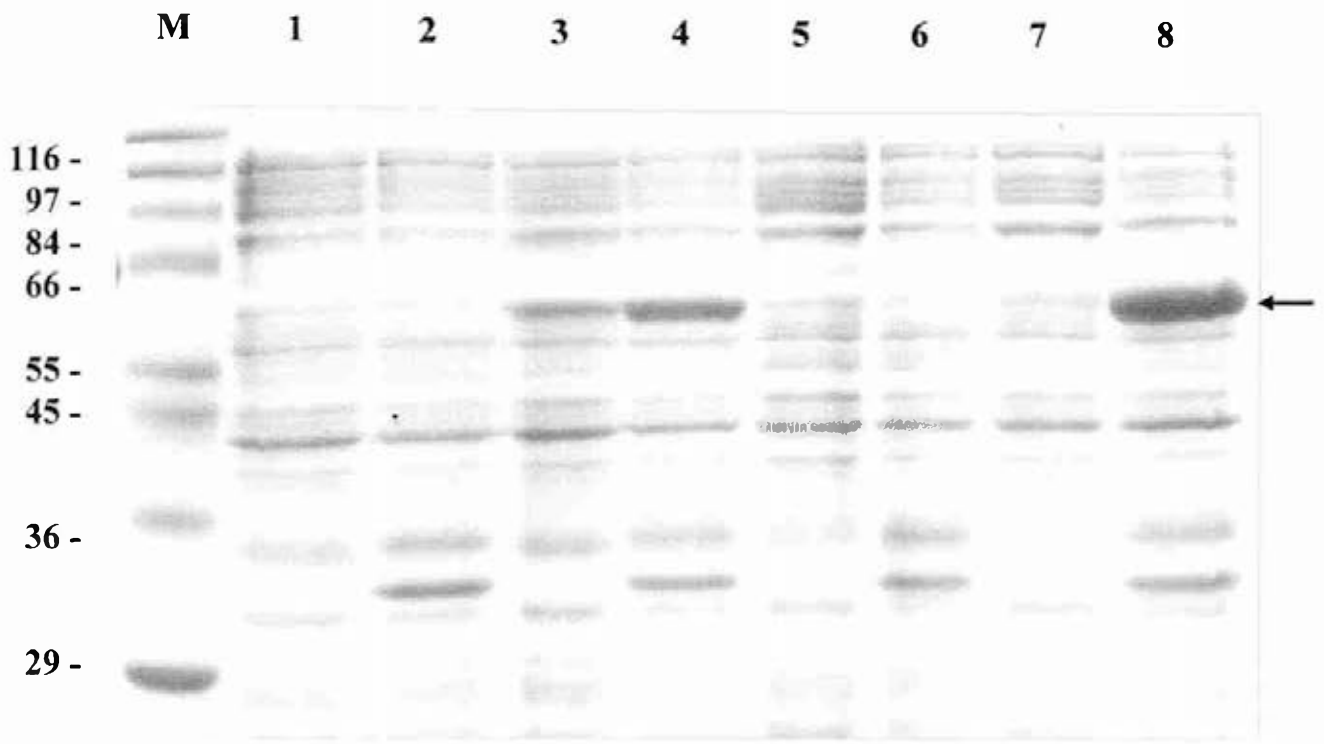

Figure 4.11. Overexpression of HCP under several growth and induction conditions. Strain RK4353/pCA24n2 was grown anaerobically in LB, 20 mM $NaNO_3$, 0.4% glucose and 10 μg/ml Cm at 20 °C and at 37 °C. At both temperatures the *t5-lac* promoter was either induced with 0.1 mM IPTG or not induced. Bacteria were broken in the French press, and cytoplasmic and insoluble fractions were separated by ultracentrifugation. **Lane M**: wide range protein Sigma marker (precise sizes in kDa are given to the left); **lane 1**: 20 °C, no IPTG, supernatant fraction; **lane 2**: 20 °C, no IPTG, pellet fraction; **lane 3**: 20 °C, 0.1 mM IPTG, supernatant; **lane 4**: 20 °C, 0.1 mM IPTG, pellet; **lane 5**: 37 °C, no IPTG, supernatant; **lane 6**: 37 °C, no IPTG, pellet; **lane 7**: 37 °C, 0.1 mM IPTG, supernatant; **lane 8**: 37 °C, 0.1 mM IPTG, pellet.

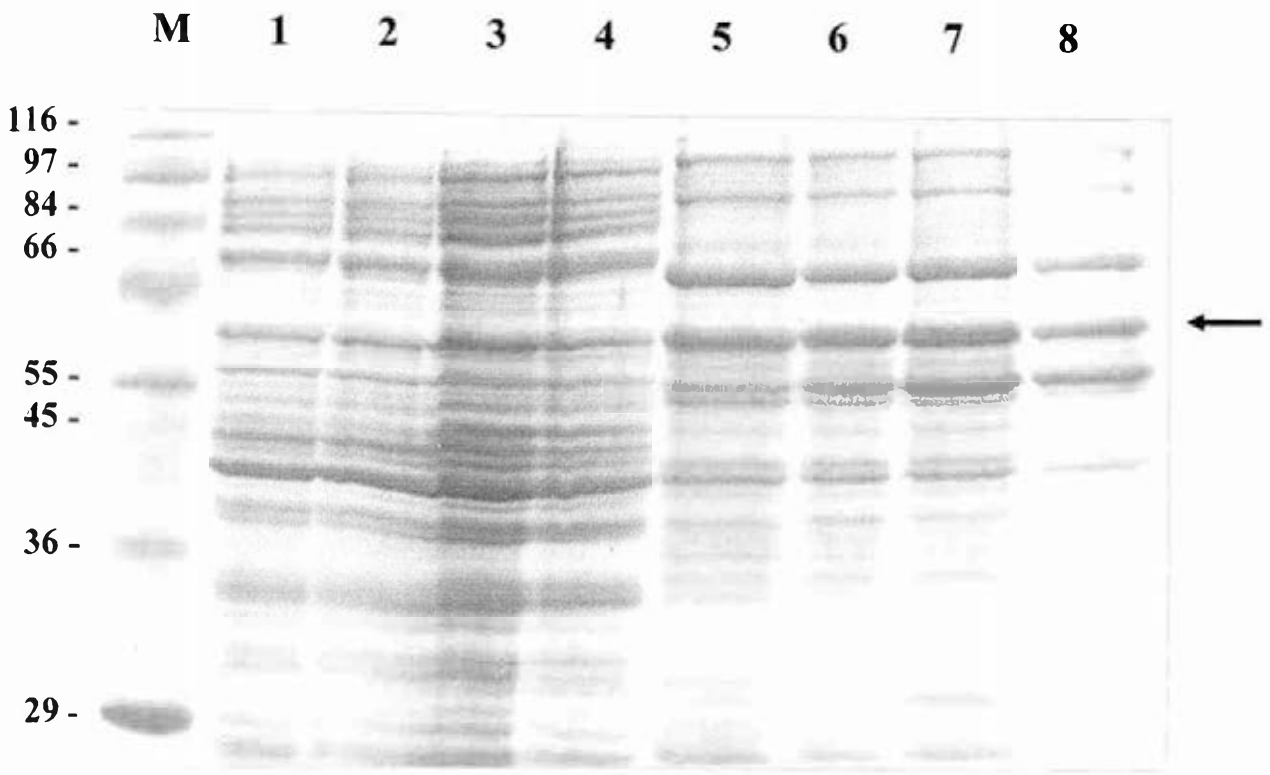

Figure 4.12. Purification of HCP on nickel-charged resin. The cytoplasmic protein fraction was incubated with Ni-NTA resin at 4 °C for 1 hour. The bound proteins were washed with 30 ml of buffer C and eluted with imidazole in buffer C at two concentrations: 0.25 M and 1 M. The concentration of eluted protein was estimated using the Folin assay. Equal amounts of protein were separated by SDS-PAGE and stained with Coomassie Blue. The arrow on the right indicates the HCP band. **Lane M**: wide range protein Sigma marker (precise sizes in kDa are given to the left); **lane 1**: initial cytoplasmic fraction; **lane 2**: filtered fraction; **lane 3**: flow through; **lane 4**: wash; **lanes 5-8**: elution with imidazole: **lane 5**: 0.25 M imidazole, first eluate; **lane 6**: as 5, second eluate; **lane 7**: 1 M imidazole, first eluate; **lane 8**: as 7, second eluate.

other cytoplasmic proteins were able to bind to the Ni-NTA resin and were eluted together with HCP upon addition of imidazole. To elute HCP separately from all of the other proteins, the Ni-NTA resin was washed with 5 ml samples of buffer containing a range of imidazole concentrations: 10 mM; 25 mM; 50 mM; 100 mM; 250 mM and 1 M. The protein fractions were separated by SDS-PAGE and stained as above. It was shown that all non-specifically bound proteins were eluted with up to 50 mM imidazole (**figure 4.13**, lanes 4-6). A substantially purified fraction of HCP was eluted with 100 mM imidazole (**figure 4.13**, lane 7). Although some HCP was also present in the 10 mM, 25 mM and 50 mM imidazole eluates, this method allowed HCP to be separated from the majority of other proteins when eluted with 100 mM imidazole. The final concentration of HCP in the last eluted fraction was 0.140 μg/μl, as determined the by Folin protein assay.

4.10. Development of a protocol for *in vitro* reduction of $NaNO_2$, $NaNO_3$ and NH_2OH by HCP

The ability of HCP to reduce $NaNO_2$, $NaNO_3$ and NH_2OH was tested with a modified methyl viologen assay. Methyl viologen is a redox active species, which is colorless when oxidized and dark blue when reduced. This assay was used to investigate whether electrons can be passed from methyl viologen via HCP to a possible substrate. Aliquots of buffer D containing nitrate, nitrite and reduced methyl viologen were added to different volumes (25, 50 and 100μl) of supernatant protein fraction from strain RK4353 and the *hcp* mutant, JCB5000, and the time required for the blue colour to vanish was measured. The anticipated result was that the reaction containing the HCP^+ supernatant might oxidize methyl viologen, and subsequently become colorless, more quickly. When normalized to the amount of the whole protein in the cytoplasmic fraction, the methyl viologen was oxidized at the same rate by HCP^+ and HCP^- cytoplasmic extracts (in about 20 seconds). This effect might be

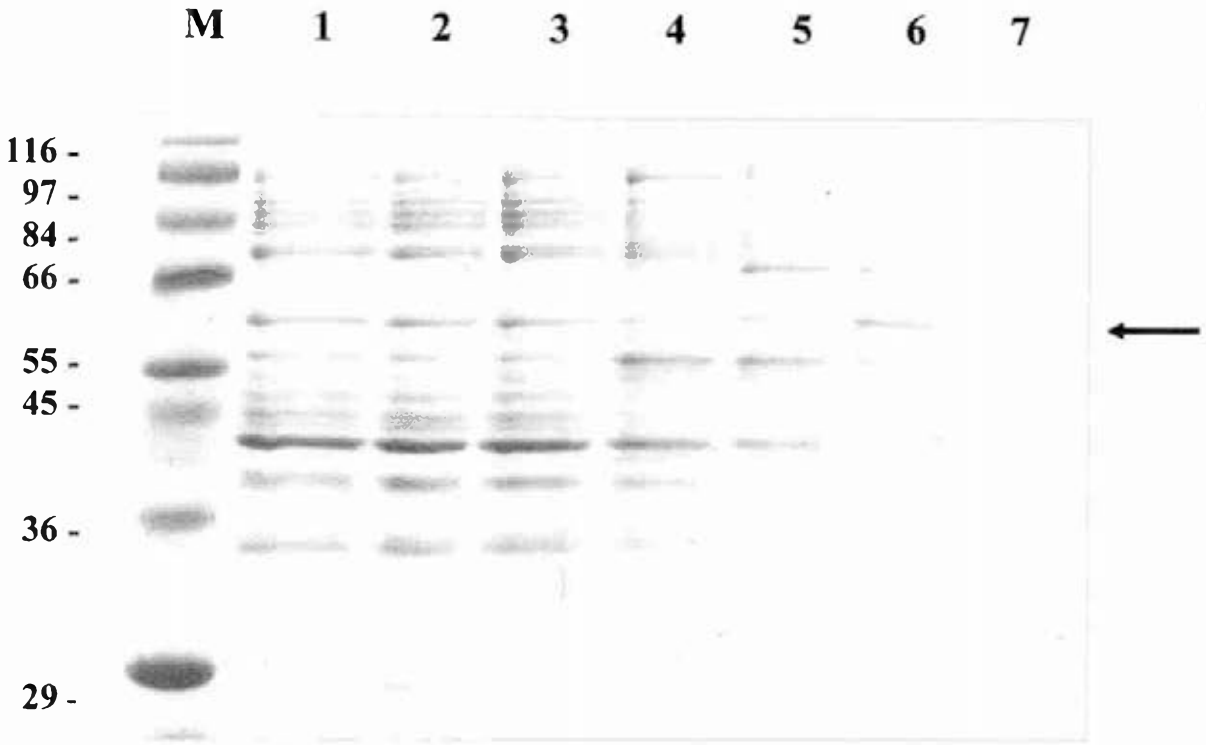

Figure 4.13. Purification of HCP on nickel-charged resin with a range of imidazole concentrations. The cytoplasmic protein fraction was loaded onto Ni-NTA resin and bound at 4 °C for 1 hour. The bound proteins were washed with 30 ml of buffer C and eluted with a range of imidazole concentrations in buffer C: 10 mM, 25 mM, 50 mM, 100 mM, 250 mM and 1 M. The arrow on the right indicates the HCP band. **Lane M**: wide range protein Sigma marker (precise sizes in kDa are given to the left); **lane 1**: initial cytoplasmic fraction; **lane 2**: flow through; **lane 3**: wash; **lanes 4-7**: elution with imidazole: **lane 4**: 10 mM; **lane 5**: 25 mM; **lane 6**: 50 mM; **lane 7**: 100 mM.

explained by the presence in both fractions of other proteins, such as nitrate reductase A, periplasmic nitrate reductase, NADH-dependent nitrite reductase and formate-dependent nitrite reductase, which can reduce nitrate or nitrite with the reduced methyl viologen as an electron donor.

4.10.1. Reduction of nitrate, nitrite and hydroxylamine by HCP partially purified on a Ni-NTA column

To test whether the purified HCP fraction can reduce nitrite, nitrate or hydroxylamine *in vitro*, buffer D containing nitrate, nitrite and hydroxylamine was added to the purified protein fractions and the time required for reduced methyl viologen to become oxidized was measured. Negative controls were buffer D left at room temperature and buffer D with formate buffer added instead of the HCP^+ fraction. A positive control was buffer D with the supernatant fraction of proteins from the *hcp*$^+$ strain, RK4353. Results of a pilot experiment with two negative and one positive control are shown in **table 4.1, a.** Buffer D on its own was completely colourless (oxidized) after 11 minutes, and after 10 minutes when mixed with the formate buffer, due to the oxidation of methyl viologen by traces of oxygen. When the supernatant fraction of proteins from the *hcp*$^+$ strain was added, buffer D became colourless in 2 to 4 minutes, possibly catalysed by some proteins, for example NAP, present in the supernatant fraction.

Nitric oxide is one of the possible substrates for HCP. To test whether nitric oxide can directly oxidize methyl viologen, nitric oxide was bubbled through buffer D above, except that purified HCP was used instead of the unpurified soluble extract. Methyl viologen was oxidized in about 7 seconds. However, the same result was observed even in the absence of purified HCP due to the direct oxidation of methyl viologen by NO. As the methyl viologen assay relies on enzyme-mediated oxidation of methyl viologen upon

Component	Components added, µl	Time for MV to become oxidized, minutes
Buffer D (negative control N1)	100	11
Buffer D with formate buffer (negative control N2)	100 + 50	10
Buffer D with supernatant fraction of proteins including HCP (positive control)	100 + 25	2

a)

Component	Components added, µl	Time for MV to become oxidized, minutes
Buffer D containing $NaNO_3$, $NaNO_2$ and NH_2OH with formate buffer (negative control)	50 + 200	> 1 hour
Buffer D with purified HCP protein fraction	50 + 200	> 1 hour

b)

Table 4.1. Time required for methyl viologen to become oxidized by the mixture of nitrate, nitrite and hydroxylamine. HCP^+ protein fractions were added to the aliquots of buffer D containing reduced methyl viologen and $NaNO_3$, $NaNO_2$ and NH_2OH as possible electron acceptors and the time required for the methyl viologen to become oxidized, was measured. **a:** pilot experiment with two negative controls and one positive control; **b:** purified HCP^+ protein fraction.

provision of the substrate of the enzyme, the possibility of NO being a substrate of HCP could not be tested using this assay.

The reduction of nitrite, nitrate and hydroxylamine by the HCP^+ fraction was investigated. As the concentration of the purified HCP was comparatively low (0.140 μg/ μl), the volume of the fraction added to buffer D was increased from 50 μl to 200 μl compared to the previous experiment. To a 50 μl aliquot of buffer D, containing nitrate, nitrite and hydroxylamine each at 0.17 M, either 200 μl of formate buffer or 200 μl of HCP^+ purified fraction were added. After 45 minutes both solutions were still blue, although the mixture with HCP fraction was clearer at the top. Oxidation of methyl viologen in both solutions took more that 1 hour (**table 4.1, b**). Nitrate, nitrite and hydroxylamine were also tested separately at a higher concentration (0.5 M), and there was also no evidence of HCP being a reductase of either nitrate, nitrite or hydroxylamine *in vitro*.

CHAPTER 5

Function of NapF, NapG and NapH proteins

5.1. Introduction

The roles of many *E. coli* iron-sulphur proteins in anaerobic electron transfer systems are less well defined than those of the *c*-type cytochromes. At the start of this project in October 2001, three putative non-haem iron-sulphur proteins other than HCP were known to be induced during anaerobic growth in the presence of nitrate or nitrite. These are NapF, NapG and NapH, all of which are encoded by the *nap* operon, and were therefore considered to be potential subunits of the periplasmic nitrate reductase. Colleagues in the laboratory, Dr. H. Brondijk and Arjaree Nilavongse, had already shown that NapH is a trans-membrane protein with four membrane spanning helices and that NapG is located in the periplasm. NapG and NapH were demonstrated to play a role in electron transfer from ubiquinol via NapC to the NapAB complex. These observations have now been published (Brondijk et al., 2002; Brondijk et al., 2004).

E. coli can synthesise both ubiquinone and menaquinone as redox mediators in the respiratory chains for nitrate reduction (Tyson et al., 1997b). The ubiquinone and menaquinone redox couples have different midpoint redox potentials. Depending on the redox state of the cell biomass, electron transport to nitrate catalysed by the periplasmic nitrate reductase can occur preferentially via either ubiquinone or menaquinone. The first aim of the work described in this chapter was to exploit strains able to synthesise both ubiquinone and menaquinone, ubiquinone alone, or menaquinone alone to determine whether the Nap system is required for redox balancing in *E. coli*. A second aim was to show whether NapG and NapH are linked specifically to quinols with high midpoint redox potentials. This chapter also investigates whether NapF, NapG and NapH play any roles in the regulation of the *napF* promoter, or the accumulation of the active Nap enzyme.

5.2. Glucose repression of the *napF* promoter

The presence of some carbon sources in the medium can repress expression of certain genes or operons whose products are involved in the utilisation of alternative carbon sources. To see whether the *napF* promoter is subject to catabolite repression, strain JCB4141 (*nap*$^+$ *ΔmenBC narL::Tn10*) was transformed with the plasmid pDF102, encoding the *napF::lacZ* fusion. The transformant was grown anaerobically in MS medium supplemented with LB and also with glucose, or glucose and nitrate, or with glycerol and nitrate. The cultures were grown until the OD_{650} was 0.3-0.5. The cells were lysed with toluene, and the β-galactosidase activity was measured. After growth in medium supplemented with glucose the activity of the *napF* promoter was about 600 units (**figure 5.1**). When the strain was grown with glucose and nitrate, the promoter activity increased to 3,800 units, suggesting that the activity of the *napF* promoter increased in response to nitrate, which is in agreement with a previously reported result (Wang et al., 1999). The activity of the *napF* promoter increased still further to 9,500 units after growth in glycerol/nitrate medium. Compared to the glycerol/nitrate medium, the activity of the promoter was 2.5-fold repressed in the glucose/nitrate medium, suggesting that the *napF* promoter is subject to catabolite repression.

5.3. Effect of deletion of *napF*, *napG*, *napH* and *napC* genes on the activity of the *napF* promoter

To find out whether NapF, NapG and NapH play a role in regulation of their own operon, strains JCB4141 (Nap$^+$ Ubi$^+$ Men$^-$), JCB4142 (*ΔnapF* Ubi$^+$ Men$^-$), JCB4143 (*ΔnapGH* Ubi$^+$ Men$^-$), JCB4144 (*ΔnapFGH* Ubi$^+$ Men$^-$) and JCB4145 (*ΔnapC* Ubi$^+$ Men$^-$) were transformed with the plasmid pDF102 carying the *napF::lacZ* fusion. The transformants were grown

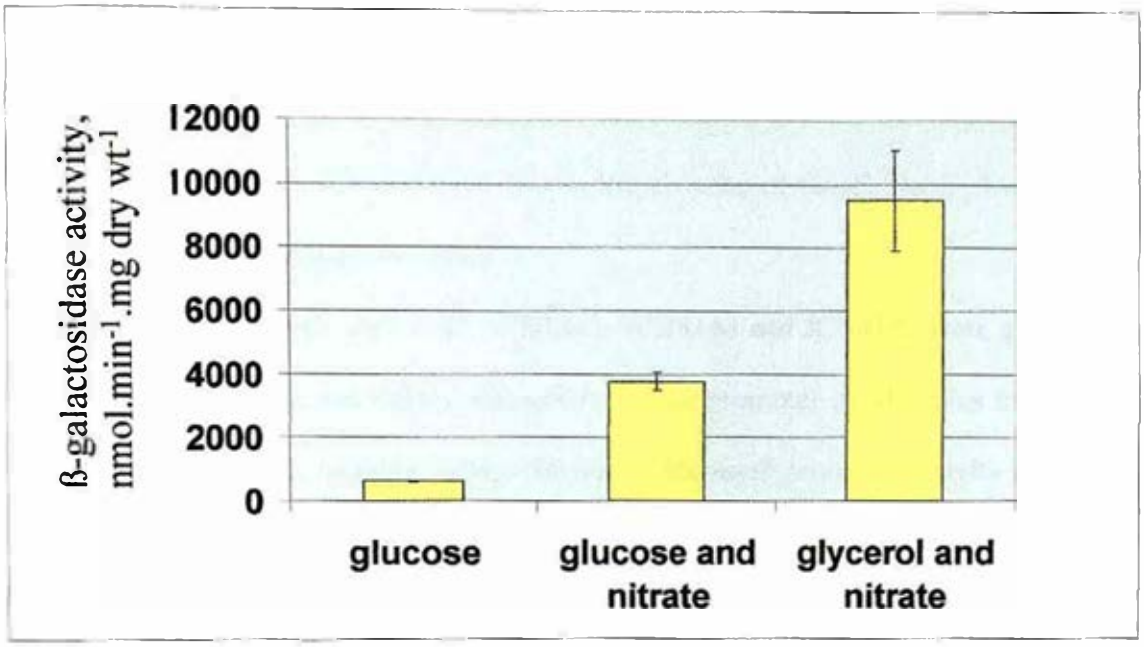

Figure 5.1. Catabolite repression and nitrate stimulation of the *napF* promoter. Strain JCB4141 (*ΔmenBC* Nap$^+$) was transformed with the plasmid pDF102, encoding the *napF::lacZ* fusion. The transformant was grown anaerobically in MS medium supplemented with LB and glucose, glucose and nitrate, or with glycerol and nitrate. The cultures were grown until the OD_{650} was 0.3-0.5. The cells were lysed with toluene, and the β-galactosidase activity was measured. The data are from two independent experiments each assayed in duplicate. The error bars are the standard deviation of the mean.

anaerobically in MS medium supplemented with glucose with or without nitrate. The β-galactosidase activity was measured as before. When the parental strain, JCB4141, expressing the Nap complex, was grown in the presence of only glucose, the activity of the *napF* promoter was about 500 units (**figure 5.2, a**). In the *napF*, *napGH*, *napFGH* and *napC* deletion mutants the activity of the *napF* promoter increased 1.56, 1.53, 1.98 and 2.82-fold, respectively (**table 5.1**). So, it was shown that in the absence of NapF, NapG, NapH and NapC the *napF* promoter activity increases.

When strains JCB4141, JCB4142, JCB4143, JCB4144 and JCB4145 were grown in the presence of both glucose and nitrate, the activity of the promoter in all strains increased compared to growth with glucose alone. However, the *napF* promoter activity in all of the strains was about 2,500 units (**figure 5.2, b**), so no increase in the promoter activity in the *napF*, *napGH* and *napC* mutants was noticed.

5.4. *Effect of deletion of napF, napG, napH* and *napC* genes on NapA activity

To find out whether NapF, NapG, NapH and NapC proteins influence the nitrate reductase activity of the NapA subunit, strains JCB4241 (Nap^+ Ubi^- Men^+), JCB4242 (*ΔnapF* Ubi^- Men^+), JCB4243 (*ΔnapGH* Ubi^- Men^+), JCB4244 (*ΔnapFGH* Ubi^- Men^-) and JCB4245 (*ΔnapC* Ubi^- Men^+) were assayed for methyl viologen dependent nitrate reductase activity. The strains were grown in MS medium supplemented with LB, glucose and nitrate until OD_{650} reached between 0.6 and 0.8 and the nitrate reductase activity was measured.

The nitrate reductase activities of the parental strain (JCB4241), *ΔnapF* strain (JCB4242) and the *ΔnapFGH* strain (JCB4244) were about 40 nmol NO_3^- reduced. min^{-1}. mg dry weight $^{-1}$ (**figure 5.3**). In the *napGH* mutant, JCB4243, the nitrate reductase activity increased 1.5-fold to about 60 units compared to the activity in the parental strain. The Nap

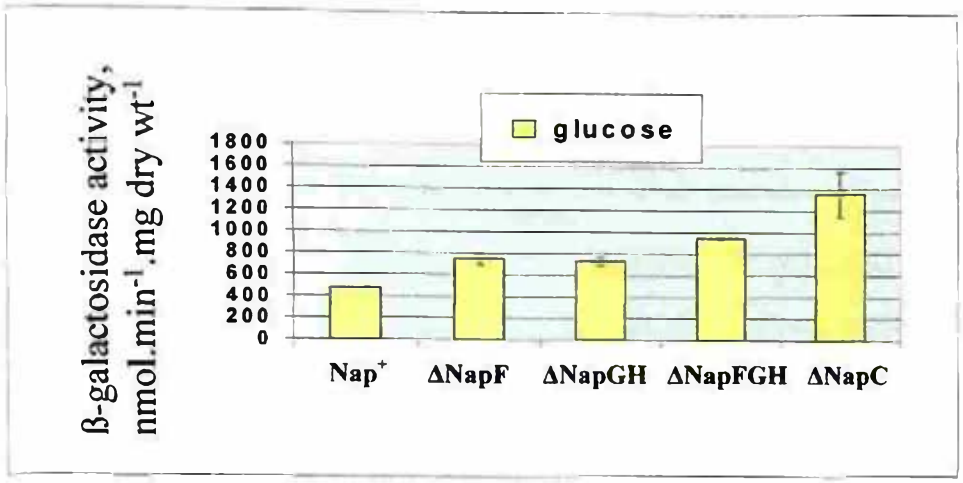

a)

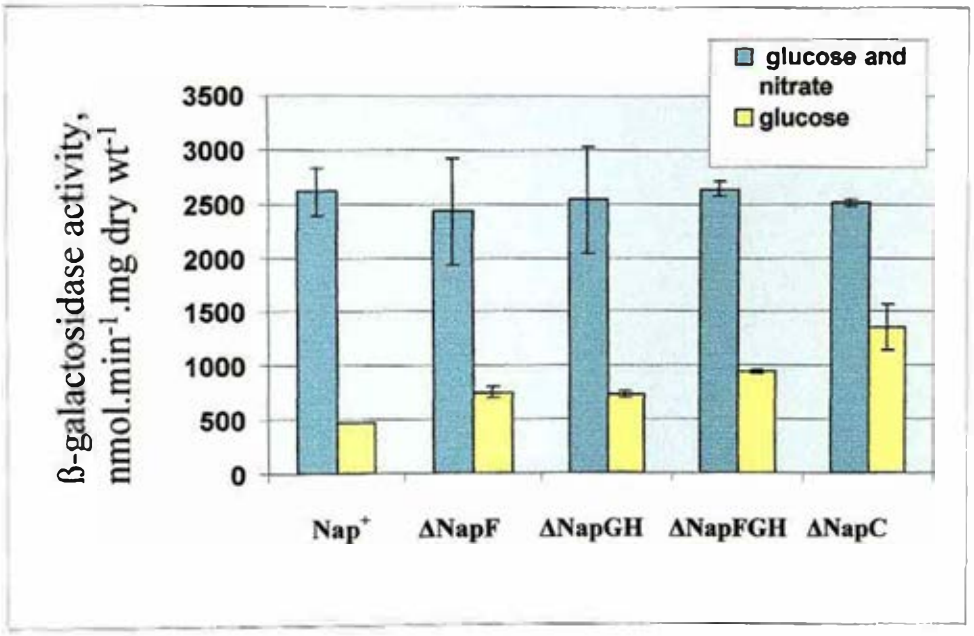

b)

Figure 5.2. Assessment of the *napF* promoter regulation in strains lacking NapF, NapGH, NapFGH and NapC. a) MS medium supplemented with glucose. **b)** MS medium supplemented with glucose and nitrate; the promoter activity after growth with glucose alone is given for comparison. Strains JCB4141 (Nap^+ Ubi^+ Men^-), JCB4142 (*ΔnapF* Ubi^+ Men^-), JCB4143 (*ΔnapGH* Ubi^+ Men^-), JCB4144 (*ΔnapFGH* Ubi^+ Men^-) and JCB4145 (*ΔnapC* Ubi^+ Men^-) were transformed with plasmid pDF102 carying the *napF::lacZ* fusion. The transformants were grown anaerobically in MS medium supplemented with glucose with or without nitrate. The cells were lysed with toluene and β-galactosidase activity was measured. The data are from two independent experiments each assayed in triplicate. The error bars are the standard deviation of the mean.

	Strain				
	JCB4141 (Nap$^+$)	**JCB4142 (*ΔnapF*)**	**JCB4143 (*ΔnapGH*)**	**JCB4144 (*ΔnapFGH*)**	**JCB4145 (*ΔnapC*)**
Ratio of increase of the *napF* promoter activity	1	1.56 ± 0.106	1.53 ± 0.063	1.98 ± 0.034	2.82 ± 0.453

Table 5.1. Ratios of induction of the *napF* promoter activity in deletion mutant strains JCB4142 (*ΔnapF*), JCB4143 (*ΔnapGH*), JCB4144 (*ΔnapFGH*) and JCB4145 (*ΔnapC*) compared to the activity in the parental strain, JCB4141. Strains JCB4141 (Nap$^+$ Ubi$^+$ Men$^-$), JCB4142 (*ΔnapF* Ubi$^+$ Men$^-$), JCB4143 (*ΔnapGH* Ubi$^+$ Men$^-$), JCB4144 (*ΔnapFGH* Ubi$^+$ Men$^-$) and JCB4145 (*ΔnapC* Ubi$^+$ Men$^-$) were transformed with the plasmid pDF102 carying the *napF::lacZ* fusion.The transformants were grown anaerobically in MS medium supplemented with glucose (**figure 5.2, a**). The β-galactosidase activity was measured and the ratios of induction of β-galactosidase activity in the deletion mutant strains compared to the Nap$^+$ parental strain were calculated. The data are from two independent experiments each assayed in triplicate and are expressed as a mean value with the standard deviation of the mean.

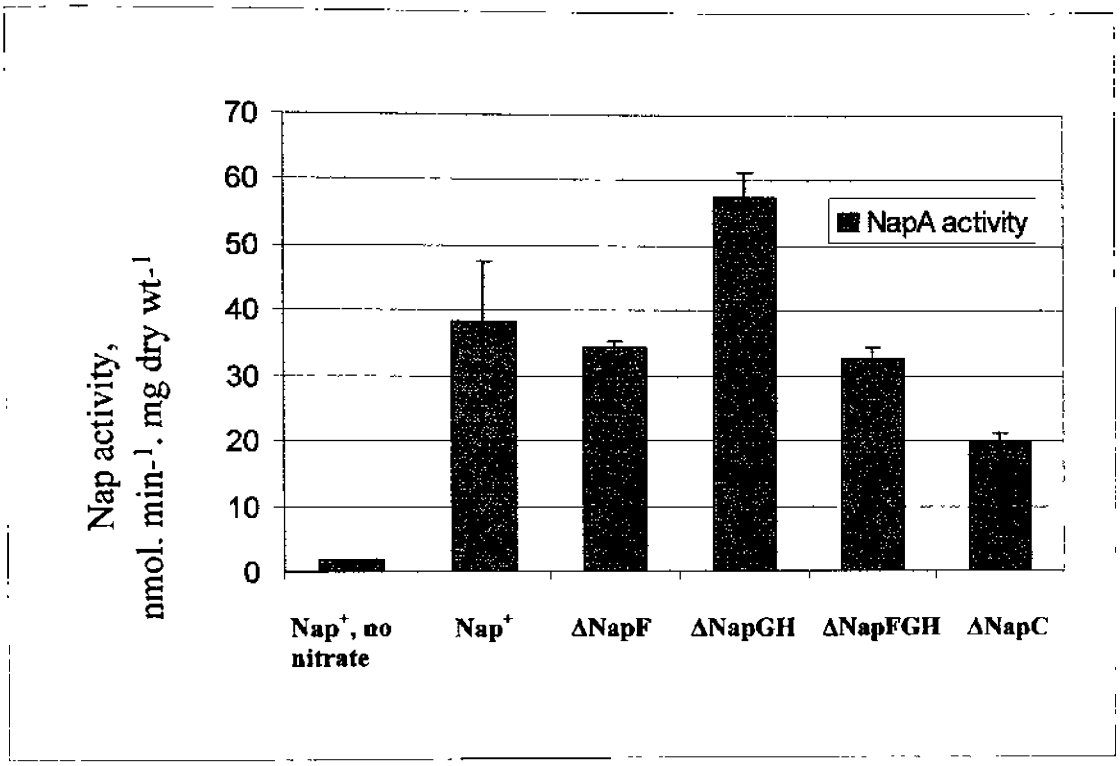

Figure 5.3. Effect of deletion of *napF*, *napG*, *napH* and *napC* genes on NapA activity in strains capable of synthesis of MK only. Strains JCB4241 (Nap^+ Ubi^- Men^+), JCB4242 (*napF* Ubi^- Men^+), JCB4243 (*napGH* Ubi^- Men^+), JCB4244 (*napFGH* Ubi^- Men^+) and JCB4245 (*napC* Ubi^- Men^+) were grown in MS medium supplemented with LB, glucose and nitrate until the OD_{650} had reached 0.6 to 0.8 and nitrate reductase activity was measured. Units of nitrate reductase activity are nmol NO_3^- reduced. min^{-1}. mg dry $weight^{-1}$. Values are the averages of data from two independent cultures. The error bars indicate the standard deviation of the mean.

activity of the *napC* mutant, JCB4245, was about half that of the parental strain. These results suggest that NapG and NapH decrease the expression or stability of the Nap electron transport complex and that NapC increases it in some way.

5.5. Effects of mutations in *napF* and *napGH* on adaptation from aerobic to anaerobic growth in strains able to synthesize both ubiquinol and menaquinol

Others in the laboratory had shown that menaquinol is a more effective electron donor to the terminal components of the Nap system than ubiquinol (Brondijk et al., 2002). Conversely, strains that are able to synthesise only ubiquinone and are defective in NapG and NapH retain only 1% of the rate of nitrate reduction of an isogenic *napGH*$^+$ strain (Brondijk et al., 2002). This implied that NapG and NapH are essential for the majority of electron transport from ubiquinol to nitrate, at least when bacteria are grown anaerobically in the presence of nitrate and the non-fermentable carbon source, glycerol.

When bacteria are grown in the presence of both glucose and nitrate, energy conservation occurs via both substrate-level phosphorylation in the process of glycolysis and via oxidative phosphorylation as a result of nitrate reduction. Also, for glycolysis and consequent growth to occur the NADH generated must be reoxidized to NAD^+, possibly by nitrate reduction. This could be achieved by reoxidizing NADH in the process of reduction of an electron acceptor. This section therefore seeks to investigate whether nitrate reduction by Nap stimulates growth during glucose fermentation. Also, the effects of deleting *napF*, *napGH* and *napC* on growth with glucose and nitrate were studied.

Strains JCB4041 (Nap$^+$ Ubi$^+$ Men$^+$), JCB4042 (*ΔnapF* Ubi$^+$ Men$^+$), JCB4042 (*ΔnapF* Ubi$^+$ Men$^+$), JCB4043 (*ΔnapGH* Ubi$^+$ Men$^+$), JCB4044 (*ΔnapFGH* Ubi$^+$ Men$^+$) and JCB4045 (*ΔnapC* Ubi$^+$ Men$^+$) were grown aerobically in LB and then subcultured and grown anaerobically in MS medium supplemented with glucose and nitrate until the late

stationary phase. The optical density of the cultures was measured every 30 minutes. As a control, the parental strain was grown in glucose medium without nitrate. The parental strain JCB4041 grown on glucose and nitrate exhibited the highest growth rate of 1 52 hour $^{-1}$ and reached the stationary phase after 5 hours of growth (**figure 5.4**). Strains JCB4043 and JCB4044 had slightly lower rates of growth of 1.48 and 1.41 hour $^{-1}$, respectively. In contrast, the strain defective in the synthesis of NapF, JCB4042, grew very poorly at a constant rather than an exponential rate, and the yield was even lower than that of strain JCB4041 grown in the absence of nitrate and conserving energy by substrate-level phosphorylation only. After 8 hours of growth, the yield of strain JCB4042 was 30% of that of the parental strain. It was concluded that NapF plays a role in nitrate-dependent growth supported by Nap and influences in some way the ability to conserve energy.

5.6. Role of NapF in adaptation from aerobic to anaerobic growth in strains able to *synthesize only* menaquinol

Similar experiments to those described in the previous section were repeated in the strains competent for synthesis of only menaquinone. The objective was to investigate whether nitrate stimulates growth during glucose fermentation and find out whether deletion of the *napF*, *napGH* and *napC* genes affects growth on glucose and nitrate. Strains JCB4241 (Nap$^+$ Ubi$^-$ Men$^+$), JCB4242 (*ΔnapF* Ubi$^-$ Men$^+$), JCB4243 (*ΔnapGH* Ubi$^-$ Men$^+$), JCB4244 (*ΔnapFGH* Ubi$^-$ Men$^+$) and JCB4245 (*ΔnapC* Ubi$^-$ Men$^+$) were grown aerobically in LB medium and then subcultured and grown anaerobically in MS medium supplemented with glucose and nitrate as above and the optical density was measured every hour (**figure 5.5**). As a control for growth due to fermentation alone, strain JCB4241 was grown on MS supplemented with glucose but without nitrate. The growth rate of strain JCB4241 in the

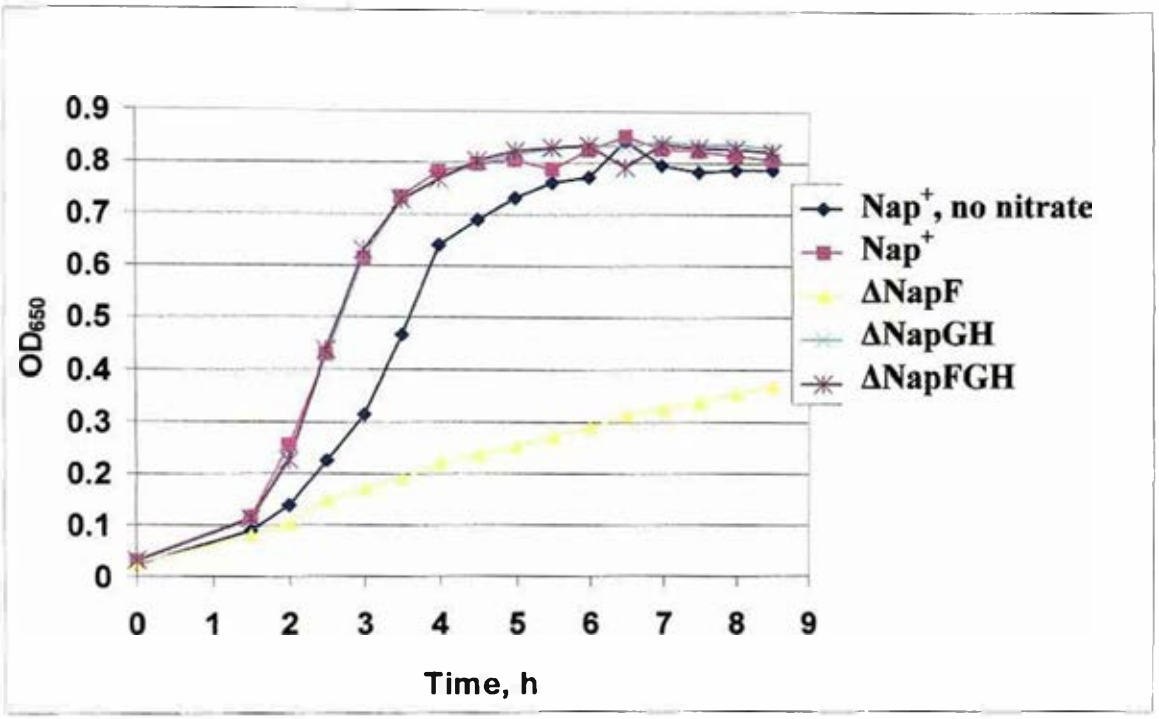

Figure 5.4. Growth on glucose and nitrate in the presence of UQ and MK. Strains JCB4041 (Nap$^+$ Ubi$^+$ Men$^+$), JCB4042 (*ΔnapF* Ubi$^+$ Men$^+$), JCB4043 (*ΔnapGH* Ubi$^+$ Men$^+$), JCB4044 (*ΔnapFGH* Ubi$^+$ Men$^+$) and JCB4045 (*ΔnapC* Ubi$^+$ Men$^+$) were grown anaerobically on MS medium supplemented with glucose and nitrate until the late stationary phase. The optical density of the cultures was measured every 30 minutes. The inocula were from aerobic cultures grown in LB medium.

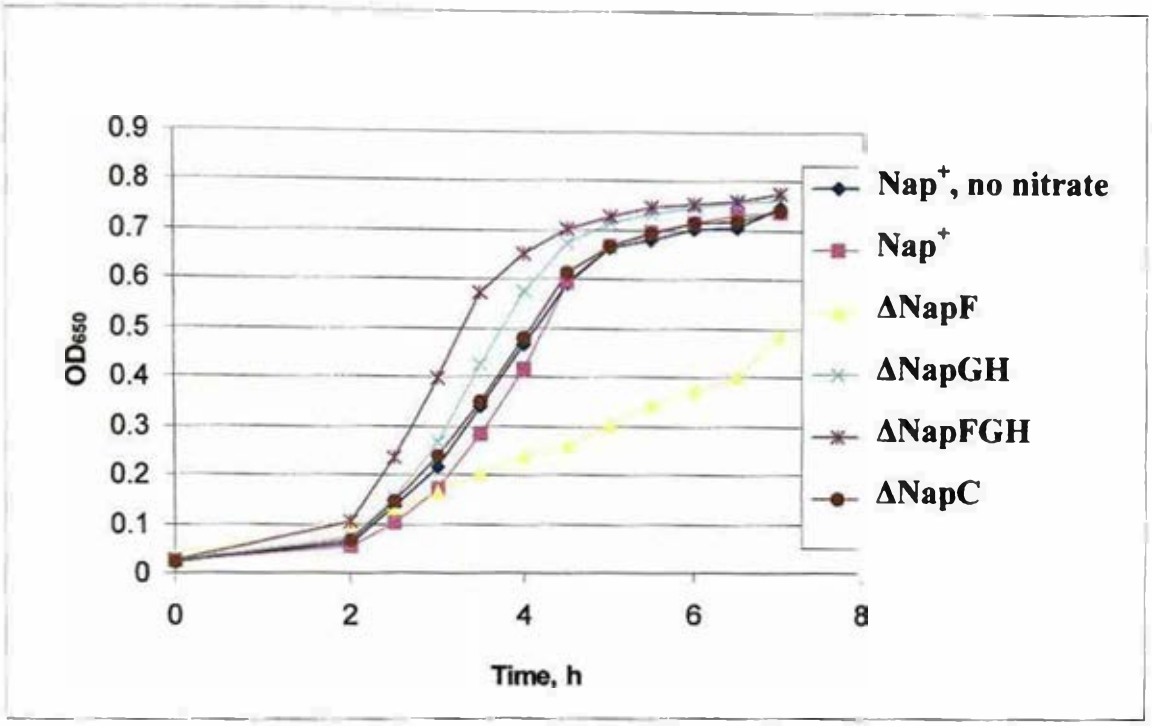

Figure 5.5. Growth on glucose and nitrate in the presence of MK only. Strains JCB4241 (Nap$^+$ Ubi$^-$ Men$^+$), JCB4242 (*ΔnapF* Ubi$^-$ Men$^+$), JCB4243 (*ΔnapGH* Ubi$^-$ Men$^+$), JCB4244 (*ΔnapFGH* Ubi$^-$ Men$^+$) and JCB4245 (*ΔnapC* Ubi$^-$ Men$^+$) were grown anaerobically until the late stationary phase in MS medium supplemented with glucose and nitrate. The inocula were from aerobic cultures grown in LB medium.

presence of nitrate was 1.27 h^{-1}. The growth rates of JCB4241 in the absence of nitrate, and of NapGH, NapFGH and NapC mutants in the presence of nitrate were 1.08, 1.13, 1.04 and 1.16 h^{-1}, respectively. The NapF mutant again grew very slowly; the growth was almost linear as in the $Ubi^{+}Men^{+}$ background and the growth rate was less than half that of the parental strain, JCB4241.

5.7. Effect of pregrowth conditions on growth of Nap^{+} and *ΔnapF* strains

In the previous experiments, cultures were inoculated with bacteria that had been grown aerobically. To see if pregrowth conditions play any role in growth of the NapF mutant under anaerobiosis, strains JCB4041 (Nap^{+}) and JCB4042 (*ΔnapF*) were first grown either aerobically or anaerobically in MS/glucose medium supplemented with nitrate. These cultures were then diluted into MS medium supplemented with glucose and nitrate and grown anaerobically until the late stationary phase. The optical density was measured throughout the growth. Both the growth rate and final yield of the NapF mutant, JCB4042, were much higher in cultures inoculated with anaerobically than aerobically grown bacteria (**figure 5.6, a**). The growth rate and yield of the Nap^{+} strain, JCB4041, inoculated with bacteria that had been grown anaerobically were just slightly higher than those inoculated with an anaerobically grown culture of JCB4042. In contrast to strain JCB4042, the growth rate of JCB4041 pregrown aerobically with nitrate was much higher than that of the same strain pregrown anaerobically (**figure 5.6, a**). So, lower growth rates and yield were obtained when the NapF mutant was pregrown aerobically, whereas the opposite results were obtained for the $NapF^{+}$ parental strain. This suggests that NapF plays some role in adaptation from aerobic to anaerobic growth.

Strain JCB4042, pregrown aerobically in MS/glucose medium without nitrate, also had lower growth rate compared to that of strain JCB4041 pregrown under the same growth

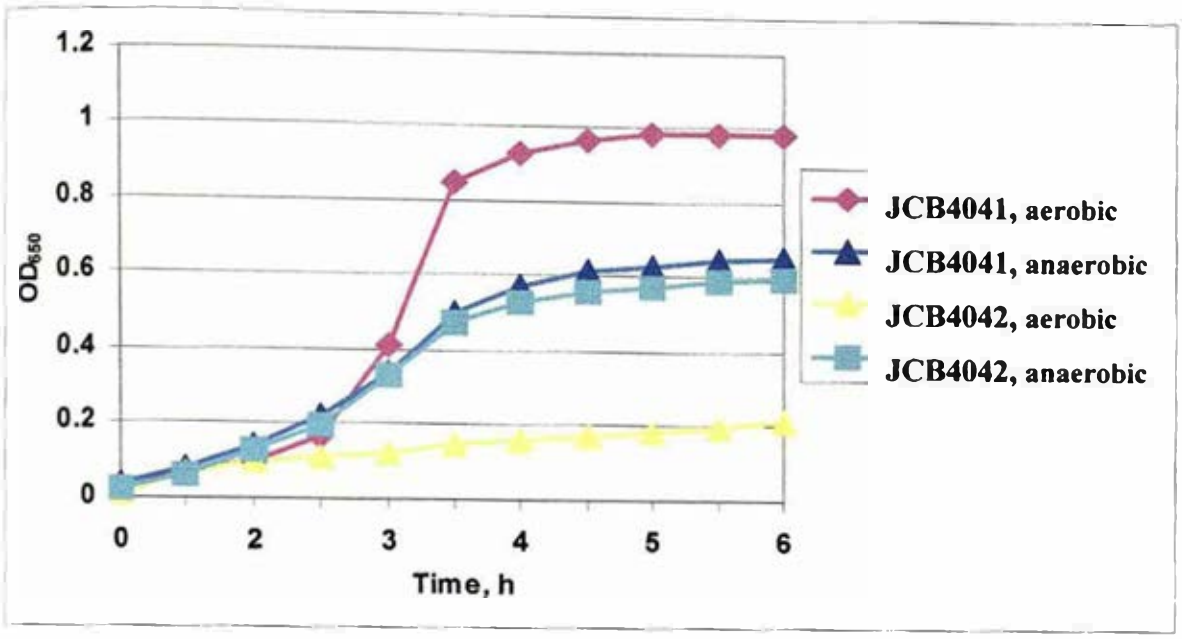

a)

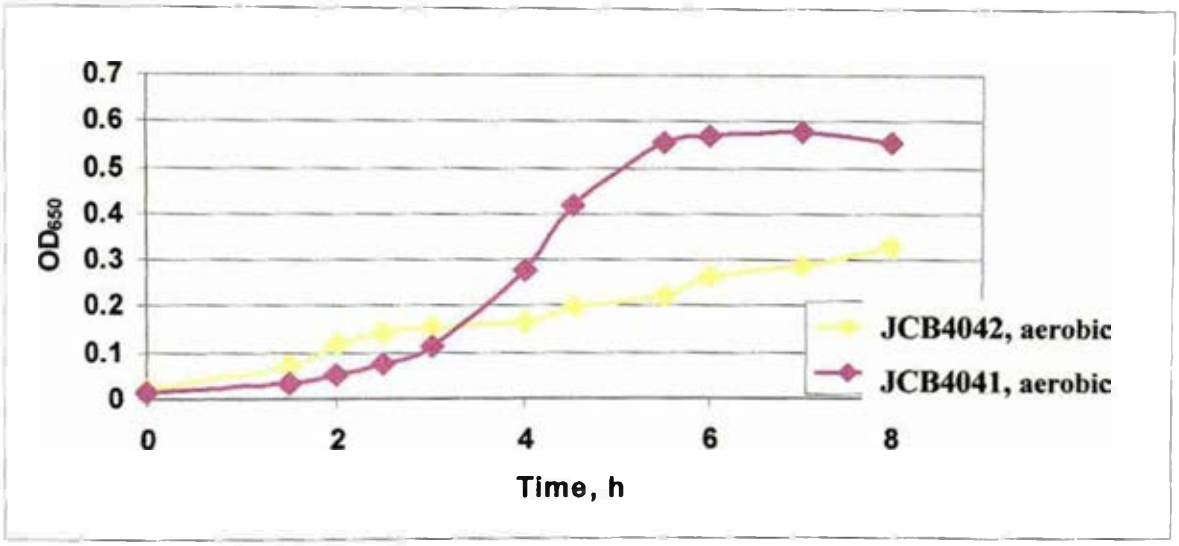

b)

Figure 5.6. Anaerobic growth of the Nap$^+$ strain, JCB4041, and NapF$^-$ strain, JCB4042, in the presence of UQ and MK depending on pregrowth conditions. Strains JCB4041 (Nap$^+$) and JCB4042 (*ΔnapF*) were first grown either aerobically or anaerobically in MS/glucose medium supplemented with nitrate. These cultures were then diluted into MS medium supplemented with glucose and nitrate and grown anaerobically until the late stationary phase. The optical density was measured throughout the growth. **a)** Aerobic pregrowth in MS medium supplemented with glucose and nitrate; **b)** Aerobic pregrowth in MS medium supplemented with glucose alone.

conditions (**figure 5.6, b**). This, probably, reflects the fact that the *napF* operon is expressed at a very low level even under aerobiosis without nitrate, which allows NapF to play its role in adaptation from aerobiosis to anaerobiosis.

5.8. A possible redox-balancing role for Nap

During glucose fermentation, cells need to reoxidise excessive reducing compounds such as NADH formed during conversion of glucose to pyruvate. *E. coli* uses fumarate reductase for redox balancing during glucose fermentation, and fumarate reductase is a menaquinone-dependent enzyme (Kroger, 1978; Soballe and Poole, 1999). In the absence of menaquinone, redox balancing must therefore be achieved by an alternative mechanism. So, strains defective in synthesis of menaquinone were used to investigate whether Nap can replace fumarate reductase in its redox-balancing role.

Strains JCB4141 (Nap^+ Ubi^+ Men^-), JCB4142 (*ΔnapF* Ubi^+ Men^-), JCB4143 (*ΔnapGH* Ubi^+ Men^-), JCB4144 (*ΔnapFGH* Ubi^+ Men^-) and JCB4145 (*ΔnapC* Ubi^+ Men^-) were grown in minimal medium supplemented with 0.4% glucose as the fermentable carbon source and 20 mM nitrate. Growth of the menaquinone deficient, Nap^+ $NarA^-$ strain JCB4141 on glucose was far more rapid in the presence of nitrate than in its absence (**figure 5.7**). The *ΔnapC, ΔmenBC* mutant, JCB4145, which is totally devoid of residual Nap activity, grew very slowly in the presence of glucose, and this rate was not increased in the presence of nitrate. There were smaller differences in the growth rates on glucose of the Ubi^+Men^+ strain, JCB4041 and Ubi^-Men^+ strain, JCB4241, compared to the Ubi^+Men^- strain JCB4141, in the presence or absence of nitrate (**figures 5.4, 5.5** and **5.7**). The ratios of growth rates with and without nitrate in Ubi^+Men^+, Ubi^-Men^+ and Ubi^+Men^- backgrounds are shown in **table 5.2.**

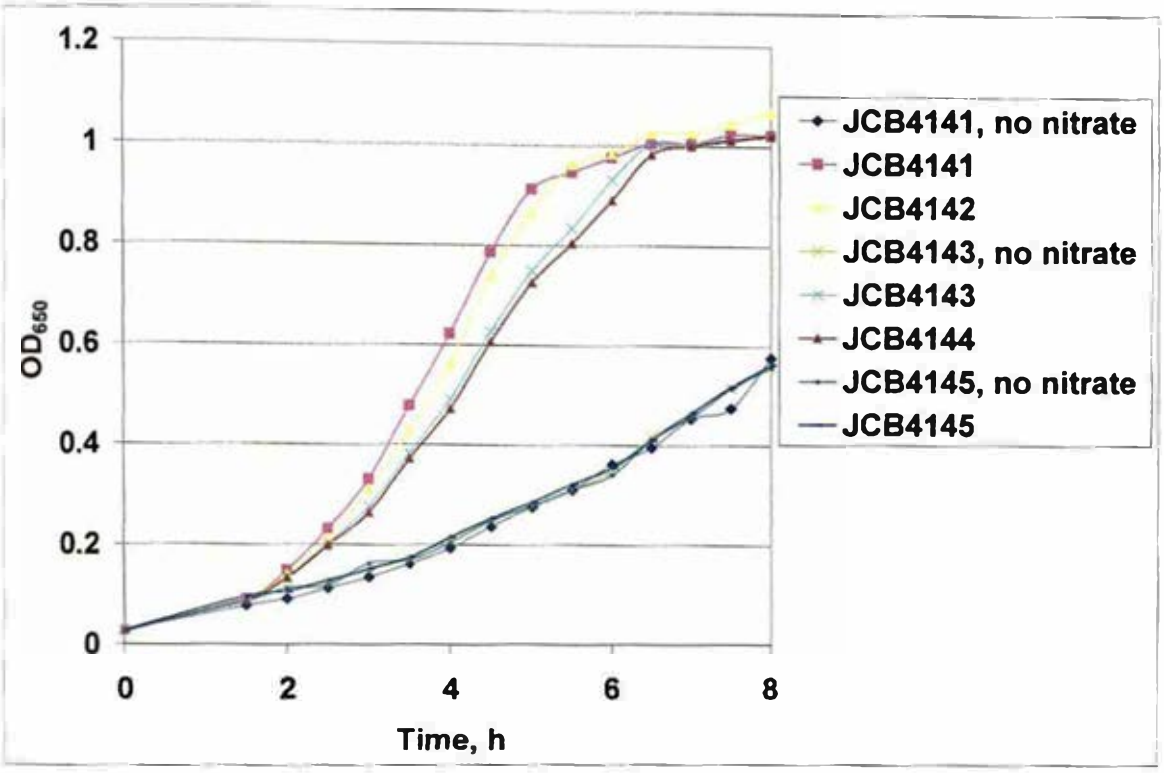

Figure 5.7. Nitrate-stimulated growth of a strain defective in synthesis of menaquinone under anaerobic growth with glucose as the fermentable carbon source. Strains JCB4141 (Nap$^+$ Ubi$^+$ Men$^-$), JCB4142 (Δ*napF* Ubi$^+$ Men$^-$), JCB4143 (Δ*napGH* Ubi$^-$ Men$^-$), JCB4144 (Δ*napFGH* Ubi$^+$ Men$^-$) and JCB4145 (Δ*napC* Ubi$^+$ Men$^-$) were grown in minimal medium supplemented with 5% (v/v) LB, 0.4% glucose as the fermentable carbon source and 20 mM nitrate. Optical density was measured every 30 minutes. Note that despite the very low rate of nitrate reduction by strain JCB4143, this strain still responds to nitrate during glucose fermentation. All five strains are defective in naphthoquinone synthesis.

Strain	Phenotype	Growth rate ($hour^{-1}$)		Ratio
		$+NO_3^-$	$-NO_3^-$	
JCB4041	Ubi^+Men^+	1.52 ± 0.04	1.00 ±0.03	1.52
JCB4141	Ubi^+Men^-	0.46 ± 0.13	0.25 ± 0.00	1.84
JCB4241	Ubi^-Men^+	1.27± 0.15	1.08 ± 0.47	1.18

Table 5.2. Rates of growth of strains JCB4041 (Ubi^+Men^+), JCB4241 (Ubi^-Men^+) and JCB4141 (Ubi^+Men^-). Strains JCB4041, JCB4241 and JCB4141 were grown anaerobically in MS medium supplemented with glucose with or without nitrate (see also figures 5.4, 5.5 and 5.7). The rates of exponential phase growth were calculated. The ratios between the rates during growth with and without nitrate are given. Values are the averages of data from two independent growth experiments. The errors indicate the standard deviation of the mean.

In the absence of nitrate, the growth rate of the *napGH* strain, JCB4143, was identical to that of the *napC* deletion mutant (**figure 5.7**). It was demonstrated before that electron transport from glycerol via ubiquinione to the NapAB complex is totally dependent on NapG and NapH subunits (Brondijk et al., 2002). Nevertheless, during glucose fermentation the growth rate of strain JCB4143 in the presence of nitrate was almost the same as that of strain JCB4141 grown under the same conditions (**figure 5.7**). These data indicate that there is a residual Nap activity even in the Δ*napGH* Δ*menBC* strain, JCB4143. This residual activity accounts for not more than 1% of total activity and therefore is too low to be measured reliably with a nitrate electrode. Nevertheless, it is apparently sufficient to replace fumarate reduction in its redox-balancing role.

5.9. Use of high and low mid-point redox potential exogenous quinols to confirm the physiological roles of NapG and NapH

The data of Brondijk et al. (2002 and 2004) all indicate that the physiological role of NapG and NapH is to facilitate electron transfer via UQH_2, but not via MKH_2, to NapC. The mid-point redox potential for the $MK:MKH_2$ couple is lower than that of the $UQ:UQH_2$ couple (-70 mV compared with +10 mV), suggesting that NapG and NapH might be required to couple the oxidation of the weaker electron donor to NapC reduction. If the mid-point redox potential for the quinone: quinol couple used is the primary determinant of whether NapG and NapH are required for electron transfer to NapC, it should be possible to reconstitute the system using exogenous quinols of *different reducing power. Preliminary* experiments established that the water-soluble UQ_0 and plumbagin are poor electron donors to the periplasmic nitrate reductase. However, rapid and reproducible rates of nitrate reduction were detected with lapochol and menadiol. The mid-point redox potential at pH 7.0 of the oxidized : reduced lapochol couple is –300 mV; that of the oxidized : reduced

menadiol couple is 0 mV. These two exogenous electron donors were therefore used to compare rates of Nap-dependent nitrate reduction by strains proficient and deficient in NapG and NapH and also mutated for the two nitrite reductases, Nir and Nrf to make sure that all nitrite that is accumulated as a result of nitrate reduction is detected and is not further reduced to ammonium. The rate of nitrate reduction by the $NapG^+$ $NapH^+$ strain, JCB4081a, in the presence of menadiol was 100 (±27) nmol of nitrite formed. min^{-1}. (mg bacterial dry mass)$^{-1}$ compared with a rate of 3 (± 2) nmol of nitrite formed. min^{-1}. (mg bacterial dry mass)$^{-1}$ for the NapG NapH-defective strain, JCB4083a (**figure 5.8**). In contrast, loss of NapG and NapH had a far smaller effect on the rate of nitrate reduction (nitrite accumulation) in the presence of the more powerful reducing agent, lapochol (**table 5.3**): the corresponding rates were 18 (± 12) and 12 (± 9) nmol of nitrite formed. min^{-1}. (mg bacterial dry mass)$^{-1}$ for strains JCB4081a and JCB4083a, respectively.

The methyl-viologen-dependent rates of nitrate reduction, which are indicative of the amount of active NapAB complex, were also lower for strain JCB4083a than for strain JCB4081a, being about 20% for the *ΔnapGH* strain compared to the parental strain (**table 5.3**). Nevertheless, this difference in amount of active NapAB complex was insufficient to account for the strikingly different dependence of nitrate reduction by menadiol on NapG and NapH (**table 5.3**).

Figure 5.8. *In vitro* reduction of nitrate to nitrite using reduced menadiol and lapochol as electron donors. Bacterial suspensions were incubated with either menadiol or lapochol in the presence of nitrate, and the concentration of nitrite in samples withdrawn at the intervals shown was determined. The strains used for these experiments were JCB4081a and JCB4083a that lacked the nitrite reductases Nir and Nrf. Menadiol (**a**) and lapochol (**b**) were reduced with sodium borohydride immediately before use.

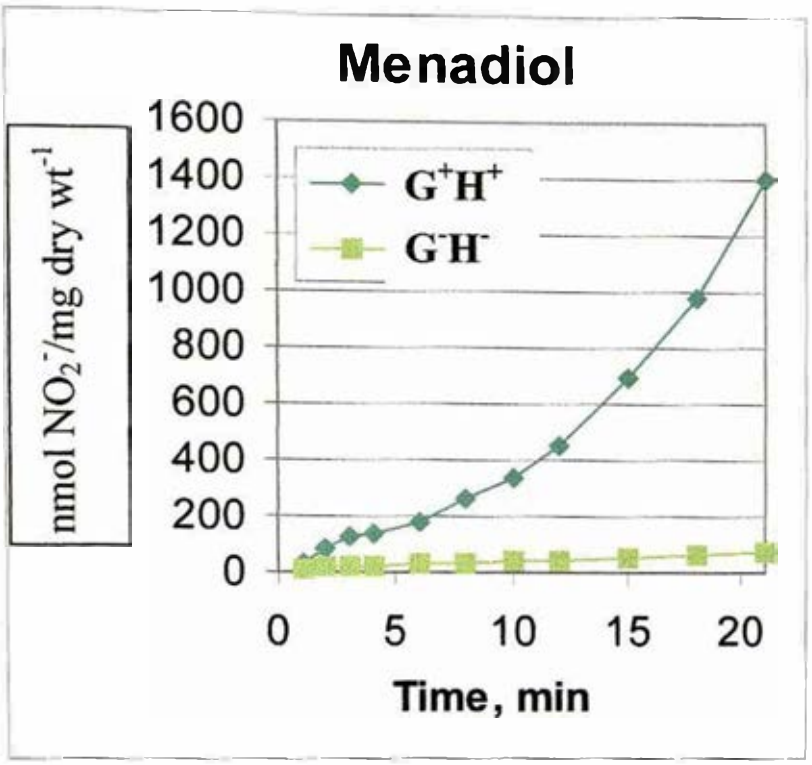
Menadiol
nmol NO_2^-/mg dry wt^{-1}
1600
1400
1200
1000
800
600
400
200
0
G^+H^+
G^-H^-
0
5
10
15
20
Time, min

a)

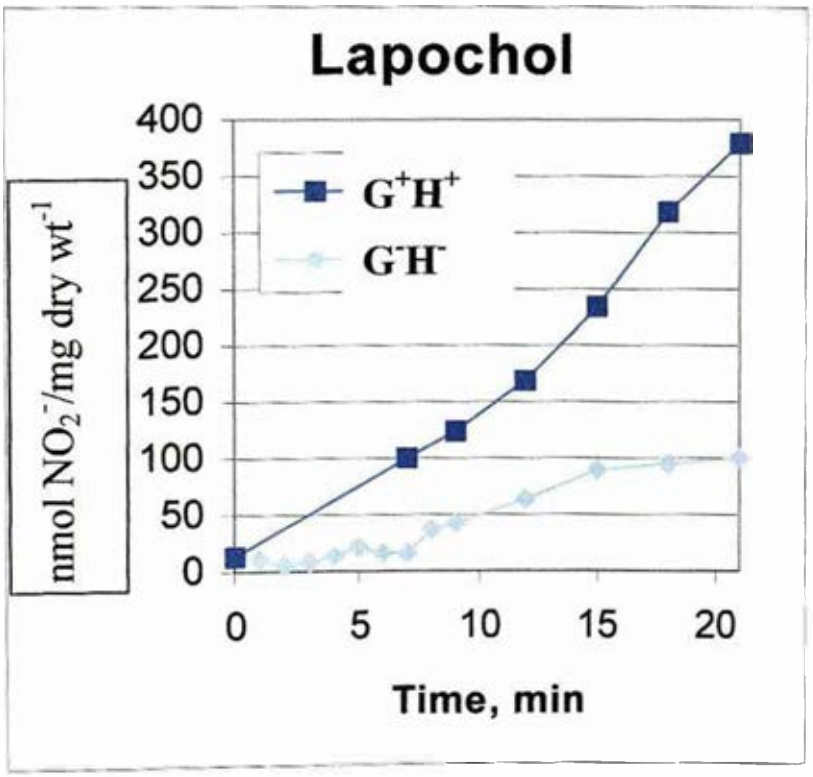
Lapochol
nmol NO_2^-/mg dry wt^{-1}
400
350
300
250
200
150
100
50
0
G^+H^+
G^-H^-
0
5
10
15
20
Time, min

b)

Strain	Nitrite production with artificial electron donors (nmol NO_2*min^{-1}*mg dry wt^{-1})			Relative activity	
	Menadiol	Lapochol	Nitrate reductase activity (MeV)	Menadiol/MeV	Lapochol/MeV
JCB4081a (Nap^+)	100 ±27	18±12	205±108	0.49	0.09
JCB4083a (*ΔnapGH*)	3±2	12±9	42±11	0.07	0.29

Table 5.3. Rates of nitrite production with artificial electron donors menadiol and lapochol in $NapGH^+$ and *ΔnapGH* strains. Menadiol and lapochol were reduced with sodium borohydride immediately before use. Samples were stirred at room temperature, and the quantity of nitrite accumulated by samples withdrawn at regular intervals was determined. Rates of nitrate reduction by the artificial electron donor, methyl viologen (MeV) were also determined as a measure of amount of active NapAB complex in the $NapGH^+$ and *ΔnapGH* strains. Values are the averages of data from at least two independent experiments, with the standard deviation of the mean indicated.

CHAPTER 6
DISCUSSION

6.1. Regulation of the gene encoding hybrid cluster protein

Previously it was shown that HCP is expressed under anaerobic conditions in the presence of nitrate or nitrite (van den Berg et al., 2000). The antibodies were raised against the *E. coli* HCP protein and Western blotting showed that more HCP accumulated during growth in medium with nitrite than with nitrate. This type of expression resembles that of the *nap* operon as the *napF* promoter is repressed in response to a high concentration of nitrate and activated in response to nitrite and a low concentration of nitrate. It was also shown that in *Shewanella oneidensis* transcription of the *hcp* gene is elevated under nitrate reducing conditions (Beliaev et al., 2002). Based on the structure of the *hcp* promoter, it was proposed that this operon might be regulated by FNR and NarL and/or NarP (**figure 3.1**). The *nar, nap, nir,* and *nrf* operons encoding proteins involved in nitrate/nitrite reduction are activated by FNR under anaerobic conditions and further regulated by either NarL or NarP when nitrate is available. The evidence that *hcp* is activated by the same regulator proteins would give an indirect indication that it is involved in the same biochemical pathways. One objective of this project was therefore to analyse the pattern of expression of the *hcp* operon.

During the shift from aerobic to anaerobic or microaerobic conditions many genes or operons are regulated by either FNR or the two-component ArcB/ArcA system (Kang et al., 2005; Salmon et al., 2005; Liu and Wulf, 2004). As expected based on previous observations, in the $fnr^{+}\Delta lac$ strain, expression of the *hcp* gene was very low during aerobic growth and induced during anaerobic growth. In the strain lacking Fnr anaerobic induction was absent (**figure 3.7**), suggesting that activation of the *hcp* promoter during anaerobic growth is mediated by FNR. There was no influence of ArcA on the *hcp* promoter under anaerobic conditions, as the promoter activity was relatively equal in both Arc^{+} and Arc^{-} strains. Nevertheless, in the fnr^{+} *arc* mutant during aerobic growth, *hcp* expression was 2.4 times higher than in $fnr^{+}arcA^{+}$ strain.

Apparently, the ArcB/ArcA system plays no direct role in the regulation of the *hcp* gene, as there is no binding site for ArcA found in the *hcp* promoter. The induction observed might therefore be due to some indirect influence of ArcA on the *hcp* promoter: ArcA for instance may activate some other protein that acts as a repressor of HCP under aerobic or microaerobic growth.

As HCP was shown to be expressed anaerobically (van den Berg et al., 2000; Beliaev et al., 2002), alternative electron acceptors such as fumarate, DMSO or TMAO were tested for their ability to activate the *hcp* promoter (**figure 3.9**). The promoter activity of the cultures in the presence of any of the three electron acceptors was approximately the same. So, as fumarate, DMSO and TMAO had no effect on transcription from the *hcp* promoter, this corroborated the hypothesis that HCP is involved in some stage of nitrogen metabolism.

It was shown in this work that the activation of the *hcp* promoter is mediated by both nitrite and nitrate and that in response to nitrite and nitrate NarP is an activator of the *hcp* promoter, whereas NarL might apparently act both as an activator and a repressor depending on the concentration of nitrate and nitrite. There has been a long discussion as to whether nitrite or nitrate is a superior anion to elicit responses mediated by the Nar system (Lee et al., 1999; Stewart and Bledsoe, 2003). It was also shown that in response to nitrite, NarX acts as a phosphatase of NarL-phosphate, which results in small amounts of NarL-phosphate (Rabin and Stewart, 1993). Experiments described in chapter 3 demonstrate that nitrite is more effective in eliciting response at the *hcp* promoter. First of all, in the parental strain, JCB302, expressing both sensor kinases, NarX and NarQ, and both response regulators, NarL and NarP, the nitrite mediated response is greater than that elicited by nitrate. Also, in the NarL$^+$NarP$^-$ strain, activity of the promoter in response to nitrite is considerably higher throughout growth.

In the NapL$^+$NarP$^-$ mutant, the activity of the promoter was increasing with growth in response to both nitrate and nitrite (**figure 3.11, c**). There are two possible explanations of the

increase of the promoter activity in response to nitrate. First, during growth nitrate is reduced to nitrite, and consequently, with growth there would be more and more nitrite accumulated. As nitrite is better in eliciting a response, it might be argued that it would result in higher promoter activity at the later stage of growth. In this regard, it is noticeable that although the promoter activity in response to nitrate is about 30% lower throughout the growth than that in response to nitrite, it eventually reaches the level of activity elicited by nitrite. This suggests that by the end of the growth in the nitrate medium, nitrite that accumulated as a result of depletion of nitrate reaches the level that is sufficient to produce optimal amounts of NarL-phosphate.

Nevertheless, if conversion of nitrate to nitrite is the sole reason for the increasing promoter activity, why would then the promoter activity increase with growth in medium supplemented with nitrite? NarL can play a dual role at some promoters acting as an activator or as a repressor (Tyson et al., 1994; Darwin et al., 1998). The tendency for the *hcp* promoter activity to increase during growth in response to either nitrite or nitrate might be due to a different action of NarL in response to different concentrations of nitrate or nitrite. The second explanation, therefore, is that at the beginning of growth with high concentration of nitrate (20 mM) almost the whole pool of NarL might become phosphorylated and consequently bind to the three NarL consensus sites at the *hcp* regulatory region (**figure 6.1, a**). Binding to some of the consensus sites might cause repression of transcription from the *hcp* regulatory region. These sites are most probably single heptamers as their location might interfere with the process of transcription by RNAP. When the concentration of nitrate decreases with growth, less NarL becomes phosphorylated. This results in release of NarL binding sites with low affinity, while the binding sites with high affinity, possibly only the 7-2-7 site, remain occupied, which causes the activation of the *hcp* promoter (**figure 6.1, b and c**). This might apply to the regulation of *hcp* transcription by NarL in response to either nitrite or nitrate. The overall higher activity of the *hcp* promoter in response to nitrite than nitrate might be due to the fact that in response to

Figure 6.1. A model of regulation of the *hcp/hcr* operon by FNR, NarL and NarP at different concentrations of nitrate or nitrite. **a**: Under anaerobic conditions in the presence of nitrate or nitrite the *hcp* promoter is activated by both FNR and NarP (P) regulatory proteins. NarL (L) acts differently in response to different concentrations of nitrate or nitrite. One of the models is that at the beginning of growth with a high concentration of nitrate (20 mM) or nitrite (2.5 mM) almost the whole pool of NarL becomes phosphorylated and consequently binds to the three NarL consensus sites at the *hcp* regulatory region. Binding to single heptamers apparently causes partial repression of transcription as it might interfere with the process of binding of RNAP. **b** and **c**: When the concentration of nitrate or nitrite decreases with growth, less NarL becomes phosphorylated. This results in release of NarL binding sites with low affinity, possibly two single heptamers, while the binding site with high affinity, possibly the 7-2-7 site, remains occupied, which leads to the full level of activation of the *hcp* promoter. The question mark means that at present it is not clear which of the two single heptamers has lower affinity for NarL-phosphate.

The rightward-facing arrow on the right is the transcription start site. The orange inverted arrows show the FNR binding site. The green arrows are NarL binding sites. The ocean-grey inverted arrows denote 7-2-7 recognition site for both NarL and NarP. Lines with arrowheads show activation; lines with straight ends show repression. The thickness of the RNAP arrow denotes the overall level of transcription of the *hcp* gene.

Concentration of NO_3^- or NO_2^-	Amount of NarL-phosphate	Binding of FNR, NarL and NarP to the *hcp* regulatory region
a: high	high	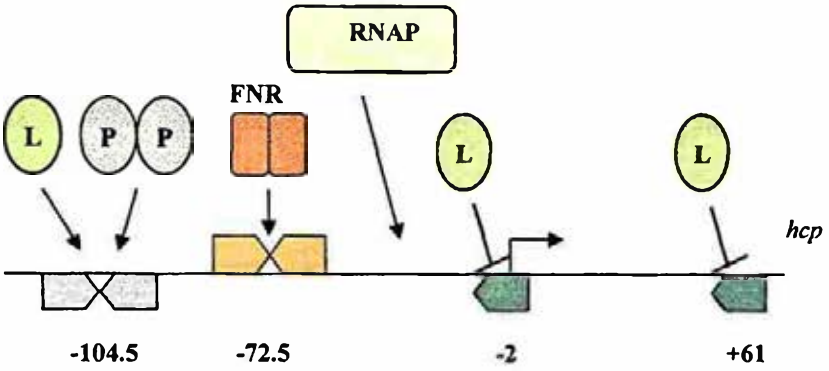
b: medium	medium	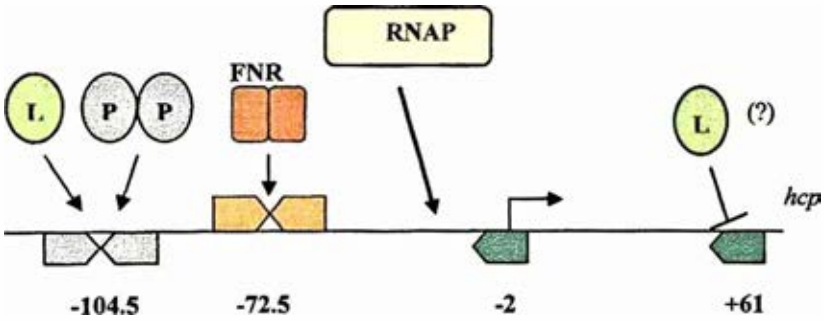
c: low	low	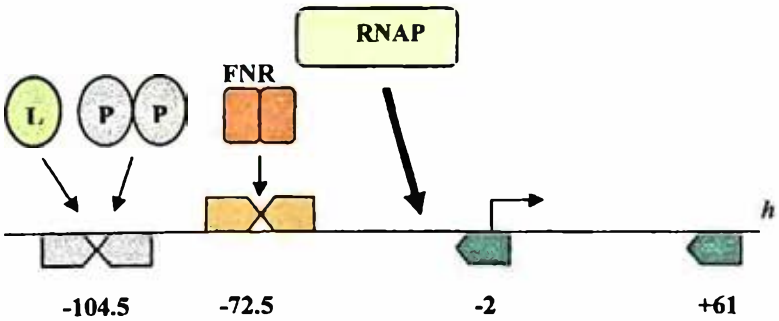

nitrite, NarL-phosphate becomes dephosphorylated by NarX, which results in a lower concentration of NarL-phosphate with higher overall activation of the *hcp* regulatory region.

It was shown by the gel retardation assays that the *hcp* promoter has three sites for binding of NarL, one being the high affinity site, and two others with lower affinity (**figure 3.12**). At present it is unclear which site out of the three has the highest and the lowest affinity, although it is possible to predict the one with the highest affinity. The 7-2-7 site has 7 out of 7 match to the consensus TACYYMT for the upstream heptamer and 5 out of 7 match for the downstream heptamer, while both single heptamers have 5 out of 7 match to the consensus. So, it is plausible to argue that under low nitrate/nitrite concentrations only the 7-2-7 site becomes occupied, and when nitrate concentrations are high, NarL binds also to the single heptamers, leading to a partial repression of the *hcp* promoter transcription. Although the two single heptamers have the same 5 out of 7 match to the consensus sequence, they differ in their ability to be recognised by NarL-phosphate as apparent from the pattern of the gel retardation assay that has three shifts (**figure 3.12**). This must assure the fine-tuning of the expression of the *hcp* promoter in response to different concentrations of nitrite or nitrate: under medium concentrations of nitrite/nitrate only one single heptamer is occupied by NapL-phosphate, while under high concentrations of the anions both heptamers become occupied.

The β-galactosidase activity of the parental strain in the presence of nitrite or nitrate showed a pattern with varying promoter activity throughout growth, which is similar in response to both nitrate and nitrite. One of the observations made on the expression of the *hcp* promoter is that NarL is superior to NarP in its regulation of the *hcp* gene. In the parental strain nitrite response is stronger, which is mediated mostly by NarL. This is evident from the pattern of nitrite-elicited activation of the *hcp* gene in single mutants expressing only NarL (**figure 3.11, c**) or only NarP (**figure 3.11, b**), which show higher response to nitrite than to nitrate and

the same response to both anions, respectively. On the other hand, NarP activates the promoter better in response to nitrate, and yet this preference is not seen in the parental strain. Two possible reasons for this can be discussed. First, in the parental strain, expressing both NarL and NarP and grown in nitrate medium, NarL-phosphate and NarP-phosphate compete for the 7-2-7 site, and NarL-phosphate binds to it but somehow fails to activate transcription to the same degree as NarP-phosphate. This would be reminiscent of regulation of the *napF* promoter where NarP can activate transcription, whereas NarL fails to do so. The second reason could be that in response to nitrate NarL binds not only to 7-2-7 site, but also to two single heptamers, as discussed above, and this prevents full activation of the promoter by NarP in response to nitrate.

Thus, the *hcp* promoter demonstrates another possibility of regulation by the Nar system, in which NarL activates preferentially in response to nitrite rather that nitrate compared to activation of nitrate by NarL (*nirB*) and activation of nitrite by NarP (*napF*). In conclusion, NarP acts as an activator of the *hcp* promoter in response to both nitrate and nitrite, whereas NarL can play a dual role as an activator or repressor, although the final outcome is activation of the promoter to different degrees as a result of different amounts of NarL-phosphate formed. When the parental strain is grown in medium supplemented with nitrate, the regulation of the *hcp* promoter is the most complex. It results from an interplay of different factors, as nitrate is converted to nitrite is the process of growth, and as both NarL and NarP, apparently activated in a different way in response to nitrate and nitrite and having different affinities, compete for the 7-2-7 binding site.

Interestingly, the *hcp* gene appears to be expressed at incredibly high levels: the activity of the gene is about 20,000 units under anaerobic growth and it further increases to 40,000 - 50,000 units upon addition of nitrate or nitrite. This is about 20- and 25-fold higher than the expression of the *nirB* promoter during anaerobic growth and anaerobic growth with nitrate, respectively (**figure 3.11, a**; see also Tyson et al., 1993; Wang and Gunsalus, 2000). Yet, the

HCP protein is apparently present in the cell cultures in quite small amounts: the Coomassie stained gels of whole protein extracts from HCP^+ and HCP^- strains failed to demonstrate any difference in the band corresponding to the HCP protein (data not shown); and only more sensitive Western analysis revealed that HCP is expressed by the parental strain, but is absent from the *hcp* mutant (**figure 4.6**). This implies that there is regulation of HCP at a post-transcriptional level.

6.2. Search of function of the hybrid cluster protein

Three lines of evidence suggest that HCP is involved in anaerobiosis and the nitrogen cycle. First, is that it is present in organisms that can exist anaerobically disregarding whether they are strict or facultative anaerobes. Apart from this no correlation between the presence of HCP and the type of organism has been noticed: the hybrid cluster protein has been found in eucaryotes, bacteria and archaea, and there is no correlation between its presence and pathogenicity as the genomes of both pathogens (*S. enterica*) and non-pathogens (*D. vulgaris*) encode it. Perhaps when the complete genome sequences of more organisms are released it will shed some more light on the function of HCP. The second line of evidence, which is consistent with the first observation, is that expression of HCP is elevated under anaerobic growth and further elevated with nitrite or nitrate (**figure 3.11, a**; see also van den Berg et al., 2000; Beliaev et al., 2002). Thirdly, some data implicate HCP in metabolism of hydroxylamine and nitric oxide (Wolfe et al., 2002, Kim et al., 2003, Cabello et al., 2004).

If in many organisms the *hcp* genes were found to be located close to another gene or genes with known function, it could be suggested that products of these genes might be functionally related. Unfortunately, the patterns of gene organisation (synteny) differ with respect to the *hcp* gene in different bacteria. In enteric bacteria the *ybjW* gene encoding HCP is preceded by *ybjE* encoding putative membrane protein and followed by *b0872* encoding

pyruvate oxidase or pyruvate dehydrogenase in *E. coli* and *S. enterica*, respectively. The *hcp* gene in *Photobacterium phosphoreum* is located next to the *rib* operon, which encodes proteins that participate in the synthesis of riboflavin from GTP and ribulose 5-phosphate (Kasai and Sumimoto, 2002). Nevertheless, this location of the *hcp* gene does not seem to be relevant to the function of the *rib* operon. The *hcp* gene of *R. capsulatus* is clustered together with the operon for nitrate assimilation, *nas*, and it has been implicated to participate in the process of nitrate, nitrite and hydroxylamine assimilation under phototrophic growth (Cabello et al., 2004).

It has been noticed that the active sites of HCP and of carbon monoxide dehydrogenase (CODH) proteins are very similar. The active site of CODH contains [3Fe-Ni-4S-2O] while HCP contains [4Fe-2S-2O]. Recently it was shown that upon substitution of the nickel atom by an iron atom in CODH, effectively creating CODH with an active cluster resembling the one of HCP, CODH exhibited hydroxylamine reductase activity (Heo et al., 2002). These findings led to the investigation and discovery of some hydroxylamine reductase activity *in vitro* for the HCP of *E. coli* (Wolfe et al., 2002). The observed hydroxylamine reductase activity of HCP was very low, reaching 458 ± 19 μmol of NH_2OH reduced min^{-1} (mg of protein)$^{-1}$. Furthermore, the K_m of the reaction for hydroxylamine was high (20 mM), suggesting that HCP might not function as a hydroxylamine reductase *in vivo*. The *R. capsulatus* HCP also exhibited relatively high K_m value of 1 mM for hydroxylamine and the basic optimum pH of 9.3 for the activity (Cabello et al., 2004). Nevertheless, it was shown that *E. coli* cells, overproducing HCP from *R. capsulatus*, tolerate hydroxylamine better during anaerobic growth (Cabello et al., 2004).

The ability of hydroxylamine to activate transcription from the *hcp* promoter was therefore tested and it was demonstrated that it does not exert any effect on the *hcp* promoter (**figure 4.4**). The promoters of some genes are not necessarily activated by the substrate of the gene product. Such an example is the *norV* gene of *E. coli*, which encodes a nitric oxide reductase, but is not induced by nitric oxide (da Costa et al., 2003). Thus, susceptibility to

hydroxylamine of the parental strain and the *hcp* mutant was studied. HCP did not protect the *E. coli* strain against toxicity of hydroxylamine *in vivo* as both HCP^+ and HCP^- strains had similar optical densities measured at different timepoints during growth with hydroxylamine (**figure 4.5**). HCP did not reduce hydroxylamine with methyl viologen as an electron donor *in vitro* (**table 4.1**). Concentration of hydroxylamine in experiments described in chapter 4 and by other authors (Cabello et al., 2004) was 0.5 mM and 10 mM, respectively. The concentration used in this work is closer to that encountered by bacteria in the natural environment. Conversely, the concentration of 10 mM is extremely high compared to natural habitats and this probably explains why HCP reacted with hydroxylamine as the latter was in vast excess.

Thus, the physiological role for HCP as a hydroxylamine reductase may well be questioned, although some authors (Cabello et al., 2004) support the possibility of HCP being the hydroxylamine reductase by noting that purified *R. capsulatus* enzymes involved in nitrogen metabolism also show high apparent K_m for their substrates and a high optimum pH *in vitro*. For example, the assimilatory nitrate reductase has an optimum pH of 9.3 and an apparent K_m for nitrate of 13 mM, and arginase shows an optimal pH of 9.0 and an apparent K_m value for arginine of 16 mM (Blasco et al., 1997; Moreno-Vivian et al., 1992).

To check whether HCP is essential for nitrate-dependent growth, the *hcp* gene was deleted from strains with different genetic backgrounds encoding both NRA and Nap, and either NRA or Nap. No difference in growth rate and yield was observed within each pair of the parental and the *hcp* deletion strains. Other authors also did not observe any discernible difference of the *hcp* mutant from the wild-type strain in a variety of assays where growth or survival was tested (Kim et al., 2003). The variables included media (LB, M9), pH (5 and 7), electron acceptors (oxygen, nitrite, nitrate), and carbon sources (glucose, glycerol, and lactate). The *hcp* mutant of *S. enterica* was also tested for increased susceptibility to mutagenesis by acidified nitrite, and no differences from the wild type cells were detected (Kim et al., 2003). It

is possible that the proper conditions have not yet been tested or that the mutants may exhibit subtle differences from the wild type. Apparently, the HCP protein is present in the cell at fairly low levels as based on some of our Coomassie gels and Western assays. In any case, the gene is dispensable under conditions tested in our experiments and by others (Kim et al., 2003).

Recently it has been shown that the *hcp* promoter from *Salmonella enterica* is upregulated under anaerobic growth conditions by acidified nitrite as a source of reactive nitrogen intermediates (Kim et al., 2003). The result was supported by the increased level of fluorescence from the *hcp::GFP* fusion in induced macrophages producing nitric oxide, which implied a role for HCP in nitric oxide detoxification (Kim et al., 2003). In our experiments, when nitric oxide saturated water was added to the *E. coli* cell culture, the activity of the promoter increased insignificantly, only 1.3-fold (data not shown) compared to 9-fold increase of activity of *S. enterica hcp*, challenged with acidified nitrite.

In *E coli*, three proteins are known to exhibit NO reductase activity: flavohemoglobin (Hmp), pentahaem cytochrome *c* nitrite reductase (NrfA), and flavorubredoxin (NorV). The flavorubredoxin gene is a part of the *norVW* operon that encodes a flavorubredoxin and NADH:(flavo)rubredoxin reductase. Activation of transcription from the *norV* promoter requires the product of a divergently transcribed regulatory gene, *norR* (Hutchings et al., 2002). As $NorR^+$ and $NorR^-$ strains did not show any significant differences in transcription from the *hcp* promoter (chapter 3), it was concluded that NorR is not a regulator of HCP. HCP also failed to protect *E. coli* against toxicity of NO *in vivo*: both HCP^+ and HCP^- strains showed similar decreases in growth rates and yield upon addition of NO saturated water (**figure 4.6**). So why is there this inconsistency of results of HCP induction by NO in *S. enterica* and *E. coli*? The *hcp* regulatory regions from *E. coli* and *S. enterica* were aligned and compared using the *gap* program and it was shown that they have 93% sequence identity (not shown). Given that *E. coli* and *S enterica* are very closely related organisms, and specifically with such a high sequence

identity in the region, similar regulation and response to a given stimulus in these two organisms would be expected. This discrepancy might be explained in two ways: either the *S. enterica* promoter was activated not by NO itself, but by some other reactive nitrogen species generated by NO, or the HCP proteins of the two organisms do differ in regulation and function. In relation to the former possibility, one of the *E. coli* NO reductases, HMP, is regulated partially by S-nitrosothiols. An *hmp* gene coregulator, Hcy, interacts with the *hmp* gene activator, MetR, preventing its binding to the *hmp* promoter. Hcy can be nitrosated by S-nitrosoglutathione, which depletes the Hcy pool size and enhances MetR binding to the *hmp* promoter (Membrillo-Hernandez et al., 1998). It might therefore be possible that HCP is regulated in a similar way.

So, what is the function of HCP? Why is there no phenotypic difference observed in the *hcp* mutant compared to the parental strain? One possibility is that the function of HCP might be masked by activity of other proteins that can fulfil the same role. Incidentally, the genome of *D. vulgaris* encodes two *hcp* genes, hcp1 and hcp2 (Haveman et al., 2004), and although the *E. coli hcp* gene is present in only one copy, masking of function of HCP might take place via some other protein. Based on the structure of HCP, the iron-sulphur clusters and channels that lead to them, the reactants must be relatively small (narrow) and reasonably soluble (Hagen, personal communication). Together with all other pieces of evidence the first two candidates to serve as HCP substrates would be hydroxylamine and nitric oxide. Nevertheless, the HCP^+ strain is not at selective advantage relative to the HCP^- mutant during growth with either hydroxylamine or nitric oxide (**figures 4.4** and **4.6**). The reason might be that HCP is not essential under the conditions tested, or that its activity is too low to be detected by the methods used. The latter would explain why *E. coli* cells overproducing HCP from the plasmid tolerated hydroxylamine better than the control cells, whereas physiologically expressed HCP did not protect the *E. coli* strain against the toxicity of hydroxylamine (Cabello et al., 2004; **figure 4.5**).

It is possible that the activity of HCP under physiological conditions is quite low, and the effect of the activity is only seen *in vivo* when the protein is present in high amounts. The next possibility is that HCP is a protein of "luxury" that is expressed to fulfil no function whatsoever. However, this is unlikely because the expression of the *hcp* gene is tightly regulated, which implies the requirement for the protein under certain conditions. The final possibility is that the right conditions have not yet been tested. Another candidate as a possible substrate of HCP then would be peroxynitrite (ONO_2^-), which is generated by the reaction of nitric oxide with superoxide. Two observations are in agreement with the possibility of peroxynitrite being the HCP substrate. The HCP protein of *Clostridium perfringens* has recently been proposed to be involved in oxidative stress (Briolat and Reysset, 2002). Also, the expression of the *hcp* gene is not zero during aerobic growth, so HCP is present under the conditions necessary for the generation of peroxynitrite.

In conclusion, HCP is a redox active protein that appears to be involved in some reaction of the nitrogen cycle. In the natural environment of *E. coli* other bacteria produce various reactive nitrogen intermediates. Nitric oxide, for example, is produced by denitrifying bacteria as an intermediate during reduction of nitrate to ammonia. Thus, it would be of advantage to have a protein that could reduce and therefore detoxify these compounds.

6.3. NapFGH

6.3.1. Regulation of the *napF* promoter

In the *napF*, *napGH*, *napFGH* and *napC* deletion mutants the activity of the *napF* promoter increased 1.56, 1.53, 1.98 and 2.82-fold, respectively (**figure 5.2, a**). As none of the proteins encoded by the *napF* operon are regulatory proteins, the regulation might occur at some other level. There might be an interaction between FNR and NapF, NapG, NapH or NapC, preventing binding of FNR to the *napF* promoter (sequestering of FNR). Alternatively, like the *nirB*

promoter (Browning et al., 2000), the *napF* promoter might be repressed under anaerobic conditions by some proteins, and for some reason this repression would be higher in the parental strain than in the NapF, NapGH, NapFGH and NapC mutants. When the same deletion mutants were grown in the presence of glucose and nitrate, the activity of the promoter in all strains increased to the same level of about 2,500 units, and the tendency of the promoter activity to increase in the deletion mutants was not noticed. This might be explained by the fact that during anaerobic growth in the presence of nitrate the *napF* promoter is regulated not only by FNR, but also by NarP and NarL, and that NarP counteracts repression by other proteins bound to the *napF* promoter.

It was shown that the *napF* promoter is 2.5-fold repressed during growth in the presence of glucose compared with growth in the presence of glycerol and fumarate (**figure 5.1**). It could be speculated that the mechanism of glucose repression at this promoter is not via the CRP protein, as there was no CRP site found at the *napF* promoter.

6.3.2. Regulation of NapA stability

It was shown that in the *napGH* mutant, JCB4243, NapA nitrate reductase activity was increased 1.5-fold compared to that of the parental strain (**figure 5.3**). This contradicts the published data for methyl-viologen-dependent activity of NapA in JCB4243 grown under the same growth conditions (Brondijk et al., 2002). When the *nap*F, *napGH* and *napFGH* mutants were grown in medium supplemented with glucose and nitrate, the nitrate reductase activity was decreased compared to the parental Nap^+ strain, JCB4241 (Brondijk et al., 2002). However, if the strains were grown in glycerol and nitrate, the nitrate reductase activity of the *napGH* was slightly increased (Brondijk et al., 2002), which is consistent with the result shown in **figure 5.3**. This increase in NapA activity in the NapGH mutant probably suggests that NapF and NapG might play some role in destabilisation of NapA or NapAB complex. This influence may

occur at the post-transcriptional level, as there was no difference observed in the level of transcription from the *napF* operon in strains expressing and lacking NapG and NapH (data not shown). It has previously been demonstrated that NapG and NapH are required for electron transport from ubiquinol to NapC and subsequently NapA, but they are not involved in oxidation of menaquinol (Brondijk et al., 2002). So, when only menaquinol is present in the membrane, as in the case of strains JCB4241 and JCB4243, NapG and NapH are not required for electron transport. It is not known why NapG and NapH might decrease the stability or assembly of NapA in the presence of only menaquinone as even if they are not involved in electron flow from menaquinol, electron transfer still occurs via the menadiol-NapC-NapB-NapA route.

It is worth noting that, in the triple NapFGH mutant, NapA activity is similar to that of the parental strain, so that the negative effect of NapG and NapH is not observed (**figure 5.3**). It has earlier been proposed that NapF plays a role in the assembly of the Fe-S cluster of NapA (Olmo-Mira et al., 2004). Can it be that NapF is involved in incorporation of Fe-S clusters of NapG and NapH as well? If this is the case, than deletion of the *napF* gene would render NapG and NapH inactive, and subsequently the negative effect of NapG and NapH on the NapA activity would disappear, which is observed in the triple *napFGH* mutant, JCB4244, compared to the double *napGH* mutant, JCB4243 (**figure 5.3**).

6.3.3. Role of NapF in adaptation to anaerobic growth

Growth experiments of strains able to synthesise both menaquinone and ubiquinone or only menaquinone demonstrated that NapF is important in adaptation of the culture from aerobiosis to anaerobiosis (**figures 5.4** and **5.5**). This might also be explained in light of the recent publication demonstrating a role for NapF from *R. sphaeroides* in assembling the Fe-S centre of the catalytic subunit of NapA (Olmo-Mira et al., 2004). If strains were pregrown anaerobically,

there would be enough of all of the Nap components synthesised at the time of inoculation. In contrast, with inocula that have been pregrown aerobically, the *napF* operon would not be expressed during transition to anaerobiosis, and the final activity of NapA would be dependent not only on rate of expression of NapA, but also on amount of the NapF protein to provide the [4Fe-4S]. At present it is unclear why this NapF influence on growth is pronounced in the Ubi^+Men^+ strain, JCB4042 and the Ubi^-Men^+ strain, JCB4242, but is not observed in the Ubi^+Men^- strain, JCB4142, especially taking into account that redox balancing by Nap is maximal in this strain. Another observation, which is difficult to explain, is why the effect of deletion of NapF in both Ubi^+Men^+ and Ubi^-Men^+ backgrounds is suppressed when NapG and NapH are deleted as well: no decrease of growth rate was observed in triple *napFGH* mutants, JCB4044 and JCB4244, compared to the respective parental strains (**figures 5.4** and **5.5**).

6.3.4. Redox balancing role of Nap during glucose fermentation

The growth rate of the $Ubi^+Men^-Nap^+$ strain, JCB4141, in the presence of the fermentable carbon source, glucose, was greatly stimulated by the addition of nitrate, but the final yield of biomass was unaffected. This increased growth rate was Nap-dependent, as shown by the lack of nitrate stimulation in the *napC* mutant, strain JCB4145 (**figure 5.7**). These data strongly suggest that Nap fulfils a redox balancing role during anaerobic growth by glucose fermentation. If this hypothesis is correct the following explanation would apply. In the Ubi^+Men^- strain, JCB4141, fumarate reductase is not functionally active as it accepts electrons from menadiol; so Nap is the only enzyme ensuring that the strain eliminates excessive reducing equivalents via the reduction of nitrate. In the strain competent for both ubiquinone and menaquinone synthesis, JCB4041, both fumarate reductase and periplasmic nitrate reductase are functional, fumarate reductase obtaining electrons from menaquinol and periplasmic nitrate reductase from both menaquinol and ubiquinol. If one activity unit were

assigned to each enzyme, then the impact of Nap on redox balancing for JCB4041 would be two out of three units, or 2/3 (1 unit for Nap linked to ubiquinol, 1 unit for Nap linked to menaquinol and 1 unit for fumarate reductase linked to menaquinol gives 3 units altogether). In the strain defective for ubiquinone but competent for menaquinone synthesis, again both fumarate reductase and periplasmic nitrate reductase are active, both receiving electrons from menaquinol. As the two enzymes are active, Nap constitutes half (1/2) of the total enzyme activity towards redox balancing. In other words, the impact of Nap on redox balancing is expected to be maximal in the $Ubi^{+}Men^{-}$ strain, JCB4141, moderate in the $Ubi^{+}Men^{+}$ strain, JCB4041 and minimal in the $Ubi^{-}Men^{+}$ strain, JCB4241, which is exactly what is observed in changes of growth rate with addition of nitrate (**tables 5.2** and **6.1**). Here the ratio in growth rate with and without nitrate is taken as a measure of impact of Nap on redox balancing during glucose fermentation.

6.3.5. NapG and NapH account for 99% of electron transport from ubiquinol to NapA

Despite the very low rates of nitrate reduction by the *napGH* mutant, strain JCB4143 (Brondijk et al., 2002), nitrate still stimulated growth to a rate only slightly lower than that of the Nap^{+} parental strain (**figure 5.7**). This growth stimulation was totally reproducible between experiments and was not due to reversion or unmasking of an additional nitrate reductase activity. Bacteria harvested at the end of these growth experiments reduced nitrate at a rate that was at most 1% of that of the parental strain, JCB4141 (Brondijk et al., 2002). This revealed that, during glucose fermentation, very low rates of nitrate reduction have profound affects on growth kinetics.

Strain	Phenotype	Expected relative impact of Nap on redox balancing	Observed ratio in the growth rates with and without nitrate
JCB4141	$Ubi^{+}Men^{-}$	1/1 (maximal)	1.84 (maximal)
JCB4041	$Ubi^{+}Men^{+}$	2/3 (medium)	1.52 (medium)
JCB4241	$Ubi^{-}Men^{+}$	1/2 (minimal)	1.18 (minimal)

Table 6.1. Relative impact of periplasmic nitrate reductase on redox balancing in strains competent for synthesis of both ubiquinone and menaquione, JCB4041, only ubiquinone, JCB4141, or only menaquinone, JCB4241. The impact of Nap on redox balancing is expected to be maximal in $Ubi^{+}Men^{-}$ strain, JCB4141, moderate in $Ubi^{+}Men^{+}$ strain, JCB4041, and minimal in $Ubi^{-}Men^{+}$ strain, JCB4241, which is precisely what is observed in changes of growth rate with addition of nitrate. Here the ratio in growth rate with and without nitrate is taken as a measure of observed impact of Nap on redox balancing during glucose fermentation. See text for the details.

6.3.6. NapG and NapH are linked to oxidation of quinols with high midpoint redox potential

The menaquinol analogue, menadiol, was an effective electron donor to Nap *in vitro*, but only in the complete Nap system. In the absence of NapG and NapH there was no nitrate reduction using menadiol. This confirms the role of NapG and NapH in the oxidation of some, but not all, quinols. Although menadiol appears to be a closer structural analogue of menaquinol than ubiquinol (Sobalte and Poole, 1999), its midpoint redox potential is closer to that of the ubiquinone : ubiquinol couple. It has been shown before that quinol analogues can behave unexpectedly based on their structural similarity to the natural quinols. The midpoint potentials of quinol analogues may be very far from those of their structural analogues and this may play a major role in determining their ability to donate electrons. Therefore, in the *in vitro* system used in this work, menadiol seems to behave more like a ubiquinol analogue rather than a menaquinol analogue.

Figure 6.2 summarises current knowledge of the roles of different Nap subunits in electron transfer from ubiquinol and menaquinol. NapG and NapH play a role in the transfer of electrons from ubiquinol via NapC and NapB to NapA. The alternative route from menaquinol to NapC is independent of NapG and NapH. This working model accounts not only for earlier work (Brondijk et al., 2002), but also for the cellular location of NapH, as determined by Western blotting using anti-Myc antibody and the topological analysis using PhoA and LacZ fusions (Brondijk *et al.*, 2004). There is a third, minor electron transfer pathway from ubiquinol directly to NapC, which is shown with blue arrows. Although this pathway accounts for less than 1% of the total rate of nitrate reduction (Brondijk et al., 2002), it is sufficient to fulfil the redox-balancing requirements during glucose fermentation. The highest impact of the periplasmic nitrate reductase on redox-balancing is in the absence of a functional fumarate reductase (**figure 5.7** and **table 6.1**).

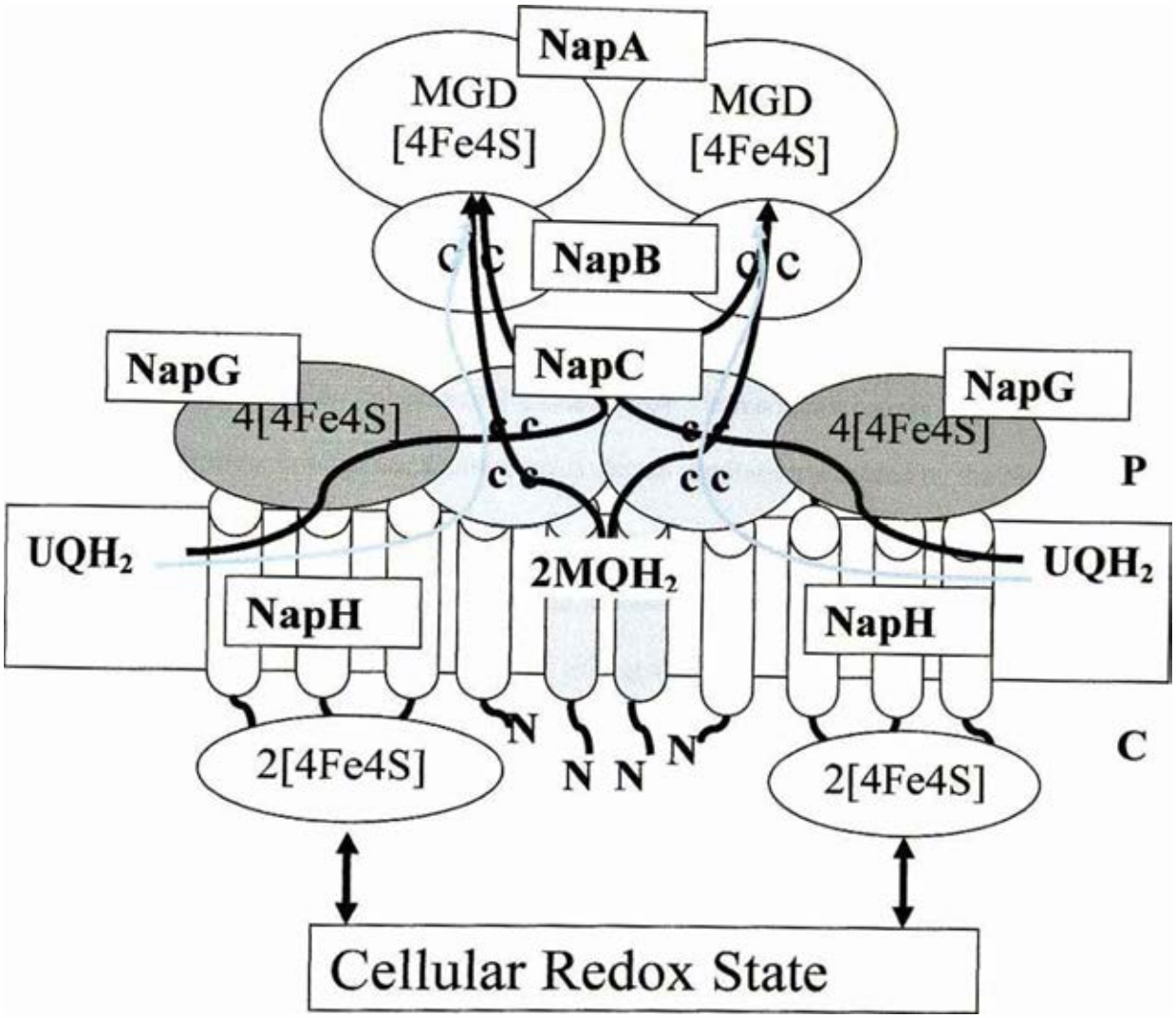

Figure 6.2. Working model for electron transfer via ubiquinone and menaquinone to the NapCBA complex in the periplasm. NapG and NapH play a role in the transfer of electrons from ubiquinol via NapC and NapB to NapA. The alternative route from menaquinol to NapC, which is independent of NapG and NapH, is also shown. There is a third, minor electron transfer pathway from ubiquinol directly to NapC (shown with the blue arrows). Although this pathway accounts for less than 1% of the total rate of nitrate reduction (Brondijk et al., 2002), it is sufficient to fulfil the redox-balancing requirements during glucose fermentation. P: periplasm; C: cytoplasm.

The demonstration that there are two, partially independent electron transfer pathways to the periplasmic nitrate reductase raises the fascinating question why both have been retained. As a facultative anaerobe, *E. coli* must be able to adapt between aerobic and anaerobic environments, most commonly living under conditions of limited oxygen supply, but also with limited supplies of alternative electron acceptors such as nitrate in their environment. Under such conditions, the higher mid-point potential ubiquinone-ubiquinol couple will be partially reduced, but the lower midpoint potential menaquinone : menaquinol couple will be essentially oxidised. Under these conditions, a slow rate of nitrate respiration provided by the NapG-NapH pathway might be sufficient to maintain redox-balanced growth. The fact that NapG and NapH are linked to oxidation of ubiquinol, which is a better electron donor under these conditions, suggests that NapG and NapH are important during the shift from aerobiosis to anaerobiosis. Conversely, in the absence of oxygen, both quinone pools will be reduced, so the more rapid menaquinol pathway will ensure rapid electron transfer not only to Nap, but also to the formate-dependent nitrite reductase, Nrf. This pathway will consume 8 electrons, making available four molecules of NAD^+ for fermentative growth for every nitrate ion reduced. Thus, for the first time, direct experimental evidence that the *E. coli* periplasmic nitrate reductase can fulfil the redox-balancing role implied by the above model has been demonstrated (**figures 5.4, 5.5, 5.7** and **table 6.1**).

6.4. Suggestions for future experiments

6.4.1. Regulation of *hcp* expression

There is plenty of scope to study the regulation of *hcp* expression. It was shown that under anaerobiosis in the *narL* or *narP* strains the *hcp* promoter activity is half of that of the parental strain. This suggests that under anaerobic conditions some proteins bind to the *hcp* promoter and prevent its full-scale activation by FNR. NarL or NarP might counteract this repression by

competing for the binding sites with these repressors, which would be reminiscent of the regulatory region of the *nirB* promoter (Browning et al., 2000). It would be interesting to find out at what sites exactly and under what conditions these proteins bind. Although immediate analysis of the *hcp* promoter does not reveal any binding sites for Fis or IHF, a progressive deletion of the promoter region from the 5′-site could reveal where the binding site of a repressor is located.

One of the peculiarities of the *hcp* promoter is that it is a class I FNR dependent promoter. Furthermore, not only a FNR binding site, but also NarP/NarL binding sites, are located upstream of the binding region of the α-CTD domain of RNAP. This is a similar arrangement to that of the *napF* promoter. It would therefore be interesting to study the specific interaction between FNR, NarP, NarL and RNAP at the *hcp* regulatory region. Some activating regions of FNR can be mutated and their effects on transcription tested.

Another question is whether the single NarL/NarP heptamers participate in *hcp* gene regulation. When NarL is expressed as the only response regulator, different levels of *hcp* promoter activation are observed at different stages of growth in response to nitrite or nitrate. One of the explanations is that the different concentrations of nitrite or nitrate result in formation of different amounts of NarL-phosphate that subsequently bind to one, two, or all three NarL binding sites. To test the hypothesis, each single heptamer could be mutated individually to see whether the tendency of the promoter activity to increase is retained or lost. It would also be feasible to study whether NarL and NarP have different affinities for the 7-2-7 site at the *hcp* promoter. This can be achieved using gel retardation assays with varying concentrations of NarL and NarP.

The β-galactosidase activity of the parental strain, $NarL^+$ $NarP^+$, in the presence of nitrite or nitrate revealed a complicated pattern of variation during growth (**figure 3.11, a**). The

activity was about 30,000 units at the beginning of growth, than it slightly decreased in the middle of growth and increased again to the previous level at the end of growth, the result being reproducible between the experiments. The reason of this varying promoter activity over the growth cycle is unclear and might be due to the fluctuating concentrations of the anions present in the medium. It would be reasonable therefore to use chemostat cultures in place of batch cultures to control precisely the medium parameters and measure the β-galactosidase activity when the steady-state condition has been reached. This would also answer how the different concentrations of nitrite and nitrate influence the level of transcription from the *hcp* promoter, which concentration of nitrite and nitrate is optimal for the highest concentrations of NarP-phosphate to be formed, and under which nitrite or nitrate concentration NarL-phosphate exerts its maximal activation of the promoter.

It was shown that the level of transcription from the *hcp* promoter in the cell culture is very high, yet the amount of the HCP protein is rather low. This implies that there is another level of HCP regulation that takes place after transcription. As mature HCP is present at quite low levels, might this post-transcriptional regulation be a key to inability to find the substrate/role of the HCP protein? Also, the *hcp* regulatory region has an A/T reach stretch of 21 nucleotides in length immediately downstream from the transcription start site, which due to its low melting temperature might be involved in regulation of *hcp* expression. It would be feasible to mutate it to increase the G/C content and test whether this influences the level of *hcp* expression.

6.4.2. The function of the hybrid cluster protein

The main question left unanswered is the physiological function of HCP. Although there is some indirect evidence that it participates in nitrite and hydroxylamine assimilation in *R.*

capsulatus, the *in vitro* enzyme activity of HCP of both *E. coli* and *R. capsulatus* is low (van den Berg et al., 2000; Cabello et al., 2004). Another possible candidate molecule for the HCP substrate could be peroxynitrite, which is formed under oxidising conditions in the presence of nitrite. An assay to measure *in vivo* peroxynitrite consumption can be developed using the *hcp*$^+$ and *hcp* strains. Although it was shown that HCP does not participate in nitrate-dependent growth, it is expressed under conditions in which there is also expression of two nitrate reductases of *E. coli*, NRA and Nap. It would be interesting to find out whether this protein interacts with any of the components encoded by the *napFDAGHBC* and *narGHIJ* operons. This can be achieved using the two-hybrid system, by subcloning in two plasmids the coding regions of two proteins of interest in frame with coding regions of two subunits of a reporter enzyme adenylate cyclase, and measuring the strength of interaction between the two subunits (Karimova et al., 2000). Although the first attempt to test this idea using a random library of *E. coli* clones did not reveal any interaction partners of HCP (Overton, unpublished work), the specific subcloning might bring some insight into the function of the hybrid cluster protein.

6.4.3. NapFGH expression and function

It was shown that in NapF, NapG and NapC mutants the anaerobic expression from the *napF* promoter is higher than that of the parental strain. The hypothesis that it is due to sequestering of the FNR by NapF, NapG and NapC can be tested with the two-hybrid system. This method would provide information on whether FNR interacts with any of the subunits of the Nap complex. It would also be feasible to dissect the *napF* promoter and make a series of the deleted *napF* variants to study whether there are any repressor binding elements upstream from the *FNR* and *NarP binding sites*.

It was demonstrated that in the *napGH* mutant the NapA activity is higher than in the parental strain, suggesting that NapG and NapH decrease stability or assembly of NapA. How

would they achieve it? NapH is an integral membrane protein and NapG is located in the periplasm, but it does not directly contact NapA. Therefore if the interaction between NapA and either of NapG and NapH is direct, it might happen in the cytoplasm before the proteins are transported/folded in the membrane. It would be also interesting to see whether the effect on NapA activity is due to NapG, NapH or both of them. This could be studied by using single *napG* and *napH* mutants.

REFERENCES

Aragao, D., Macedo, S., Mitchell, E.P., Romao, C.V., Liu, M.Y., Frazao, C., Saraiva, L.M., Xavier, A.V., LeGall, J., van Dongen, W.M., Hagen, W.R., Teixeira, M., Carrondo, M.A., and Lindley, P. (2003) Reduced hybrid cluster proteins (HCP) from *Desulfovibrio desulfuricans* ATCC 27774 and *Desulfovibrio vulgaris* (Hildenborough): X-ray structures at high resolution using synchrotron radiation *J Biol Inorg Chem* **8**: 540-548.

Arnoux, P., Sabaty, M., Alric, J., Frangioni, B., Guigliarelli, B., Adriano, J.M., and Pignol, D (2003) Structural and redox plasticity in the heterodimeric periplasmic nitrate reductase *Nat Struct Biol* **10**: 928-934.

Bagramyan, K., Vassilian, A., Mnatsakanyan, N., and Trchounian, A. (2001) Participation of *hyf*-encoded hydrogenase 4 in molecular hydrogen release coupled with proton-potassium exchange in *Escherichia coli Membr Cell Biol* **14**: 749-763.

Ballantine, S.P., Boxer, D.H. (1985) Nickel-containing hydrogenase isoenzymes from anaerobically grown *Escherichia coli* K-12 *J Bacteriol* **163**: 454-459.

Bedzyk, L., Wang, T., and Ye, R.W. (1999) The periplasmic nitrate reductase in *Pseudomonas sp.* strain G-179 catalyzes the first step of denitrification *J Bacteriol* **181**: 2802-2806.

Beinert, H., Holm, R.H., and Munck, E. (1997) Iron-sulfur clusters: nature's modular, multipurpose structures *Science* **277**: 653-659.

Beliaev, A.S., Thompson, D.K., Khare, T., Lim, H., Brandt, C.C., Li, G., Murray, A.E., Heidelberg, J.F., Giometti, C.S., Yates, J., Nealson, K.H., Tiedje, J M., and Zhoui, J. (2002) Gene and protein expression profiles of *Shewanella oneidensis* during anaerobic growth with different electron acceptors *OMICS* **6**: 39-60.

Bell, A., Busby, S. (1994) Location and orientation of an activating region in the *Escherichia coli* transcription factor, FNR *Mol Microbiol* **11**: 383-390.

Bell, A.I., Gaston, K.L., Cole, J.A., and Busby, S.J. (1989) Cloning of binding sequences for the *Escherichia coli* transcription activators, FNR and CRP: location of bases involved in discrimination between FNR and CRP *Nucleic Acids Res* **17**: 3865-3874.

Bell, L.C., Richardson, D.J., and Ferguson, S.J. (1990) Periplasmic and membrane-bound respiratory nitrate reductases in *Thiosphaera pantotropha*. The periplasmic enzyme catalyzes the first step in aerobic denitrification *FEBS Lett* **265**: 85-87.

Bentley, R., Meganathan, R. (1982) Biosynthesis of vitamin K (menaquinone) in bacteria *Microbiol Rev* **46**: 241-280.

Berks, B.C., Ferguson, S.J., Moir, J.W., and Richardson, D.J. (1995a) Enzymes and associated electron transport systems that catalyse the respiratory reduction of nitrogen oxides and oxyanions *Biochim Biophys Acta* **1232**: 97-173.

Berks, B.C., Richardson, D.J., Reilly, A., Willis, A.C., and Ferguson, S.J. (1995b) The *napEDABC* gene cluster encoding the periplasmic nitrate reductase system of *Thiosphaera pantotropha Biochem J* **309**: 983-992.

Berks, B.C., Sargent, F., De Leeuw, E., Hinsley, A.P., Stanley, N.R., Jack, R.L., Buchanan, G., and Palmer, T. (2000a) A novel protein transport system involved in the biogenesis of bacterial electron transfer chains *Biochim Biophys Acta* **1459**: 325-330.

Berks, B.C., Sargent, F., and Palmer, T. (2000b) The Tat protein export pathway *Mol Microbiol* **35**: 260-274.

Blasco, F., Guigliarelli, B., Magalon, A., Asso, M., Giordano, G., and Rothery, R.A. (2001) The coordination and function of the redox centres of the membrane-bound nitrate reductases *Cell Mol Life Sci* **58**: 179-193.

Blasco, F., Iobbi, C., Ratouchniak, J., Bonnefoy, V., and Chippaux, M. (1990) Nitrate reductases of *Escherichia coli*: sequence of the second nitrate reductase and comparison with that encoded by the *narGHJI* operon *Mol Gen Genet* **222**: 104-111.

Blasco, F., Nunzi, F , Pommier, J., Brasseur, R., Chippaux, M., and Giordano, G. (1992a) Formation of active heterologous nitrate reductases between nitrate reductases A and Z of *Escherichia coli Mol Microbiol* **6**: 209-219.

Blasco, F., Pommier, J., Augier, V., Chippaux, M., and Giordano, G. (1992b) Involvement of the *narJ* or *narW* gene product in the formation of active nitrate reductase in *Escherichia coli Mol Microbiol* **6**: 221-230.

Blasco, R., Castillo, F., and Martinez-Luque, M. (1997) The assimilatory nitrate reductase from the phototrophic bacterium, *Rhodobacter capsulatus* E1F1, is a flavoprotein *FEBS Lett* **414**: 45-49.

Blattner, F.R., Plunkett, G., Bloch, C.A., Perna, N.T., Burland, V., Riley, M., Collado-Vides, J., Glasner, J.D., Rode, C.K., Mayhew, G.F., Gregor, J., Davis, N.W., Kirkpatrick, H.A., Goeden, M.A., Rose, D.J., Mau, B., and Shao, Y. (1997) The complete genome sequence of *Escherichia coli* K-12 *Science* **277**: 1453-1474.

Böhm, R., Sauter, M., and Bock, A. (1990) Nucleotide sequence and expression of an operon in *Escherichia coli* coding for formate hydrogenlyase components *Mol Microbiol* **4**: 231-243.

Bonnard, N., Tresierra-Ayala, A., Bedmar, E.J., and Delgado, M.J. (2005) Molybdate-dependent expression of the periplasmic nitrate reductase in *Bradyrhizobium japonicum Biochem Soc Trans* **33**: 127-129.

Bonnefoy, V., Ratouchniak, J., Blasco, F., and Chippaux, M. (1997) Organization of the *nar* genes at the *chlZ* locus *FEMS Microbiol Lett* **147**: 147-149.

Brigé, A., Leys, D., Meyer, T.E., Cusanovich, M.A., and Van Beeumen, J J (2002) The 1.25 A resolution structure of the diheme NapB subunit of soluble nitrate reductase reveals a novel cytochrome c fold with a stacked heme arrangement *Biochemistry* **41**: 4827-4836.

Brigé, A., Leys, D., and Van Beeumen, J.J. (2001) Crystallization and preliminary X-ray analysis of the recombinant dihaem cytochrome *c* (NapB) from *Haemophilus influenzae Acta Crystallogr D Biol Crystallogr* **57**: 418-420.

Briolat, V., Reysset, G. (2002) Identification of the *Clostridium perfringens* genes involved in the adaptive response to oxidative stress *J Bacteriol* **184**: 2333-2343.

Brondijk, T.H., Fiegen, D., Richardson, D.J , and Cole, J.A. (2002) Roles of NapF, NapG and NapH, subunits of the *Escherichia coli* periplasmic nitrate reductase, in ubiquinol oxidation *Mol Microbiol* **44**: 245-255.

Brondijk, T.H., Nilavongse, A , Filenko, N., Richardson, D.J., and Cole, J A. (2004) NapGH components of the periplasmic nitrate reductase of *Escherichia coli* K-12: location, topology and physiological roles in quinol oxidation and redox balancing *Biochem J* **379**: 47-55.

Browning, D.F., Cole, J.A., and Busby, S.J. (2000) Suppression of FNR-dependent transcription activation at the *Escherichia coli nir* promoter by Fis, IHF and H-NS: modulation of transcription initiation by a complex nucleo-protein assembly *Mol Microbiol* **37**: 1258-1269.

Bruckner, R., Titgemeyer, F. (2002) Carbon catabolite repression in bacteria: choice of the carbon source and autoregulatory limitation of sugar utilization *FEMS Microbiol Lett* **209**: 141-148.

Busby, S., West, D., Lawes, M., Webster, C., Ishihama, A., and Kolb, A. (1994) Transcription activation by the *Escherichia coli* cyclic AMP receptor protein. Receptors bound in tandem at promoters can interact synergistically *J Mol Biol* **241**: 341-352.

Cabello, P., Pino, C., Olmo-Mira, M.F., Castillo, F., Roldan, M.D., and Moreno-Vivian, C. (2004) Hydroxylamine assimilation by *Rhodobacter capsulatus* E1F1: requirement of the *hcp* gene (hybrid cluster protein) located in the nitrate assimilation *nas* gene region for hydroxylamine reduction *J Biol Chem* **279**· 45485-45494

Cartron, M.L., Roldan, M D., Ferguson, S.J., Berks, B.C., and Richardson, D.J. (2002) Identification of two domains and distal histidine ligands to the four haems in the bacterial c-type cytochrome NapC; the prototype connector between quinol/quinone and periplasmic oxido-reductases *Biochem J* **368**: 425-432.

Castillo, F., Dobao, M.M., Reyes, F., Blasco, R., Roldan, M.D., Gavira, M., Caballero, F.J., Moreno-Vivian, C., and Martinez-Luque, M. (1996) Molecular and Regulatory Properties of the Nitrate Reducing Systems of *Rhodobacter Curr Microbiol* **33**: 341-346.

Chang, L., Wei, L.I., Audia, J.P., Morton, R.A., and Schellhorn, H.E. (1999) Expression of the *Escherichia coli* NRZ nitrate reductase is highly growth phase dependent and is controlled by RpoS, the alternative vegetative sigma factor *Mol Microbiol* **34**: 756-766.

Chiang, R.C., Cavicchioli, R., and Gunsalus, R.P. (1997) 'Locked-on' and 'locked-off' signal transduction mutations in the periplasmic domain of the *Escherichia coli* NarQ and NarX sensors affect nitrate- and nitrite-dependent regulation by NarL and NarP *Mol Microbiol* **24**: 1049-1060.

Choe, M., Reznikoff, W.S. (1993) Identification of the regulatory sequence of anaerobically expressed locus *aeg-46 5 J Bacteriol* **175**: 1165-1172.

Christen, S., Gee, P., and Ames, B N. (1996) Mutagenicity of nitric oxide in base pair-specific *Salmonella* tester strains: TA7000 series *Methods Enzymol* **269**: 267-278.

Clegg, S. (2002) Nitrate and nitrite transport across the cytoplasmic membrane of *Escherichia coli* K-12. PhD thesis. The University of Birmingham.

Clegg, S., Yu, F., Griffiths, L., and Cole, J.A. (2002) The roles of the polytopic membrane proteins NarK, NarU and NirC in *Escherichia coli* K-12: two nitrate and three nitrite transporters *Mol Microbiol* **44**: 143-155.

Cole, J.A., Brown, C.M. (1980) Nitrite reduction to ammonia by fermentative bacteria: a short circuit in the biological nitrogen cycle *FEMS Microbiol Lett* **7**: 65-72.

Cole, S.T., Condon, C., Lemire, B.D., and Weiner, J.H. (1985) Molecular biology, biochemistry and bioenergetics of fumarate reductase, a complex membrane-bound iron-sulfur flavoenzyme of *Escherichia coli Biochim Biophys Acta* **811**: 381-403.

Cole, J.A., Wimpenny, J.W. (1968) Metabolic pathways for nitrate reduction in *Escherichia coli Biochim Biophys Acta* **162**: 39-48.

Compan, I., Touati, D. (1994) Anaerobic activation of *arcA* transcription in Escherichia coli: roles of Fnr and ArcA *Mol Microbiol* **11**: 955-964.

Cooper, S.J., Garner, C.D., Hagen, W.R., Lindley, P.F., and Bailey, S. (2000) Hybrid-cluster protein (HCP) from *Desulfovibrio vulgaris* (Hildenborough) at 1.6 A resolution *Biochemistry* **39**: 15044-15054.

da Costa, P.N., Teixeira, M., and Saraiva, L.M. (2003) Regulation of the flavorubredoxin nitric oxide reductase gene in *Escherichia coli*. nitrate repression, nitrite induction, and possible post-transcription control *FEMS Microbiol Lett* **218**: 385-393.

Cruz-Ramos, H., Crack, J., Wu, G , Hughes, M.N., Scott, C., Thomson, A.J., Green, J., and Poole, R.K. (2002) NO sensing by FNR: regulation of the *Escherichia coli* NO-detoxifying flavohaemoglobin, Hmp *EMBO J* **21**: 3235-3244.

Darwin, A.J., Stewart, V. (1995a) Expression of the *narX, narL, narP*, and *narQ* genes of *Escherichia coli* K-12: regulation of the regulators *J Bacteriol* **177**: 3865-3869.

Darwin, A J., Stewart, V. (1995b) Nitrate and nitrite regulation of the Fnr-dependent *aeg-46.5* promoter of *Escherichia coli* K-12 is mediated by competition between homologous response regulators (NarL and NarP) for a common DNA-binding site *J Mol Biol* **251**: 15-29.

Darwin, A., Stewart, V. (1996). The NAR modulon systems: nitrate and nitrite regulation of anaerobic gene expression. In: Regulation of gene expression in *Escherichia coli*. Lin, E.C.C , Lynch A.S. (eds). Chapman and Hill, New York, pp: 343-359.

Darwin, A.J., Tyson, K.L., Busby, S.J , and Stewart, V. (1997) Differential regulation by the homologous response regulators NarL and NarP of *Escherichia coli* K-12 depends on DNA binding site arrangement *Mol Microbiol* **25**: 583-595.

Darwin, A.J., Ziegelhoffer, E.C., Kiley, P.J , and Stewart, V. (1998) Fnr, NarP, and NarL regulation of *Escherichia coli* K-12 *napF* (periplasmic nitrate reductase) operon transcription *in vitro J Bacteriol* **180**: 4192-4198.

Datsenko, K.A., Wanner, B.L. (2000) One-step inactivation of chromosomal genes in *Escherichia coli* K-12 using PCR products *Proc Natl Acad Sci U S A* **97**: 6640-6645.

Delgado, M.J., Bonnard, N., Tresierra-Ayala, A., Bedmar, E.J., and Muller, P. (2003) The *Bradyrhizobium japonicum napEDABC* genes encoding the periplasmic nitrate reductase are essential for nitrate respiration *Microbiology* **149**: 3395-3403.

Dias, J.M., Than, M.E., Humm, A., Huber, R., Bourenkov, G.P., Bartunik, H D., Bursakov, S., Calvete, J., Caldeira, J., Carneiro, C., Moura, J.J., Moura, I., and Romao, M.J. (1999) Crystal structure of the first dissimilatory nitrate reductase at 1.9 A solved by MAD methods *Structure Fold Des* **7**: 65-79.

Dobbek, H., Svetlitchnyi, V., Gremer, L., Huber, R., and Meyer, O. (2001) Crystal structure of a carbon monoxide dehydrogenase reveals a [Ni-4Fe-5S] cluster *Science* **293**: 1281-1285.

Dominy, C.N., Deane, S.M., and Rawlings, D E. (1997) A geographically widespread plasmid from *Thiobacillus ferrooxidans* has genes for ferredoxin-, FNR-, prismane- and NADH-oxidoreductase-like proteins which are also located on the chromosome *Microbiology* **143**: 3123-3136.

Dong, X.R., Li, S.F., and Demoss, J.A. (1992) Upstream sequence elements required for NarL-mediated activation of transcription from the *narGHJI* promoter of *Escherichia coli J Biol Chem* **267**: 14122-14128.

Drennan, C.L., Heo, J., Sintchak, M.D., Schreiter, E., and Ludden, P.W. (2001) Life on carbon monoxide: X-ray structure of *Rhodospirillum rubrum* Ni-Fe-S carbon monoxide dehydrogenase *Proc Natl Acad Sci U S A* **98**: 11973-11978.

Eaves, D.J., Grove, J., Staudenmann, W., James, P., Poole, R.K., White, S A., Griffiths, I., and Cole, J.A. (1998) Involvement of products of the *nrfEFG* genes in the covalent attachment of haem *c* to a novel cysteine-lysine motif in the cytochrome c552 nitrite reductase from *Escherichia coli Mol Microbiol* **28**: 205-216.

Ellington, M.J., Bhakoo, K.K., Sawers, G., Richardson, D.J., and Ferguson, S J. (2002) Hierarchy of carbon source selection in *Paracoccus pantotrophus*: strict correlation between reduction state of the carbon substrate and aerobic expression of the *nap* operon *J Bacteriol* **184**: 4767-4774.

Ellington, M.J., Richardson, D.J., and Ferguson, S.J. (2003a) *Rhodobacter capsulatus* gains a competitive advantage from respiratory nitrate reduction during light-dark transitions *Microbiology* **149**: 941-948.

Ellington, M.J., Sawers, G., Sears, H.J., Spiro, S , Richardson, D.J., and Ferguson, S.J. (2003b) Characterization of the expression and activity of the periplasmic nitrate reductase of *Paracoccus pantotrophus* in chemostat cultures *Microbiology* **149**: 1533-1540.

Feelisch, M , Stamler J.S. (1996). Donors of nitrogen oxides. In: Feelisch, M., Stamler, J.S. (eds.) Methods in nitric oxide research John Wiley and Sons, New York, N.Y. pp: 71-115.

Gangeswaran, R., Eady, R.R. (1996) Flavodoxin 1 of *Azotobacter vinelandii*: characterization and role in electron donation to purified assimilatory nitrate reductase *Biochem J* **317**: 103-108.

Gangeswaran, R., Lowe, D.J., and Eady, R.R. (1993) Purification and characterization of the assimilatory nitrate reductase of *Azotobacter vinelandii Biochem J* **289**: 335-342.

Garavelli, J.S., Huang, H. Z,.and Miller, D. J. (2000) Protein Sci. Meet., abstr. 131.

Gates, A J., Hughes, R.O., Sharp, S.R., Millington, P.D., Nilavongse, A., Cole, J.A., Leach, E.R., Jepson, B., Richardson, D.J., and Butler, C.S. (2003) Properties of the periplasmic nitrate reductases from *Paracoccus pantotrophus* and *Escherichia coli* after growth in tungsten-supplemented media *FEMS Microbiol Lett* **220**: 261-269.

Gavira, M., Roldan, M.D., Castillo, F., and Moreno-Vivian, C. (2002) Regulation of *nap* gene expression and periplasmic nitrate reductase activity in the phototrophic bacterium *Rhodobacter sphaeroides* DSM158 *J Bacteriol* **184**: 1693-1702.

Gennis, R.B., Stewart, V. (1996) Respiration. In: *Escherichia coli* and *Salmonella.* Neidhardt, F.C. (ed). 217-261.

Georgellis, D., Kwon, O., and Lin, E.C. (2001) Quinones as the redox signal for the arc two-component system of bacteria *Science* **292**: 2314-2316.

Goldman, B.S., Lin, J.T., and Stewart, V. (1994) Identification and structure of the *nasR* gene encoding a nitrate- and nitrite-responsive positive regulator of *nasFEDCBA* (nitrate assimilation) operon expression in *Klebsiella pneumoniae* M5al *J Bacteriol* **176**: 5077-5085.

Gon, S., Patte, J.C., Mejean, V., and Iobbi-Nivol, C. (2000) The *torYZ* (*yecK bisZ*) operon encodes a third respiratory trimethylamine N-oxide reductase in *Escherichia coli J Bacteriol* **182**: 5779-5786.

Green, J., Guest, J R. (1994) Regulation of transcription at the *ndh* promoter of *Escherichia coli* by FNR and novel factors *Mol Microbiol* **12**: 433-444.

Green, J., Sharrocks, A D., Green, B., Geisow, M., and Guest, J.R. (1993) Properties of FNR proteins substituted at each of the five cysteine residues *Mol Microbiol* **8**: 61-68.

Grove, J., Tanapongpipat, S., Thomas, G., Griffiths, L., Crooke, H., and Cole, J. (1996) *Escherichia coli* K-12 genes essential for the synthesis of c-type cytochromes and a third nitrate reductase located in the periplasm *Mol Microbiol* **19**: 467-481.

Haddock, B.A., Kendall-Tobias, M W. (1975) Functional anaerobic electron transport linked to the reduction of nitrate and fumarate in membranes from *Escherichia coli* as demonstrated by quenching of atebrin fluorescence *Biochem J* **152**: 655-659

Harborne, N.R., Griffiths, L., Busby, S.J., and Cole, J.A. (1992) Transcriptional control, translation and function of the products of the five open reading frames of the *Escherichia coli nir* operon *Mol Microbiol* **6**: 2805-2813.

Haveman, S A., Greene, E.A., Stilwell, C.P., Voordouw, J.K., and Voordouw, G. (2004) Physiological and gene expression analysis of inhibition of *Desulfovibrio vulgaris* hildenborough by nitrite *J Bacteriol* **186**: 7944-7950.

Heo, J., Wolfe, M.T., Staples, C.R., and Ludden, P.W. (2002) Converting the NiFeS carbon monoxide dehydrogenase to a hydrogenase and a hydroxylamine reductase *J Bacteriol* **184**: 5894-5897.

Hinks, J.A., Evans, M.C., De Miguel, Y., Sartori, A.A., Jiricny, J., and Pearl, L.H. (2002) An iron-sulfur cluster in the family 4 uracil-DNA glycosylases *J Biol Chem* **277**: 16936-16940.

Hussain, H., Grove, J., Griffiths, L., Busby, S., and Cole, J. (1994) A seven-gene operon essential for formate-dependent nitrite reduction to ammonia by enteric bacteria *Mol Microbiol* **12**: 153-163.

Hutchings, M.I., Mandhana, N., and Spiro, S. (2002) The NorR protein of *Escherichia coli* activates expression of the flavorubredoxin gene *norV* in response to reactive nitrogen species *J Bacteriol* **184**: 4640-4643.

Ingledew, W.J., Poole, R.K. (1984) The respiratory chains of *Escherichia coli Microbiol Rev* **48** 222-271.

Ishizuka, H., Hanamura, A., Inada, T., and Aiba, H. (1994) Mechanism of the down-regulation of cAMP receptor protein by glucose in *Escherichia coli*: role of autoregulation of the *crp* gene *EMBO J* **13**: 3077-3082.

Iuchi, S., Chepuri, V., Fu, H.A., Gennis, R.B., and Lin, E C. (1990) Requirement for terminal cytochromes in generation of the aerobic signal for the arc regulatory system *in Escherichia coli*: study utilizing deletions and *lac* fusions of *cyo* and *cyd J Bacteriol* **172**: 6020-6025.

Iuchi, S., Lin, E.C. (1988) *arcA* (*dye*), a global regulatory gene in *Escherichia coli* mediating repression of enzymes in aerobic pathways *Proc Natl Acad Sci U S A* **85**: 1888-1892.

Jayaraman, P.S., Cole, J.A., and Busby, S.J. (1989) Mutational analysis of the nucleotide sequence at the FNR-dependent *nirB* promoter in *Escherichia coli Nucleic Acids Res* **17**: 135-145

Jayaraman, P.S., Gaston, K L., Cole, J.A., and Busby, S.J. (1988) The *nirB* promoter of *Escherichia coli*: location of nucleotide sequences essential for regulation by oxygen, the FNR protein and nitrite *Mol Microbiol* **2**: 527-530.

Jayaraman, P.S., Peakman, T.C., Busby, S.J., Quincey, R.V., and Cole, J.A. (1987) Location and sequence of the promoter of the gene for the NADH-dependent nitrite reductase of *Escherichia coli* and its regulation by oxygen, the Fnr protein and nitrite *J Mol Biol* **196**: 781-788.

Jetten, M.S , Cirpus, I., Kartal, B., van Niftrik, L., van de Pas-Schoonen, K.T., Sliekers, O., Haaijer, S., van der Star, W., Schmid, M., van, d., V, Schmidt, I., Harhangi, H., van Loosdrecht, M., Gijs, K.J., Op, d.C., and Strous, M. (2005) 1994-2004: 10 years of research on the anaerobic oxidation of ammonium *Biochem Soc Trans* **33**: 119-123.

Jetten, M.S., Wagner, M., Fuerst, J., van Loosdrecht, M., Kuenen, G., and Strous, M. (2001) Microbiology and application of the anaerobic ammonium oxidation ('anammox') process *Curr Opin Biotechnol* **12**: 283-288.

Jia, W., Cole, J.A. (2005) Nitrate and nitrite transport in *Escherichia coli Biochem Soc Trans* **33**: 159-161.

Johnson, M.K. (1998) Iron-sulfur proteins: new roles for old clusters *Curr Opin Chem Biol* **2**. 173-181.

Jones, H.M., Gunsalus, R.P. (1987) Regulation of *Escherichia coli* fumarate reductase (*frdABCD*) operon expression by respiratory electron acceptors and the *fnr* gene product *J Bacteriol* **169**: 3340-3349.

Jones, R.W., Garland, P.B. (1977) Sites and specificity of the reaction of bipyridylium compounds with anaerobic respiratory enzymes of *Escherichia coli*. Effects of permeability barriers imposed by the cytoplasmic membrane *Biochem J* **164**: 199-211

Jones, R.W., Lamont, A., and Garland, P.B. (1980) The mechanism of proton translocation driven by the respiratory nitrate reductase complex of *Escherichia coli Biochem J* **190**: 79-94.

Jormakka, M., Byrne, B., and Iwata, S. (2003) Protonmotive force generation by a redox loop mechanism *FEBS Lett* **545**: 25-30.

Jormakka, M., Tornroth, S., Abramson, J., Byrne, B., and Iwata, S. (2002a) Purification and crystallization of the respiratory complex formate dehydrogenase-N from *Escherichia coli Acta Crystallogr D Biol Crystallogr* **58**: 160-162.

Jormakka, M., Tornroth, S., Byrne, B., and Iwata, S. (2002b) Molecular basis of proton motive force generation: structure of formate dehydrogenase-N *Science* **295**. 1863-1868.

Kang, Y., Weber, K.D., Qiu, Y., Kiley, P.J., and Blattner, F.R (2005) Genome-wide expression analysis indicates that FNR of *Escherichia coli* K-12 regulates a large number of genes of unknown function *J Bacteriol* **187**: 1135-1160.

Karimova, G., Ullmann, A., and Ladant, D. (2000) A bacterial two-hybrid system that exploits a cAMP signaling cascade in *Escherichia coli Methods Enzymol* **328**: 59-73.

Kasai, S., Sumimoto, T. (2002) Stimulated biosynthesis of flavins in *Photobacterium phosphoreum* IFO 13896 and the presence of complete *rib* operons in two species of luminous bacteria *Eur J Biochem* **269**: 5851-5860.

Kiley, P.J., Beinert, H. (1998) Oxygen sensing by the global regulator, FNR: the role of the iron-sulfur cluster *FEMS Microbiol Rev* **22**: 341-352.

Kim, C.C., Monack, D., and Falkow, S. (2003) Modulation of virulence by two acidified nitrite-responsive loci of *Salmonella enterica* serovar Typhimurium *Infect Immun* **71** 3196-3205.

Kitagawa, M., Ara, T., Arifuzzaman M., Ioka-Nakamichi, T., Inamoto, I., Toyonaga, H., Mori., H. A complete set of ORF clones of *Escherichia coli* ASKA library (A Complete Set of *E. coli* K-12 ORF Archive): Unique Resources for Biological Research. *In preparation*

Kolb, A., Igarashi, K., Ishihama, A., Lavigne, M., Buckle, M., and Buc, H. (1993) *E. coli* RNA polymerase, deleted in the C-terminal part of its alpha-subunit, interacts differently

with the cAMP-CRP complex at the *lacP1* and at the *galP1* promoter *Nucleic Acids Res* **21**: 319-326.

Kroger, A. (1978) Fumarate as terminal acceptor of phosphorylative electron transport *Biochim Biophys Acta* **505**: 129-145.

Krockel, M., Trautwein, A.X., Arendsen, A.F., and Hagen, W.R. (1998) The prismane protein resolved--Mossbauer investigation of a 4Fe cluster with an unusual mixture of bridging ligands and metal coordinations *Eur J Biochem* **251**: 454-461.

Kwon, O., Georgellis, D., and Lin, E.C. (2000) Phosphorelay as the sole physiological route of signal transmission by the arc two-component system of *Escherichia coli J Bacteriol* **182**: 3858-3862.

Lee, A.I., Delgado, A., and Gunsalus, R.P. (1999) Signal-dependent phosphorylation of the membrane-bound NarX two-component sensor-transmitter protein of *Escherichia coli*: nitrate elicits a superior anion ligand response compared to nitrite *J Bacteriol* **181**: 5309-5316.

Lehmann, Y., Meile, L., and Teuber, M. (1996) Rubrerythrin from *Clostridium perfringens*: cloning of the gene, purification of the protein, and characterization of its superoxide dismutase function *J Bacteriol* **178**: 7152-7158.

Li, J., Kustu, S., and Stewart, V. (1994) In vitro interaction of nitrate-responsive regulatory protein NarL with DNA target sequences in the *fdnG, narG, narK* and *frdA* operon control regions of *Escherichia coli* K-12 *J Mol Biol* **241**: 150-165.

Lin, J.T., Stewart, V. (1998) Nitrate assimilation by bacteria *Adv Microb Physiol* **39**: 1-30.

Liu, H.P., Takio, S., Satoh, T., and Yamamoto, I. (1999) Involvement in denitrification of the *napKEFDABC* genes encoding the periplasmic nitrate reductase system in the denitrifying phototrophic bacterium *Rhodobacter sphaeroides* f. sp. denitrificans *Biosci Biotechnol Biochem* **63**: 530-536.

Liu, X., De Wulf, P. (2004) Probing the ArcA-P modulon of *Escherichia coli* by whole genome transcriptional analysis and sequence recognition profiling *J Biol Chem* **279**: 12588-12597.

Lowry, O.H., Rosebrough, N.J., Farr, A.L., and Randall, R.J. (1951) Protein measurement with the Folin phenol reagent *J Biol Chem* **193**: 265-275.

Lumppio, H.L., Shenvi, N.V., Summers, A.O., Voordouw, G., and Kurtz, D.M.J. (2001) Rubrerythrin and rubredoxin oxidoreductase in *Desulfovibrio vulgaris*: a novel oxidative stress protection system *J Bacteriol* **183**: 101-108.

Lynch, A.S., Lin, E.C. (1996) Transcriptional control mediated by the ArcA two-component response regulator protein of *Escherichia coli*: characterization of DNA binding at target promoters *J Bacteriol* **178**: 6238-6249.

Macedo, S., Aragao, D., Mitchell, E.P., and Lindley, P. (2003) Structure of the hybrid cluster protein (HCP) from *Desulfovibrio desulfuricans* ATCC 27774 containing molecules in the oxidized and reduced states *Acta Crystallogr D Biol Crystallogr* **59**: 2065-2071.

Macedo, S., Mitchell, E.P., Romao, C.V., Cooper, S.J., Coelho, R., Liu, M.Y., Xavier, A.V., LeGall, J., Bailey, S., Garner, D.C., Hagen, W.R., Teixeira, M., Carrondo, M.A., and Lindley, P. (2002) Hybrid cluster proteins (HCPs) from *Desulfovibrio desulfuricans* ATCC 27774 and *Desulfovibrio vulgaris* (Hildenborough): X-ray structures at 1.25 A resolution using synchrotron radiation *J Biol Inorg Chem* **7**: 514-525.

MacMicking, J., Xie, Q W., and Nathan, C. (1997) Nitric oxide and macrophage function *Annu Rev Immunol* **15**: 323-350.

Magalon, A., Rothery, R.A., Giordano, G., Blasco, F., and Weiner, J.H. (1997) Characterization by electron paramagnetic resonance of the role of the *Escherichia coli* nitrate reductase (NarGHI) iron-sulfur clusters in electron transfer to nitrate and identification of a semiquinone radical intermediate *J Bacteriol* **179**: 5037-5045.

Maniatis, T., Fritsch, E. and Sambrook, J. (1982) Molecular Cloning. A Laboratory Manual. Cold Spring Harbour Press, New York.

Marritt, S.J., Farrar, J.A., Breton, J.L., Hagen, W.R., and Thomson, A.J. (1995) Characterization of the prismane protein from *Desulfovibrio vulgaris* (Hildenborough) by low-temperature magnetic circular dichroic spectroscopy *Eur J Biochem* **232**: 501-505.

McNicholas, P.M., Gunsalus, R.P. (2002) The molybdate-responsive *Escherichia coli* ModE transcriptional regulator coordinates periplasmic nitrate reductase (*napFDAGHBC*) operon expression with nitrate and molybdate availability *J Bacteriol* **184**: 3253-3259

Membrillo-Hernandez, J., Coopamah, M.D., Channa, A., Hughes, M.N., and Poole, R.K. (1998) A novel mechanism for upregulation of the *Escherichia coli* K-12 *hmp* (flavohaemoglobin) gene by the 'NO releaser', S-nitrosoglutathione: nitrosation of homocysteine and modulation of MetR binding to the *glyA-hmp* intergenic region *Mol Microbiol* **29**: 1101-1112.

Menon, N.K., Robbins, J., Wendt, J.C., Shanmugam, K.T., and Przybyla, A.E. (1991) Mutational analysis and characterization of the *Escherichia coli hya* operon, which encodes [NiFe] hydrogenase 1 *J Bacteriol* **173**: 4851-4861.

Miki, K, Lin, E.C. (1975) Electron transport chain from glycerol 3-phosphate to nitrate in *Escherichia coli J Bacteriol* **124**: 1288-1294.

Moreno-Vivian, C., Cabello, P., Martinez-Luque, M., Blasco, R, and Castillo, F. (1999) Prokaryotic nitrate reduction: molecular properties and functional distinction among bacterial nitrate reductases *J Bacteriol* **181**: 6573-6584.

Moreno-Vivian, C., Soler, G., and Castillo, F. (1992) Arginine catabolism in the phototrophic bacterium *Rhodobacter capsulatus* E1F1. Purification and properties of arginase *Eur J Biochem* **204**: 531-537.

Moura, I., Tavares, P., Moura, J.J., Ravi, N., Huynh, B.H., Liu, M.Y., and LeGall, J. (1992) Direct spectroscopic evidence for the presence of a 6Fe cluster in an iron-sulfur protein isolated from *Desulfovibrio desulfuricans* (ATCC 27774) *J Biol Chem* **267**: 4489-4496.

Nasser, W., Schneider, R., Travers, A., and Muskhelishvili, G. (2001) CRP modulates *fis* transcription by alternate formation of activating and repressing nucleoprotein complexes *J Biol Chem* **276**: 17878-17886.

Nathan, C., Shiloh, M.U. (2000) Reactive oxygen and nitrogen intermediates in the relationship between mammalian hosts and microbial pathogens *Proc Natl Acad Sci U S A* **97**: 8841-8848.

Nilavongse, A. (2003) The function and localization of subunits of the *Escherichia coli* periplasmic nitrate reductase. PhD thesis. The University of Birmingham.

Nohno, T., Noji, S., Taniguchi, S., and Saito, T. (1989) The *narX* and *narL* genes encoding the nitrate-sensing regulators of *Escherichia coli* are homologous to a family of prokaryotic two-component regulatory genes *Nucleic Acids Res* **17**: 2947-2957.

Ogawa, K., Akagawa, E., Yamane, K., Sun, Z.W., LaCelle, M., Zuber, P., and Nakano, M.M. (1995) The *nasB* operon and *nasA* gene are required for nitrate/nitrite assimilation in *Bacillus subtilis J Bacteriol* **177**: 1409-1413.

Olmo-Mira, M.F., Gavira, M., Richardson, D.J., Castillo, F., Moreno-Vivian, C, and Roldan, M.D. (2004) NapF is a cytoplasmic iron-sulfur protein required for Fe-S cluster assembly in the periplasmic nitrate reductase *J Biol Chem* **279**: 49727-49735.

Parkhill, J., Wren, B.W., Mungall, K, Ketley, J.M., Churcher, C., Basham, D., Chillingworth, T., Davies, R.M., Feltwell, T., Holroyd, S., Jagels, K., Karlyshev, A.V., Moule, S., Pallen, M.J., Penn, C.W., Quail, M.A., Rajandream, M A., Rutherford, K.M., van Vliet, A.H., Whitehead, S., and Barrell, B.G. (2000) The genome sequence of the food-borne pathogen *Campylobacter jejuni* reveals hypervariable sequences *Nature* **403**: 665-668.

Page, L., Griffiths, L., and Cole, J.A. (1990) Different physiological roles of two independent pathways for nitrite reduction to ammonia by enteric bacteria *Arch Microbiol* **154** 349-354.

Philippot, L., Hojberg, O. (1999) Dissimilatory nitrate reductases in bacteria *Biochim Biophys Acta* **1446**: 1-23.

Pierik, A.J., Hagen, W R., Dunham, W.R., and Sands, R.H. (1992a) Multi-frequency EPR and high-resolution Mossbauer spectroscopy of a putative [6Fe-6S] prismane-cluster-containing protein from *Desulfovibrio vulgaris* (Hildenborough). Characterization of a supercluster and superspin model protein *Eur J Biochem* **206**: 705-719

Pierik, A.J., Wolbert, R.B., Mutsaers, P.H., Hagen, W.R., and Veeger, C. (1992b) Purification and biochemical characterization of a putative [6Fe-6S] prismane-cluster-containing protein from *Desulfovibrio vulgaris* (Hildenborough) *Eur J Biochem* **206**: 697-704.

Poock, S.R., Leach, E.R., Moir, J.W., Cole, J.A., and Richardson, D.J. (2002) Respiratory detoxification of nitric oxide by the cytochrome c nitrite reductase of *Escherichia coli J Biol Chem* **277**: 23664-23669.

Pope, N.R., Cole, J.A. (1984) Pyruvate and ethanol as electron donors for nitrite reduction by *Escherichia coli* K12 *J Gen Microbiol* **130**: 1279-1284.

Postma, P.W., Lengeler, J.W., and Jacobson, G.R. (1993) Phosphoenolpyruvate: carbohydrate phosphotransferase systems of bacteria *Microbiol Rev* **57**: 543-594.

Potter, L., Angove, H., Richardson, D., and Cole, J. (2001) Nitrate reduction in the periplasm of gram-negative bacteria *Adv Microb Physiol* **45**: 51-112

Potter, L.C., Cole, J A. (1999) Essential roles for the products of the *napABCD* genes, but not *napFGH*, in periplasmic nitrate reduction by *Escherichia coli* K-12 *Biochem J* **344**: 69-76.

Potter, L C., Millington, P., Griffiths, L., Thomas, G.H., and Cole, J.A. (1999) Competition between *Escherichia coli* strains expressing either a periplasmic or a membrane-bound nitrate reductase: does Nap confer a selective advantage during nitrate-limited growth? *Biochem J* **344**: 77-84.

Poyart, C., Berche, P., and Trieu-Cuot, P. (1995) Characterization of superoxide dismutase genes from gram-positive bacteria by polymerase chain reaction using degenerate primers *FEMS Microbiol Lett* **131**: 41-45.

Rabin, R.S., Stewart, V. (1992) Either of two functionally redundant sensor proteins, NarX and NarQ, is sufficient for nitrate regulation in *Escherichia coli* K-12 *Proc Natl Acad Sci U S A* **89**: 8419-8423.

Rabin, R S., Stewart, V. (1993) Dual response regulators (NarL and NarP) interact with dual sensors (NarX and NarQ) to control nitrate- and nitrite-regulated gene expression in *Escherichia coli* K-12 *J Bacteriol* **175**: 3259-3268.

Reyes, F., Gavira, M., Castillo, F., and Moreno-Vivian, C (1998) Periplasmic nitrate-reducing system of the phototrophic bacterium *Rhodobacter sphaeroides* DSM 158: transcriptional and mutational analysis of the *napKEFDABC* gene cluster *Biochem J* **331**: 897-904.

Reyes, F., Roldan, M.D., Klipp, W., Castillo, F., and Moreno-Vivian, C. (1996) Isolation of periplasmic nitrate reductase genes from *Rhodobacter sphaeroides* DSM 158: structural and functional differences among prokaryotic nitrate reductases *Mol Microbiol* **19**: 1307-1318.

Rhodius, V.A , Busby, S.J. (1998) Positive activation of gene expression *Curr Opin Microbiol* **1**: 152-159.

Richard, D.J., Sawers, G., Sargent, F., McWalter, L , and Boxer, D.H. (1999) Transcriptional regulation in response to oxygen and nitrate of the operons encoding the [NiFe] hydrogenases 1 and 2 of *Escherichia coli Microbiology* **145**: 2903-2912.

Richardson, D.J. (2000) Bacterial respiration. a flexible process for a changing environment *Microbiology* **146**. 551-571.

Richardson, D J. (2001) Introduction: nitrate reduction and the nitrogen cycle *Cell Mol Life Sci* **58**: 163-164.

Richardson, D J., Berks, B.C., Russell, D.A., Spiro, S., and Taylor, C.J. (2001) Functional, biochemical and genetic diversity of prokaryotic nitrate reductases *Cell Mol Life Sci* **58**: 165-178.

Richardson, D.J., McEwan, A.G., Page, M.D., Jackson, J.B , and Ferguson, S.J. (1990) The identification of cytochromes involved in the transfer of electrons to the periplasmic NO_3^- reductase of *Rhodobacter capsulatus* and resolution of a soluble NO_3^--reductase--cytochrome-*c*552 redox complex *Eur J Biochem* **194**: 263-270.

Richardson, D.J., Wehrfritz, J.M , Keech, A., Crossman, L.C., Roldan, M.D., Sears, H.J., Butler, C.S., Reilly, A., Moir, J.W., Berks, B.C., Ferguson, S.J., Thomson, A.J., and Spiro, S. (1998) The diversity of redox proteins involved in bacterial heterotrophic nitrification and aerobic denitrification *Biochem Soc Trans* **26**: 401-408.

Rothery, R.A., Blasco, F , and Weiner, J.H. (2001) Electron transfer from heme *b*L to the [3Fe-4S] cluster of *Escherichia coli* nitrate reductase A (NarGHI) *Biochemistry* **40**: 5260-5268.

Rowe, J.J., Ubbink-Kok, T., Molenaar, D., Konings, W.N., and Driessen, A.J. (1994) NarK is a nitrite-extrusion system involved in anaerobic nitrate respiration by *Escherichia coli Mol Microbiol* **12**: 579-586.

Rubio, L.M , Herrero, A., and Flores, E. (1996) A cyanobacterial *narB* gene encodes a ferredoxin-dependent nitrate reductase *Plant Mol Biol* **30**: 845-850.

Saffarini, D.A., Nealson, K.H. (1993) Sequence and genetic characterization of *etrA*, an *fnr* analog that regulates anaerobic respiration in *Shewanella putrefaciens* MR-1 *J Bacteriol* **175**: 7938-7944.

Salmon, K.A., Hung, S.P., Steffen, N.R., Krupp, R., Baldi, P., Hatfield, G.W., and Gunsalus, R.P. (2005) Global gene expression profiling in *Escherichia coli* K12: effects of oxygen availability and ArcA *J Biol Chem* **280**: 15084-15096.

Savery, N.J., Lloyd, G.S., Kainz, M., Gaal, T., Ross, W., Ebright, R.H., Gourse, R.L., and Busby, S.J. (1998) Transcription activation at Class II CRP-dependent promoters: identification of determinants in the C-terminal domain of the RNA polymerase alpha subunit *EMBO J* **17**: 3439-3447.

Schröder, I., Wolin, C.D., Cavicchioli, R., and Gunsalus, R.P (1994) Phosphorylation and dephosphorylation of the NarQ, NarX, and NarL proteins of the nitrate-dependent two-component regulatory system of *Escherichia coli J Bacteriol* **176**: 4985-4992.

Sears, H.J., Bennett, B., Spiro, S., Thomson, A.J., and Richardson, D.J. (1995) Identification of periplasmic nitrate reductase Mo(V) EPR signals in intact cells of *Paracoccus denitrificans Biochem J* **310**: 311-314.

Sears, H.J., Sawers, G., Berks, B.C., Ferguson, S.J., and Richardson, D.J. (2000) Control of periplasmic nitrate reductase gene expression (*napEDABC*) from *Paracoccus pantotrophus* in response to oxygen and carbon substrates *Microbiology* **146**: 2977-2985.

Self, W.T., Grunden, A.M., Hasona, A., and Shanmugam, K.T. (2001) Molybdate transport *Res Microbiol* **152**: 311-321.

Self, W.T., Hasona, A., and Shanmugam, K.T. (2004) Expression and regulation of a silent operon, *hyf*, coding for hydrogenase 4 isoenzyme in *Escherichia coli J Bacteriol* **186**: 580-587.

Shaw, D.J., Guest, J R. (1982) Nucleotide sequence of the *fnr* gene and primary structure of the Fnr protein of *Escherichia coli Nucleic Acids Res* **10**: 6119-6130.

Shaw, D.J., Rice, D.W., and Guest, J R. (1983) Homology between CAP and Fnr, a regulator of anaerobic respiration in *Escherichia coli J Mol Biol* **166**: 241-247.

Showe, M.K., Demoss, J.A. (1968) Localization and regulation of synthesis of nitrate reductase in *Escherichia coli J Bacteriol* **95**: 1305-1313.

Siddiqui, R.A., Warnecke-Eberz, U., Hengsberger, A., Schneider, B., Kostka, S., and Friedrich, B. (1993) Structure and function of a periplasmic nitrate reductase in *Alcaligenes eutrophus* H16 *J Bacteriol* **175**: 5867-5876.

Silvestro, A., Pommier, J., Pascal, M.C., and Giordano, G. (1989) The inducible trimethylamine N-oxide reductase of *Escherichia coli* K12: its localization and inducers *Biochim Biophys Acta* **999**: 208-216.

Simon, J., Sanger, M., Schuster, S.C., and Gross, R. (2003) Electron transport to periplasmic nitrate reductase (NapA) of *Wolinella succinogenes* is independent of a NapC protein *Mol Microbiol* **49**: 69-79.

Soballe, B., Poole, R.K. (1999) Microbial ubiquinones: multiple roles in respiration, gene regulation and oxidative stress management *Microbiology* **145**: 1817-1830.

Spiro, S., Guest, J.R. (1990) FNR and its role in oxygen-regulated gene expression in *Escherichia coli FEMS Microbiol Rev* **6**: 399-428.

Steenhoudt, O., Keijers, V., Okon, Y., and Vanderleyden, J. (2001) Identification and characterization of a periplasmic nitrate reductase in *Azospirillum brasilense* Sp245 *Arch Microbiol* **175**: 344-352.

Stewart, V (1993) Nitrate regulation of anaerobic respiratory gene expression in *Escherichia coli Mol Microbiol* **9**: 425-434.

Stewart, V. (1994) Regulation of nitrate and nitrite reductase synthesis in enterobacteria *Antonie Van Leeuwenhoek* **66**: 37-45.

Stewart, V. (1998) Bacterial two-component regulatory systems. In: Busby, S.J, Thomas, C.M., Brown, N.L. (eds.) Molecular microbiology. *NATO ASI series, series H. cell biology* **103**: 141-158.

Stewart, V. (2003) Biochemical Society Special Lecture. Nitrate- and nitrite-responsive sensors NarX and NarQ of proteobacteria *Biochem Soc Trans* **31**: 1-10.

Stewart, V., Berg, B.L. (1988) Influence of *nar* (nitrate reductase) genes on nitrate inhibition of formate-hydrogen lyase and fumarate reductase gene expression in *Escherichia coli* K-12 *J Bacteriol* **170**: 4437-4444.

Stewart, V., Bledsoe, P.J. (2003) Synthetic *lac* operator substitutions for studying the nitrate- and nitrite-responsive NarX-NarL and NarQ-NarP two-component regulatory systems of *Escherichia coli* K-12 *J Bacteriol* **185**: 2104-2111.

Stewart, V., Bledsoe, P.J., and Williams, S.B. (2003) Dual overlapping promoters control *napF* (periplasmic nitrate reductase) operon expression in *Escherichia coli* K-12 *J Bacteriol* **185**: 5862-5870.

Stewart, V., McGregor, C.H. (1982) Nitrate reductase in *Escherichia coli* K-12: involvement of *chlC*, *chlE*, and *chlG* loci *J Bacteriol* **151**: 788-799.

Stock, A.M., Robinson, V.L., and Goudreau, P.N. (2000) Two-component signal transduction *Annu Rev Biochem* **69**: 183-215.

Stokkermans, J.P., Houba, P.H., Pierik, A.J., Hagen, W.R., van Dongen, W.M., and Veeger, C. (1992a) Overproduction of prismane protein in *Desulfovibrio vulgaris* (Hildenborough): evidence for a second S = 1/2-spin system in the one-electron reduced state *Eur J Biochem* **210**: 983-988.

Stokkermans, J.P., van den Berg, W.A., van Dongen, W.M., and Veeger, C. (1992b) The primary structure of a protein containing a putative [6Fe-6S] prismane cluster from *Desulfovibrio desulfuricans* (ATCC 27774) *Biochim Biophys Acta* **1132**: 83-87.

Stolz, J.F., Basu, P. (2002) Evolution of nitrate reductase: molecular and structural variations on a common function *Chembiochem* **3**: 198-206.

Tanapongpipat, S., Reid, E., Cole, J.A., and Crooke, H. (1998) Transcriptional control and essential roles of the *Escherichia coli ccm* gene products in formate-dependent nitrite reduction and cytochrome c synthesis *Biochem J* **334**: 355-365.

Taylor, B.L., Zhulin, I.B. (1999) PAS domains: internal sensors of oxygen, redox potential, and light *Microbiol Mol Biol Rev* **63**: 479-506.

Thomas, G., Potter, L., and Cole, J.A. (1999) The periplasmic nitrate reductase from *Escherichia coli*: a heterodimeric molybdoprotein with a double-arginine signal sequence and an unusual leader peptide cleavage site *FEMS Microbiol Lett* **174**: 167-171.

Tyson, K.L., Bell, A.I., Cole, J.A., and Busby, S.J. (1993) Definition of nitrite and nitrate response elements at the anaerobically inducible *Escherichia coli nirB* promoter: interactions between FNR and NarL *Mol Microbiol* **7**: 151-157.

Tyson, K., Busby, S., and Cole, J. (1997a) Catabolite regulation of two *Escherichia coli* operons encoding nitrite reductases: role of the Cra protein *Arch Microbiol* **168**: 240-244.

Tyson, K.L., Cole, J A., and Busby, S.J. (1994) Nitrite and nitrate regulation at the promoters of two *Escherichia coli* operons encoding nitrite reductase: identification of common target heptamers for both NarP- and NarL-dependent regulation *Mol Microbiol* **13**: 1045-1055.

Tyson, K., Metheringham, R., Griffiths, L., and Cole, J.A (1997b) Characterisation of *Escherichia coli* K-12 mutants defective in formate-dependent nitrite reduction: essential roles for *hemN* and the *menDBCE* gene cluster. *Archives of Microbiology* **168**: 403-411.

Unden, G., Schirawski, J. (1997) The oxygen-responsive transcriptional regulator FNR of *Escherichia coli*: the search for signals and reactions *Mol Microbiol* **25**: 205-210.

Varga, M.E., Weiner, J.H. (1995) Physiological role of GlpB of anaerobic glycerol-3-phosphate dehydrogenase of *Escherichia coli Biochem Cell Biol* **73**: 147-153.

van de Graaf, A.A , Mulder, A., de Bruijn, P., Jetten, M.S., Robertson, L.A., and Kuenen, J.G. (1995) Anaerobic oxidation of ammonium is a biologically mediated process *Appl Environ Microbiol* **61**: 1246-1251.

van den Berg, W.A., Hagen, W.R., and van Dongen, W.M. (2000) The hybrid-cluster protein ('prismane protein') from *Escherichia coli.* Characterization of the hybrid-cluster protein, redox properties of the [2Fe-2S] and [4Fe-2S-2O] clusters and identification of an associated NADH oxidoreductase containing FAD and [2Fe-2S] *Eur J Biochem* **267**: 666-676.

van den Berg, W.A., Stevens, A.A., Verhagen, M.F., van Dongen, W.M., and Hagen, W.R. (1994) Overproduction of the prismane protein from *Desulfovibrio desulfuricans* ATCC 27774 in *Desulfovibrio vulgaris* (Hildenborough) and EPR spectroscopy of the [6Fe-6S] cluster in different redox states *Biochim Biophys Acta* **1206**: 240-246.

Wallace, B.J., Young, I.G. (1977) Role of quinones in electron transport to oxygen and nitrate in *Escherichia coli.* Studies with a *ubiA- menA-* double quinone mutant *Biochim Biophys Acta* **461**: 84-100.

Wang, H., Gunsalus, R P (2000) The *nrfA* and *nirB* nitrite reductase operons in *Escherichia coli* are expressed differently in response to nitrate than to nitrite *J Bacteriol* **182**: 5813-5822.

Wang, H., Tseng, C.P., and Gunsalus, R.P. (1999) The *napF* and *narG* nitrate reductase operons in *Escherichia coli* are differentially expressed in response to submicromolar concentrations of nitrate but not nitrite *J Bacteriol* **181**: 5303-5308.

Weidner, U., Geier, S., Ptock, A., Friedrich, T., Leif, H., and Weiss, H. (1993) The gene locus of the proton-translocating NADH: ubiquinone oxidoreductase in *Escherichia coli.* Organization of the 14 genes and relationship between the derived proteins and subunits of mitochondrial complex I *J Mol Biol* **233**: 109-122

Weiner, J.H , MacIsaac, D.P., Bishop, R.E , and Bilous, P.T (1988) Purification and properties of *Escherichia coli* dimethyl sulfoxide reductase, an iron-sulfur molybdoenzyme with broad substrate specificity *J Bacteriol* **170**: 1505-1510.

Williams, S.B., Stewart, V. (1997) Discrimination between structurally related ligands nitrate and nitrite controls autokinase activity of the NarX transmembrane signal transducer of *Escherichia coli* K-12 *Mol Microbiol* **26**: 911-925.

Wimpenny, J.W., Cole, J.A. (1967) The regulation of metabolism in facultative bacteria. 3. The effect of nitrate *Biochim Biophys Acta* **148**: 233-242.

Wing, H.J., Williams, S.M., and Busby, S.J. (1995) Spacing requirements for transcription activation by *Escherichia coli* FNR protein *J Bacteriol* **177**: 6704-6710.

Wissenbach, U., Kroger, A., and Unden, G. (1990) The specific functions of menaquinone and demethylmenaquinone in anaerobic respiration with fumarate, dimethylsulfoxide, trimethylamine N-oxide and nitrate by *Escherichia coli Arch Microbiol* **154**: 60-66.

Wolfe, M.T., Heo, J., Garavelli, J.S., and Ludden, P.W. (2002) Hydroxylamine reductase activity of the hybrid cluster protein from *Escherichia coli J Bacteriol* **184**: 5898-5902.

Wood, N.J., Alizadeh, T., Bennett, S., Pearce, J., Ferguson, S.J., Richardson, D.J., and Moir, J.W. (2001) Maximal expression of membrane-bound nitrate reductase in *Paracoccus* is induced by nitrate via a third FNR-like regulator named NarR *J Bacteriol* **183**: 3606-3613.

Wu, H., Tyson, K.L., Cole, J.A., and Busby, S.J. (1998) Regulation of transcription initiation at the *Escherichia coli nir* operon promoter: a new mechanism to account for co-dependence on two transcription factors *Mol Microbiol* **27**: 493-505.